

A new approach to automated energy performance and fault detection and diagnosis of HVAC systems

DEVELOPMENT OF THE 4S3F METHOD

Arie Taal

A new approach to automated energy
performance and fault detection and diagnosis
of HVAC systems

Development of the 4S3F method

Arie Cornelis Taal

A new approach to automated energy performance
and fault detection and diagnosis of HVAC systems
Development of the 4S3F method

PROEFSCHRIFT

ter verkrijging van de graad van doctor aan de Technische Universiteit
Eindhoven, op gezag van de rector magnificus prof.dr.ir. F.P.T. Baaijens,
voor een commissie aangewezen door het College voor Promoties, in het
openbaar te verdedigen op 23 november 2021 om 13:30 uur

door

Arie Cornelis Taal

geboren te Den Haag, Nederland

Dit proefschrift is goedgekeurd door de promotoren en de samenstelling van de
promotiecommissie is als volgt:

Voorzitter: prof.dr.ir.T.A.M.Salet

1e promotor: prof.ir. W. Zeiler

2de promotor: prof.dr.ir. L.C.M. Itard (Delft University of Technology)

leden: prof. dr.ir.-arch. D. Saelens (KU Leuven University)

prof. dr. ir. P.J.C.J de Wilde (University of Plymouth)

prof. dr. ir. Z. Lukszo (Delft University of Technology)

prof. dr. A.H.M.E. Reinders

prof. dr. ir. J.L.M. Hensen

Het onderzoek of ontwerp dat in dit proefschrift wordt beschreven is uitgevoerd in overeenstemming met de TU/e Gedragscode Wetenschapsbeoefening.



A catalogue record is available from the Eindhoven University of
Technology Library

ISBN: 978-90-386-5409-6

Bouwstenen 325

Printed by TU/e print services-Dereumaux

Eindhoven, The Netherlands

© Arie Taal, 2021

Copyright of the cover page images belongs to The Hague University of
Applied Sciences.

Summary

The Heating Ventilation and Air Conditioning (HVAC) sector is responsible for a large part of the total worldwide energy consumption, a significant part of which is caused by incorrect operation of controls and maintenance. HVAC systems are becoming increasingly complex, especially due to multi-commodity energy sources, and as a result, the chance of failures in systems and controls will increase. Therefore, systems that diagnose energy performance are of paramount importance. However, despite much research on Fault Detection and Diagnosis (FDD) methods for HVAC systems, they are rarely applied. One major reason is that proposed methods are different from the approaches taken by HVAC designers who employ process and instrumentation diagrams (P&IDs). This led to the following main research question:

Which FDD architecture is suitable for HVAC systems in general to support the set up and implementation of FDD methods, including energy performance diagnosis?

First, an energy performance FDD architecture based on information embedded in P&IDs was elaborated. The new FDD method, called the **4S3F method**, combines systems theory with data analysis. In the 4S3F method, the detection and diagnosis phases are separated. The symptoms and faults are classified into 4 types of symptoms (deviations from balance equations, operating states (OS) and energy performance (EP), and additional information) and 3 types of faults (component, control and model faults).

Second, the 4S3F method has been tested in four case studies. In the first case study, the symptom detection part was tested using historical Building Management System (BMS) data for a whole year: the combined heat and power plant of the THUAS (The Hague University of Applied Sciences) building in Delft, including an aquifer thermal energy storage (ATES) system, a heat pump, a gas boiler and hot and cold-water hydronic systems. This case study showed that balance, EP and OS symptoms can be extracted from the P&ID and the presence of symptoms detected.

In the second case study, a proof of principle of the fault diagnosis part of the 4S3F method was successfully performed on the same HVAC system extracting possible component and control faults from the P&ID. A Bayesian Network diagnostic, which mimics the way of diagnosis by HVAC engineers, was applied to identify the probability of all possible faults by interpreting the symptoms. The diagnostic Bayesian network (DBN) was set up in accordance with the P&ID, i.e., with the same structure. Energy savings from fault corrections were estimated to be up to 25% of the primary energy consumption, while the HVAC system was initially considered to have an excellent performance.

In the third case study, a demand-driven ventilation system (DCV) was analysed. The analysis showed that the 4S3F method works also to identify faults on an air ventilation system.

Sensors are the heart of an FDD system, being able to diagnose sensor faults automatically is essential. In the fourth case study, model faults were introduced for soft sensor faults and the application of additional symptoms, e.g., from other detection methods. Furthermore, redundant balances have been applied for systems and subsystems that support sensor diagnosis.

The case studies demonstrated that the 4S3F method unambiguously diagnosed the causes of failures. In addition, they showed that the 4S3F architecture largely solves the problems present with existing FDD methods which could be realized by a strict discrimination between causes (faults) and effects (symptoms) allowing multiple detection methods to be used. The diagnosis by DBNs supports simultaneous multi-level diagnosis of multiple faults and overcomes by posterior probabilities of the possible faults problems related to incorrect results due to measurement inaccuracies and uncertainties in the FDD method. Furthermore, it was demonstrated that as well energy performance FDD and component FDD is applicable with the 4S3F architecture. Next to this, classifications for symptoms and faults were presented. Sensitivity analysis on the set probabilities in the DBN of the case studies showed that the absolute values are subordinate to the relative ones.

In the present study a step forward has been made towards a systematic and automated multi-system and multi-level fault and energy performance diagnosis. The 4S3F architecture holds great promise for energy performance and component FDD of HVAC systems as its utility has been demonstrated. A first step towards automation of detection and diagnosis has been achieved to minimize the effort for setting up the 4S3F method and for analysis purposes. Next to this, further research is needed to extend DBN models for missing HVAC systems and detection rules. In addition, the DBNs must be further developed for the set probabilities and for the optimal relationships between faults and symptoms. Research should also be done on the integration of additional data from inspection and maintenance and the integration with specific FDD methods provided by component suppliers.

Acknowledgments

This doctoral journey has been a long, challenging and emotional process and this dissertation would not have been possible without the support and assistance of people to whom I would like to dedicate this section and express my gratitude. First, I would like to thank my supervisors Prof. Laure Itard and Prof. Wim Zeiler who gave me the opportunity to carry out this PhD research. Laure helped me through my down periods through her enthusiasm, her tireless guidance and support throughout the process. Wim, through his critical feedback, by putting me on the track of the DBN approach and the support for finishing the thesis. Many thanks to them for their advice and experience. I would like to thank the members of the committee, prof. dr.ir.-arch. D. Saelens, prof. P.J.C.J. de Wilde, prof. dr. Z. Lukszo, prof. A.H.M.E. Reinders and prof. J.L.M. Hensen for their time and valuable feedback on my draft thesis. I would also like to thank the committee chair, prof.dr.ir.T.A.M. Salet for his time during the defense. My thanks go to The Hague University of Applied Sciences who made my PhD possible through financial support and the department of Mechanical Engineering, who understood the struggle I experienced as a part-time researcher next to teacher duties. In addition, the lecturers from the Energy and Buildings and Energy in Transition research groups who have supported me over time. Special thanks to the members of the Energy and Buildings research group of The Hague University of Applied Sciences for their feedback support during my PhD work: Frans Jooststens, Dirk Jan Schagen and Jan-Peter Vos who helped me through dips. Also, Joep de Groot for editing submitted conference papers. I would also like to thank the other colleagues from The Hague University of Applied Sciences who had asked for years about the progress of my PhD research. In addition, Rob van der Werf and Baldiri Salcedo Rahola for the finishing touch of the dissertation, and Shalika Walker, Silvie van Dam and Veerle Peeters for their support for the submission of this thesis. And finally, Madeleine who accepted the much time I spent in the evenings and weekends with the PhD research.

Table of contents

| | |
|--|----|
| Summary..... | 5 |
| Acknowledgments | 7 |
| List of figures | 12 |
| List of tables | 17 |
| Nomenclature | 18 |
| 1. Introduction..... | 21 |
| 1.1. Background..... | 21 |
| 1.2. State of the art on automated FDD methods for energy performance evaluation of HVAC systems..... | 23 |
| 1.3. HVAC engineering practices | 26 |
| 1.4. Objectives, scope, and research questions..... | 30 |
| 1.5. Research methodology..... | 31 |
| 1.6. Thesis outline | 33 |
| References..... | 35 |
| 2. A reference architecture for the integration of automated energy performance fault diagnosis into HVAC systems | 41 |
| 2.1. Introduction..... | 41 |
| 2.2. Energy performance FDD and HVAC design..... | 44 |
| 2.3. Proposed reference architecture for automated energy performance diagnosis..... | 48 |
| 2.4. Conclusions and recommendations | 61 |
| References..... | 63 |
| 3. P&ID-based symptom detection for automated energy performance in HVAC systems | 69 |
| 3.1. Introduction..... | 69 |
| 3.2. 4S3F architecture for Energy Performance Diagnosis | 70 |
| 3.3. Pre-processing..... | 71 |
| 3.4. Generic approach to symptom detection | 72 |
| 3.5. Case study: the heat and cold generation system of the building of The Hague University of Applied Sciences in Delft | 78 |
| 3.6. System and subsystem selection in the case study | 81 |
| 3.7. Symptom detection in the case study | 81 |

| | |
|--|-----|
| 3.8. Evaluation of the results of the automated symptom detection process..... | 88 |
| 3.9. Detection time span..... | 89 |
| 3.10. Conclusion and recommendations..... | 93 |
| Appendix 3A. Threshold values and results from annual detection..... | 96 |
| Appendix 3B. Results from daily detection..... | 98 |
| Appendix 3C. Results from monthly detection..... | 104 |
| References..... | 105 |
| 4. P&ID-based automated fault identification for energy performance diagnosis in HVAC systems: 4S3F method, development of DBN models and application to an ATES system..... | 108 |
| 4.1. Introduction..... | 108 |
| 4.2. 4S3F architecture for energy performance detection and diagnosis..... | 110 |
| 4.3. The fault identification approach based on the 4S3F method..... | 112 |
| 4.4. The thermal energy plant at The Hague University of Applied Sciences in Delft..... | 118 |
| 4.5. Detected symptoms in the case study..... | 122 |
| 4.6. Automated fault isolation in the case study..... | 124 |
| 4.7. Effects of a DBN with only aggregated systems A to H (Level B)..... | 131 |
| 4.8. Fault analysis, correction and effect on energy usage..... | 133 |
| 4.9. Sensitivity analysis of the assumed probabilities in the fault layer..... | 136 |
| 4.10. Conclusions and recommendations..... | 136 |
| Appendix 4A. Control systems for roof heating, and cold water, hot water, condenser and evaporator supply temperatures..... | 139 |
| Appendix 4B. DBN models with only aggregated systems A to H without capacity or OS symptoms..... | 141 |
| References..... | 142 |
| 5. Fault detection and diagnosis for indoor air quality in DCV systems: Application of 4S3F method and effects of DBN probabilities..... | 145 |
| 5.1. Introduction..... | 145 |
| 5.2. The 4S3F FDD method for indoor air quality..... | 148 |
| 5.3. Faults and symptoms of demand-controlled air ventilation systems..... | 149 |
| 5.4. 4S3F model for DCV systems in a case study..... | 150 |
| 5.5. Monitoring results and descriptive analysis of BMS data..... | 156 |
| 5.6. Application of the 4S3F method: Detected symptoms..... | 158 |
| 5.7. Application of the 4S3F method: Diagnosis results..... | 158 |

| | |
|---|-----|
| 5.8. Evaluation of the diagnosis results..... | 161 |
| 5.9. Sensitivity analysis of the set probabilities | 162 |
| 5.10. Conclusions and recommendations..... | 165 |
| Appendix 5A. Symptoms and faults of a DCV system..... | 167 |
| Appendix 5B. The construction of the 4S3F DBN..... | 169 |
| References..... | 171 |
| 6. Fault Detection, Diagnosis and Correction for hard and soft sensors in Building Energy Management Systems: A new extension of the 4S3F framework. | 175 |
| 6.1. Introduction..... | 175 |
| 6.2. 4S3F framework for building energy performance..... | 177 |
| 6.3. Generic pre-processing models for soft sensors..... | 177 |
| 6.4. Generic approach for detection of symptoms related to sensors | 179 |
| 6.5. Generic approach for sensor fault isolation..... | 180 |
| 6.6. Generic approach of sensor corrections | 185 |
| 6.7. The thermal energy plant in the building of The Hague University in Delft | 186 |
| 6.8. Hard and soft sensors in the case study..... | 189 |
| 6.9. Fault symptom detection in the case study..... | 190 |
| 6.10. Sensor fault identification in the case study | 191 |
| 6.11. Correction of sensor faults in the case study | 196 |
| 6.12. Sensitivity analysis of the assumed probabilities in the fault layer | 197 |
| 6.13. Conclusions and recommendations..... | 198 |
| Appendix 6A. Detection symptoms results..... | 200 |
| Appendix 6B. Corrections in the case study | 205 |
| References..... | 208 |
| 7. Discussion..... | 212 |
| 7.1. Study outcomes..... | 212 |
| 7.2. Limitations of the study | 220 |
| 8. Conclusions | 223 |
| 8.1 Overall conclusions..... | 223 |
| 8.2. Recommendations..... | 225 |
| 8.3. Further research..... | 226 |
| References..... | 230 |

| | |
|----------------------------|-----|
| About the author | 231 |
| List of publications | 232 |
| Bouwstenen..... | 233 |

List of figures

| | |
|---|-----|
| Figure 1.1. Phases of an FDD process | 22 |
| Figure 1.2. Classification of FDD methods | 24 |
| Figure 1.3. Examples of P&IDs..... | 24 |
| Figure 1.4. Schematic diagram of the thesis | 30 |
| | |
| Figure 2.1. The (simplified) HVAC schematic diagram of the heat and cold generation system in the THUAS building..... | 46 |
| Figure 2.2. Energy exchange based on Figure 2.1..... | 50 |
| Figure 2.3. Relationship between types of symptoms and faults | 52 |
| Figure 2.4. An aggregated system consisting of two sub-systems..... | 54 |
| Figure 2.5. HVAC schematic diagram of a heat pump system | 55 |
| Figure 2.6. Black box model of a heat pump system | 55 |
| Figure 2.7. A generic DBN model for a water-to-water heat-pump system and its control system. | 57 |
| Figure 2.8. Summary of the architecture for automated energy performance FDD. | 62 |
| | |
| Figure 3.1. 4S3F DBN structure | 71 |
| Figure 3.2. Inside the THUAS building..... | 79 |
| Figure 3.3. The relevant aggregated systems at Level a) and b) consisting of systems A to H..... | 79 |
| Figure 3.4. Principal scheme (P&ID) of the heat and cold generation system of HHS | 80 |
| Figure 3.5. Daily COP of the heat pump system..... | 91 |
| | |
| Figure 3B.1 Daily energy performance factors of the heat pump | 98 |
| Figure 3B.2 Measured capacity of the heat exchanger (TSA) of the ATES system throughout the year 2013. | 98 |
| Figure 3B.3 Daily efficiencies of systems B, C, D, G and H..... | 99 |
| Figure 3B.4 Energy signature of Thw_supply | 101 |
| Figure 3B.5 Energy signature of Thw_return | 101 |
| Figure 3B.6 Energy signature of Tcw_supply | 101 |
| Figure 3B.7 Energy signature of Tcw_return | 101 |
| Figure 3B.8 Energy signature of Tevap_in..... | 102 |
| Figure 3B.9 Energy signature of Tevap_out..... | 102 |
| Figure 3B.10 Energy signature of Tcond_out..... | 102 |
| Figure 3B.11 Energy signature of Tcold_well_in..... | 103 |
| Figure 3B.12 Energy signature of Tcold_well_out..... | 103 |
| Figure 3B.13 Energy signature of Twarm_well_in..... | 103 |
| Figure 3B.14 Energy signature of Twarm_well_out..... | 103 |

| | |
|--|-----|
| Figure 4.1 4S3F architecture for automated energy performance detection and diagnosis | 111 |
| Figure 4.2 4S3F DBN structure | 112 |
| Figure 4.3 P&ID heat pump system..... | 116 |
| Figure 4.4 DBN schematic diagram of a heat pump system..... | 116 |
| Figure 4.5 The implemented prior node properties of a fault called <i>Control roof heating</i> in GeNie..... | 117 |
| Figure 4.6 The implemented conditional node probabilities of a symptom..... | 118 |
| Figure 4.7 The atrium of the THUAS building..... | 119 |
| Figure 4.8 A staff room in the THUAS building..... | 119 |
| Figure 4.9 The heat exchanger (8)..... | 119 |
| Figure 4.10 The headers (14) and (15)..... | 119 |
| Figure 4.11 Principal diagram (P&ID) of the thermal energy plant at THUAS | 120 |
| Figure 4.12 The relevant aggregated systems at Level A and at Level B..... | 121 |
| Figure 4.13 Flow sensor FT28-03..... | 122 |
| Figure 4.14 Control of the ATES system..... | 125 |
| Figure 4.15 Control of the regeneration system..... | 125 |
| Figure 4.16 Overall DBN model at Level B with systems A to H..... | 127 |
| Figure 4.17 DBN model of the cold water system A..... | 128 |
| Figure 4.18 DBN model of the ATES system B..... | 129 |
| Figure 4.19 DBN model of the heat pump..... | 129 |
| Figure 4.20 DBN model of the boiler system D. system C..... | 129 |
| Figure 4.21 DBN model of the hot water system E..... | 129 |
| Figure 4.22 DBN model of the roof system F..... | 130 |
| Figure 4.23 DBN model of the cold water hydronic system G..... | 130 |
| Figure 4.24 DBN model of the hot water hydronic system H..... | 130 |
| Figure 4.25 Posterior fault probabilities after diagnosis..... | 130 |
| Figure 4.26 DBN model at Level B..... | 132 |
| Figure 4.27 Posterior Present fault probabilities after diagnosis..... | 132 |
| Figure 4.28 Incorrect fault isolation..... | 133 |
| Figure 4.29 Primary energy consumption for the emitter systems and the ATES system..... | 135 |
| | |
| Figure 4A.1 Control roof heating system..... | 139 |
| Figure 4A.2 Control of the supply temperature of the cold water system | 139 |
| Figure 4A.3 Control of the supply temperature of the hot water system | 140 |
| Figure 4A.4 Control of the condenser outlet water temperature..... | 140 |
| Figure 4A.5 Control of the evaporator outlet water temperature..... | 140 |
| | |
| Figure 4B.1 DBN model at Level B without capacity symptoms..... | 141 |

| | |
|---|-----|
| Figure 4B.2 DBN model at Level B without Operational State symptoms | 141 |
| Figure 4B.3 DBN model at Level B without capacity and Operational State symptoms..... | 142 |
| Figure 5.1. The 4S3F model: Relations between fault and symptom types. | 148 |
| Figure 5.2. P&ID of a VAV system..... | 150 |
| Figure 5.3. Considered building section | 151 |
| Figure 5.4. DBN model of DCV system in the case study..... | 155 |
| Figure 5.5. CO ₂ concentrations in room 1.067, 1.069, 1.071 and 1.075. | 156 |
| Figure 5.6. Air flow rate to room 1.067 | 157 |
| Figure 5.7. CO ₂ concentration in room 1.067 | 157 |
| Figure 5.8. Occupancy of room 1.067 | 157 |
| Figure 5.9. Presence during weekdays..... | 157 |
| Figure 5.10. Mean air flow rate during weekdays | 157 |
| Figure 5.11. Detected symptoms a to m..... | 159 |
| Figure 5.12. Faults 1 to 9 | 160 |
| Figure 5.13. Effects prior probability <i>Damper</i> | 162 |
| Figure 5.14. Effects prior probability <i>CO2 control</i> | 162 |
| Figure 5.15. Effects conditional probability <i>Damper</i> | 163 |
| Figure 5.16. Effects conditional probability <i>CO2 control</i> | 163 |
| Figure 5.17. DBN model for symptom <i>high CO2 and no qV</i> | 163 |
| Figure 5.18. Diagnosis deviation by different set prior and conditional probabilities related to symptom <i>High CO2 and qV=0</i> | 164 |
| Figure 5.19. Effects on posterior probabilities at changed set probabilities to symptom <i>High CO2 and qV=0</i> | 165 |
| Figure 5B.1 DBN model for symptom <i>High CO2 and low qV</i> | 169 |
| Figure 5B.2 Estimation of symptom probabilities | 170 |
| Figure 5B.3 Estimation of fault probabilities..... | 170 |
| Figure 6.1. 4S3F structure..... | 177 |
| Figure 6.2. Header with unknown temperature..... | 178 |
| Figure 6.3. Model for a three-way valve..... | 178 |
| Figure 6.4. Adapted structure 4S3F model | 181 |
| Figure 6.5. The generic DBN structure for 4S3F sensor fault diagnosis. | 181 |
| Figure 6.6. Generic DBN model for the energy balance model of headers. | 182 |
| Figure 6.7. Generic DBN model for the mass balance of headers | 182 |
| Figure 6.8. Example of a DBN Negligible energy node. | 183 |
| Figure 6.9. Example of a DBN NE node | 183 |
| Figure 6.10. Example of DBN model with an additional symptom..... | 184 |
| Figure 6.11. Prior probabilities of the additional node <i>FDD TT01</i> | 184 |
| Figure 6.12. Inside the THUAS building..... | 187 |
| Figure 6.13. Aggregated systems in block scheme form. | 187 |

| | |
|---|-----|
| Figure 6.14. HVAC P&ID of the heat and cold generation system of THUAS including soft sensors. | 188 |
| Figure 6.15. Overall DBN model of the thermal energy plant as built in GeNie... | 193 |
| Figure 6.16. The implemented DBN model for the heat pump system (C) | 194 |
| Figure 6.17. Fault probabilities of sensors FT28 | 195 |
| Figure 6.18. Fault probabilities of sensors FT29 | 195 |
| Figure 6.19. Fault probabilities of sensors TT04 | 195 |
| Figure 6.20. Fault probabilities of sensor TT29_07 | 195 |
| | |
| Figure 6A.1 Deviations of the heat exchanger ATES (8) before corrections | 200 |
| Figure 6A.2 Deviations of the heat pump (12) | 200 |
| Figure 6A.3 Deviations of the ATES system before corrections. | 201 |
| Figure 6A.4 Deviations of the heat pump system before corrections. | 201 |
| Figure 6A.5 Deviations of the boiler system before corrections. | 201 |
| Figure 6A.6 Deviations of the hydronic system cold water before corrections | 201 |
| Figure 6A.7 Deviations of the hydronic system hot water before corrections | 201 |
| Figure 6A.8 Deviations of the thermal energy plant before corrections. | 201 |
| Figure 6A.9 Daily EER _{hp} before corrections | 202 |
| Figure 6A.10 Daily COP _{hp} before corrections | 202 |
| Figure 6A.11 Deviation between TT04_04 and TT04_05 before corrections | 203 |
| Figure 6A.12 Temperatures TT04_04 and TT04_05 before corrections | 203 |
| Figure 6A.13 Temperatures TT04_01 and TT04_02 before corrections | 203 |
| Figure 6A.14 Negligible energy heat pump system | 204 |
| Figure 6A.15 Negligible energy boiler system | 204 |
| Figure 6A.16 Negligible energy roof system | 204 |
| | |
| Figure 6B.1 Deviations of the ATES system after corrections | 206 |
| Figure 6B.2 Deviations of the heat pump system after corrections | 206 |
| Figure 6B.3 Deviations of the boiler system after corrections | 206 |
| Figure 6B.4 Deviation of the hydronic system cold-water after corrections | 206 |
| Figure 6B.5 Deviations of the hydronic system hot water after corrections | 206 |
| Figure 6B.6 Deviations of the whole system after corrections. | 206 |
| Figure 6B.7 Measured EER _{hp} after corrections | 207 |
| Figure 6B.8 Deviations between TT04_04 and TT04_05 after bias correction of TT04_04. | 207 |
| Figure 6B.9 Energy exchange boiler system after corrections | 208 |
| Figure 6B.10 Energy exchange roof after corrections | 208 |
| Figure 6B.11 Energy exchange systems headers (4) and (5) after corrections | 208 |
| Figure 6B.12 Energy exchange system (3) after corrections | 208 |
| | |
| Figure 7.1 Separated detection and diagnosis phases in the 4S3F method. | 213 |
| Figure 7.2 The 4S3F structure in a DBN model | 214 |

Figure 7.3 Faults and symptoms present in the case studie.215
Figure 7.4 Extraction of a DBN model from a P&ID 216
Figure 7.5 An aggregated system consisting of two sub-systems.216
Figure 7.6 DBN model at level B containing components at level C.217

List of tables

| | |
|---|-----|
| Table 1.1 Energy performance measures | 23 |
| Table 2.1. Symptoms detected during the 28-days measurement period | 60 |
| Table 3.1. Overview of the detection results | 88 |
| Table 3A.1. Annual detection results: energy balance symptoms | 96 |
| Table 3A.2. Measured annual EPFs and reference annual EPFs | 96 |
| Table 3A.3. Thresholds for set-point values and symptoms of control-based indicators | 97 |
| Table 3A.4. Thresholds for design-based indicators and symptom detection | 97 |
| Table 3C.1 Monthly energy balance symptoms of boiler system D | 104 |
| Table 3C.2 Monthly SCOP symptoms of the heat pump on a daily basis | 104 |
| Table 3C.3 Symptoms for the capacity of the boiler | 104 |
| Table 3C.4 Monthly OS symptoms | 105 |
| Table 4.1 Fault-symptom relation table for a heat pump system. | 115 |
| Table 4.2 Overview of the detection results from BMS data for the 31 possible symptoms found in the year 2013 | 123 |
| Table 4.3 Main relations between the 31 symptoms and the 18 faults to build the DBN models | 126 |
| Table 4.4 Influence of prior probabilities on the outcomes of the posterior fault Present probabilities | 136 |
| Table 5.1 Overview of faults and corresponding symptoms in the case study (we have renumbered the faults and symptoms in Table 5A.1) | 153 |
| Table 5A.1 Faults and symptoms related to the DCV system of Figure 5.3 | 168 |
| Table 5B.1 Conditional node properties symptom High CO ₂ and low qV | 169 |
| Table 5B.2 Calculated probabilities symptom High CO ₂ and low qV from the fault states. | 170 |
| Table 5B.3 Noisy-Max type for the symptom node High CO ₂ and low qV in the DBN example | 171 |
| Table 6.1 Posterior Present probabilities depending on state of FDD TT01 | 184 |
| Table 6.2 Detected symptoms related to faults. | 192 |
| Table 6.3 Influence of prior probabilities on the posterior probabilities | 197 |

Nomenclature

Abbreviations

| | |
|---------|---|
| ABCAT | Automated Building Commissioning Analysis Tool |
| Absent | Absence of a fault or symptom |
| ASHRAE | American Society of Heating, Refrigerating and Air Conditioning Engineers |
| ATES | Aquifer Thermal Energy Storage |
| AFI | automated fault isolation |
| AHU | air handling unit |
| BEMS | Building Energy Management System |
| BMS | Building Management System |
| DBN | Diagnostic Bayesian Network |
| DCV | Demand controlled ventilation |
| EP | Energy Performance |
| EPBD | Energy Performance of Buildings Directive |
| ES | Energy signature |
| EU | European Union |
| EUI | Energy use intensity |
| EWMA | Exponential weighted moving averages |
| F | Fault |
| FDD | Fault Detection and Diagnosis |
| FT | Flow transmitter |
| HVAC | Heat, Ventilation and Air conditioning |
| IAQ | Indoor air quality |
| ICT | Information and communications technology |
| IEA | International Energy Agency |
| KPI | Key performance indicator |
| NE | negligible energy |
| OS | Operational State |
| P&ID | Proces & Instrumentation Diagram |
| PCA | Principal Component Analysis |
| PIR | Passive infrared |
| Present | Presence of a fault or symptom |
| S | Symptom |
| SVM | Support Vector Machine |
| TC | temperature controller |
| THUAS | The Hague University of Applied Sciences |
| TSA | heat exchanger |
| TT | temperature transmitter |
| VAV | Variable air volume |
| 4S3F | Four faults and three symptoms |

Symbols

| | | |
|--------------------|---------------------------------------|--|
| COP | Coefficient of performance | [-] |
| CO ₂ | CO ₂ concentration | [ppm] |
| E | Energy | [kW] |
| EER | Energy efficiency ratio | [-] |
| n _{tot} | Number of detections | [days, hours] |
| n _{fault} | Number of fault detections | [days, hours] |
| P | Power | [kW] |
| P | Probability | [0...100 %] |
| PER | primary energy ratio | [-] |
| PIR | presence | [0,1] |
| PF | Performance factor | [-] |
| q _v | Volume flow rate | [m ³ /h] or [m ³ /s] |
| SCOP | Seasonal coefficient of performance | [-] |
| SEER | Seasonal energy efficiency ratio | [-] |
| T | Temperature | [°C] |
| Q | Heat | [kJ] |
| W | Work | [kJ] |
| δ | Threshold outliers during a time span | [%] |
| ε | Deviation from expected value | [%] |
| η | efficiency | [%] |

Indices

| | |
|-------|--|
| cond | condenser |
| cw | cold water |
| exp | expected |
| evap | evaporator |
| hp | heat pump |
| hw | hot water |
| LL | lower limit |
| load | load of cold water into the cold well of the ATES system |
| max | maximum |
| mea | measured |
| min | minimum |
| mod | module |
| pr | primary |
| reg | regeneration |
| roof | roof system THUAS building |
| syst | system |
| systB | ATES system (depicted as system B) |
| systC | heat pump system (depicted as system C) |

| | |
|--------|--|
| systD | boiler system (depicted as system D) |
| systG | hydronic system for heat distribution (depicted as system G) in the thermal plant of THUAS |
| systH | hydronic system for cold distribution (depicted as system H) in the thermal plant of THUAS |
| td | thermodynamic |
| TSA | heat exchanger |
| UL | upper limit |
| unload | unload of cold water from the cold well of the ATES system. |

1. Introduction

1.1. Background

Worldwide minimization of energy demand is of highest importance to reduce the consumption of fossil energy and thereby, associated environmental problems. One way to reduce energy demand is to minimize waste energy in energy systems. From the main energy demand categories namely, transport, industrial and built environment, the building sector accounts for almost 33% [1] of the total worldwide energy usage. From this 33%, about 20-25% [2, 3] are identified to be unnecessary energy losses or waste energy, meaning that a worldwide energy reduction of 6-8 % may be possible if the intra-building energy systems function properly. The main building energy systems are lighting systems, appliances, ICT devices, and HVAC systems. The energy losses arise for a large part in the process of control and handling of faults in HVAC systems (Heating, Ventilation and Air Conditioning systems).

In practice, faults in building installations are not easily noticeable because automated systems which diagnose such faults are not commonly used. Nevertheless, regulations from government, especially the Energy Performance Building Directive (EPBD) [4] in the European community will enforce applications of energy management systems. With these applications, methods will be developed to continuously control energy consumption, efficiency and unnecessary energy losses in all kinds of HVAC systems [5]. Because of ‘multi-commodity’ energy sources integrated to buildings (e.g., solar panels being combined with an aquifer thermal energy storage (ATES) system, a heat pump and a boiler in one building heating system), HVAC systems are becoming more and more complex. Therefore, fault monitoring and fault repair in systems and controls is becoming increasingly important.

Moreover, when dealing with built environment, indoor climate is of the utmost importance. A better indoor climate results in higher comfort, better performances [6], and less complaints from users. Therefore, a proper control of the HVAC system is not only about controlling energy consumption for heating, cooling and electricity, but also about maintaining thermal comfort and indoor air quality. The system control problem is therefore multi-objective which makes the control complex.

For the operational control of the efficient energy consumption of HVAC systems, it is a necessity to have continuous commissioning, see e.g., Djuric [7], applying fault diagnosis systems to avoid energy waste by malfunctioning of an HVAC system. In practice, automated fault diagnostic systems are only scarcely used despite many proposed methods in IEA EBC (International Energy Agency Energy in Buildings

and Communities) annexes [8-12]. Research is therefore necessary to underline the importance of the application of energy performance methods in practice by removing current obstacles. Handbook [13] presents how building performance analyses can be approached. In this study, the focus is on automated methods.

So-called FDD (fault detection and diagnosis) is used to identify malfunctioning HVAC components and controls. In FDD methods faults are diagnosed by detection of symptoms. Because unnecessary energy wastages in an HVAC system and undesirable indoor climate arise from malfunctioning HVAC components and controls, they can also be considered as symptoms caused by faults. Therefore, an energy performance diagnosis system can also be understood as an FDD system. That is why the focus here is on FDD methods as starting point for energy performance diagnosis. In this thesis when the term FDD is used, it always includes energy performance diagnostic.

In practice, setting up and managing reliable, affordable and scalable HVAC FDD systems for continuous commissioning are still difficult and expensive tasks, as mentioned in [14] whereby automated FDD systems are only rarely used despite many suggested methods. Next, existing FDD methods are different from HVAC design methods and require a separate setup and realization procedure. In addition, several methods are used for different HVAC components and systems and the diagnosis systems are therefore very specific. Furthermore, these FDD systems do not work properly when a sensor is broken, if contradictory information is collected from different sensors, or if there are too few sensors placed to perform a diagnosis. The latter is a problem in existing systems. In addition, most methods are not fully automated and HVAC experts must proactively look for errors and act accordingly because errors are not identified, only the presence of failures. The present research aims at an energy performance diagnosis method that overcomes above mentioned problems and can be set up with the least possible effort and can be integrated with existing and new FDD approaches.

In general, an FDD process consists of phases as shown in Figure 1.1:

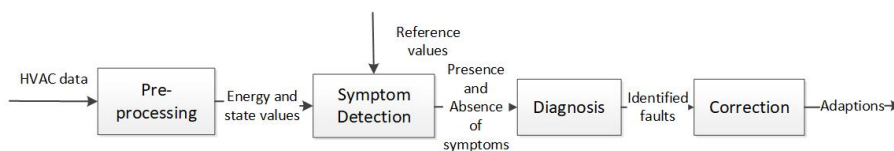


Figure 1.1. Phases of an FDD process

- Step 1: Pre-processing - Raw data from data loggers or from the building (energy) management system ((B(E)MS) is converted in processable format for FDD as energy data and other metrics. In this stage, incomplete and corrupted data is filtered. Furthermore, values from soft sensors (see [15]) are estimated.

Then, the FDD finds place:

- Step 2: Symptom detection – Presence or absence of symptoms indicating malfunction.
- Step 3: Diagnosis - Faults causing the detected symptoms are identified. In this stage faults are isolated and fault effects on energy performance and comfort are quantified.

End after diagnosis:

- Step 4: Correction – In this stage decisions are made for repair and adjustments.

In general, it's interesting to see that there is no loop back after correction. This because after adjusting/repair a new steady state will develop.

The focus in the present study is on the detection and diagnosis phases.

1.2. State of the art on automated FDD methods for energy performance evaluation of HVAC systems

A preliminary literature study conducted on energy performance measures¹ (reference values for energy performance estimation) and FDD methods for HVAC systems to identify the main features of FDD methods are presented in this section. In Chapters 2-7 more literature has been further discussed. In an energy performance FDD method, the measured energy performance should be compared with the expected one from energy performance measures. Several reviews considering energy performance measures were published [16-17]. In reference [18] the EU presents a method for energy performance calculations.

Table 1.1 presents a summary of these energy performance metrics.

Table 1.1 Energy performance measures

| <i>Energy performance measure</i> | <i>Example</i> |
|-----------------------------------|--|
| Energy use intensity (EUI) | Energy consumption per area unit: kWh/m ² |
| Energy signature (ES) | Energy vs. outdoor temperature. Indoor temperature vs. outdoor temperature. |
| Dimensionless key figures | Coefficient of performance (COP). Efficiency |

The simplest mathematical measure for energy consumption purposes presented in literature is a benchmarking approach in which the energy consumptions in buildings are compared with those of similar buildings: the energy use intensity (EUI), which

¹ The terms indicator and metrics are also used for this, the first of which is used in the published journal articles.

indicates energy consumption (e.g., kWh/m²), see [16 and 21]. Next to this, so called energy signatures are popular [22-24]. In graphics energy performance metrics are presented. For instance, daily energy consumption and indoor temperature vs outdoor temperature. Furthermore, there are dimensionless energy performance key figures, as the coefficient of performance (COP) for heat pumps [25], and approaches in which energy performance measures are compared with results from (simulation) models [21,26-27]. These energy performance measures are applied at different system levels: from component to whole building level, see e.g., [28].

The discussions in the above articles show that low HVAC performance is caused by errors in the design, implementation, operation, or maintenance of HVAC systems, and in the integration of HVAC with the actual use of buildings and actual building materials such as the shell insulation that deviates from the original design. It is remarkable that most FDD methods have been very specifically developed to deal with failure of HVAC components and effects on energy performance are hardly considered. In addition, effects of process control, maintenance, actual building characteristics and building use on energy performance are rarely studied. Summarizing, although there are some developments in this area, a generic FDD method for energy performance purposes using energy performance measures is not common.

Nevertheless, the FDD approaches can serve as a basis to be applied for energy performance evaluation. An overview of methods used in such applications is discussed below. First, the different generic types of FDD methods are discussed and Figure 1.2 presents an overview of these methods, derived from Kim and Katipamula [5], based on [29].

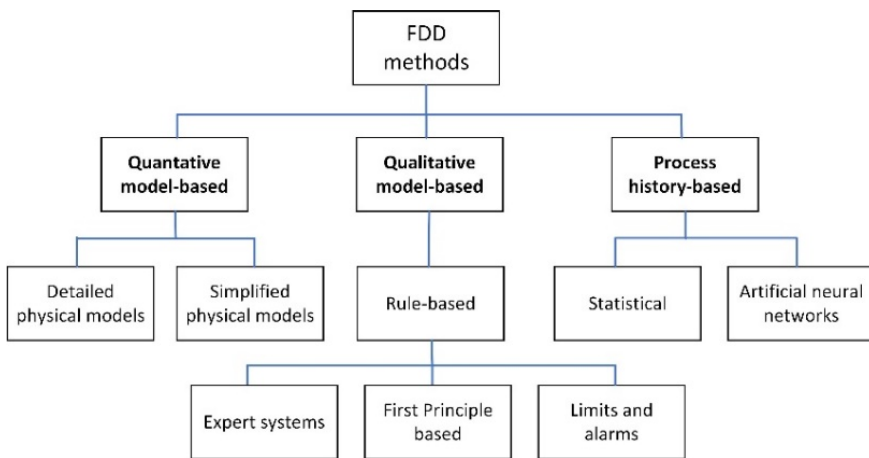


Figure 1.2. Classification of FDD methods
(Derived from [5]).

They classify FDD methods into quantitative, qualitative, and process history-based methods:

- **Quantitative models** are based on physical models, e.g., from simulation models (could be detailed) or physical balances (simplified) and are also called model-based methods [30].
- The most common applied **qualitative methods** are rule-based in which rules are known from HVAC design experts [31] such as expected state values (e.g., temperatures). In addition, alarms and exceeds of limits indicate faults and rules based on first principles are applied.
- **The process history-based methods** (also called data-driven methods) have gained in popularity during the last decades. These methods are based on measured data from which patterns are identified. The pattern recognition leads to fault isolation. Several data-driven methods have been proposed. Commonly mentioned are supervised methods using black boxes in which physical output (e.g., energy usage) is calibrated against historical data (e.g., regression methods and artificial neural networks [32-33]). They also include classification methods as SVM (support vector machine) which divide a data set in faulty and unfaulty outcomes for the HVAC operation [34-36] and PCA (principal component analysis) methods [36 and 38] which reduce a higher dimensional space into a lower dimensional space.

In above classification no distinction has been made between detection and diagnosis.

In the last decades, hybrid methods are applied (not shown in Figure 1.2). As example, gray box methods for FDD using a highly simplified physical model which parameters are determined by historical data (see for instance ABCAT [39]).

For HVAC's these FDD methods are applied for components and (sub)systems. Most HVAC FDD methods are developed for components as chillers [40-41], AHUs (air handling units) [42], sensors [43-44] and VAV (Variable Air Volume) boxes [45-46]. In addition to these FDD for separate components, specific HVAC systems with multiple components are considered, see for example [47] which discusses an HVAC system including a chiller, a cooling tower, a heat exchanger and hydraulic systems. Despite all research, all these methods still have shortcomings. Set-up of FDD rules is still a labour-intensive exercise because each HVAC system is unique and demands HVAC expertise and knowledge of the building. In case of models, often simulation expertise is needed. Most methods and models are developed for specific subsystems like chillers, VAV systems, and AHUs. In addition, measurement points present in one study are not always available in another system. On the other hand, data-driven

methods require large amounts of data from installations, while it is generally unknown if the installation is functioning properly or not. Another problem is that not enough data could be made available from the HVAC systems (at least one year data), making this method less suitable.

Moreover, most literature studies are theory-based and do not consider real-time measurements which embed unknown faulty measurement data. Some FDD methods are detection methods only and do not distinguish between symptoms and faults.

Integration of these different methods in one generalized methodology is difficult or even impossible to realize. All these methods diagnose faults on different levels: from component level to whole system level. When a multi-level approach is present, it is either top-down or bottom-up in sequences incorporating multiple types of methods [48]. It is also noticeable that the diagnosis approach often strongly depends on the detection method used. For instance, when diagnosing sensor faults using PCA methods there is a one-on-one correlation between symptoms and faults [49]. Hence, libraries with generic FDD models for all kind of HVAC systems are still missing.

Furthermore, most available FDD methods result in a binary outcome for (presence of) symptoms and faults leading to faulty outcomes by inaccuracies in measurement data and the applied FDD method. Therefore, studies over the past decade have focused on minimizing the false diagnosis results through adapted, complex FDD methods optimized for a specific HVAC component. To overcome this problem, the application of diagnosis methods based on probabilities is promising, like Bayesian statistics, which predict fault chances from presence and absence of symptoms. One of such method is the diagnostic Bayesian network (DBN) method, see [50-53]. The DBN method can also largely overcome the other above-mentioned problems because it can handle with simultaneous multi-level diagnosis, modularity, simple extension of symptoms or faults, little data points, different types of symptoms and faults, and even with contradictory and redundant symptoms.

All considered, most FDD methods are still complex, tens of different methods must be used at subsystem or component level for a specific (unique) building and there is no integration at system level. A reference architecture for HVAC FDD is missing which embeds different methods and structures of the FDD process. However, a DBN-based method seems to overcome problems in other methods.

1.3. HVAC engineering practices

The literature study shows that most proposed FDD methods are designed and implemented without considering HVAC systems design. HVAC system design is based on first principles systems, as mass and energy balances, and from systems science that systems can be divided in subsystems and aspect systems. It is common use to apply schematics which grow from raw to detail (e.g., ASHRAE's handbook

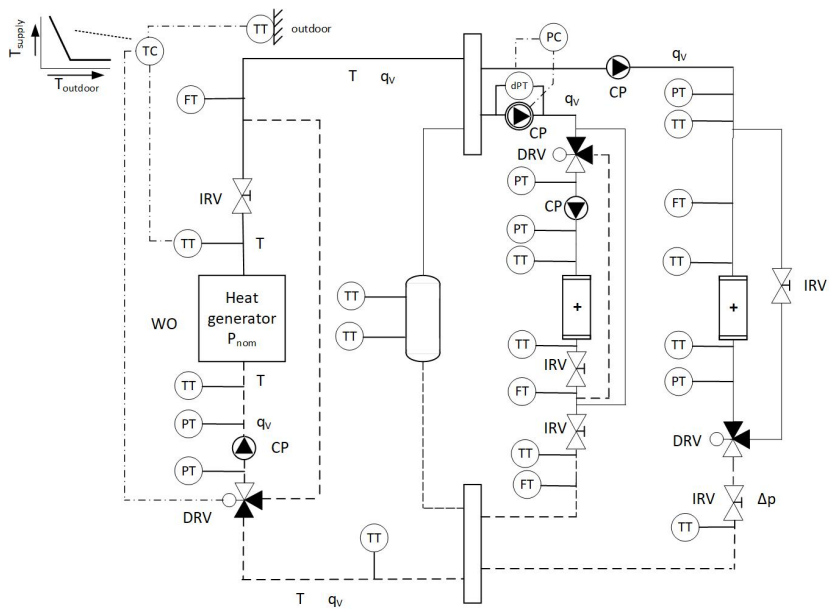
[54] and design manual [55]). In the design stage, HVAC designers determine the specifications of the components, sub-systems and systems and their control. They capture it into P&IDs ²(Process and instrumentation diagrams) in which the main HVAC and control components are represented with all their interconnections as well as all mass (fuel, water, air), electric energy and signal transfer channels, by which thermal energy flows can be easily computed. Guidelines for setting up HVAC modules are available.

Figure 1.3 shows such P&ID diagrams based on Dutch guidelines for measurement points [56], hydronic hot water [57] and cold water [58] modules. Figure 1.3 (a) and (b) present representative P&IDs for hot and cold-water systems in which a thermal energy generator is present. Figure 1.3 (c) presents the air handling unit and (d) an example of an (air) end-user system. A P&ID contains components (presented as symbols) which are linked by pipes, ducts and signals, and contain sensors (depicted as transmitters) and actuators (e.g., electric motors of valves) which are coupled via controllers. Furthermore, the nominal power of components is often shown (see Pnom in figure (a)), and the controlled and designed temperatures and flow rates at design conditions on the P&IDs (T and qv in the figures). All-over, P&IDs contain information about components, controls and expected state values which are important for energy performance analysis.

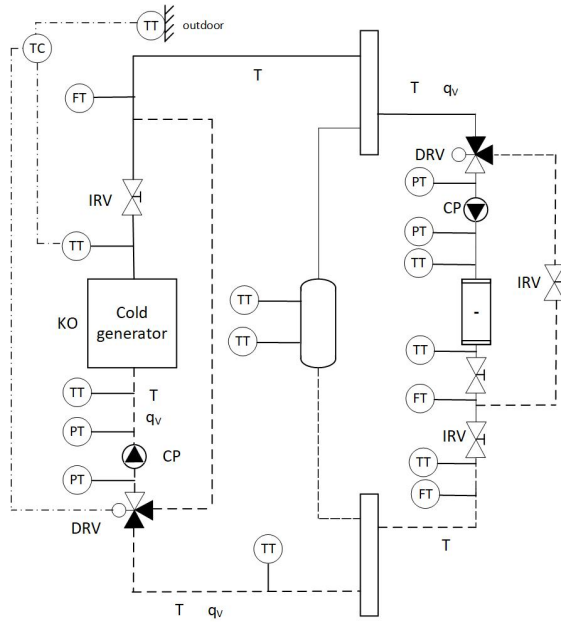
From the P&ID two types of faults can be distinguished: **component faults** (such as pumps, valves, boilers, sensors) and **control faults** (settings in controllers, such as TC and CC). Faults of this kind could lead to **energy performance (EP) symptoms**, such as low coefficients of performance (COPs). From the P&ID, the sensors needed to estimate the exchanged energy amounts for energy performance measures can be estimated. These faults also lead to symptoms such as unwanted temperatures (measured by de sensors TT, CT, PT in the presented P&IDs) or unexpected states of actuators (pumps, valves). These symptoms can be stated as **operational state (OS) symptoms**. Finally, for the diagnosis to take place with correct measurements, the idea is to use mass, energy, and pressure **balance symptoms** to rule out sensor errors.

The above types of symptoms and faults are generic, useful, and available for any multi-level HVAC installation and can be extracted from P&IDs.

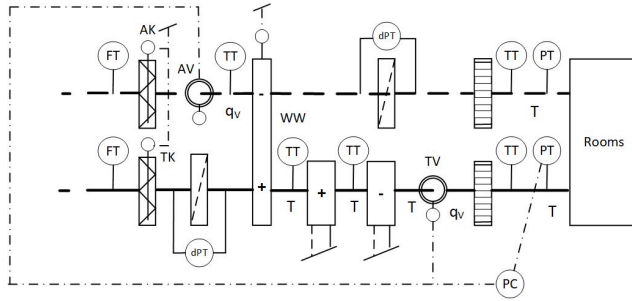
² Also called piping and instrumentation diagrams and depicted as PDF's (process flow diagrams).



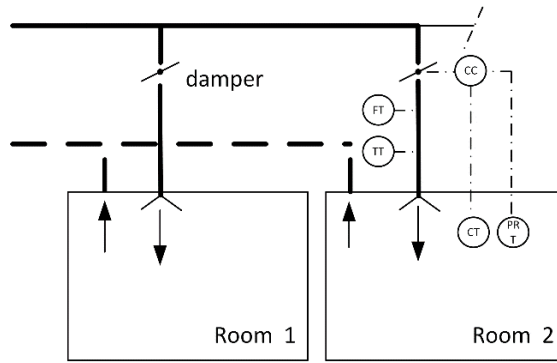
(a) hot water system



(b) cold water system

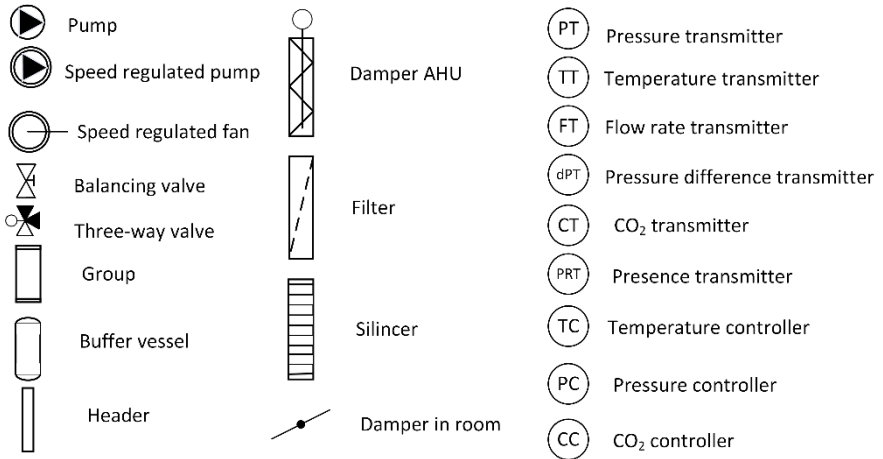


(c) Air handling unit (AHU)



(d) End-user ventilation system

Nomenclature:



T=Temperature; qv= flow rate; p=pressure

Figure 1.3 Examples of P&IDs.

1.4. Objectives, scope, and research questions

Despite much research in this area, major shortcomings result in lack of applications of FDD. Set-up of FDD models is labour intensive because each HVAC system is unique and the set-up demands HVAC, information technology (IT), data analytics, or modelling expertise. IT and data analytics experts have generally little expertise in HVAC, and for them it is difficult to understand the physical meaning of the data they handle. HVAC and building modellers on the contrary lack knowledge on IT and data analytics methods. In addition, FDD methods lack the ability to integrate diagnosis simultaneously on different system levels: component to whole system level. Next to this, most methods are detection methods, which detect that a fault is present but do not isolate the causes of the faults. Moreover, methods are specific for each subsystem like chillers, VAV systems, AHU units, and even specific per supplier. There are no standardized methods and as an effect, libraries with FDD models are missing. All considered, the HVAC FDD methods are still complex and there is need for a structured approach to FDD, integrating expertise, components, and methods.

This research is motivated by the absence of a general FDD architecture and modular FDD approach for HVAC systems addressing the issues mentioned in Section 1.1. This led to the idea of a reference architecture for energy performance FDD incorporating multiple symptom detection methods in a systematic and organized way based on information embedded in P&IDs. Methods based on this architecture can determine fault probabilities at all levels of an HVAC system, regardless of the layout and components of this HVAC system.

The study hypothesizes that FDD can become an integral and automated part of the HVAC system and its control design activities. This would save money and avoid building energy management system (BEMS) design faults. In the end, HVAC and control engineers are best able to determine energy performance measures, alarm thresholds and which sensors are needed.

Above leads to following hypothesis:

It should be possible to develop an automated and standardized fault detection and diagnosis (FDD) method for HVAC's energy performance diagnostic purposes based on systems theory, information from HVAC process and instrumentation diagrams (PIDs) and integrating diverse FDD methods already demonstrated.

The objective is to find out which FDD architecture meets the hypothesis. The main result to be achieved is a proposal for this FDD architecture. With the information known from the design, reflected in P&IDs, a method can be set up which diagnoses both energy performance and component faults. Moreover, automation of the methods in this architecture are worked out for as well detection as diagnosis purposes. A classification of symptoms and faults, and suggestions for detection and

diagnosis rules are presented. In addition, a start for libraries for detection and diagnosis models is set up. This PhD research focus on the useability of DBN's for as well energy performance as well component FDD. The scientific contribution is that a step forward could be made for a systematic and automated multi-system and multi-level energy performance diagnosis in which FDD of components is embedded.

Following this focus and hypothesis, the main research question of this thesis is formulated.

Which FDD architecture is suitable for HVAC systems in general to support the set up and implementation of FDD methods, including energy performance diagnosis?

In addition, the next sub-questions are defined:

1. How can HVAC process and instrumentation diagrams (P&IDs) be used as starting point for setting up an HVAC-FDD system, including energy performance diagnosis.
2. How can the multiple system and subsystem levels in HVAC systems be reflected in and made useful for the FDD system?
3. Which methods need to be applied for symptom detection of the main categories of faults?
4. Can the proposed FDD architecture easily be automated and applied on existing HVAC systems?

1.5. Research methodology

From P&IDs, two types of faults can be extracted: **component and control faults** which lead to three types of symptoms: **energy performance, operational state and balance symptoms**. This is used as a starting point for the development of a novel FDD architecture for HVAC energy performance. The above types of symptoms and faults are generic and usable and available for any HVAC installation at multi-level. In addition, other symptoms may be available, such as maintenance and inspection information, user complaints, and information from embedded component FDD. However, this information is not always available. It is proposed that this fall under the container term **additional symptom**.

Models have sometimes been drawn up for the symptoms, for example for soft sensors, to determine a value. This also makes faults possible. This is referred to as **model faults**.

As a result, 4 types of symptoms and 3 types of faults are identified in the so-called **4S3F** (4 symptoms and 3 faults) method.

The following methodology is applied in this research. The idea of the proposed 4S3F architecture is discussed theoretically first and with experiences from this, the proof of concept is made in four case studies.

The case studies are conducted on an actual HVAC system with real measurement data from The Hague University of Applied Sciences (THUAS) building in Delft. This building mainly contains classrooms, offices for lecturers and other staff members, and a restaurant. It was selected because it has a complex HVAC system with an advanced control system, and extensive measurement data is available for analysing energy consumption and indoor climate. In addition, it is an operational HVAC system with a reputation for working properly and apparently being energy efficient. In winter, heat is generated by a heat pump. When the heat loads are high, a gas boiler can deliver additional heat. The heat source of the heat pump is warm ground water delivered by the warm well of an ATES (Aquifer thermal energy storage) system. The ATES system can also deliver heat to the parking lanes on the roof to keep it free of ice. In the summer months, cold water from the cold well of the ATES system delivers cooling. When cooling loads are high, the heat pump produces additional cold at the evaporator side. During the summer, heat from the heat pump condenser and the roof collector can be used to regenerate the warm well of the ATES system, as the annual thermal energy extracted from and pumped into the wells has to be balanced under the Dutch regulations. Cold and heat are delivered to the rooms of the building by a thermal floor system which acts as a Thermally Activated Building System (TABS) and by ceiling radiation panels where hot or cold water is circulated. The hot and cold-water groups are divided in south and north groups which are further divided into sub-groups for the air handling in de air handling units, the ceiling and the floor equipment. A demand driven air ventilation system is present in which the air flow rates to the rooms are controlled by CO₂ concentration and occupancy.

The first case study is conducted on the thermal energy plant of THUAS with the use of a P&ID to investigate which rules can be applied to detect energy balance, energy performance and operational status symptoms while ignoring sensor failures. In the next case study, fault diagnosis is performed on this HVAC system to examine the desired structure and parameters for the 4S3F DBN determining component and control faults. In the third case study, to demonstrate that the 4S3F method is generic to all types of HVAC systems, it was developed for an air ventilation system to isolate faults. Finally, in the final case study of the 4S3F method research is conducted on soft (model-based) and hard (component-based) sensor errors with additional symptoms.

1.6. Thesis outline

The thesis outline is shown in Figure 1.4. First, the structure of the 4S3F FDD architecture based on 4 types of symptoms and 3 types of faults is developed and discussed in Chapter 2. This FDD architecture is based on system information from P&IDs. The whole HVAC system can be divided in systems with the help of P&ID schemes. In the Chapters 3 to 6, the FDD architecture is worked out in experiments to demonstrate that the 4S3F concept, is feasible for different kinds of systems. First, in Chapter 3, the symptom detection phase with balance, operational state and energy performance symptoms is designed and tested on the historical data of the thermal energy plant of the THUAS building which generates heat and cold using a heat pump, a gas boiler and an aquifer thermal energy storage system. The focus is on energy consumption.

Next, in chapter 4 the identification of energy performance related faults applying Bayesian theory is discussed. Considering fault identification as part of diagnosis, the research focuses on mimicking the approach an HVAC expert would apply. This approach is a probabilistic one, in which the expert generally operates by eliminating causes that are not likely to happen and focuses on the most likely faults leading to the symptoms observed. For this part the research therefore focuses on a probabilistic approach of fault isolation based on the presence and absence of symptoms. The analysis of possible faults leads to their categorization into 2 different types: component and control faults. The research focuses on how to (automatically) identify faults in these two categories. Here too, the method is applied on historical BMS (building management system) data from THUAS building.

To show that the 4S3F method is generic it is applied on another HVAC subsystem and aspect system: an HVAC end-user system in which the energy performance is focussed healthy climate. Its usage is shown for an actual DCV system with real BMS data in Chapter 5. And at last, to show that FDD can further on be integrated, component FDD is discussed in Chapter 6. The backbone of any FDD method is the sensor data, and hence inaccuracies or even completely faulty data can complicate the FDD process. For this purpose, a part of the research also focuses on researching how to extend the method to cope with hard and soft sensor faults. Soft sensor faults are model type faults arise when models are used to estimate missing data. In this section, additional symptoms are considered.

In Chapter 7 the research results and limitations are discussed. Finally, the conclusions and recommendations for further research on FDD method integrating energy performance diagnosis are presented in Chapter 8.

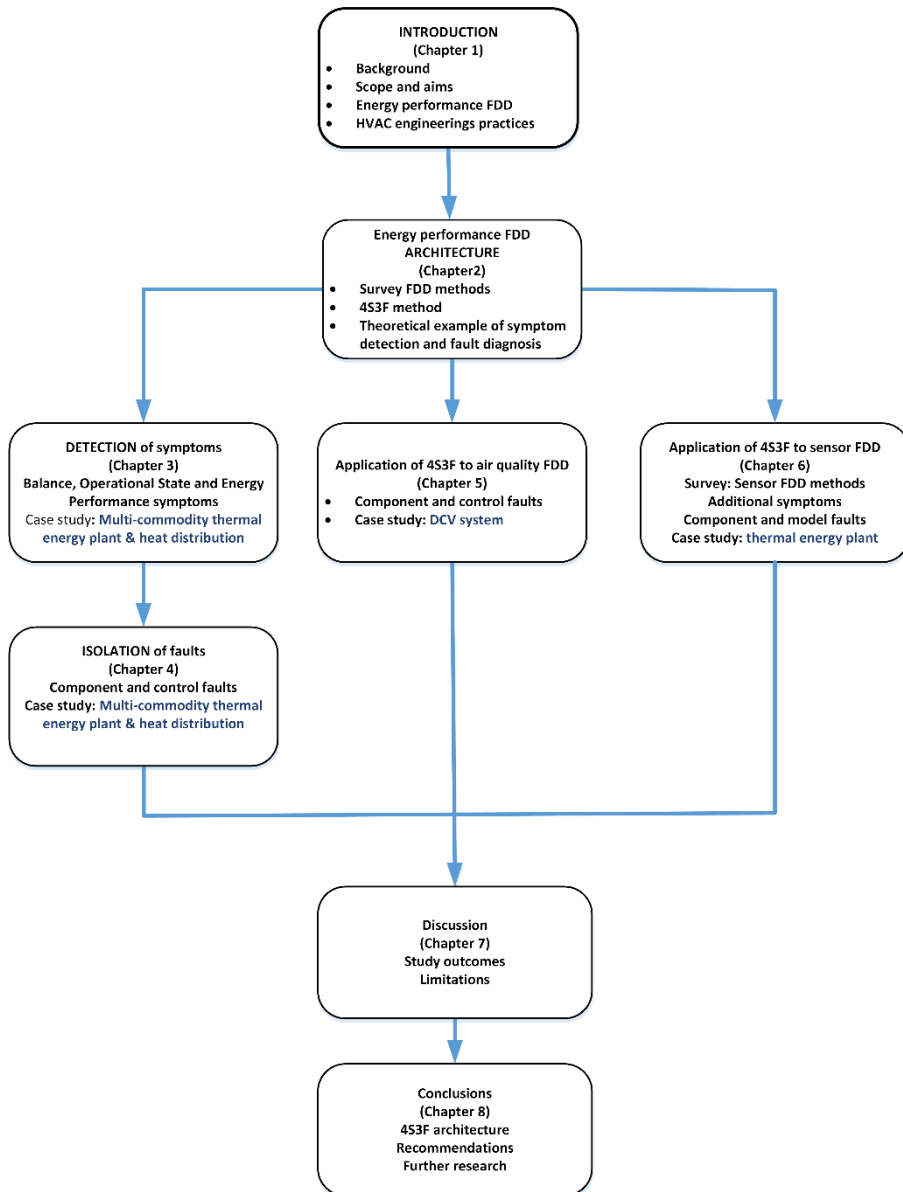


Figure 1.4 Schematic diagram of the thesis.

Summarized, the thesis outline is organized as follow:

- Chapter 1: Introduction
- Chapter 2: A reference architecture for the integration of automated energy performance fault diagnosis into HVAC systems: the 4S3F approach.
- Chapter 3: P&ID-based symptom detection for automated energy performance in HVAC systems: balance, operational state and energy performance symptoms.
- Chapter 4: Automated energy performance isolation for complex HVAC systems: Application of 4S3F diagnosis method on an ATEs system: component and control faults.
- Chapter 5: Effect of prior and conditional probabilities in the 4S3F diagnosis method: Application to IAQ control in DCV systems.
- Chapter 6: Fault Detection, Diagnosis and Correction for hard and soft sensors in Building Energy Management Systems: A new extension of the 4S3F framework: addition of model faults and additional symptoms.
- Chapter 7: Discussions and limitations.
- Chapter 8: Conclusions and recommendations.

References

- [1] IEA, World Energy Balances: Overview (2020). OECD/IEA, Paris. <https://www.iea.org/reports/world-energy-balances-overview#world>.
- [2] P. de Wilde, The gap between predicted and measured energy performance of buildings: A framework for investigation. Automation in Construction 41 (2014): 40-49. <https://doi.org/10.1016/j.autcon.2014.02.009>.
- [3] C. van Dronkelaar, M. Dowson, C. Spataru, D. Mumovic, A review of the Regulatory Energy Performance Gap and Its Underlying Causes in Non-domestic Buildings. Frontiers in Mechanical Engineering (2016): 1-17. <https://doi.org/10.3389/fmech.2015.00017>.
- [4] Energy performance of buildings. Directive 2010/31/EU (2020). The European Union. <http://data.europa.eu/eli/dir/2010/31/oj>.
- [5] W. Kim, S. Katipamula, A Review of Fault Detection and Diagnostics Methods for Building Systems. Science and Technology for the Built Environment, 24(1) (2017): 3-21, <https://doi.org/10.1080/23744731.2017.1318008>.

- [6] Boerstra, A. C. *Personal control over indoor climate in offices: impact on comfort, health and productivity*. PhD thesis (2016). Technische Universiteit Eindhoven.
- [7] N. Djuric, V. Novakovic, Review of possibilities and necessities for building lifetime commissioning, *Renewable and Sustainable Energy Reviews* 13 (2009): 486-492. <https://doi.org/10.1016/j.rser.2007.11.007>.
- [8] Technical Synthesis Report annex 34. Computer Aided Evaluation of HVAC System Performance (2006). IEA. www.ecbcs.org.
- [9] IEA ECBS Annex 40. Commissioning of Building HVAC Systems for Improving Energy Performance (2013). IEA. <http://www.buildup.eu/en/explore/links/iea-ecbcs-annex-40-commissioning-building-hvac-systems-improving-energy-performance> .
- [10] IEA ECBS Annex 47. Cost Effective Commissioning of Existing and Low Energy Buildings (2013). IEA. <https://www.buildup.eu/en/explore/links/iea-ecbcs-annex-47-cost-effective-commissioning-existing-and-low-energy-buildings>
- [11] H. Yoshino, T. Hong, N. Nord, IEA EBC annex 53: Total energy use in buildings— Analysis and evaluation methods. *Energy and Buildings* 152 (2017): 124-136. <https://doi.org/10.1016/j.enbuild.2017.07.038>.
- [12] Annex 58 Reliable Building Energy Performance Characterization Based on Full Scale Dynamic Measurements (2017). [EBC PSR Annex 58.pdf \(iea-ebc.org\)](http://www.iea-ebc.org/annex/58/PSR_Annex_58.pdf).
- [13] P. de Wilde, Building performance analysis (2018). John Wiley & Sons Ltd. ISBN 9781119341925.
- [14] Y. Zhao, T. Li, X. Zhang*, C. Zhang, Artificial intelligence-based fault detection and diagnosis methods for building energy systems: Advantages, challenges and the future, *Renewable and Sustainable Energy Reviews* 109 (2019): 85-101. <https://doi.org/10.1016/j.rser.2019.04.021>.
- [15] L. Haorong, Y. Daihong, J. Braun, A review of virtual sensing technology and application in building systems, *HVAC&R Research*, 17(5) (2011): 619-645, <https://www.tandfonline.com/doi/abs/10.1080/10789669.2011.573051>.
- [16] W. Chung. Review of building energy-use performance benchmarking methodologies. *Applied Energy* 88 (2011):1470-1479. <https://doi.org/10.1016/j.apenergy.2010.11.022>.
- [17] Y. Wei, X. Zhang, Y. Shi, L. Xia, S. Pan, J. Wu, M. Han, A review of data-driven approaches for prediction and classification of building energy consumption. *Renewable and Sustainable Energy Reviews* 82 (2018): 1027-1047. <https://doi.org/10.1016/j.rser.2017.09.108>.

- [18] E.H. Borgstein, R. Lamberts, J.L.M. Hensen, Evaluating energy performance in non-domestic buildings: A review. *Energy and Buildings* 128 (2016): 734-755. <https://doi.org/10.1016/j.enbuild.2016.07.018>.
- [19] Z. Li, Y. Han, P.Xu, Methods for benchmarking building energy consumption against its past or intended performance: An review. *Applied Energy* 124 (2014): 325-334. <https://doi.org/10.1016/j.apenergy.2014.03.020>.
- [20] EN 15316-1:2017. Energy performance of buildings - Method for calculation of system energy requirements and system efficiencies - Part 1: General and Energy performance expression, Module M3-1, M3-4, M3-9, M8-1, M8-4.
- [21] J. Liu, H. Chen, J. Liu, Z. Li, R. Huang, L. Xing, An Energy performance evaluation methodology for individual office building with dynamic energy benchmarks using limited information. *Applied Energy* 206 (2017): 193-205. <https://doi.org/10.1016/j.apenergy.2017.08.153>
- [22] BuildingEQ. <http://www.buildup.eu/en/practices/cases/building-eq-tools-and-methods-linking-epbd-and-continuous-commissioning> .
- [23] R. Hitchin, I. Knight, Daily energy consumption signatures and control charts for air-conditioned buildings. *Energy and Buildings* 112 (2016): 101-109. <https://doi.org/10.1016/j.enbuild.2015.11.059>.
- [24] L. Belussi, L. Danza, Method for the prediction of malfunctions of buildings through real energy consumption analysis: Holistic and multidisciplinary approach of Energy Signature. *Energy and Buildings* 55 (2012): 715-720. <https://doi.org/10.1016/j.enbuild.2012.09.003>.
- [25] H. Wang, P. Xu, X. Lu, D. Yuan, Methodology of comprehensive building energy performance diagnosis for large commercial buildings at multiple levels. *Applied Energy* 169 (2016): 14-27. <https://doi.org/10.1016/j.apenergy.2016.01.054>.
- [26] J. Cho, S. Shin, J. Kim, H. Hong, Development of an energy evaluation methodology to make multiple predictions of HVAC&R system energy demand for office buildings. *Energy and Buildings* 80 (2014): 169-183. <https://doi.org/10.1016/j.enbuild.2014.04.046>.
- [27] T. Maile, V. Bazjanac, M. Fisher, A method to compare simulated and measured data to assess building energy performance. *Building and Environment* 56 (2012): 241-251. <https://doi.org/10.1016/j.buildenv.2012.03.012>.
- [28] H. Wang, P. Xu, X. Lu, D. Yuan, Methodology of comprehensive building energy performance diagnosis for large commercial buildings at multiple levels. *Applied Energy* 169 (2016): 14-27. <https://doi.org/10.1016/j.apenergy.2016.01.054>.

- [29] S. Katipamula, M.R. Brambley, Methods for fault detection, diagnostics, and prognostics for building systems – A review, Part I. HVAC&R Research 11 (2005): 3-25. <https://doi.org/10.1080/10789669.2005.10391123>
- [30] S. Wang, J. Wang, Law-Based Sensor Fault Diagnosis and Validation for Building Air-Conditioning Systems. HVAC&R Research, 5:4 (1999): 353-380. <https://doi.org/10.1080/10789669.1999.10391243>
- [31] J. Schein, S.T. Bushby, A Hierarchical Rule-based Fault Detection Diagnostic Method for HVAC Systems, HVAC&R Research 12 (2006): 111-125. <https://doi.org/10.1080/10789669.2006.10391170>
- [32] Z. Du, B. Fan, X. Jin, J. Chi, Fault detection and diagnosis for buildings and HVAC systems using combined neural networks and subtractive clustering analysis, Building and Environment 73 (2014): 1-11, <https://doi.org/10.1016/j.buildenv.2013.11.021>.
- [33] W. Lee, J. House, N. Kyong, Subsystem level fault diagnosis of a building's air-handling unit using general regression neural networks, Applied energy 77 (2004): 153-170. [https://doi.org/10.1016/S0306-2619\(03\)00107-7](https://doi.org/10.1016/S0306-2619(03)00107-7).
- [34] K. Sun, G. Li, H. Chen, J. Liu, J. Li, W. Hu, A novel efficient SVM-based fault diagnosis method for multi-split air conditioning system's refrigerant charge fault amount, Applied Thermal Engineering 108 (2016): 989-998. <https://doi.org/10.1016/j.applthermaleng.2016.07.109>.
- [35] H. Han, B. Gu, J. Kang, Z. Li, Study on a hybrid SVM model for chiller FDD applications, Applied Thermal Engineering 31 (2011): 582-592. <https://doi.org/10.1016/j.applthermaleng.2010.10.021>.
- [36] J. Liang, R. Du, Model-based Fault Detection and Diagnosis of HVAC systems using Support Vector Machine method. International Journal of Refrigeration 30 (2007): 1104-1114. <http://dx.doi.org/10.1016/j.ijrefrig.2006.12.012>.
- [37] F. Xiao, S. Wang, X. Xu, G. Ge, An isolation enhanced PCA method with expert-based multivariate decoupling for sensor FDD in air-conditioning systems. Applied Thermal Engineering 29 (2009): 712-722. <https://doi.org/10.1016/j.applthermaleng.2008.03.046>
- [38] S. Wang, F. Xiao, AHU sensor fault diagnosis using principal component analysis method. Energy and Buildings 36 (2004): 147-160. <https://doi.org/10.1016/j.enbuild.2003.10.002>
- [39] J. Bynum, D. Claridge, J. Curtin, Development and testing of an Automated Building Commissioning Analysis Tool (ABCAT). Energy and Buildings 55 (2012): 607-617. <https://doi.org/10.1016/j.enbuild.2012.08.038>.

- [40] A. Beghi, R. Brignoli, L. Cecchinato, G. Menegazzo, M. Rampozzo, F. Simmini, Data-driven Fault Detection and Diagnosis for HVAC water chillers. *Control Engineering Practice* 53 (2016): 79-91. <https://doi.org/10.1016/j.conengprac.2016.04.018>
- [41] X. Zhao, Lab test of three fault detection and diagnostic methods' capability of diagnosing multiple simultaneous faults in chillers, *Energy and Buildings* 94 (2015): 43–51. <https://doi.org/10.1016/j.enbuild.2015.02.039>
- [42] Y. Yu, D. Woradachjurnoen, D. Yu, A review of fault detection and diagnosis methodologies on air-handling units, *Energy and Buildings* 82 (2014): 550-562. <https://doi.org/10.1016/j.enbuild.2014.06.042>
- [43] S. Wang, J. Wang, Law-Based Sensor Fault Diagnosis and Validation for Building Air-Conditioning Systems. *HVAC&R Research*, 5:4 (1999): 353-380. <http://dx.doi.org/10.1080/10789669.1999.10391243>
- [44] N. Kocyigit, Fault and sensor error diagnostic strategies for a vapor compression refrigeration system by using fuzzy inference systems and artificial neural network, *international journal of refrigeration* 50 (2015): 69-79. <https://doi.org/10.1016/j.ijrefrig.2014.10.017>
- [45] H. Wang, Y. Chen, C. Chan, J. Qin, A Robust Fault Detection and Diagnosis Strategy for Pressure-independent VAV Terminals of Real Office Buildings, *Energy and Buildings* 43 (2011): 1774-1783. <https://doi.org/10.1016/j.enbuild.2011.03.018>
- [46] H. Wang, Y. Chen, C. Chan, J. Qin, An online fault diagnosis tool of VAV terminals for building management and control systems, *Automation in Construction* 22 (2012): 203-211. <https://doi.org/10.1016/j.autcon.2011.06.018>
- [47] S. Wang, Q. Zhou, F. Xiao, A system-level fault detection and diagnosis strategy for HVAC systems involving sensor faults, *Energy and Buildings* 42 (2010): 477–490. <https://doi.org/10.1016/j.enbuild.2009.10.017>
- [48] D. Choiniere, DABOTM: A BEMS assisted on-going commissioning tool. *Proceedings of the National Conference on Building Commissioning* (2008).
- [49] F. Xiao, S. Wang, X. Xu, G. Ge, An isolation enhanced PCA method with expert-based multivariate decoupling for sensor FDD in air-conditioning systems, *Applied Thermal Engineering* 29 (2009): 712-722. <https://doi.org/10.1016/j.applthermaleng.2008.03.046>
- [50] F. Xiao, Y. Zhao, J. Wen, S. Wang, Bayesian network based FDD strategy for variable air volume terminals. *Automation in Construction* 41 (2014): 106-118. <https://doi.org/10.1016/j.autcon.2013.10.019>

- [51] Y. Zhao, J. Wen, F. Xiao, X. Yang, S. Wang, Diagnostic Bayesian networks for diagnosing air handling units faults – part I: Faults in dampers, fans, filters and sensors. *Applied Thermal Engineering* 111 (2017): 1272-1286. <https://doi.org/10.1016/j.applthermaleng.2015.09.121>
- [52] Y. Zhao, J. Wen, S. Wang, ‘Diagnostic Bayesian networks for diagnosing air handling units faults – Part II: Faults in coils and sensors,’ *Applied Thermal Engineering* 90 (2015): 145-157. <https://doi.org/10.1016/j.applthermaleng.2015.07.001>.
- [53] Y. Zhao, S. Wang, An intelligent chiller fault detection and diagnosis methodology using Bayesian belief network. *Energy and Buildings* 57 (2013): 278–288. <https://doi.org/10.1016/j.enbuild.2012.11.007>
- [54] ASHRAE Handbook, HVAC Systems and Equipment. American Society of Heating, Refrigerating and Air Conditioning Engineers (2012). ASHRAE.
- [55] Air-Conditioning System Design Manual, Second Edition (2007). ASHRAE Press.
- [56] Meetpunten en meetmethoden voor klimaatinstallaties (2014), ISSO-publicatie 31, Stichting ISSO, Rotterdam, The Netherlands.
- [57] Ontwerp van hydraulische schakelingen voor verwarmen (1998), ISSO-publicatie 44, Stichting ISSO, Rotterdam, The Netherlands.
- [58] Ontwerp van hydraulische schakelingen voor koelen (2005), ISSO-publicatie 47, Stichting ISSO, Rotterdam, The Netherlands.

2. A reference architecture for the integration of automated energy performance fault diagnosis into HVAC systems

This chapter has been published as:

Arie Taal, Laure Itard, Wim Zeiler, “A reference architecture for the integration of automated energy performance fault diagnosis into HVAC systems”, *Energy & Buildings* **179** (2018):144-155.

In this chapter, the 4S3F architecture is presented in which detection takes place with four types of symptoms (based on balance, energy performances, operational states, and additional information). Diagnosis of 3 types of faults (component, control, and model faults) is conducted with Bayesian statistics with DBNs (Diagnostic Bayesian Networks) in which faults and symptoms are linked together. In a DBN, posterior probabilities of faults are estimated from the results of the detection. The symptoms and faults can be extracted from HVAC P&IDs.

2.1.Introduction

Building energy management systems (BEMS) will become increasingly important, due to the increasing complexity of building services and the ongoing demand for high levels of indoor comfort and a healthy indoor environment, combined with stringent legal or agreed requirements regarding savings on operational energy use (e.g., the Energy Performance of Buildings Directive or EPBD [1] in Europe). Buildings account for 30%-40% of the total energy consumption of Western countries. Many studies have demonstrated that, in the operational phase, buildings actually use more energy than the amounts predicted by energy simulations during the design phase (de Wilde [2]). Dronkelaar et al. [3] estimate a performance gap of 34%. This gap is due in part to uncertainty in the modelling of energy calculations in the design phase, as well as to differences in occupant behaviour and changes in building use over time (e.g., changing room functions and building occupancy). Malfunction and degradation of components and control of heating, ventilation and air conditioning (HVAC) and lighting systems due to ageing also contribute to higher energy consumption (in some cases, 10%-20% higher than necessary). Mills [4] reports excess energy usage of 16% for existing buildings and 13% for new buildings. Despite the great focus on commissioning in the past decade, energy consumption is still higher than expected. Recently, Jing et al. [5] demonstrated that the cooling energy for 30 office buildings was on average 16% higher than designed due to

operational errors. Furthermore, HVAC and electrical installations are becoming more complex due to networks of energy conversion systems and storage – both local (in the building) and non-local (outside the building) – in addition to the distribution of the control of HVAC and lighting systems across centralised (e.g., at level of an Air Handling Unit), decentralised (e.g., at zone level) and end-user levels (e.g., at room level), which increases the probability of operational faults.

Despite examples of application in continuous commissioning (see Djuric [6] who presents a review on lifetime commissioning and Verhelst et al. [7]) and preventive maintenance for HVAC, automated energy performance diagnosis features are currently seldom applied in practice in building energy management systems (BEMS). These BEMSs are either stand-alone applications or are integrated as application within the building management system (BMS)³ itself.

At the same time, increasing amounts of data are being collected in buildings by building automation systems, due to decreases in the cost of sensors and to broader developments (the Internet of Things), which could support energy performance diagnosis further. In general, BMS can store up to millions of data points, only a very small portion of which is currently used, leaving a huge potential for energy savings untouched. To make these data useful at large scale, generic energy diagnosis methods are needed.

Energy performance diagnosis is usually limited to simple graphics (e.g., plots showing actual energy use and supply temperatures against outdoor temperatures). Although such graphics are valuable and although they can help in the initial diagnosis of HVAC malfunctions, the enormous potential of the data collected by the BMS has remained largely unexplored. The practical usability of energy diagnosis systems is further reduced by the necessity of having an expert to interpret thoroughly the graphics.

To be suitable for making automated diagnoses, a BEMS would have to identify energy waste, poor air quality or thermal discomfort, in addition to estimating the causes of such problems. Potential causes can be categorised as relating to faults in design, implementation, operations or maintenance (see [6, 8, 9]) and in hard and soft faults. Examples of hard faults are design faults including miscalculations of the capacity of components of the HVAC systems, incorrectly installed capacities that differ from the designed capacities and faulty connections between HVAC devices. Soft faults are errors in the control rules that have been designed and implementation faults which could include wrong settings in the control systems. Both types of faults

³ The BMS, also known as building automation system, generally stores monitoring data, regulates the control systems and is used as support for maintenance, safety, operational and facility management activities.

are known to pose serious problems in practice. Operational and maintenance faults include incorrect changes in HVAC control rules, room occupancies that are higher or lower than designed, unexpected occupancy behaviours, the ageing of components and all related faults (e.g., poor air quality, reduced efficiency, breakdowns). Operational faults also lead to sub-optimal operational energy performance (e.g., low efficiency of components, incorrect temperature or pressure levels resulting from control rules that are not suitable to the specific actual operational mode). Recent fault detection and diagnosis (FDD) case studies in Australia [10] showed that energy savings between 15 to 28 % are possible by implementation of HVAC FDD systems.

Despite all this, FDD tools are still not widely used. The main reasons for the absence of high-level automated diagnosis of a building's energy systems in practice are related to the complex and time-consuming nature of the tasks, which must be customised to each building as noted by Kim and Katipamula [11], who presented recently an overview of FDD methods for HVAC systems, and the absence of standards for modular diagnosis tools. Moreover, such a diagnostic tool is usually designed separately from the HVAC system and BMS, with no systematic integration with these systems. It is common that HVAC engineers use schematic HVAC diagrams to describe the HVAC system and its components (e.g., see [12,13]). These schematics are also used to describe the control systems. In BMS's these schematics are applied as user-interface.

In this article, we explore the possibility of linking the design of diagnostic tools to that of the HVAC and control systems based on the same system approach as used in HVAC schematic diagrams as a means of advancing and automating energy performance diagnosis features. Such integration could decrease the effort required to incorporate basic automated diagnosis features into the systems, as they are designed at the same time and by the same experts as the HVAC and control systems. We propose a reference architecture for energy performance fault detection and diagnosis (EP FDD), applicable for all types of HVAC systems. As indicated by the name itself, FDD methods always consist of two steps [6]: detection and diagnosis, in the same way that a doctor diagnoses a disease based on the symptoms he detects. First (observable) symptoms are detected, then the fault (disease) leading to these symptoms is diagnosed. The well-accepted term 'FDD' may be slightly confusing, as it seems that faults are detected first. In fact, it is not a fault that is detected, but a symptom. The diagnosis uses all detected symptoms to find out the fault⁴. Of course, in simple cases, symptoms and faults are identical (e.g., a sensor in frozen state is symptom and fault at the same time), but in most cases a single symptom (e.g., a too

⁴ In that sense, it would be more appropriate to use the term Symptom Detection and Fault Diagnosis (SDFD) instead of FDD. However, as FDD is a well-accepted term it will be used in this paper.

low efficiency of a heat pump) will need diagnostic work to find out the cause (the fault). In the reference architecture presented in this paper⁵, we propose a generic systematic approach of symptom detection (including existing methods). The fault diagnosis itself is based on diagnostic Bayesian networks (DBN) in which faults are diagnosed based on the occurrence or absence of simultaneous symptoms. Both the detection and diagnosis approaches are inspired by and remain very close to HVAC diagrams.

In the second section of this article, we address briefly fault detection and diagnosis methods for building energy performance and explain how HVAC system engineers work with HVAC schematics. Section 3 describes the proposed architecture for Energy Performance FDD and shows validations through a simulation experiment and results from a case study. In Section 4, we present conclusions about the architecture, followed by recommendations for the implementation of the proposed reference architecture.

2.2. Energy performance FDD and HVAC design

The International Energy Agency (IEA) established Annexes 34 [14], 40 [15], 47 [16], 53 [17] and 58 [18] as well on the subject of continuous commissioning, which focus on operational energy performance analysis (automated or non-automated) as well on energy diagnostic tools. In the EU, the implementation of the EPBD has also led to the development of prototypes for energy diagnostic tools [19,20].

Literature includes several FDD methods for HVAC systems. See [11,21,22,23,24,25], which present complete overviews of FDD methods relating to energy performance. FDD methods are commonly classified as quantitative model-based, qualitative model-based and process history-based [26,27]. Most of the quantitative model-based methods apply mathematical physical models, also called white box models, examples are presented in [8, 19, 20, 28, 29, 30]. The qualitative model-based methods look at the state of a system and its component. Most of them are rule-based and use if-then-else rules, see [31], based on expert rules and on measured operational states. In the process-history based methods, also referred as data-driven methods, historical BMS data is used to estimate trends, patterns and outliers. Patterns can be extracted from energy signatures ([18,32,33,34,35]) which consist of scatter diagrams and carpet plots for energy consumption and state values like supply temperatures. These data-drive methods may use also regression methods [30,34] and grey boxes [36] energy models in which the parameters are estimated by historical data. Other authors have used more abstract mathematical methods like principal component analysis (PCA) [37,38], artificial neural networks (ANN)

⁵ This research was founded by SIA (Taskforce for Applied Research), which is part of the Netherlands Organization for Scientific Research (NWO).

[39,40] and support vector machines (SVM) [41,42], especially to detect faults in components like sensors.

Despite the availability of methods, FDD tools are not commonly applied in practice, especially not when it comes to their application to energy performance diagnosis. A first reason for this is that the methods that have been developed are highly specific to components and systems, like certain types of sensors, chillers, air handling units, and variable volume systems, and this makes broad application and standardization difficult. Second, the construction of FDD models is very time consuming and HVAC engineers are therefore reluctant to build such a model. Third, in case of data-driven models it is very difficult to know the extent to which historical data represent correct operation. Fourth, none of the existing approaches can be easily expanded to accommodate novel energy systems (e.g., smart energy grids [43,44], in which energy generators, distribution systems and consumers are linked, thermally activated building systems [45], aquifer thermal energy systems (ATES) systems [46], adaptive facades [47]) or even new combination of components. Thousands of different combinations of components can be encountered in HVAC systems, therefore the development of FDD methods specific to one system should not be recommended. Fifth, different FDD methods are proposed for HVAC components, controls, indoor environment and energy performance and an integrated overall approach is clearly lacking. Sixth, generic automation of energy performance FDD has yet to be realized. In most cases only the monitoring of data through the BMS is automated, as well as the detection of some critical symptoms and energy experts are needed to diagnose the faults.

Finally, the above-mentioned energy-performance FDD methods have yet to be integrated into HVAC designs. A method that could be directly and easily implemented during the HVAC design process would offer several important advantages:

- It could become an integral part of the HVAC system and its control design activities. This would save money and avoid BEMS design faults.
- Control engineers are best able to determine which sensors are needed.
- HVAC engineers are best able to determine energy performance metrics and alarm thresholds.

The subject of this paper is therefore the development of a reference architecture for energy performance FDD which would incorporate on a systematic and organized way multiple symptom detection methods (based either on quantitative or qualitative models or on process history) and use one diagnosis method to determine the faults over all levels of an HVAC system, whatever the lay-out and components of this HVAC system may be.

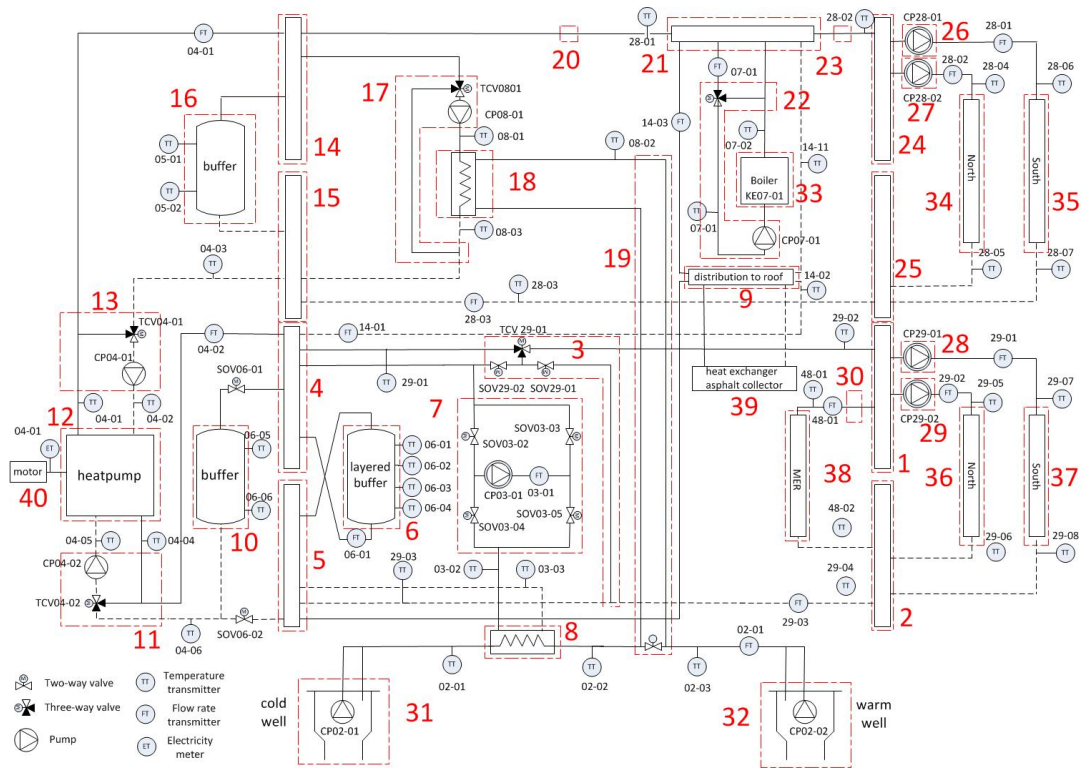


Figure 2.1. The (simplified) HVAC schematic diagram of the heat and cold generation system in the THUAS building.

In the design stage, HVAC designers always use system theory (whether consciously or unconsciously) to determine the specifications of the objects (components, sub-systems and systems) and their control. Designers create HVAC schematic diagrams that describe the functionality of the systems. In these HVAC schematics, the main HVAC and control components are represented by symbols connected by lines representing water, air or signal transfer.

In Figure 2.1, we present a simplified (e.g., the control systems are not depicted) example of an HVAC schematic diagram for the heat and cold generation in the building of The Hague University of Applied Science (THUAS) in Delft, which serves as the specific case for this study. Such systems have been common in non-domestic buildings built in the Netherlands in the past 15 years. All of the main sub-systems of the complete system are shown and numbered. The purpose of this diagram is to show the complexity of current HVAC systems due to the presence of many modular sub-systems, like heat pumps, boilers, heat exchangers, valves, pumps and sensors. All these components can be faulty, which results in very complex energy performance FDD systems. Such HVAC diagrams are used during the design phase to determine the capacities, dimensions and controls of the components according to energy, mass and pressure balances. During the operational phase, experts use the same diagrams (which are usually presented in the user interface of the BMS) to diagnose faults in the system. The solid lines in Figure 2.1 depict supply pipes and the dashed ones return pipes. The diagram contains a boiler (33), a heat pump (12) and an ATES system (components 7, 8, 17, 18, 19, 31 and 32). The cold-water system (28, 29, 30, 36, 37 and 38) used to distribute cold in the building and the hot water system (26, 27, 34 and 35) used to distribute heat can be seen on the right part of the diagram. The diagram contains sensors for flux (noted in this figure as FT) and temperature (noted in this figure as TT). These diagrams can be based on national or international standards. For example, national standards are available in the Netherlands by ISSO 44 and 47 [48,49] and in Norway by NS 3451, noted by Djuric and Novakovic in [50], which can be used for constructing generation, distribution, node (headers and buffers) and emitter systems (in-room terminal systems) as presented in draft prEN 15603:2013 [51]. Guidelines are also available for the measurement points for energy monitoring (e.g., [52,53]).

None of the existing frameworks for constructing energy-performance diagnoses indicated in literature overviews are consistent with (or based on) approaches to design and operations that are based on the modularity present in HVAC diagrams. As demonstrated in the following discussion, such an approach is promising, not only because it is better suited to the thinking processes of energy and HVAC experts and to the design of the system to be diagnosed, but also because it makes it possible to overcome the following main problems which are addressed in detail in Section 2.3.

- Energy diagnosis at the level of modular sub-systems and systems as a whole is far from being fully automated.
- No standardised generic diagnostic tools are available yet.
- There is no open framework based on a reference architecture within which detection methods can easily be adapted, extended, or replaced.
- Unreliable sensor data leads to unreliable or faulty diagnoses.
- Implementation is costly.

2.3. Proposed reference architecture for automated energy performance diagnosis

In this section a reference architecture for automated energy performance diagnosis is proposed which would overcome the problems mentioned in section 2. In this architecture a strong distinction is made between the detection and diagnosis stages. In the detection phase multiple methods can be applied to estimate symptoms and in the diagnosis phase one method is applied, which identifies the faults that lead to the detected symptoms. In the same way that a doctor diagnoses the probability of a disease based on detected symptoms, energy waste in a building can be diagnosed according to energy-related symptoms that have been detected. Diagnoses can be applied simultaneously at the level of individual components (analogous to a diagnosis at the level of individual organs) and of entire buildings or HVAC systems (analogous to the holistic approach of a doctor asking about fever, fatigue or nutritional patterns). In medical diagnoses, the presence and absence of symptoms are used simultaneously to estimate the probabilities of a specific disease. Symptoms can be estimated using a variety of detection methods. For example, in the medical world, a diagnosis might be based on blood and urine tests, in addition to the observation of physical and mental phenomena.

Like the human body, HVAC systems consist of sub-systems that work together simultaneously. In both cases, diagnoses must be based on the simultaneous analysis of various sub-systems and aggregated systems, which are connected by components that transport energy, mass and information. This is the foundation of system theory. The input of an energy system affects its output in a known way: the laws of conservation of energy, mass and pressure. It would therefore be logical to use mass, energy and pressure systematically as a foundation for diagnosis. For energy, the law of conservation is the first law of thermodynamics and for pressure, it is Bernoulli's law. Although Wang and Wang [54] have applied energy balances to correct biased faults in sensors of a chilling plant, it has never been applied on a systematic way for HVAC systems and sub-systems. In the next sections we will show how the laws of conservations can be used to generically detect symptoms, and how they can be complemented with three other types of symptoms. In Section 2.3.1 symptom detection in the reference architecture is described followed by the diagnosis in

Section 2.3.2. Section 2.3.3 is about simultaneous multi-level detection and diagnosis. Next, in Section 2.3.4 the reference architecture is demonstrated in a virtual (simulation) experiment, followed in Section 2.3.5 by results with actual data over a period of 28 days. Finally, the sensitivity of the method to the number of sensors and to prior probabilities in the DBN models is discussed in Section 2.3.6.

2.3.1. Detection of symptoms

In FDD methods for energy performance, several symptom detection methods are encountered. In quantitative model-based methods detection is made by comparing actual energy performances with simulated ones ([21,54]). In rule-based methods by using the operational state of systems, components and controls, see e.g., [26,27]. In data-driven detection methods by tracking deviations from supposedly correct operational patterns. Sometimes additional information based on maintenance and inspection data is used too [31]. Because many symptoms are encountered, we propose to classify them into four categories that will be explained in detail hereafter. These four categories are based on our observations how HVAC experts carry out energy diagnostic in practice. We further link these four categories to the theoretical approaches found in literature.

1. Balance symptoms: based on balance deviations. This is a quantitative model-based approach, based on system theory. However, it does not use complex white box models, but just balance equations.
2. Energy Performance (EP) symptoms: based on deviations in energy performance metrics. Both quantitative and qualitative model-based approaches can be applied here (see explanations further in this section).
3. Operational state (OS) symptoms: based on deviations in the operational state from the expected state. This is either a qualitative model-based approach or a data-driven approach, in which historical data can be used to estimate outliers.
4. Additional symptoms: based on additional information. This may be based on historical data or on maintenance or inspection data, but also on the results from a specific FDD method included in a component by the producer.

The first type of symptoms is generic, while the last is generally system specific. Although second and third types are generic, their set values are not. They are explained in further details hereafter.

Balance deviation, which is directly linked to laws of mass, energy and pressure conservation and system theory, forms the foundation for the detection of symptoms. To estimate the balances, quantitative (thermodynamic) models are used. However, opposite to most models found in literature, these models are very simple. If the

timespan used for energy calculation is large enough to eliminate transient effects, these models are reduced to the fact that the sum of the inputs to a system or subsystem should be equal to the sum of the outputs. As all systems and sub-systems are described in the HVAC schematic diagrams, it is easy to describe the balances simultaneously with HVAC systems and to implement them in the BEMS simultaneously with the HVAC control system.

An example of heat and work exchanges between (aggregated) systems based on Figure 2.1 is presented in Figure 2.2. In this figure the systems 1 to 39 are shown in red for 8 aggregated systems. Heat amounts between systems can be calculated from temperatures and flow rates at the in- and outlet sides of each system

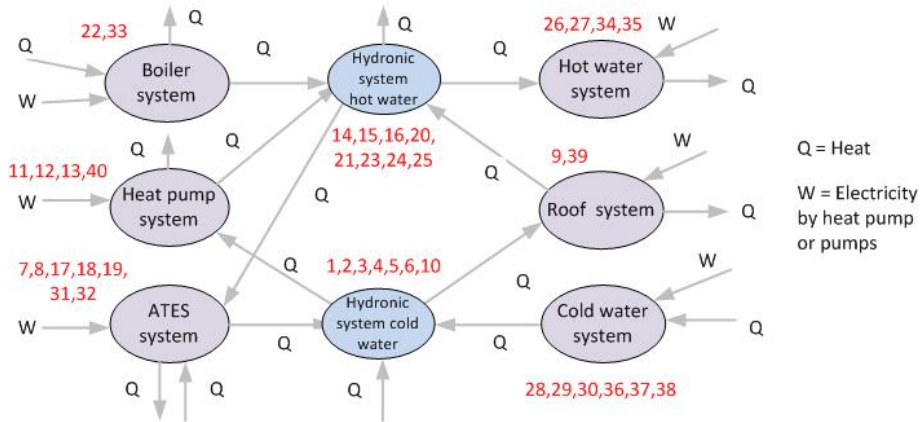


Figure 2.2. Energy exchange based on Figure 2.1.

Similarly, EP deviations offer a generic way of detecting symptoms, by comparing the performance of specific components relative to product specifications and the performance of systems to simulation results, benchmark values or guidelines. Examples include comparing efficiencies (the efficiency of a heat exchanger) and performance factors of components to product specifications (e.g., the coefficient of performance (COP) of a heat pump) or the yearly energy consumption to a benchmark. Energy performance metrics based on seasonal values can be used, and also shorter times can be applied (day, hour etc.). The level of detail of the EP metrics is not fixed in the reference architecture. Depending on aims and costs benchmark metrics can be used or results from simulation models. The EP symptoms can be estimated by a mix of quantitative models (if the actual EP has to be calculated, as is often the case with the COP value) and qualitative models (comparison with expected values).

Further, OS deviations emerge from the comparison between measured state values (e.g., a supply temperature or energy signatures) and their control set points. These

symptoms can be detected by the use of qualitative models and history-based regression models.

Additional information can further enhance the diagnosis. This additional information can contain results of specific component FDD methods already integrated in components by suppliers. With regard to monitoring faults, additional information may include the maintenance state of sensors. With regard to energy performance, it could include maintenance and inspection information on components (to rule out the presence of faults in these components) or historical data trends (e.g., decrease of COPs of systems over the years due to ageing). Such additional information is relatively specific to systems or buildings, however, and it is likely to be more cumbersome to implement.

2.3.2. Diagnosis

Diagnoses by HVAC experts are usually based on a probabilistic approach, starting from the most visible symptoms and being further refined by determining which other symptoms are present or absent. DBN diagnoses offer a promising solution in this area, as they are based on processes that are similar to the operational methods of HVAC experts. DBN draws upon a Bayesian statistical approach, which closely resembles system theory and in which the probability of faults is calculated according to the occurrence of symptoms. The outputs of the DBN are not Booleans but can take all possible values between 0 and 100 %, which can help to reduce Type I and II errors. Symptoms and faults can be represented in a network model (the DBN), which has been applied in the field of healthcare (see e.g., [55,56]). Although it has also been applied in the context of fault detection in HVAC components and systems [57-60], it has yet to be applied at the level of entire HVAC systems or for purposes of energy performance diagnosis. In addition, DBN is well suited to coping with simultaneous symptoms and indeterminate information. Moreover, as noted by Zhao [58], DBN even generates outcomes when conflicting symptoms are detected. Most of the faults referred to in literature are specified by type of HVAC component⁶ and control (e.g., chiller, air handling units and control of supply temperature) and aspect (e.g., fouling of a heat exchanger, biased or frozen sensor). However, our experience is that faults in data pre-processing and in the models used for FDD models occur often as well. All these faults can be divided into three general categories:

1. Component faults: installation or design of too low or too high capacities; fouling and degradation of components due to ageing and failure. Sensors

⁶ Here we define a component as a component, sub-system or system in which energy is exchanged or transformed.

are considered as components as well. These component faults are also referred to as hard faults in literature [6].

2. Control faults: incorrect set-points for controllers, timer settings, on-off control of components, software faults.
3. Model faults: faults in the quantitative models that are used to estimate missing and derived measurements or parameters. Both control faults and model faults are also referred to as soft faults in literature [6].

The relationship between the four types of symptoms and three types of faults is depicted in Figure 2.3 and explained further below. These relationship diagrams can be used directly and very easily to construct a DBN, as will be shown in Section 2.3.4.

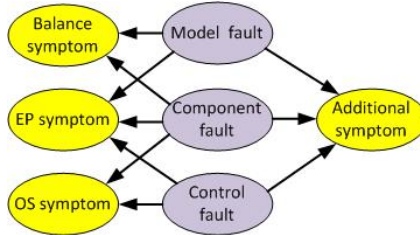


Figure 2.3. Relationship between types of symptoms and faults.
(EP: Energy Performance; OS: Operational State)

As shown in the figure, there are a multiple relationship between symptoms and faults. A model fault cannot, by nature, cause an OS symptom (an OS is measured by essence and is not the result of a calculation), however it can impact both balance and EP symptoms. A given component fault can lead to balance symptom (e.g., forthcoming from a sensor fault), EP symptom (e.g., forthcoming from the degradation of a generator), OS symptoms (e.g., failure to obtain the supply temperature due to low heat-pump capacity) and additional symptoms (e.g., breakdown of a pump). In the same way, control faults can lead to OS and EP symptoms, but will never affect balance symptoms.

An HVAC system like the one of Figure 2.1 consists of commercial HVAC products consisting in turn of components and sub-components that can be faulty. For example, a heat pump consists of an evaporator, a compressor, an electromotor, a condenser, an expansion valve, sensors and a control system. Our reference architecture focuses on the main components of the HVAC system as bought from suppliers (e.g., heat pump, distribution pumps, boilers and heat exchangers) and do not take into account their sub-components. We assume that producers of HVAC components will eventually deliver their own FDD methods for estimating faults in their sub-systems (whether now or in the future). We therefore propose an architecture that helps to estimate faults in trade components but that does not go inside these components. However, the architecture supports the integration of results

of external FDD methods as additional symptoms, which makes this architecture generic and expandable during the service life of the equipment.

2.3.3. Simultaneous multi-level diagnosis

Some methods (see references in section 2.2) propose a hierarchical multi-level approach. In the top-down approach, the energy performance analysis starts at the level of the building as a whole, proceeding to the investigation of lower levels only if symptoms are detected in the initial diagnosis. One important disadvantage of the top-down approach is that it may fail to reveal faults at lower levels (e.g., in components or control systems), thus making it impossible to optimise energy consumption. Also, a decision tree is needed to analyse the correct subsystems. On the other hand, a bottom-up approach could lead to time-consuming diagnosis and correction analysis of sub-systems, yielding only marginal energy savings at the whole-building level. Furthermore, because energy analyses are performed separately at different levels without any integration between levels, any diagnosis produced in this way remain uncertain and difficult to interpret, due to the indeterminate character of the fault isolation (see further in this section).

We therefore propose an integral approach that diagnoses faults through simultaneous diagnosis on multi-levels. The system as a whole can be divided into sub-systems (see Figure 2.2), which also contain sub-systems (e.g., the numbered sub-systems displayed in the HVAC diagram in Figure 2.1, other subsystems, more or less aggregated are possible too). Note that all these systems and sub-systems can contain control systems, which are not shown here. For example, a heat pump has its own control system (for safety purposes), and it can contain an embedded control for supply temperature, which in turn involves the evaporator and condenser modules. Higher-level controls can also be connected by lower-level sensors and actuators. For example, the heat pump can be switched on and off by a time schedule at the level of the HVAC system.

Symptom detection takes place simultaneously at the level of aggregated systems and at the level of the sub-systems. In this approach, the problem of fault isolation is not as indeterminate as in a top-down or bottom-up approach, given the availability of more equations and the attainment of a certain level of redundancy. In the following discussion, this approach is explained according to a simple generic example in which sensor faults in a thermal system consisting of two connected systems (see Figure 2.4) must be isolated. Input and output of thermal energy can be calculated from data produced by two temperature sensors and one flow sensor. Considering a large enough time period, for instance one day, a steady-state model can be applied to detect energy balance symptoms. The connection between the systems makes it possible to consider three systems in the analysis: A, B and the aggregated system C. If only system A is considered, six sensor faults are possible, while only two balance equations (one for energy, one for mass), therefore two symptoms, are present. The

degree of indeterminacy of the diagnose is 4. If the neighbouring system (B) and the aggregated system (C) are also taken into account (see Figure 2.2), nine sensor faults are possible, while six balance equations are available (three energy balances and three mass balances, therefore 6 symptoms). The diagnosis is therefore less indeterminate, as the degree of indeterminacy decreases to 3. The more sub-systems and aggregated systems are used, the more determined the diagnosis will be. When OS and EP symptoms are considered according to state values for different operating modes of the HVAC system – as when the system is off (e.g., the inlet water temperature has to be equal to the outlet water temperature) and additional symptoms (e.g., the water flow is zero when a pump is off) are added – the number of equations increases, and faults can be identified almost exactly.

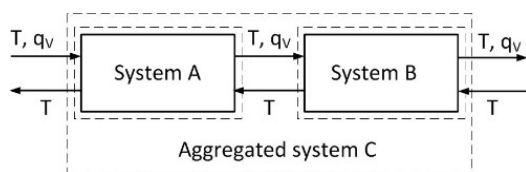


Figure 2.4. An aggregated system consisting of two sub-systems.

2.3.4. Application of the reference architecture on an HVAC system

The proposed reference architecture is applied below for a relatively simple part of the THUAS HVAC system, in order to demonstrate how to construct a DBN model based on the HVAC schematic diagram. We use the HVAC diagram of the heat-pump system (see Figure 2.5), which consists of systems 11, 12, 13 and 40 in Figure 2.1, aggregated to the ‘Heat pump system’ in Figure 2.6. A heat pump is a thermodynamic machine that upgrades thermal energy from low to high temperature levels. Heat from a heat source is delivered to the evaporator of the heat pump, while the pump’s condenser supplies this heat to the heat distribution part of the HVAC system at a higher temperature. The heat pump is powered by a compressor. The HVAC diagram of the heat-pump system is depicted with its two control systems, which are located on the evaporator and condenser sides of the heat pump (see Figure 2.5). The heat pump and pumps CP1 and CP2 are switched on when heat is needed. The inlet hot water is a mixture of the return hot water (which is measured with the temperature sensor TT4) and the outlet hot water from the condenser (hot-water supply). The temperature of the hot-water supply, which is measured by the temperature sensor TT3, is set by the controller TC2, which actuates the position of the three-way valve TCV2. Once the valve is open, the pump CP2 is activated, and the heat pump starts. In the same way, TC1 controls the temperature of the cold-water supply with the valve TCV1. The temperature sensors TT4 and TT1, and the flow sensors FT1 and FT2 are installed for monitoring purposes.

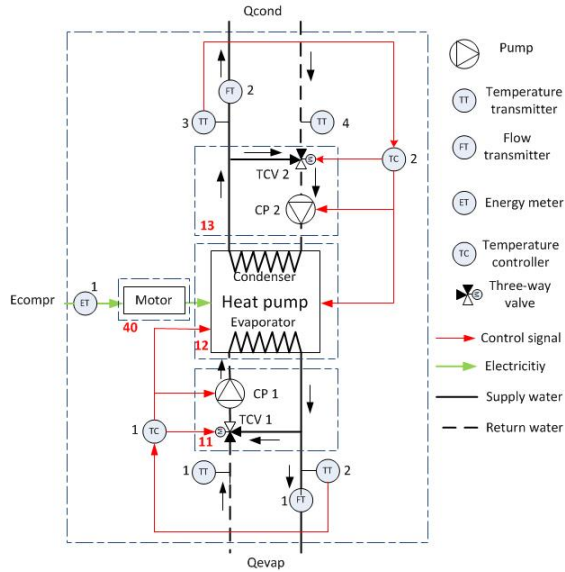


Figure 2.5. HVAC schematic diagram of a heat pump system

Figure 2.6 shows also the heat pump system as a black box. The heat exchanged towards other coupled systems are Q_{cond} and Q_{evap} which are calculated from flow rate and temperature sensors.

Given the generic character of such a water-to-water heat-pump system, once it has been translated into a DBN model, it can be used in many other HVAC systems. A library of such generic models could therefore be constructed.

In this example, we focus on symptoms of types 1 to 3 (Balance, EP and OS, see Section 2.3.1), as they are generic.

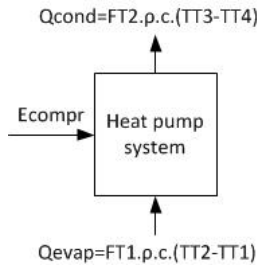


Figure 2.6 Black box model of a heat pump system

- The energy balance on the total heat-pump system A is non-zero (balance symptom). This is the only possible balance symptom as it is impossible to make balances on systems 11,12,13,40, as they are not equipped with the sensors needed to make such a balance.

- The actual COP of the heat pump (System 12) is lower than the COP specified by the heat-pump producer (EP symptom). No other Energy Performance symptoms can be determined as the only specifications found in the suppliers' documentation is the COP of the heat pump.
- The temperature of the hot-water supply from System 13 on the condenser side (TT3) differs from specifications (e.g., too high; OS symptom).
- The temperature of the cold-water supply from System 11 at the outlet of the evaporator (TT2) differs from specifications (e.g., too low; OS symptom). These two values (TT2 and TT3) are the only ones being controlled, so no other operational symptoms can be determined.

Note that in case more data would be available, additional symptoms could be added, like an additional EP symptom if benchmark values for heat pumps are known, additional symptoms (type 4) in case time series of COP values in past years are known or OS symptoms if the specific values of FT2 or FT1 are indicated in the commissioning documents. For the following analysis, we consider only the four symptoms described above.

If one or more of these symptoms is observed, the fault(s) leading to these symptoms has to be determined. All three types of possible faults (see Section 2.3.2) can be encountered, leading to 15 possible faults (each control, component and sensor described in Figure 2.4 can be faulty, as well as each model; the possible faults arise in fact from a simple inventory of these controls, components, sensors and models).

- Two control faults for the water outlet temperature of the condenser and evaporator (there are only two controllers TC2 and TC1).
- Twelve component faults: seven sensor faults, a heat-pump fault, two pump faults (CP1 and CP2) and two valve faults (TCV1 and TCV2).
- One model fault for the heat balance of the heat-pump system (this is the only model used).

Based on system theory (as represented in the HVAC diagram presented in Figure 2.5 and on the descriptions above), the corresponding generic DBN for the heat pump is depicted in Figure 2.7. We refer to [58,59] for further detailed explanation on the working of DBNs, as describing DBN's is not the purpose of this paper. Note however, that the DBN of Figure 2.7 can be easily constructed and understood when looking at Figure 2.5.

The four possible symptoms that can be observed in the detection layer are presented in yellow. The blue nodes are related to Qevap and Qcond which have values that must be calculated from the sensor data. For example, the energy of the compressor and the amounts of heat exchanged in the condenser and evaporator must be calculated from the BMS data (using the volume flow and two temperatures) before

the heat pump's COP can be calculated, or before the balance in the heat pump can be established. Note that in Figure 2.7, we have aggregated faults in TC2, TCV2 and CP2 in one fault node 'Control Thw' (idem 'Control Tcw' for TC1, TCV1 and CP1), as these three faults would lead to the exact same symptoms and cannot be differentiated, therefore. Differentiation would only be possible if an additional OS symptom on FT2 would exist. As this is not the case (no set point value is known in this specific case), differentiation is not possible yet.

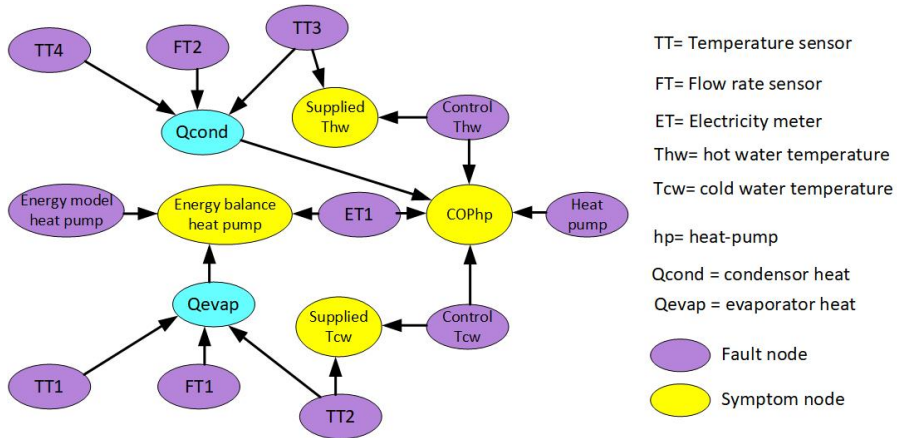


Figure 2.7. A generic DBN model for a water-to-water heat-pump system and its control system.

All possible faults (i.e., faults that could lead to specific symptoms) are presented in purple. Their number is limited to 15, the approach is generic, and it can be applied to almost all kinds of heat pump systems.

For example, consider the possible symptom 'too low COP of heat pump' (indicated as *COPhp* in Figure 2.7), which is obtained through comparison of actual COP values to the heat-pump specifications. As indicated in the DBN there are six direct causes that can lead to the occurrence of this symptom: a malfunctioning heat pump, the (calculated) evaporator heat, the (calculated) condenser heat, the measured compressor work ET1 (this meter measures the heat pump's electricity usage E_{compr}) or incorrect control of the supplied hot or cold-water temperatures (or a broken valve or pump). If the problem is in 'Control Thw' it would probably also cause a symptom in the measured temperature of the hot-water supply. The term 'probably' is used, as one cannot be 100% certain that this will occur, given the possibility that the error in the hot-water system could be compensated by a fault in sensor TT3. The occurrence of the two symptoms '*COPhp*' and 'Supplied hot water

temperature' would therefore indicate that a fault in 'Control Thw' is more likely to be the cause of the observed symptoms.

The symptom 'energy balance heat-pump' can be affected only by faults in the (calculated) condenser heat and the (calculated) evaporator heat (therefore by faults in TT1, FT2, TT3, TT1, FT1 or TT2), as well as by a fault in the electricity meter ET1, or a fault in the heat pump's energy model (e.g., due to the neglect of heat losses). The combination of the symptoms 'energy balance heat pump' and 'COPhp' would reduce strongly the number of possible faults as this symptom combination could be caused only by a problem in the calculated condenser heat (Q_{cond})⁷.

A problem in the condenser heat (Q_{cond}) can be due to incorrectly measured values of TT3, TT4 or FT2 by faulty sensors. In that case, the present symptom of low COP could be false, as the problem is caused by a biased sensor, while the COP is actually correct but measured incorrectly. In this way, FDD of components (including sensors), controls and energy performance are completely integrated with each other. Generic DBN models can be constructed easily for all kinds of HVAC systems, and they can consist of DBN sub-models for energy generation, distribution and emitter systems. The development of an open library of such standard models (like we did for the heat pump) would help HVAC and control engineers to build quickly a whole HVAC DBN model, by assembling the basic models.

2.3.5. Virtual simulation experiment with two symptoms detected

The reference architecture applied on the heat pump system of Figure 2.5 with usage of the DBN model shown in Figure 2.7 was first tested using a simulation experiment. In DBN two kind of nodes, parent and child nodes, are distinguished. Parent nodes have so called prior probabilities for states which are independent of other nodes while child nodes have conditional probabilities depending on the state of parent nodes and other child nodes. In the proposed DBN for energy performance diagnosis, fault nodes (purple in Figure 2.7) are parent nodes, while symptoms (yellow in Figure 2.7) are child nodes (see e.g., [58]). For the sake of simplicity, we distinguish in this paper only two events for the parent nodes: true (there is no fault) or false (there is a fault), and we assign to the parent nodes prior probabilities of 95% and 5% for the true and false states (for a discussion on the sensitivity of the results to these choices, see Section 2.3.7). In other words, all fault nodes (purple) have a probability of 5% to be faulty and we do not consider the possibilities of parent nodes being 'a bit faulty'. Also, for purposes of simplification, we assume that, if a parent node is false, the conditional probability that the child nodes will be false is 95%. It is therefore possible that a symptom will be absent despite the presence of a fault, given that faults

⁷ Neglecting here for the sake of demonstration the fact that both faults could appear simultaneously while not being caused by a common fault (e.g., this could happen in the case where TC2 and TT4 are both faulty)

can compensate each other. The DBN model depicted in Figure 2.7 with the aforementioned probabilities has been implemented in GeNie [61], a DBN software application.

In fault diagnosis, false probabilities of all fault nodes are estimated simultaneously according to the observed occurrence or absence of symptoms. In our virtual simulation experiment, we assume two symptoms are detected: the COP of the heat pump is low (EP symptom) and the condenser outlet temperature is too high (OS symptom). No other symptoms are detected. These two symptoms are fed into the DBN model, which yields the fault probabilities for the control of the hot-water supply temperature ‘Control Thw’ (or broken valve TCV2 or broken pump CV2, see previous section) (98%), for the heat pump (5%) and for sensor TT3 (3%). The other fault nodes indicate no fault probability. As expected in this simple experiment, the DBN shows clearly that the low COP has been caused by the control of the supply hot-water temperature ‘Control Thw’. Similar experiments were conducted with other possible combinations of symptoms, leading to the determination of the expected faults. This experiment shows a correct fault diagnosis despite the strong simplifications made for the values of the prior and conditional probabilities.

2.3.6. Application to the heat pump system in THUAS building

The reference architecture has been tested on the HVAC system shown in Figure 2.1 for 28 days in November and December 2013. Actual 4-minutes data from the BMS was available. The results for the heat pump system of Figure 2.5 are presented below. Daily balances were set up for systems 11, 12 and 13 (see Figure 2.5). This was possible because, opposite to what was done in Section 2.3.4, all systems connected to the heat pump system (see Figure 2.1) were taken into account. For energy performance symptoms daily heat pump COPs for heating and cooling were considered. When the absolute deviation between measured value and specified EP value is higher than 5 %, a symptom is detected. Considering OS symptoms, daily temperature values when the system is off (on Sundays only) were taken into account. When the system is off, TT04-06, TT04-04 and TT04-05 should be equal, as well as TT04-03, TT04-01 and TT04-02. As threshold value, we considered that the temperature difference should be lower than 0.4 K.

The detection process during these 28 days resulted in balance symptoms, energy performance symptoms and operational state symptoms as summarized in Table 2.1. Next, these symptoms were fed to the DBN model. In this model prior probabilities were set to 95 % and conditional probabilities to 98 %. The diagnosis was carried out daily and resulted in a fault probability for the sensor TT04-04 varying between 60 and 100 % during the considered 28 days. The fault probabilities for sensors TT04-05 and TT04-05 varied between 0 and 40 % during the same period. Checks in the system showed that TT04-04 was wrongly placed.

Table 2.1. Symptoms detected during the 28-days measurement period

| Detected symptom | Symptom type | Additional Explanation |
|---------------------------------------|--------------------|--|
| <i>Balance system 11 wrong</i> | Balance | System 11: Evaporator group heat pump |
| <i>Balance system 12 wrong</i> | Balance | System 12: Heat pump |
| <i>COP_{cooling} too high</i> | Energy Performance | COP _{cooling} is defined as heat to evaporator of the heat pump divided by compressor work. According to the specifications this COP should be lower than 3.5 |
| <i>Deviation TT04-04–TT04-05</i> | Operational state | Deviation water temperatures in evaporator group. See Figure 2.2 for these sensors (deviation higher than 0.4 K). |
| <i>Deviation TT04-04–TT04-06.</i> | Operational state | Deviation water temperatures in evaporator group. See Figure 2.2 for these sensors (deviation higher than 0.4 K). |

Because the fault probabilities of sensor TT04-04 are much higher than those for TT04-05 and TT04-06 and occurred all days of the measurement period, we proposed an automated bias correction for sensor TT04-04. From the expected operational states (values of TT04-06 and TT04-05 on Sundays) we estimated the bias to be 1.2 K. After correction of the BMS value data for TT04-04 with this bias, we have applied the symptom detection and fault diagnosis process all over again. Not a single symptom was detected, showing this way the possibility for automated correction of biases.

2.3.7. Influence of the number of sensors and probability values of the nodes in the DBN

The DBN model can easily be extended with symptoms and faults if needed for specific systems. Another advantage of these DBNs is that the diagnosis generates results even if few symptoms are present. In our simulation experiment (Section 2.3.5), if the supply temperatures TT1 and TT3 had not been measured (as commonly occurs in practice), the heat pump, ‘*Control Thw*’ and ‘*Control Tcw*’ would have had a fault probability of 35.1%. All other fault properties would have been less than or equal to 1%. Despite the fact that the diagnosis would not have detected unambiguously a fault in the heat pump, ‘*Control Thw*’ or ‘*Control Tcw*’, the model converges at least to these three possible faults. Thus, also when few sensors are available, which can be the case for older HVAC systems, the reference architecture is valuable.

In the literature (see [11]), the estimation of the prior and conditional probabilities has been identified as a disadvantage of DBN. To our view, the exact value of the diagnosis outcomes in our framework is not as relevant to the diagnosis as are the relative probabilities of the various faults. As demonstrated in this experiment, precise probability values are not needed in order to isolate faults. This was also

shown in the case study in Section 2.3.7. Furthermore, we have conducted the diagnosis several times with differing prior probabilities varying between 80 and 98% in different combinations. In all cases it led to the identification of TT04-04 as being the fault.

2.4. Conclusions and recommendations

In this article, we propose a reference architecture integrating energy diagnosis and FDD systems into a single framework, remaining very close to HVAC diagrams and the manner in which HVAC systems and their associated control systems are designed. It has been constructed by analogy with how HVAC experts carry out diagnostics. In this architecture detection of symptoms and diagnosis of faults finds place separately.

In the first stage, symptom detection, four types of symptoms are used: balance, energy performance, operational state and additional symptoms. The first three types are generic (although the set point values of EP and OS symptoms are case specific) and the complete list of the possible symptoms can easily be described at the same time and by the same engineers constructing the HVAC diagrams and their control systems.

In the second stage, the diagnosis itself, three possible types of faults, model, component and control faults are identified. Here again, a complete list of possible faults can easily be obtained by listing all components, controls and models in the HVAC diagram. All possible symptoms and faults are then connected to each other in a DBN model following closely the connections between systems and the measurement points as indicated in the HVAC diagram. The DBN model is then fed with the detected symptoms and estimates automatically the fault probabilities which lead to the observed symptoms. The diagnose takes place simultaneously through all levels of the system. This architecture is summarised in Figure 2.8.

One of the strengths of this reference architecture is that specific already existing methods for symptom detection, like quantitative, qualitative and data-driven methods can be used to search for deviations in EP, OS and additional symptoms.

In the design phase, next to the generic balance symptoms, simple rules for the identification of OS and EP symptoms can be used (like comparison with product specification), while, in a later stage, more complex methods can be introduced if needed. Because the approach is generic and systematic, the method can be applied to almost all HVAC systems.

By developing a library of detection models and DBN models for sub-components (in this paper we showed a generic model for a heat pump) the implementation of an energy performance FDD system during the HVAC design will be fastened. Because the DBN model consists of systems and sub-systems with the same four types of

symptoms and three types of faults a simultaneous multi-level diagnosis is possible, thereby strongly increasing the ability of the DBN to diagnose faults precisely. A simulation experiment and a case study with actual measurements have shown the capabilities of the reference architecture.

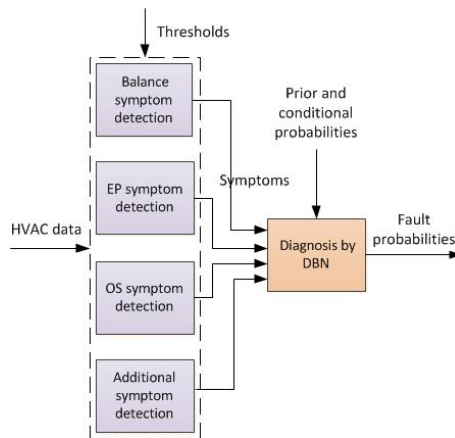


Figure 2.8. Summary of the architecture for automated energy performance FDD.

The proposed reference architecture for energy performance diagnosis largely overcomes the problems stated in the introduction:

- It simplifies the implementation of the BEMS, as the structure of the DBN resembles that of HVAC schematic diagrams. Because both models are constructed of connected sub-systems, they can be easily constructed at the same time and by the same designers of the HVAC system and its control system.
- It addresses the problem that one symptom can be caused by more faults and that one fault can cause diverse symptoms, as the DBN method generates fault probabilities in the same way that HVAC experts arrive at diagnoses.
- It integrates fault diagnosis and energy performance analysis in one framework.
- It allows fully automated detection and diagnosis.
- It allows the application of all kinds of FDD methods for symptom detection purposes and the easy replacement and extension of detection methods (e.g., with the FDD methods of suppliers of HVAC components and control systems).
- It enables the simultaneous diagnosis of aggregated systems and sub-systems and offers therefore a modular approach.

In future research, a number of points that needs further exploration and demonstration should be addressed, like optimal time intervals for the analysis of diverse balance, EP and OS symptoms, the influence of the prior and conditional probabilities in the DBN models (the subject was touched in our paper, but need further demonstration), the implementation of HVAC operating modes as additional symptoms or OS symptoms and the application of the reference architecture to in-room terminal systems (e.g., demand controlled ventilation at room level).

References

- [1] Energy performance of buildings — Overarching EPB assessment – Part 1: General framework and procedures ISO/WD 52000-1 (2015).
<https://ec.europa.eu/energy/en/topics/energy-efficiency/buildings>.
- [2] P. de Wilde, The gap between predicted and measured energy performance of buildings: A framework for investigation. *Automation in Construction* 41 (2014), 40-49. <https://doi.org/10.1016/j.autcon.2014.02.009>.
- [3] C. van Dronkelaar, M. Dowson, C. Spataru, D. Mumovic, A review of the Regulatory Energy Performance Gap and Its Underlying Causes in Non-domestic Buildings. *Frontiers in Mechanical Engineering* (2016).
<https://doi.org/10.3389/fmech.2015.00017>.
- [4] E. Mills, A Golden Opportunity for Reducing Energy Costs and Greenhouse Gas Emissions. California Energy Commission (2009).
<https://escholarship.org/uc/item/7dq5k3fp>.
- [5] R. Jing, M. Wang, R. Zhang, N. Li, Y. Zhao, A study on energy performance of 30 commercial office buildings in Hong Kong. *Energy and Buildings* 144 (2017), 117-128. <https://doi.org/10.1016/j.enbuild.2017.03.042>.
- [6] N. Djuric, V. Novakovic, Review of possibilities and necessities for building lifetime commissioning, *Renewable and Sustainable Energy Reviews* 13 (2009), 486-492. <https://doi.org/10.1016/j.rser.2007.11.007>.
- [7] J. Verhelst, G. van Ham, D. Saelens, L. Hensen, Model selection for continuous commissioning of HVAC-systems in office buildings: A review. *Renewable and Sustainable Energy Reviews* 76 (2017), 673-686.
<https://doi.org/10.1016/j.rser.2017.01.119>.
- [8] L. Kallab, R. Chbeir, P. Bourreau, P. Brassier, M. Mrissa, HIT2GAP: Towards a better building energy management. *Energy Procedia* 122 (2017), 895-900.
<https://doi.org/10.1016/j.egypro.2017.07.399>.

- [9] S. Wu, J. Sun, Cross-level fault detection and diagnostics of building HVAC systems. *Building and Environment* 46 (2011), 1558-1566. <https://doi.org/10.1016/j.buildenv.2011.01.017>.
- [10] RP1026: Evaluation of Next-Generation Automated Fault Detection & Diagnosis (FDD) tools for Commercial Building Energy Efficiency, Part I: FDD Case Studies in Australia (2018). Low Carbon Living, CRC.
- [11] W. Kim, S. Katipamula, A Review of Fault Detection and Diagnostics Methods for Building Systems. *Science and Technology for the Built Environment*, 24:1 (2017), 3-21. <https://doi.org/10.1080/23744731.2017.1318008>.
- [12] ASHRAE Handbook, HVAC Systems and Equipment. American Society of Heating, Refrigerating and Air Conditioning Engineers. (2012). ASHRAE.
- [13] ASHRAE. Air-Conditioning System Design Manual, Second Edition (2007). ASHRAE Press.
- [14] Technical Synthesis Report annex 34. Computer Aided Evaluation of HVAC System Performance (2006). IEA. www.ecbcs.org.
- [15] IEA ECBS Annex 40. Commissioning of Building HVAC Systems for Improving Energy Performance (2013). <http://www.buildup.eu/en/explore/links/iea-ecbcs-annex-40-commissioning-building-hvac-systems-improving-energy-performance>
- [16] IEA ECBS Annex 47. Cost Effective Commissioning of Existing and Low Energy Buildings (2013). <https://www.buildup.eu/en/explore/links/iea-ecbcs-annex-47-cost-effective-commissioning-existing-and-low-energy-buildings>
- [17] H. Yoshino, T. Hong, N. Nord, IEA EBC annex 53: Total energy use in buildings— Analysis and evaluation methods. *Energy and Buildings* 152 (2017), 124-136. <https://doi.org/10.1016/j.enbuild.2017.07.038>.
- [18] Annex 58 Reliable Building Energy Performance Characterization Based on Full Scale Dynamic Measurements (2017), IEA. [EBC_PSR_Annex_58.pdf \(iea-ebc.org\)](http://www.iea-ebc.org/EBC_PSR_Annex_58.pdf)
- [19] BuildingEQ (2018). <http://www.buildingeq.eu>
- [20] G. Anzaldi, A. Corchero, H. Wicaksono, K. McGlenn, A. Gerdelan, M. Dibley, Knoholem: Knowledge-Based Energy Management for Public Buildings Through Holistic Information Modeling and 3D Visualization (2013). https://doi.org/10.1007/978-3-319-02332-8_5.

- [21] S. Wang, Y. Chengchu, F. Xiao, Quantitative energy performance assessment methods for existing buildings. *Energy and Buildings* 55 (2012) 873-888. <https://doi.org/10.1016/j.enbuild.2012.08.037>.
- [22] W. Chung, Review of building energy-use performance benchmarking methodologies. *Applied Energy* 88 (2011), 1470-1479. <https://doi.org/10.1016/j.apenergy.2010.11.022>.
- [23] Z. Li, Y. Han, P. Xu, Methods for benchmarking building energy consumption against its past or intended performance: A review. *Applied Energy* 124 (2014), 325-334. <https://doi.org/10.1016/j.apenergy.2014.03.020>.
- [24] E.H. Borgstein, R. Lamberts, J.L.M. Hensen, Evaluating energy performance in non-domestic buildings: A review. *Energy and Buildings* 128 (2016), 734-755. <https://doi.org/10.1016/j.enbuild.2016.07.018>.
- [25] Y. Wei, X. Zhang, Y. Shi, L. Xia, S. Pan, J. Wu, M. Han, A review of data-driven approaches for prediction and classification of building energy consumption. *Renewable and Sustainable Energy Reviews* 82 (2018), 1027-1047. <https://doi.org/10.1016/j.rser.2017.09.108>.
- [26] S. Katipamula, M.R. Brambley, Methods for fault detection, diagnostics, and prognostics for building systems – A review, Part I. *HVAC&R Research* 11 (2005), 3-25. <https://doi.org/10.1080/10789669.2005.10391123>
- [27] S. Katipamula, M.R. Brambley, Methods for fault detection, diagnostics, and prognostics for building systems – A review, Part II. *HVAC&R Research* 11 (2005), 169-187. <https://doi.org/10.1080/10789669.2005.10391133>
- [28] J. Cho, S. Shin, J. Kim, H. Hong, Development of an energy evaluation methodology to make multiple predictions of HVAC&R system energy demand for office buildings. *Energy and Buildings* 80 (2014), 169-183. <https://doi.org/10.1016/j.enbuild.2014.04.046>.
- [29] T. Maile, V. Bazjanac, M. Fisher, A method to compare simulated and measured data to assess building energy performance. *Building and Environment* 56 (2012), 241-251. <https://doi.org/10.1016/j.buildenv.2012.03.012>.
- [30] H. Wang, P. Xu, X. Lu, D. Yuan, Methodology of comprehensive building energy performance diagnosis for large commercial buildings at multiple levels. *Applied Energy* 169 (2016) 14-27. <https://doi.org/10.1016/j.apenergy.2016.01.054>.
- [31] D. Choiniere, D. DABOTM: A BEMS assisted on-going commissioning tool. *Proceedings of the National Conference on Building Commissioning*, (2008).

- [32] L. Belussi, L. Danza, Method for the prediction of malfunctions of buildings through real energy consumption analysis: Holistic and multidisciplinary approach of Energy Signature. *Energy and Buildings* 55 (2012), 715-720. <https://doi.org/10.1016/j.enbuild.2012.09.003>.
- [33] A. Costa, M. Keane, J. Torrens, E. Corry, Building operation and energy performance: Monitoring, analysis and optimization toolkit. *Applied Energy* 101 (2013), 310-306. <https://doi.org/10.1016/j.apenergy.2011.10.037>.
- [34] R. Hitchin, I. Knight, Daily energy consumption signatures and control charts for air-conditioned buildings. *Energy and Buildings* 112 (2016), 101-109. <https://doi.org/10.1016/j.enbuild.2015.11.059>.
- [35] L. Zhao, J. Zhang, R. Liang, Development of an energy monitoring system for large public buildings. *Energy and Buildings* 66 (2013), 41-48. <https://doi.org/10.1016/j.enbuild.2013.07.007>.
- [36] J. Bynum, D. Claridge, J. Curtin, Development and testing of an Automated Building Commissioning Analysis Tool (ABCAT). *Energy and Buildings* 55 (2012) 607-617. <https://doi.org/10.1016/j.enbuild.2012.08.038>.
- [37] F. Xiao, S. Wang, X. Xu, G. Ge, An isolation enhanced PCA method with expert-based multivariate decoupling for sensor FDD in air-conditioning systems. *Applied Thermal Engineering* 29 (2009), 712-722. <https://doi.org/10.1016/j.applthermaleng.2008.03.046>
- [38] Y. Guo, G. Li, H. Chen, Y. Hu, H. Li, J. Liu, M. Hu, W. Hu, Modularized PCA method combined with expert-based multivariate decoupling for FDD in VRF systems including indoor unit faults, *Applied Thermal Engineering* 115 (2017), 744-755. <https://doi.org/10.1016/j.applthermaleng.2017.01.008>
- [39] Z. Du, B. Fan, X. Jin, J. Chi, Fault detection and diagnosis for buildings and HVAC systems using combined neural networks and subtractive clustering analysis, *Building and Environment* 73 (2014), 1-11, <https://doi.org/10.1016/j.buildenv.2013.11.021>.
- [40] W. Lee, J. House, N. Kyong, Subsystem level fault diagnosis of a building's air-handling unit using general regression neural networks, *Applied energy* 77 (2004), 153-170. [https://doi.org/10.1016/S0306-2619\(03\)00107-7](https://doi.org/10.1016/S0306-2619(03)00107-7).
- [41] K. Sun, G. Li, H. Chen, J. Liu, J. Li, W. Hu, A novel efficient SVM-based fault diagnosis method for multi-split air conditioning system's refrigerant charge fault amount, *Applied Thermal Engineering* 108 (2016), 989-998. <https://doi.org/10.1016/j.applthermaleng.2016.07.109>.

- [42] H. Han, B. Gu, J. Kang, Z. Li, Study on a hybrid SVM model for chiller FDD applications, *Applied Thermal Engineering* 31 (2011), 582-592. <https://doi.org/10.1016/j.applthermaleng.2010.10.021>.
- [43] H. Lund, S. Werner, R. Wiltshire, S. Svendsen, J. Thorsen, F. Hvelplund, B. Mathiesen, 4th Generation District Heating (4GDH): Integrating smart thermal grids into future sustainable energy systems, *Energy* 68 (2014), 1-11. <https://doi.org/10.1016/j.energy.2014.02.089>.
- [44] M. Tuballa, M. Abundo, A review of the development of Smart Grid technologies, *Renewable and Sustainable Energy Reviews* 59 (2016), 710-725. <https://doi.org/10.1016/j.rser.2016.01.011>.
- [45] L. Navarro, A. de Gracia, S. Colclough, M. Browne, S. McCormack, P. Griffiths, L. Cabeza, Thermal energy storage in building integrated thermal systems: A review. Part 1. active storage system, *Renewable Energy* 88 (2016), 526-547. <https://doi.org/10.1016/j.renene.2015.11.040>.
- [46] P. Fleuchaus, B. Godschalk, I. Stober, P. Blum, Worldwide application of aquifer thermal energy storage – A review, *Renewable and Sustainable Energy Reviews* 94 (2018), 861-876. <https://doi.org/10.1016/j.rser.2018.06.057>.
- [47] C. Kasalini, R. Loonen, D. Costola, J. Hensen, Climate adaptive building shells: State-of-the-art and future challenges, *Renewable and Sustainable Energy Reviews* 25 (2013), 483-493. <https://doi.org/10.1016/j.rser.2013.04.016>.
- [48] Het ontwerp van hydraulische schakelingen voor verwarmen, ISSO-publicatie 44 (1998). ISSO.
- [49] Ontwerp van hydraulische schakelingen voor koelen, ISSO-publicatie 47. (2013). ISSO.
- [50] N. Djuric, V. Novakovic, Correlation between standards and the lifetime commission, *Energy and Buildings* 42 (2010), 510-521. <https://doi.org/10.1016/j.enbuild.2009.10.020>.
- [51] Energy performance of Buildings – Overarching standard EPBD, prEN 15603:2013:E (2013). CEN.
- [52] K.L. Gillespie, P. Haves, R.J. Hitchcock, J. Deringer, K.L. Kinney, A Specifications Guide for Performance Monitoring Systems (2007). <https://buildingdata.energy.gov/cbrd/resource/795>.
- [53] C.D. Barley, M. Deru, S. Pless, P. Torcellini, Procedure for Measuring and Reporting Commercial Building Energy Performance. Technical Report NREL/TP-

550-38601 (2005). Golden, CO: National Renewable Energy Lab. www.nrel.gov/docs/fy06osti/38601.pdf.

[54] S. Wang, J. Wang, Law-Based Sensor Fault Diagnosis and Validation for Building Air-Conditioning Systems. HVAC&R Research, 5:4 (1999), 353-380. <https://doi.org/10.1080/10789669.1999.10391243>

[55] P. Lucas, Bayesian networks in medicine: A model-based approach to medical decision making. Proceedings of the EUNITE Workshop on Intelligent Systems in Patient Care, Vienna, (2001), 73–97.

[56] A. Zogarecki, P. Orzechowski, K. Holownia, A System for Automated General Medical Diagnosis using Bayesian Networks, Studies in health technology and informatics 192 (2013) 461-465. <https://www.ncbi.nlm.nih.gov/pubmed/23920597>.

[57] F. Xiao, Y. Zhao, J. Wen, S. Wang, ‘Bayesian network based FDD strategy for variable air volume terminals,’ Automation in Construction 41 (2014): 106-118. <https://doi.org/10.1016/j.autcon.2013.10.019>.

[58] Y. Zhao, J. Wen, S. Wang, ‘Diagnostic Bayesian networks for diagnosing air handling units faults – Part II: Faults in coils and sensors,’ Applied Thermal Engineering 90 (2015), 145-157. <https://doi.org/10.1016/j.applthermaleng.2015.07.001>.

[59] K. Verbert, R. Babuska, B. De Schutter, Combining knowledge and historical data for system-level fault diagnosis of HVAC systems, Engineering Applications of Artificial Intelligence 59 (2017), 260-273. <https://doi.org/10.1016/j.engappai.2016.12.021>

[60] M. Hu, H. Chen, L. Shen, G. Li, Y. Guo, H. Li, J. Li, W. Hu, A machine learning Bayesian network for refrigerant charge faults of variable refrigerant flow air conditioning system. Energy and Buildings 158 (2018) 668-676. <https://doi.org/10.1016/j.enbuild.2017.10.012>.

[61] GeNie 2.1 (2016). Bayesfusion. <http://download.bayesfusion.com>,

3. P&ID-based symptom detection for automated energy performance in HVAC systems

This chapter has been published as:

Arie Taal, Laure Itard, “P&ID-based symptom detection for automated energy performance in HVAC systems”, *Automation in construction* **119** (2020) 103344

In this chapter, a set of symptom detection methods based on balances, energy performance and operational states is discussed which can be extracted from HVAC P&IDs. Detection is applied in a case study for the thermal energy plant of the building of the Hague University of Applied Sciences.

3.1. Introduction

Energy use in the operational phase of buildings is higher than predicted, for instance by energy simulations, during the design phase, see e.g., [1]. Continuous commissioning by a building energy management system (BEMS) can help to reduce this unnecessarily high energy consumption. However, fully automated building energy analysis systems including fault detection and diagnosis (FDD) are not often applied in practice. An important reason is that these systems are not setup and implemented simultaneously with the heating, ventilation and air conditioning (HVAC) system. In the present article, the authors develop further the symptom detection - which indicates the presence of faults - part of the 4S3F (four categories of symptoms and three categories of faults) method for energy purposes and apply it to a case study of a thermal energy generation system. The 4S3F approach using process and instrumentation diagrams (P&IDs) remains close to the way HVAC experts diagnose problems. A first draft of this method, described in [2], in which the 4S3F architecture was tested on a simple case, presented the following four types of symptoms:

- Balance based
- Energy Performance based
- Operational State based
- Additional based

Despite many studies of fault detection methods, there is still no classification of detection models with generic key performance indicators (KPIs) and associated detection rules, and the implications of detection time spans. The current article demonstrates the proposed automated symptom detection part of the 4S3F method as

applied to the thermal energy plant of the THUAS (The Hague University of Applied Sciences) building in Delft, the Netherlands, using the data in the building management system (BMS). The HVAC system that was considered has a gas boiler and a heat pump combined with an aquifer thermal energy storage (ATES) system for the storage and supply of both heat and cold. The analysis covers a whole year, thus examining the annual energy performance of the heating and cooling systems, based on 16-minute data and demonstrates the practical usability of the 4S3F architecture for an existing HVAC system.

The 4S3F diagnosis basic architecture for energy performance is briefly presented in Section 3.2. Section 3.3 presents the pre-processing part needed for energy performance diagnosis, and Section 3.4 studies the generic approach to symptom detection. This section is in two parts. The first describes the KPIs and the second the rules relating to these KPIs. Much attention is paid to the development of suitable generic key energy performance and operational state indicators. Section 3.5 describes the HVAC system considered for a case study. Sections 3.6 and 3.7 describe the implementation of the symptom detection in the case study. Section 3.8 evaluates the case study results, and Section 3.9 discusses the detection time span. Finally, Section 3.10 draws conclusions and recommendations concerning the implementation of the 4S3F diagnosis framework.

3.2. 4S3F architecture for Energy Performance Diagnosis

3.2.1. BMS-data based energy diagnosis

The generic structure of the processes in a BEMS consists of pre-processing, symptom detection, diagnosis and correction phases. A BEMS can be an extension of a BMS controlling an HVAC system.

In the pre-processing phase, the measurement data is prepared for the calculation of energy performance indicators. Measurement data is obtained from the BMS (or from data loggers if there is no BMS) and is usually stored in a database. Such data is susceptible to corruption due to measurement errors (e.g., sensor inaccuracy, drifting sensors) or missing data. Data correction for such instances is performed in the pre-processing phase. In addition, measurement data is not in the proper form for energy performance calculations. For example, thermal energy flows must be calculated from temperature and flow-rate sensors, missing flow rates or temperatures must be estimated using other BMS data and product specifications (resulting in soft sensor values; for soft sensors to use in HVAC systems, see e.g., [3]), and outliers must be filtered (which can be done automatically: see e.g., the BuildingEQ project [4]).

In the detection phase, symptoms of malfunctioning are detected. Faults are then diagnosed based on the observed symptoms. The last phase is the correction phase,

in which it is decided which faults must be corrected, based on performance and investment considerations.

3.2.2. Applied 4S3F reference architecture for energy performance diagnosis

This section presents the broad outline of the 4S3F architecture (see [2] for a detailed explanation of that architecture). The automated energy performance FDD process starts with the detection of observable malfunctioning symptoms, based on the measurement points and set points in the BMS and the P&IDs which contain HVAC components and control components (actuators, sensors and controllers). These symptoms are categorised into four main types (4S), see Figure 3.1: balance symptoms (energy, mass and pressure based), energy performance (EP) symptoms, operational state (OS) symptoms, and symptoms based on additional information, e.g., maintenance information.

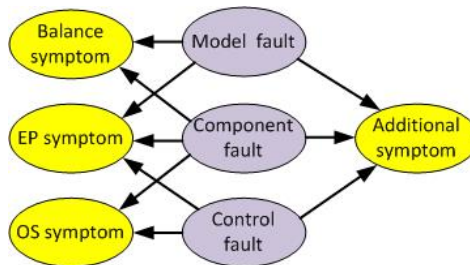


Figure 3.1. 4S3F DBN structure

The results of the symptom detection phase are supplied to a diagnostic Bayesian network (DBN) model as shown in Figure 3.1. This model links symptoms to possible faults. We distinguish three types of faults: faults in the models used to estimate missing energy data or to set up balance models, component faults, and finally faults in control components. We define components as being not only trade components but also all HVAC subsystems at different aggregation levels. The direction of the arrows is from the faults to the symptoms. Hence Figure 3.1 shows which symptoms may be caused by a specific fault. At fault isolation in the 4S3F method, the faults are estimated from the presence and absence of symptoms. The components and controls, and detection rules, can be easily extracted from the HVAC P&ID. The present paper addresses only the symptom detection part (4S) of the 4S3F framework.

3.3. Pre-processing

On the one hand, the pre-process consists of estimating energy data automatically and continuously from the available BMS data. Missing and faulty data are corrected and calculations or assumptions for missing data points are made. This correction

process can also be carried out using the 4S3F method and will be reported in another paper. In the case study for this paper all the data used had already been corrected and checked to be valid. On the other hand, an important part of the pre-process consists of the identification and selection of the systems considered for energy performance diagnosis. We propose carrying out this step once in the time interval using the HVAC P&ID and following the procedure described in Sections 3.4.1 and 3.4.2.

3.3.1. Selection of the systems and subsystems

For the purpose of energy performance diagnosis, the HVAC system is divided into subsystems based on the availability of data that can be used to estimate relevant key performance indicators. We propose identifying three system levels for components:

- a. The whole HVAC system.
- b. Aggregated systems according to international classification agreements such as EN15316-1 [5] in which heating systems can be categorised into generator, distribution and emitter systems.
- c. Subsystems consisting of trade components (e.g., boiler and heat pump).

It is essential when choosing the aggregation levels of the various subsystems that it must be possible to measure their performance and/or make energy balances: in other words, there should be enough sensors to perform the task.

A more detailed level (e.g., components of a heat pump such as a compressor) has not been considered because we assume that FDD methods are or will be available for trade components (see [6], which presents a review of such methods for HVAC components such as chillers). The 4S3F method can of course be applied easily to trade components as well.

3.4. Generic approach to symptom detection

The symptom detection process determines the presence and absence of symptoms. As shown in Section 3.2, these can be balance, energy performance (EP) and operational state (OS) symptoms. We do not discuss the possibility of using additional information (e.g., from facility managers) as symptoms in this paper.

Like pre-processing, symptom detection is done in two stages. Firstly, all the possible symptoms are listed once in the time interval during the setup of the diagnosis system, based on the P&ID. Secondly, symptoms are detected per hour, day, week, month or year (see later in this article) using automated comparison of measured values with expected values.

Section 3.4.1 introduces generic symptom detection models which can be applied regardless of the HVAC system to estimate balance, EP and OS symptoms. The rules for this are elaborated in Section 3.4.2.

3.4.1. Generic symptom detection models for thermal energy plants

3.4.1.1. Generic energy balance symptoms

As dimensionless balance indicators we use efficiencies, in terms of heat losses in the diverse systems and components, and mechanical efficiencies. These efficiencies follow either directly from the energy balances that are made concurrently in all subsystems at various aggregation levels as shown in Section 3.3.1 or from efficiency rules of heat exchangers (e.g., using the NTU-method, as described in [7] or compulsory seasonal balances (e.g., for ATES systems, see [8] which presents a review of system performance studies of such systems). If the useful energy output of a system is much lower than the input (i.e., the efficiency is low), there is energy wasted in the system and this is a symptom that the system under consideration is not working properly. The number of systems for which efficiencies can be calculated depends of course on the measurement points present in the P&ID. Examples of formulas for these efficiencies are described in Section 3.7 and need to be implemented only once in the time interval.

3.4.1.2. Generic energy performance (EP) symptoms

A thorough literature study of possible energy performance factors was conducted. The literature includes several applications of energy performance indicators to buildings and their systems. Benchmarking approaches with simplified methods in which the energy consumptions in the buildings are compared with those of similar buildings are very common: for example, energy use intensity (EUI), which indicates energy consumption (e.g., kWh/m²) (see Chung 2011 [9] and Liu et al. [10]). However, these approaches are very rough and do not take advantage of the full potential of energy diagnostics, because they are based on the comparison of buildings and systems that are not always identical in design and use, and only aggregated seasonal or yearly data is used. Additionally, these indicators are not detailed enough to allow for the identification of HVAC-specific faults.

Another approach, this time building-specific, is the use of black-box, grey-box or white-box models. Kim and Katipamula [6] presented an overview of FDD methods for HVAC systems. Wei et al. [11], Borgstein et al. [12] and Li et al. [13] presented reviews of methods for energy performance purposes. Black-box models, which are data-driven methods using e.g., ANNs (artificial neural networks) or regression models (see e.g., [14] and [15]), compare the actual energy consumptions with past performances. However, it is impossible to estimate to what extent past performances were optimal, and the setup of a data-driven model can be time-consuming.

Furthermore, the practical usability of such models is limited, because identified correlations may not be the result of causal relationships and may not have a physical meaning. Moreover, taking transient effects into account is a complex process. In grey-box models, such as RC (resistance and capacity) network models for buildings and system, the diagnosis is aided by a simple model, the parameters of which are determined by data-driven optimisation methods (see for instance ABCAT [16]). The white-box approach uses complex models based on physics (e.g., a simulation tool such as EnergyPlus, which was applied in the KnoholEM project [17]). See also Maile et al. [18], where simulation tools were proposed. These approaches are, however, also extremely time-consuming (especially the calibration procedure) and depend on the availability of reliable data for a well-functioning HVAC system. In addition, the energy performance indicators are generally not dimensionless but expressed in terms of energy intensity use, whereas in design practice dimensionless energy performance indicators such as efficiency, coefficient of performance (COP) and energy efficiency ratio (EER) are commonly used (see e.g., [14]). The main advantage is that these indicators are building-independent and reference values can be found in handbooks, guidelines and product descriptions or are known from HVAC design. We propose combining these dimensionless indicators with a few non-dimensionless indicators, related to actual energy rates of components (see e.g., DABO [19]). For instance, inadequate heat pump capacity could lead to higher energy consumption by a gas boiler at peak load, and excessive capacity could lead to higher energy consumption due to lower performance at partial load.

Finally, we noticed energy waste outliers: unexpected electrical energy consumption by fans during non-working periods, for instance. The BuildingEQ [4] project developed energy signature tools to estimate deviations between actual and expected energy values.

Based on the foregoing, we propose the following classification of key (energy) performance indicators:

- Performance factors, for instance COPs and EERs. The measured COPs and EERs can be compared with product, design or guideline specifications. Mismatch can be considered as a symptom of malfunctioning.
- Capacity indicators, which can show that inadequate or excessive capacity has been installed.
- Energy outliers, which indicate energy waste.

3.4.1.3. Generic operational state (OS) symptoms

In addition to EP indicators, KPIs not directly related to energy amounts can be used to compare the operational performance of control components with pre-set values (e.g., actual temperature versus set-point temperature). DABO [19] compares actual

supply water temperatures with set points. Several other studies [20 to 24] present examples of the use of energy signatures, presenting operational state values such as supply air and water temperatures in time series and scatter plots.

Based on these studies, the following operational state indicators can be considered:

- Control-based OS indicators. These check the quality of state properties against set points in the control system, for instance supply temperatures. Large numbers of wrong actual values (in comparison with the set-point value) are symptomatic of malfunctioning. These control-based rules need to be defined in relation to the operational mode of the HVAC system (e.g., the cold well pump in the ATES system has to be on when the outlet cold well temperature is analysed).
- Design-based OS indicators. There are state values that are not controlled in the control system but that were used as a starting point for the design of the HVAC system and are expected to be achieved during operation: the supply water temperature from the cold well of the ATES system, for instance. Comparing the actual values with the design values helps to identify symptoms. The fact that design temperatures are not met could indicate that the system is not working properly, as a result of wrong HVAC design or control.

Set-point values and design values are known to the HVAC designers and generally referred to in the HVAC P&ID, in such a way that they can be listed very simply.

3.4.1.4. Generic additional symptoms

As well as the balance, EP and OS symptom indicators, additional information about HVAC systems can be used as symptoms, for instance:

- Maintenance information from which a component fault can be excluded.
- Result from an FDD method supplied by a component manufacturer.
- User satisfaction with thermal indoor climate.

3.4.2. Rules for symptom detection

In practice, measurement accuracy and precision are essential factors in the accurate determination of symptoms. Furthermore, the transient behaviour of the HVAC components affects reliable symptom detection, and the detection time interval, e.g., hourly, daily and annual, is of great importance.

To deal with this, the detection rules need to use lower and upper limits for the threshold values. A symptom is detected when the deviation ε of an energy balance, an energy performance indicator or an operational state indicator ε is higher or lower than the threshold values ε_{\min} and ε_{\max} . Eq. (3.1) shows when the deviation ε is acceptable.

$$\varepsilon_{min} < \varepsilon < \varepsilon_{max} \quad (3.1)$$

Eq. (4.2) is the equation for calculating the deviation ε in the case of energy balance and EP symptom detection.

$$\varepsilon = \frac{X_{mea} - X_{exp}}{X_{exp}} \quad (3.2)$$

where:

X_{mea} = measured symptom indicator.

X_{exp} = expected symptom indicator.

The denominator X_{exp} indicates a characteristic value for the symptom indicator. The values for ε_{min} and ε_{max} depend on the type of rule and HVAC design, required control accuracy and measurement inaccuracies.

3.4.2.1 Rules for the detection of energy balance symptoms

The energy balance symptoms relate to dimensionless indicators (efficiencies).

For efficiencies Eq. (3.1) becomes with (3.2):

$$\varepsilon = \frac{\eta_{mea} - \eta_{exp}}{\eta_{exp}} > \varepsilon_{min} \quad (3.3)$$

For instance, ε_{min} for efficiencies of heat distribution systems could be -5% due to measurement inaccuracies and transient behaviour. ε_{max} is not relevant as it would indicate higher efficiencies than expected and can therefore not be considered as a symptom.

3.4.2.2 Rules for the detection of energy performance symptoms

Eq. (4.1) transformed for dimensionless performance factors is shown in Eq. (3.4):

$$\varepsilon = \frac{PF_{mea} - PF_{exp}}{PF_{exp}} > \varepsilon_{min} \quad (3.4)$$

where:

PF = performance factor [-]

The dimensionless performance factors can be COPs and EERs. Acceptable deviations for COPs and EERs could be 5% ($\varepsilon_{min} = -5\%$). Here too, ε_{max} is not considered because a positive deviation would indicate a better COP than expected and cannot therefore be considered as faulty.

For the non-dimensionless performance factors related to capacity, a symptom is detected when the difference between the measured value P_{mea} and the nominal value

P_{nom} (e.g., the installed capacity) is lower than a threshold ε_{min} or higher than ε_{max} . See Eq. (3.5).

$$\varepsilon_{min} < \frac{P_{mea} - P_{nom}}{P_{nom}} < \varepsilon_{max} \quad (3.5)$$

ε_{min} could be -10% whereas ε_{max} could be higher than 10%, depending on the effect of component capacity on energy performance at partial load.

For the performance factors related to energy outliers, for instance to detect unexpected energy consumption by pumps outside working hours, we propose the following equation:

$$\frac{E_{mea} - E_{exp}}{E_{exp}} < \varepsilon_{max} \quad (3.6)$$

where:

E_{mea} = measured energy consumption [J]

E_{exp} = expected energy consumption [J]

3.4.2.3 Rules for the detection of operational state symptoms

For operational state thresholds, we apply rules relating to the state variable under consideration. Eq. (3.7) shows the rule for temperatures:

$$\varepsilon_{min} < \Delta T < \varepsilon_{max} \quad (3.7)$$

where ΔT is the temperature deviation from the set-point or design value.

In addition, the number of faults in a time span, for instance a week, month or year, should be considered. This is because a deviation occurring only a few times will not have a large impact on energy use, whereas if it happens often the repercussions could be substantial. We propose simply using the number of faulty values n_{fault} divided by the whole number of measurements in the period under consideration. A symptom is observed when this ratio δ is larger than the threshold δ_{max} (for instance 10%). See Eq. (3.8).

$$\delta = \frac{n_{fault}}{n_{tot}} > \delta_{max} \quad (3.8)$$

δ_{max} is estimated separately for lower (δ_{LL}) and upper (δ_{UL}) limits of the state values because negative and positive deviations may be symptoms of differing faults. The lower limit is linked to $\Delta T < \varepsilon_{min}$ and the upper limit to $\Delta T > \varepsilon_{max}$.

3.4.2.4 Additional conditions linked to system dynamics and time spans

Additional conditions are needed to eliminate measurement outliers and effects of transient behaviour. In addition to threshold, the dynamic of the system under consideration should be taken into account. An additional condition could be that

only measurements after a certain time span are taken into account. Also, a generator's energy and temperature measurements are considered only when the generator is on.

Detection can take place at very different time intervals, from the storage interval in the BMS to annually. Using a small interval (such as the 16-minute storage interval in our case study) does not necessarily yield better symptom description, as this interval may be far below the response time of many components and would therefore necessitate the use of dynamic indicators. For instance, calculating a COP on the basis of 16-minute data makes no sense, as the COP is low at start-up because the generator and hydronic systems have to be warmed up or cooled down. In the same way, the COP is very high when the generator is stopped, and thermal energy is still being delivered by the hydronic systems. Conversely, aggregating the data at annual level substantially limits the possibilities for intervention, and some malfunctioning processes may not be observed. For a real-time diagnosis system, time periods of one hour, day, week or month are therefore preferable. This is discussed in Section 3.9. When to use which period is beyond the scope of this paper, but an automated approach in which detection at different time levels is used will be preferable in practice. For the sake of demonstration, Section 3.7 presents symptom detection results in the case study on an annual basis only for balance, energy performance and operational state indicators as well as the threshold values and additional conditions used.

3.5. Case study: the heat and cold generation system of the building of The Hague University of Applied Sciences in Delft

The 4S3F method was tested on the THUAS building in Delft. This was selected because it has a complex HVAC system with an advanced control system, and extensive measurement data is available for analysing energy consumption and indoor climate. In addition, it is an operational HVAC system with a reputation for working properly and apparently being energy efficient.

The building mainly contains classrooms, offices for lecturers and other personnel, an atrium (see Figure 3.2), and a restaurant.

In winter, heat is generated by a heat pump. When the heat loads are high, a gas boiler can deliver additional heat. The heat source of the heat pump is warm water delivered by the warm well of an ATES system. The ATES system can also deliver heat to the parking lane on the roof to keep it free of ice. Such ATES systems are common in the Netherlands: more than 2,000 of them have been installed in recent years and their operation is known to be often sub-optimal.

In the summer months, cold water from the cold well of the ATES system delivers cooling. When cooling loads are high, the heat pump produces additional cold at the

evaporator side. During the summer, heat from the heat pump condenser and the roof collector can be used to regenerate the warm well of the ATES system, as the annual thermal energy extracted from and pumped into the wells has to be balanced under the Dutch regulations.



Figure 3.2. Inside the THUAS building

As the 4S3F framework is based on HVAC P&IDs, Figure 3.3 shows the overall principal P&ID layout with all the possible heating and cooling states of the HVAC system. The systems depicted are connected by lines which represent pipes. Each system has inlet and outlet pipes. The outlet pipes of the thermal energy plant are themselves supply pipes to the systems (34 to 38) and the inlet pipes of the energy plant are return pipes from these systems. Cold and heat are delivered to the rooms of the building by a thermal floor system which acts as a Thermally Activated Building System (TABS) and by ceiling radiation panels where water is circulated. The hot water groups (34) and (35) as well the cold-water groups (36) and (37) consist of South and North groups which are divided into sub-groups (not shown) for air handling, the ceiling and the floor equipment.

Heat is produced by a heat pump (12) and a boiler (33). The heat pump extracts heat from the ATES system. Warm groundwater flows from the warm well (32) to the cold well (31) and delivers heat through a heat exchanger (8). When more heat is needed than the heat pump can deliver, the boiler provides the rest. The existing buffers (6), (10) and (16) are needed for the stable functioning of the HVAC installation when operating under partial load.

A heat regeneration system, comprising subsystems (17) to (19), is provided to feed additional heat into the warm well of the aquifer system. Because the THUAS building needs more heat than cold, this is necessary (and mandatory) to keep both wells in thermal balance.

The hot water header (14) delivers heat to the boiler header (21), to the heat storage vessel (16) and to the regeneration unit (17). The return water is collected in the collector (15).

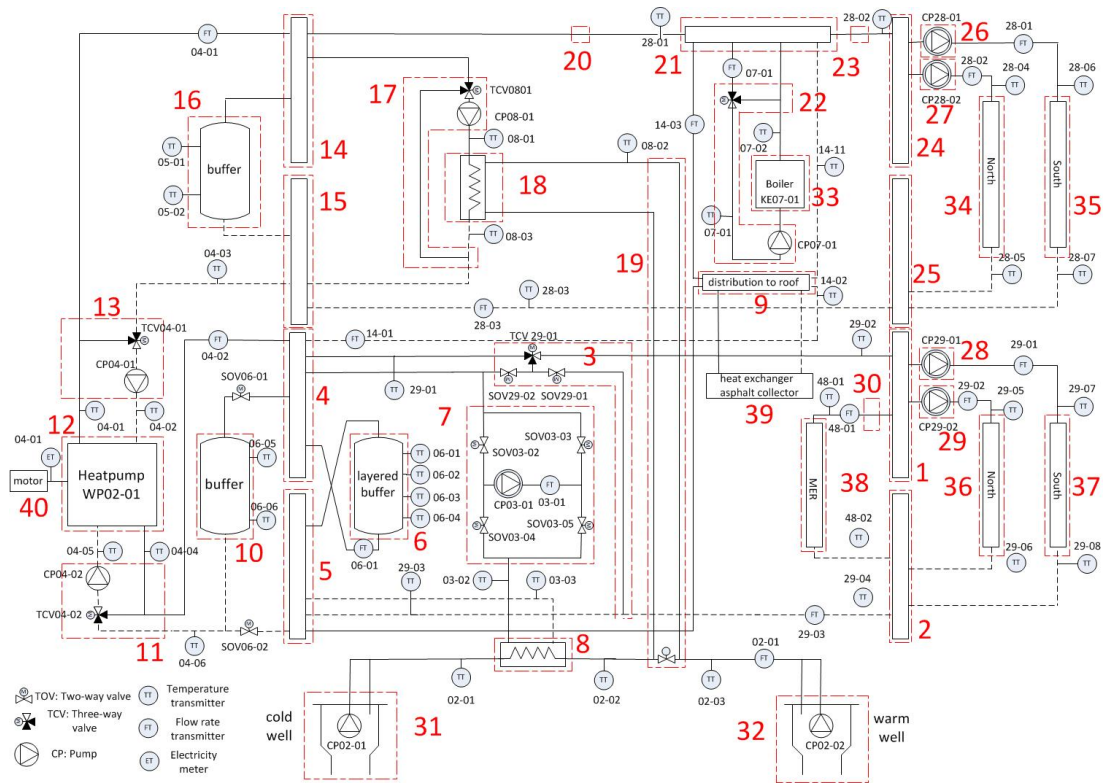


Figure 3.3 Principal scheme (P&ID) of the heat and cold generation system of HHS
(Controllers are not depicted)

The main cold-water header (4) delivers cold water to the header (1) and to the heat exchanger of the ground storage installation (8). The cold-water header (5), which acts as a collector of warmed up return cold water from the building and the heat exchanger of the ATES system, delivers warm water to the roof (39) (so as to keep it ice-free) and to the evaporator group (11) of the heat pump (12). In the summer, the roof delivers also heat to the warm well of the ATES system.

The header (1) in the cooling group delivers cold to the building sections and Air Handling Units located with a North (N) and South (S) orientation ((36) and (37)), and also to a server room (MER) (38).

The sensors and actuators are the ones that were installed when the system was built in 2009. Figure 3.4 shows 42 temperature sensors and 13 flow meters. There is also thermal energy metering (not shown) in the hot and cold-water groups, at systems (3), (27), (28), (17), (21) and (22). Pressure metering (also not shown) is provided for the control of pumps CP28-01, CP28-02, CP29-01 and CP29-02. The electricity consumption of the heat pump compressor (40) is measured by meter ET04-01. These measurements are stored in the BMS at 16-minute intervals. The codes of the sensors and actuators (beginning with 02 to 48) as implemented in the BMS were supplied by the designer of the HVAC system.

An entire year, 2013, was taken for the case study because of the availability of an almost complete dataset.

System and subsystem selection will be outlined in Section 3.6 and symptom detection in Section 3.7.

3.6. System and subsystem selection in the case study

The whole HVAC system considered in the case study is shown in the P&ID of Figure 3.3 and represented by the system boundaries depicted by the dotted line in Figure 3.4. Aggregated systems at level b), as described in Section 3.3.1, are arranged in Figure 3.4 into generator (systems B, C and D), hydronic (systems G and H) and emitter systems (systems A, E and F). In this figure the work W02, W03, W04, W07 and W08 corresponds to the work of pumps CP02_01 and CP02_02, CP03_01, CP04_01 and CP04_02, CP07_01 and CP08_01, shown in Figure 3.4. The compressor work of the heat pump Whp is measured by electricity meter ET04_01.

The subsystems (components) at level c) are shown by the numbers (1) to (40) in Figure 3.3. This division into systems and subsystems follows directly from the HVAC P&ID and is therefore very easy to implement for designers of HVAC systems.

3.7. Symptom detection in the case study

This section applies the principles developed in Section 4 to the case study and shows the main detection results. We refer to the tables in Appendix 3A, which provide more detailed information on the detection process.

For the sake of simplicity, a detection period of one year has been taken. We consider shorter detection periods in Section 3.9. First, we address the balance symptoms (Section 3.7.1), then the energy performance symptoms (Section 3.7.2), and finally the operational state symptoms (Section 3.7.3). Section 3.7.4 discusses the symptoms present and absent in the case study.

3.7.1. Energy balance symptoms in the case study

The energy balance indicators (efficiencies (η)) specific to the HVAC system of THUAS are presented below.

For the once-in-the-time-interval implementation in the BEMS to calculate the efficiencies, the heat transfer ΔQ between systems was calculated using Eq. (3.9) for each 16 minutes, based on the flow rates and temperatures at the start time of each 16-minute interval.

$$\Delta Q = q_v \cdot \rho \cdot c \cdot \Delta T \cdot \Delta t \quad (3.9)$$

where:

ΔQ = exchanged heat [kJ]

$\Delta t = t_{\text{end}} - t_{\text{start}} = 960$ s.

t_{end} = end-time calculation stored in BMS [s]

t_{start} = start-time calculation stored in BMS [s]

q_v = water flow rate at start time [m³/s]

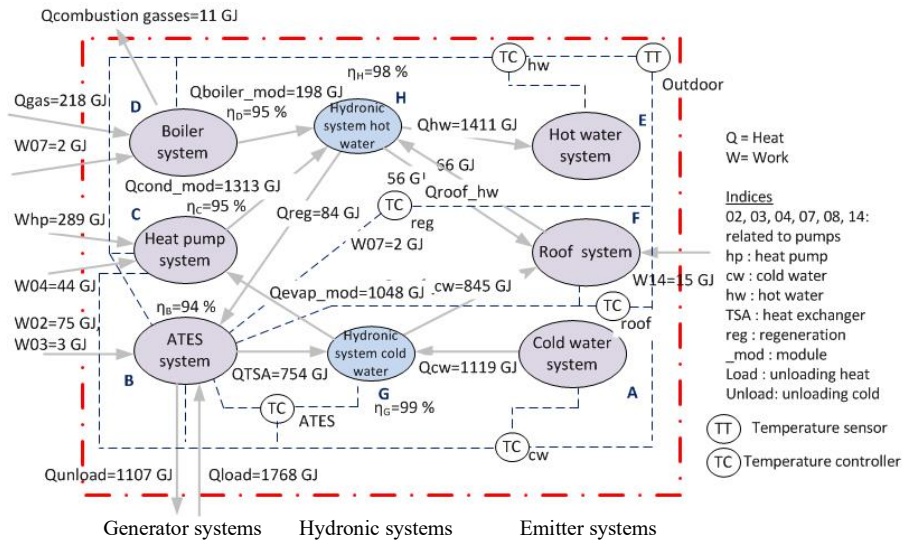
ρ = water density = 1000 kg/m³

c = specific heat of water = 4.18 kJ/kgK

ΔT = difference between supply and return temperatures at start time [K]

Eq. (3.9) can easily be programmed once in the BMS or in a separate BEMS when setting up the diagnosis system based on the P&ID. The efficiencies of the systems during a certain period are then calculated based on these ΔQ s. For instance, the efficiency of system H (see Figure 3.4 which shows the annual exchanged energy values) is calculated using:

$$\eta_H = \frac{Q_{hw} + Q_{reg}}{Q_{cond_mod} + Q_{boiler_mod} + Q_{roof_hw}} \quad (3.10)$$



- System A: 28, 29, 30, 36, 37 and 38.
- System B: 8, 17, 18, 19, 31 and 32.
- System C: 11, 12, 13 and 40.
- System D: 22 and 33.
- System E: 26, 27, 34 and 35.
- System F: 9 and 39.
- System G: 1, 2, 3, 4, 5, 6 and 10.
- System H: 14, 15, 16, 20, 21, 23, 24 and 25

Figure 3.4 The relevant aggregated systems at Level a) and b) consisting of systems A to H

We assume an expected efficiency of $\eta_{exp}=98\%$ (i.e., 2% heat losses) for all thermal energy balances, and a symptom when the arbitrary threshold $\varepsilon_{min}=-3\%$ is exceeded. This means that when using Eq. (3.3), a symptom is detected when the efficiency is lower than 95%. One exception is made for the ATEs system. The expected efficiency η_{exp} is set to 96% because of dissipation by the ATEs pumps and higher thermal energy losses underground, which leads to symptom detection when the efficiency is lower than 93%.

In addition to these efficiencies based on the application of system theory to the HVAC P&ID, efficiencies relating to heat exchange performance can be defined.

Eq. (3.11) is the equation for the annual efficiency of the heat balance of the ATEs system (depicted in Figure 3.4) which under the Dutch regulations needs to be 100%. Please note that η_{reg} , which is discussed in [26], can only be used in the case of annual analysis.

$$\eta_{reg} = 1 - \frac{abs(Q_{load} - Q_{unload})}{\max(Q_{load}, Q_{unload})} \quad (3.11)$$

Eq. (3.12) shows the annual efficiency of the heat exchanger of the ATEs system (see Figure 3.4 and system 8 in Figure 3.3, which shows the heat exchanger (8) and sensors TT02_01, TT02_02 and TT03_03), based on temperature efficiency⁸ instead of the NTU method (this is an arbitrary choice).

$$\eta_{TSA} = \frac{Q_{unload}}{Q_{unload, \max}} = \frac{\sum(TT02_{01} - TT02_{02})}{\sum(TT02_{01} - TT03_{03})} \quad (3.12)$$

According to the design, this efficiency should be at least 87%. It is assumed that a deviation threshold of 5% is acceptable.

3.7.2. Energy performance symptoms in the case study

This section presents the equations used to estimate the EP factors for performance factors, capacities and energy outliers.

3.7.2.1. Performance factors

Eqs. (3.13) to (3.15) show the performance factors for the aggregated systems under consideration: the hot water system E, the cold-water system A and the roof system F. SCOP_{hw} is the seasonal COP for the heat supply to the hot water system E. SEER_{cw} (Seasonal energy efficiency ratio cold water) defines the ratio between the cold supply to the cold-water system A and the energy consumption of the heat pump and the pumps in cooling mode. SCOP_{roof} denotes the SCOP for the roof heating. See Figure 3.4, which shows the energy amounts.

$$SCOP_{hw} = \frac{Q_{hw}}{W_{hp} + W_{02} + W_{03} + W_{04} + W_{07} + Q_{gas}} \quad (3.13)$$

$$SEER_{cw} = \frac{Q_{cw}}{W_{hp} + W_{02} + W_{03} + W_{04}} \quad (3.14)$$

$$SCOP_{roof} = \frac{Q_{roof_cw}}{W_{14} + W_{02} + W_{03}} \quad (3.15)$$

W₁₄ is the work of the pumps in the roof collector group (not shown in Figures 3.3 and 3.4). It only includes W_{hp}, W₀₂, W₀₃, W₀₄, W₀₇ and W₁₄ by the heat pump and the pumps needed for the thermal energy Q under consideration.

Eqs. (3.16) and (3.17) show the SCOP and SEER for the heat pump.

⁸ This is not energy efficiency as with the NTU method. It indicates to what extent the outlet temperature TT02-02 of the ATEs water reaches the inlet temperature TT03-03 of the distribution cold-water. If this efficiency is 100%, they would be equal.

$$SCOP_{hp} = \frac{Q_{cond_mod}}{W_{hp}} \quad (3.16)$$

$$SEER_{hp}^9 = \frac{Q_{evap_mod}}{W_{hp}} \quad (3.17)$$

Eq. (3.18) defines the SCOP for heat regeneration. SCOP_{reg} can be considered as a generic energy performance factor for ATES systems. W₁₄, W₀₈ and W₀₂ are the pump energy for heat regeneration purposes.

$$SCOP_{reg} = \frac{Q_{reg}}{W_{14}+W_{08}+W_{02}} \quad (3.18)$$

When the heat pump is simultaneously generating cold and heat for the emitter systems A, E and F, the electricity is divided proportionally based on the thermal energy supplied to systems A, E and F.

In this paper, we assume that a symptom is present when the measured SCOP or SEER is 5% lower than the expected value. International references for performance factors are not available, as the ATES system in the THUAS building is typical for the Netherlands. For the expected value, such as PF_{exp} in Eq. (3.4), we therefore use the Dutch guideline ISSO 39 [26], which describes thermal energy generation plants with ATES systems. These expected values can be found in Table 3A.2.

3.7.2.2. Capacities

The actual capacities can be determined by identifying the maximum heat flows P occurring during the measurement period. These values are compared with the nominal power of the apparatus and the heat and cold demand (see Table A.2). A threshold of $\varepsilon_{min}=-10\%$ is applied. Positive deviations would show that the system is working better than expected and are not therefore considered as symptoms.

3.7.3. Operational state symptoms in the case study

The approach using OS rules is also generic and can be set up once, for instance using a guideline. In most cases the thresholds are specific and need to be programmed only once in the particular BEMS, although default values can be used as well. Only design values of the temperature type are used in this paper. It goes without saying that far more rules than shown in this paper can be implemented: for instance, concerning pump flows and the heat shares delivered by the heat pump and boiler, or the cold delivered by the ATES system and the heat pump, or comparisons between design

⁹ Here we define SEER as the seasonal quotient of heat supplied to the evaporator of the heat pump and the work supplied when the heat pump functions simultaneously in both heat and cold production mode.

water flow values and measured values. We have omitted this from the present paper for the sake of simplicity.

Control-based rules are described first with the results of the detection process, followed by design-based rules for the year considered. As an additional condition, the measured values are considered if the system under consideration is operating for at least 30 minutes.

The detection period is a full year. For every day the mean weighted measured operational state value is calculated using the 16-minute values. If there are no measured values, that day is ignored. Thus, we have at most $n_{\text{tot}}=365$ in the detection period under consideration in Eq. (3.8).

3.7.3.1. Control-based rules

In the case study we consider the control set points of the systems' inlet and outlet temperatures. The supply water temperature of the hot and cold-water emitter systems E (Thw_supply) and A (Tcw_supply) is set by the control system. In addition, the outlet temperatures of the water to the evaporator (Tevap_out) and condenser (Tcond_out) from the heat pump have specific set-point values. The inlet water temperatures to the cold and warm wells of the ATES system (Tcold_well_in and Twarm_well_in) are also controlled.

In the case study the average daily deviation $\varepsilon=\Delta T$, as shown in Eq. (3.7), is calculated to estimate OS symptoms. When the additional conditions mentioned in Section 4.2.4 are met, the value 1 is added to the counter n_{tot} in Eq. (3.8) for the whole year. In addition, a detected symptom is counted as 1, otherwise as 0, and added to the annual fault counter n_{fault} in Eq. (3.8).

For the supply temperatures in the hot water circuit the assumed threshold ε_{max} is 3 K, due to control accuracy and transient behaviour. However, the control of the cold water has to be more accurate, as these values greatly affect the performance of the ATES system. Accurate cold-water controls are therefore provided, with three-way valves as actuators. An arbitrary threshold of 1 K is thus taken into account.

The inlet temperatures to the warm and cold wells of the ATES are essential and therefore controlled strictly, yielding an assumed threshold of 1 K.

Table 3A.3 shows the controlled values, which are derived from the design specification of the HVAC system of the THUAS building as shown in the HVAC P&ID.

3.7.3.2. Design-based rules

For the design-based rules we consider the water temperatures of systems A, B, C and E, for which either the inlet or outlet design temperatures are known. These temperatures are not controlled. We assume the same thresholds that have been

applied to the control-based temperatures, i.e., 3 K at the warm water side and 1 K at the cold-water side.

Table 3A.4 does not show the lower limit δ_{LL} and the upper limit δ_{UL} everywhere: where they are absent, the threshold can be ignored because negative and positive deviations have different meanings. For instance, if Thw_return is too low it will not decrease the COP of the heat pump, whereas it will if it is too high. In the same way a higher $Twarm_well_out$ and $Tevap_in$ are favourable. And a high Tcw_return helps to feed high-temperature heat into the warm well of the ATES system. Finally, a low $Tcold_well_out$ is desirable to avoid additional cooling by the heat pump. These rules are generally known by HVAC designers.

3.7.4. Symptoms detected in the case study

Appendix 3A shows results from the symptom detection process, which are discussed below.

3.7.4.1. Results from energy balances

Table 3A.1 shows the results for energy balance symptoms. Rules for the efficiencies η of the systems B to D and G and H do not generate symptoms, because all the annual deviations remain higher than ε_{min} during the year under consideration. The heat exchanger TSA of the ATES system also shows no symptoms, but the efficiency η_{reg} is far below the expected value, showing that the ATES system is unbalanced.

3.7.4.2. Results from energy performances

The results and reference values for the detection of EP symptoms are shown for the year 2013 in Table 3A.2. Most of the EP indicators are true, even better than the reference values, indicating high performance. For the SCOPs and SEERs, no symptoms are detected, except for SCOProof, which is more than 5% lower than the expected value.

In terms of capacity, most of the measured values are almost the same as the designed values. However, the maximum heat transfer power produced by the heat exchanger of the ATES system is much lower than the designed value and a symptom is therefore found. The capacity of the cold-water system A is also lower than designed and a symptom is detected here too. Symptoms of energy outliers were not found and are not therefore reported in Table 3A.2.

Only three EP factors are false and should be considered as symptoms: SCOProof, Pcw and PTSA.

3.7.4.3. Results from operational states

The detection process (see Table 3A.3) reveals a symptom of malfunctioning for four operational states: for the supply temperatures of the hot water system E, the cold-water system A and the inlet temperatures of the cold water well and warm water

well. Table 3A.4 summarises the design-based rules for detection purposes and the results of the detection process. One symptom is detected: the outlet temperature from the warm well.

Overview of the symptoms detected

Table 3.1 summarises the results of the annual detection process.

Table 3.1. Overview of the detection results
(P= symptom detected, A symptom absent)

| Energy balance symptoms | | Energy performance symptoms | | | | Operational state symptoms | | | |
|-------------------------|-----|-----------------------------|-----|----------|-----|----------------------------|-----|----------------|-----|
| Efficiency | A/P | Performance factor | A/P | Capacity | A/P | Control-based | A/P | Design-based | A/P |
| η_{systB} | A | SCOP _{hw} | A | Phw | A | Thw_supply | P | Thw_return | A |
| η_{systC} | A | SEER _{ew} | A | Pcw | P | Tcw_supply | P | Tcw_return | A |
| η_{systD} | A | SCOP _{proof} | P | Php | A | Tcond_out | A | Tevap_in | A |
| η_{systG} | A | SCOP _{preg} | A | Proof | A | Tevap_out | A | Tcold_well_out | A |
| η_{systH} | A | SCOP _{hp} | A | Preg | A | Tcold_well_in | P | Twarm_well_out | P |
| η_{TSA} | A | SEER _{hp} | A | PTSA | P | Twarm_well_in | P | | |
| η_{reg} | P | | | Pboiler | A | | | | |

As can be seen, nine symptoms were automatically detected as present and 22 as absent.

3.8. Evaluation of the results of the automated symptom detection process

For the analysis of the results on an annual basis, the 16-minute and daily data from the BMS were analysed using energy signature graphs for the whole year 2013, which are presented in Appendix B. Below we discuss the results from some of these energy signature graphs. In addition, interviews were conducted with the building manager and logbooks were consulted which did not lead to additional symptoms.

3.8.1. Evaluation of energy balance symptoms

In addition to the annual efficiencies as shown in Table 3A.1, the daily efficiencies of systems B, C, D, G and H are estimated (see Figure 3B.3). Most deviations remain under the set thresholds, which supports the reliability of the annual detection results for the energy balance symptoms. 3.8.2. Evaluation of EP symptoms

3.8.2.1. Performance factors

The daily COP and EER values of the heat pump fluctuate realistically (see Figure 3B.2) around the set thresholds with some outliers. The main causes of these outliers

are transient behaviour and the fact that the actual COPs and EERs depend on varying water temperatures.

The SEER_{cw} (60) (see Table 3A.2) was much higher than expected. Additional analysis of the energy data showed that cold was only provided by the cold well of the ATES system, whereas it was expected during design that the heat pump would deliver 10% of the cold, yielding a lower SEER_{cw} of 40.

3.8.2.2. Capacities

As for the capacities, 16-minute capacities were checked for the whole the year using graphs and symptoms were not missed. The inadequate capacity of the heat exchanger of the ATES system (PTSA) was correctly diagnosed (see Figure 3B.2, which shows the 16-minute graph): the actual capacity remains far below the design value (840 kW) throughout the year.

3.8.3. Evaluation of OS symptoms

Visual inspection of the energy signatures for the control-based and design-based operational states (see Figures 3B.4 to 3B.14) shows that they are close to the set point where symptoms are absent.

3.9. Detection time span

The detection process is described in Section 3.7 for a period of one year. However, where a symptom was found, it is quite clear, as the graphs in Appendix 3B show, that daily, weekly or monthly analysis could have enabled the symptoms to be found earlier. Conversely, a short period-level analysis can lead to the identification of a symptom that ultimately rarely occurs (for example, 3.1% of the days in Figure 3B.9). It is conceivable that the BEMS would simply warn that there is a potential fault and would only report a real problem after successive days, e.g., by using moving average methods, taking previous results into account to exclude temporary sensor outliers and effects of transient behaviour. This section discusses the use of shorter detection periods. We present results from monthly and daily symptom detection using rules from Section 3.7.

3.9.1. Monthly and daily detection of energy balance symptoms

Monthly detection

Outliers are not found for systems B, C, G and H using monthly detection based on Eq. (3.3). However, the boiler system D (see Table 3C.1) shows two outliers. We note that the exchanged energy of the boiler system was estimated using soft sensors for the flow rate and the return temperature at the boiler header (shown as (21) in

Figure 3.3), which introduces inaccuracies. The presence of hard sensors could lead to lower deviations.

Daily detection

Daily detection for energy balance symptoms (see Figure 3B.3) yields reasonable results. Only five false detection results were found, i.e., five outliers in 1825 detection results (<0.3%).

3.9.2. Monthly and daily detection of energy performance symptoms

Here we discuss the detection time span for EP symptoms. EP symptom detection is more complicated in monthly and daily detection due to operational conditions.

3.9.2.1. Performance factors

First, we address performance factors. As an example, we discuss the COP of the heat pump because this is one of the most important KPIs of the thermal energy plant. As this COP is strongly dependent on outdoor temperature levels, it is not acceptable to use the annual expected value, such as SCOP_{hp}=4 in Table 3A.2 (see Figure 3B.2), which shows many outliers. The effects of the water temperatures at the heat pump's evaporator and condenser, which are highly dependent on outdoor temperatures, must be considered. The thermodynamic efficiency η_{td} for several conditions could be estimated using the documentation on the heat pump installed. In the range of operational water temperatures in the case study they are between 0.37 and 0.39. Multiplying an assumed value of 0.38 by the COP of the Carnot process yields the expected performance COP_{exp}:

$$COP_{exp} = \eta_{td} \cdot COP_{Carnot} = \eta_{td} \cdot \frac{T_{high}}{T_{high} - T_{low}} \quad (3.19)$$

where:

T_{high} =T_{cond_out} and T_{low} =T_{evap_out} at which η_{td} is calculated.

Monthly detection

As can be seen from Table 3C.2, from June to August symptoms for the heat pump were incorrectly detected as present. However, in those months the heat pump was off most of the time. Transient behaviour strongly affected the results. To neglect this effect, we propose ignoring detection results from months in which a component is off most of the time.

Daily detection

Figure 3.5 shows a part of the daily COP of the heat pump and the expected values, taking thresholds of 5% into account. Here again the upper and lower limits are

calculated based on Eq. (3.4) for the thresholds. The measured values are showed in blue.

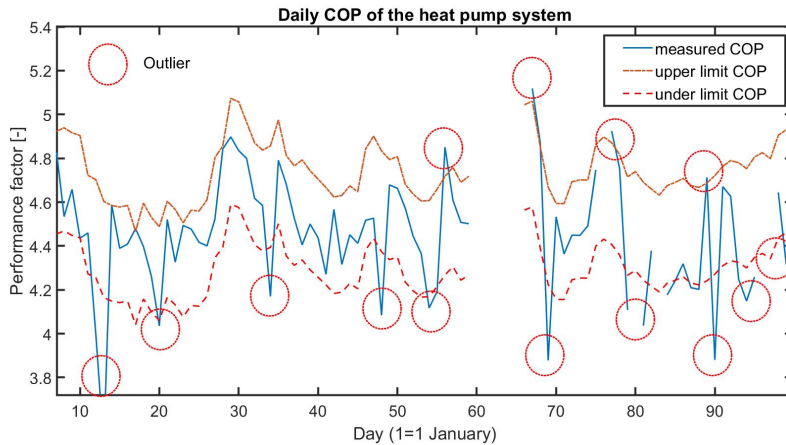


Figure 3.5. Daily COP of the heat pump system

As can be seen, the actual daily COP follows the expected COP. The heat pump was on for 165 days, with the upper limit exceeded by 21 days and the lower limit by 37 days, caused by transient behaviour and variation in the heat pumps' thermodynamic efficiency η_{td} .

3.9.2.2. Capacities

We take the boiler capacity as an example to show the monthly maximum heat flux in the gas boiler. There is no point in detecting capacity symptoms on a daily basis, because the nominal capacity is only achieved under full load conditions, which are not present every day. However, Table 3C.3 shows for example that the boiler capacity can be detected correctly for the winter months, when there is significant heat consumption by the boiler.

3.9.3. Monthly and daily detection of operational state symptoms

Monthly detection

The number of hours is considered in monthly detection, as opposed to the number of days in annual detection. Only hours that meet the additional condition that the system is on for 30 minutes are considered. Table 3C.4 shows for example results for T_{cond_out} , T_{cw_supply} and $T_{cold_well_in}$. False detections are highlighted in yellow. $T_{cold_well_in}$ shows no false detection results. However, T_{cond_out} and T_{cw_supply} are incorrectly detected as present or absent in some months, which may be due to assumed thresholds that are too low and transient behaviour.

Daily detection

Daily detection of operational state symptoms based on Eq. (3.7) makes no sense because we know from Figures 3B.4 to 3B.14 that this yields many wrong detections.

3.9.4. Conclusions and recommendations for daily and monthly detection time spans

Overall, we note that daily detection of energy efficiencies yields acceptable detection results. The outliers for the boiler system efficiencies show the need to avoid complex soft sensors as much as possible. In the case of new HVAC systems, the necessary measuring points must be present to avoid complex models for estimating exchanged energy quantities.

Research into additional conditions as mentioned in 3.4.2.4 is needed: for instance, to take into account hours in which the exchanged energy is higher than a certain threshold. This would avoid incorrect monthly detections of the COP of the heat pump and the boiler capacity, as shown in Appendix C. However, it would also be possible to start up the energy plant, e.g., daily, weekly or monthly, at different full load modes to estimate symptoms earlier.

To increase the reliability of the detection results, especially when using daily detection, we propose researching the use of smoothing techniques which calculate the average deviation based on two or more days, to compensate for daily outliers. In addition to a CUSUM (cumulative sum control chart), one could apply the EWMA (exponentially weighted moving average) chart method (see [27] for implementation).

We also recommend researching the application of this to daily binary detection outcomes (e.g., -1: too low, 0: correct, 1: too high).

Daily detection of the capacities of thermal energy systems makes no sense because full load does not occur every day and start-up every day requires a great deal of energy in full-load mode. However, this is a realistic solution for distribution systems (pump, fans and valves).

Another approach which is applicable to all KPIs is to give a warning that could not lead to direct action on the part of the technical manager or to an automated fault diagnosis. Diagnosis could take place after structural false detections.

3.10. Conclusion and recommendations

Current symptom detection methods for energy diagnosis in HVAC systems are not standardised and there is still no classification of detection models with generic key performance indicators and associated detection rules. This paper presents a classification of symptoms into three categories: balance, energy performance and operational states, that covers a large part of encountered symptoms. Detection models and KPIs are developed for these 3 categories. Generic detection rules for energy diagnosis in heating, ventilation and air conditioning (HVAC) systems are proposed which are consistent with HVAC process and instrumentation diagrams (P&IDs) as used by engineers to design and operate these systems. It has been applied successfully to the thermal energy plant of the THUAS school building. One whole year was taken as the detection period. However, monthly and daily detection also yielded adequate results. Section 3.10.1 summarises the results for the detection framework in more detail and Section 3.10.2 draws conclusions from the case study. Section 3.10.3 proposes recommendations for the standardisation of symptom detection.

3.10.1. Results of the detection framework based on the 4S3F method

The proposed framework for energy performance analysis falls into four phases: pre-processing, detection, diagnosis and correction. This article focuses on the symptom detection phase based on the 4S3F architecture, which contains four types of symptoms and three types of faults. The three main types of symptoms are discussed, and rules and thresholds are developed:

- Balance symptoms: efficiencies.
- Energy performance (EP) symptoms: performance factors such as COPs and EERs, capacities such as nominal heat and cold rates and flow rates, and energy outliers such as unexpected energy consumption.
- Operational state (OS) symptoms: control-based symptoms such as controlled supply temperatures, and design-based symptoms such as expected return temperatures from energy users.

The approach discussed is congruent with the way engineers design an HVAC system. The HVAC designer uses the P&IDs for detection purposes. In the pre-processing phase, systems and aggregated systems are determined once by the HVAC designer. For the detection process, the same HVAC designer must list all the possible symptoms (balance, EP and OS based) once that could be occurring in the system based on the measurement points in the P&ID. Each of the symptoms relates to the equations and models described in the present paper, which could easily be compiled into a standard guideline.

The detection process can be fully automated by using generic detection models for aggregated systems such as generator, hydronic and emitter systems. These equations have to be programmed in the BEMS once, preferably producing symptoms at day, week, month, season and annual level.

The next step is to use these symptoms to identify the faults causing them, using the 4S3F methods and DBNs: this will be discussed in detail in another paper. However, the simple fact of having an automated symptom detection system covering a wide range of parameters is already very helpful for energy performance diagnosis.

3.10.2. Conclusions from the case study

The case study successfully demonstrated the symptom detection part of the 4S3F framework for a thermal energy plant with an ATEs system. One whole year, with 16-minute time interval, historical data was examined to show how symptoms leading to faults can be detected automatically.

The evaluation has shown that no symptoms were overlooked or incorrectly detected.

Section 3.9 discussed time spans shorter than one year, showing that the proposed symptom detection method can be used for daily and monthly detection, provided that the recommendations in Section 3.9.4 are followed.

In our case study, an HVAC commissioning engineer would focus on the nine symptoms detected to optimise the system. In a subsequent paper, we will show that by redesigning the control rules a 25% annual primary energy saving could be achieved in the case study, which is a thermal heat plant with a reputation for working well. This indicates that far more energy savings would be possible if such symptom detection methods were used more widely.

3.10.3. Recommendations for further research

Although the results are promising, further research is needed. We have not considered developing the fault identification model with a DBN included in the 4S3F framework here.

Further research is needed into the question of which threshold values should be used for the KPIs and that of which symptom detection period (hourly, daily or seasonable) is needed for which systems and subsystems. Given the question of KPI thresholds, research into dynamic KPIs for hourly and daily detection is recommended. It also needs to be examined whether the HVAC can be started up automatically daily, weekly or monthly by the BMS in different HVAC modes to hasten the detection of symptoms.

In addition, a guideline on the minimum BMS dataset needed to estimate energy amounts to and from systems would be helpful. It could be worthwhile to expand the list of symptoms: for instance, with OS symptoms concerning flow rates, valves and

pumps. Additional symptoms from maintenance logbooks and commissioning reports were not included but could offer additional possibilities.

For automation purposes, a generic library of symptom detection models is needed from which EP models can be selected in a specific case. A start has been made in this paper.

Appendix 3A. Threshold values and results from annual detection

This appendix presents information on threshold values for the four types of symptoms in the 4S3F method in tables. Detection results from annual detection are also presented.

As shown in Table 3A.1, a symptom is present (depicted as **P**) for η_{reg} . The other symptoms are absent (**A**).

Table 3A.1. Annual detection results: energy balance symptoms

(**A**: symptom absent; **P**: symptom present)

| System | Efficiency | Efficiency in accordance with guideline ISO 39 [26] or design | Measured efficiency | Symptom detection |
|--------------------------------|----------------|---|---------------------|-------------------|
| ATES system (B) | η_{systB} | 0.93 | 0.94 | A |
| Heat pump system (C) | η_{systC} | 0.95 | 0.95 | A |
| Boiler system (D) | η_{systD} | 0.95 | 0.95 | A |
| Hydronic cold-water system (G) | η_{systG} | 0.95 | 0.99 | A |
| Hydronic cold-water system (H) | η_{systH} | 0.95 | 0.98 | A |
| ATES system (B) | η_{TSA} | 0.87 | 0.97 | A |
| ATES system (B) | η_{reg} | 1 | 0.63 | P |

Table 3A.2 presents the results for the energy performance factors (EPFs)

Table 3A.2. Measured annual EPFs and reference annual EPFs

(**A**: indicates symptom absent; **P**: symptom present)

| System | EP factor | EP factor in accordance with guideline ISO 39 [27] or design | Measured SPF | Symptom detected |
|---|-----------------------|--|--------------|------------------|
| Whole system (B to D, and H and G) | SCOP _{hw} | 3 | 3 | A |
| Whole system (B to D, and H and G) | SEER _{cw} | 40 | 60 | A |
| ATES system (B) | SCOP _{reg} | 20 | 22.3 | A |
| Heat pump system (C) | SCOP _{hp} | 4 | 4.5 | A |
| Heat pump system (C) | SEER _{hp} | 3.2 | 3.6 | A |
| Roof system (F) | SCOP _{proof} | 20 | 16.7 | P |
| Hot water capacity (E) | Phw | 597 kW | 540 kW | A |
| Cold water capacity (A) | Pcw | 742 kW | 450 kW | P |
| Roof collector capacity (F) | Proof | 576 kW | 531 kW | A |
| Heat pump capacity (C) | Php | 247 kW | 270 kW | A |
| Gas boiler capacity (D) | Pboiler | 327 kW | 400 kW | A |
| Capacity of heat exchanger TSA from ATES system (8) | PTSA | 840 kW | 590 kW | P |
| Heat regeneration capacity of ATES system (B) | Preg | 237 kW | 250 kW | A |

Tables 3A.3 and 3A.4 present results for operational state symptoms. As can be seen, five operational state symptoms were detected.

Table 3A.3. Thresholds for set-point values and symptoms of control-based indicators

(A: symptom absent P: symptom present)

| | Controlled value | Measured by sensor (see Figure 3.6) | Thresholds | Symptom detected | |
|---|--|--|-------------------------|------------------|---|
| | | | | δ [%] | |
| Hot water supply (E) (Thw_supply, Figure 5.2.) | Winter mode: varying linearly between 45 and 35°C at outdoor temperatures between -10 and 15°C. Summer mode: 30°C. | TT28_02 | $\epsilon_{\max} = 3$ K | δ [%] | |
| | | | $\delta_{LL} = 10\%$ | 11.1 | P |
| | | | $\delta_{UL} = 10\%$ | 0.9 | A |
| Cold water supply (A) (Tew_supply, Figure 5.3.) | Varying linearly between 15 to 11°C at outdoor temperatures between 15 and 25°C. | TT29_02 | $\epsilon_{\max} = 1$ K | δ [%] | |
| | | | $\delta_{LL} = 10\%$ | 0.5 | A |
| | | | $\delta_{UL} = 10\%$ | 22.8 | P |
| Outlet of cold-water heat pump (C) (Tcond_out, Figure 5.4) | 8.5°C in winter mode. | TT04_01 | $\epsilon_{\max} = 3$ K | δ [%] | |
| | | | $\delta_{LL} = 10\%$ | 3.1 | A |
| | | | $\delta_{UL} = 10\%$ | 4.0 | A |
| Outlet of evaporator (C) (Tevap_out, Figure 5.5) | 7°C in winter mode. | TT04_04 | $\epsilon_{\max} = 1$ K | δ [%] | |
| | | | $\delta_{LL} = 10\%$ | 0.9 | A |
| | | | $\delta_{UP} = 10\%$ | 3.1 | A |
| Inlet of cold water well (B) (Tcold_well_in, Figure 5.6) | 7.5°C | TT02_01 | $\epsilon_{\max} = 1$ K | δ [%] | |
| | | | $\delta_{LL} = 10\%$ | 0.0 | P |
| | | | $\delta_{UL} = 10\%$ | 68.5 | A |
| Inlet of warm water well (B) (Twarm_well_in, Figure 5.7) | 17.5°C, 20°C in regeneration mode. | TT02_03 | $\epsilon_{\max} = 1$ K | δ [%] | |
| | | | $\delta_{LL} = 10\%$ | 18.9 | P |
| | | | $\delta_{UL} = 10\%$ | 8.3 | A |

Table 3A.4. Thresholds for design-based indicators and symptom detection

(A: symptom absent P: symptom present)

| | Design value | Measured by sensor (see Figure 3.6) | Thresholds | No symptom detected | |
|--|---|--|---|---------------------|---|
| | | | | δ [%] | |
| Hot water return (E) (Thw_return, Figure 5.8) | 35°C in winter mode, 24°C in summer mode | TT28_03 | $\epsilon_{\max} = 3$ K $\delta_{UL} = 10\%$ | 69.9 | A |
| Cold water return (A) (Tew_return, Figure 5.9) | 19°C | TT29_04 | $\epsilon_{\max} = 1$ K $\delta_{LL} = 10\%$ | 9.2 | A |
| Input of evaporator (C) (Tevap_in Figure 5.10) | 12°C in winter mode, 19°C in summer mode | TT04_05 | $\epsilon_{\max} = 1$ K $\delta_{UL} = 10\%$ | 0.0 | A |
| Outlet of cold water well (B) (Tcold_well_out, Figure 5.11) | 8.5°C in summer mode | TT02_01 | $\epsilon_{\max} = 1$ K $\delta_{UL} = 10\%$ | 7.8 | A |
| Outlet of warm water well (B) (Twarm_well_out, Figure 5.12) | 16.5°C in winter mode | TT02_03 | $\epsilon_{\max} = 1$ K $\delta_{LL} = 10\%$ | 48.7 | P |

Appendix 3B. Results from daily detection

This appendix presents results from daily detection.

Figure 3B.1 shows the daily COPs and EERs of the heat pump system.

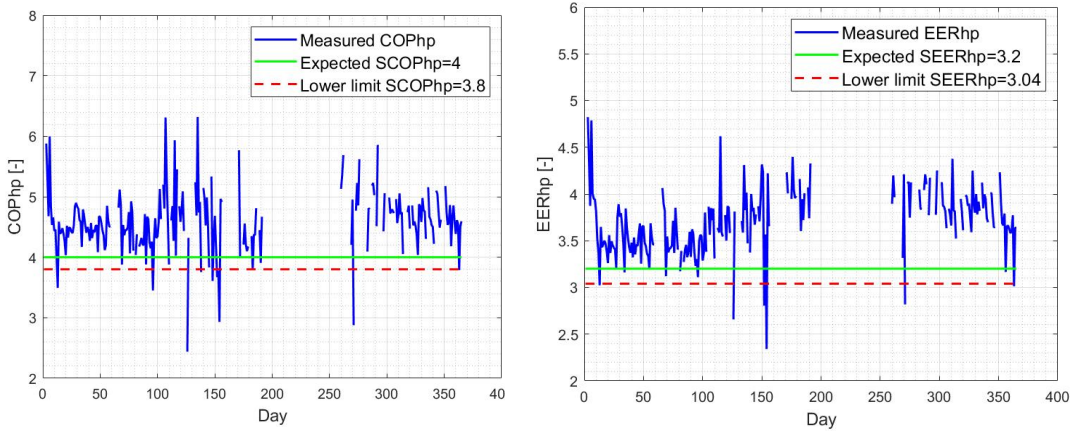


Figure 3B.1 Daily energy performance factors of the heat pump

The maximum heat flux of the heat exchanger TSA of the ATES system is shown in Figure 3B.2 based on 16-minute time spans. Positive values are present when the warm well is used, negative when the cold well is used.

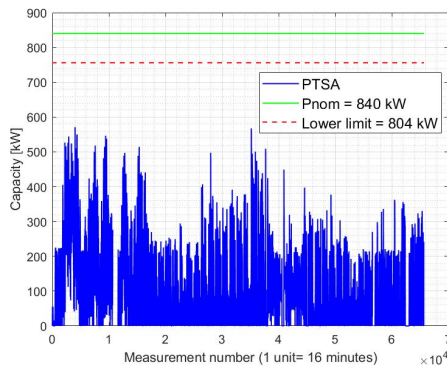
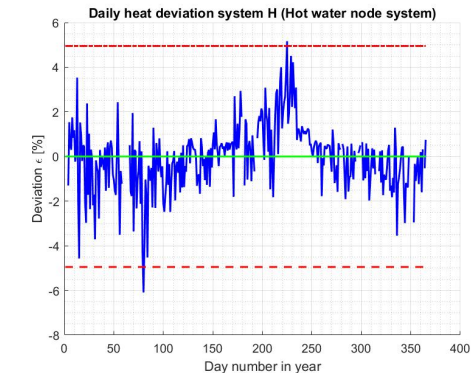
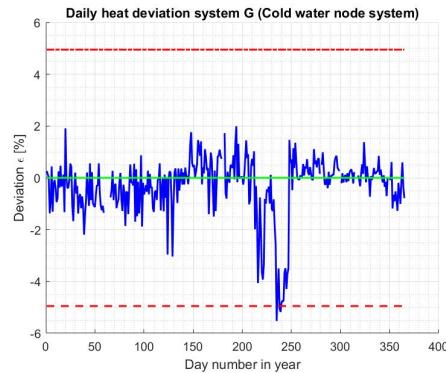
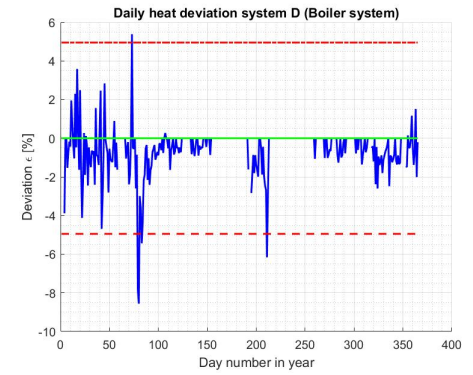
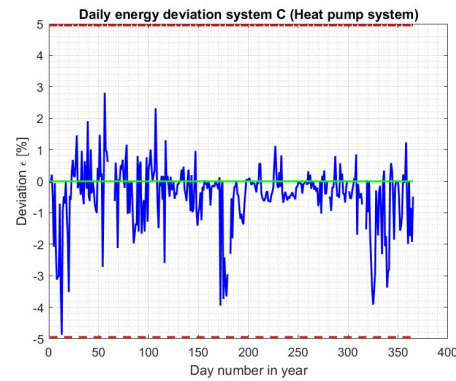
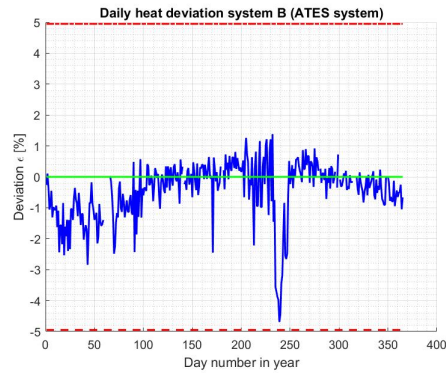


Figure 3B.2 Measured capacity of the heat exchanger (TSA) of the ATES system throughout the year 2013.

Figure 3B.3 shows the daily deviations of the systems B to D, G and H. As can be seen, they almost all remain under the thresholds.



- Measured
- Expected
- Upper limit $\epsilon_{\max} = 5\%$
- Lower limit $\epsilon_{\min} = -5\%$

Figure 3B.3 Daily efficiencies of systems B, C, D, G and H

Figures 3B.4 to 3B.14 show energy signatures for operational states. One year was taken as the detection period. Each point indicates the result of one day. A detected symptom is indicated as **P** and as **A** when absent. n_{tot} represents the number of days for which the system that affects the operational state is active. As a reference, each figure shows the values expected from the control set points or the design values. The acceptable limits ε_{min} and ε_{max} for ΔT are shown as presented in Tables 3A.3 and 3A.4. In these graphs ‘no symptom detected’ is indicated by an **A** (absent) and ‘a symptom detected’ by a **P** (present), in line with Tables 3A.3 and 3A.4. A value in brackets indicates that a threshold was not seen.

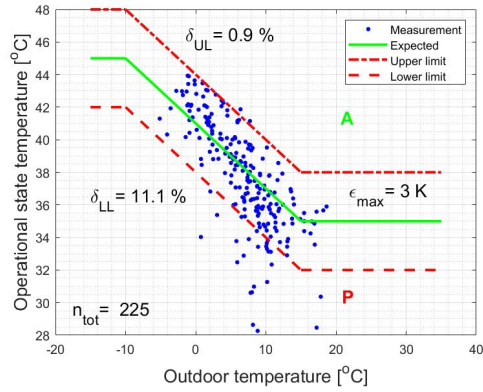


Figure 3B.4 Energy signature of Thw_supply

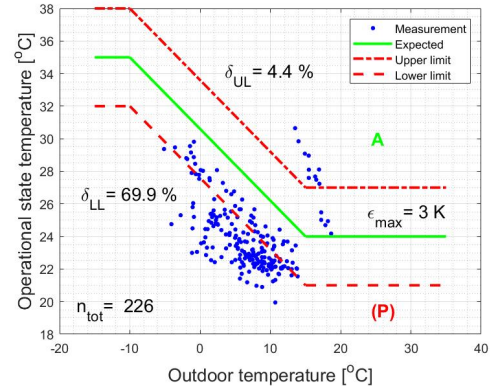


Figure 3B.5 Energy signature of Thw_return

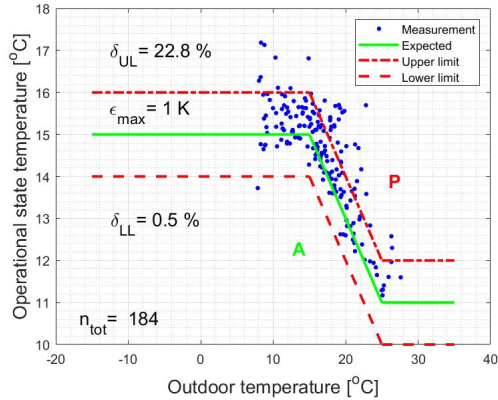


Figure 3B.6 Energy signature of Tcw_supply

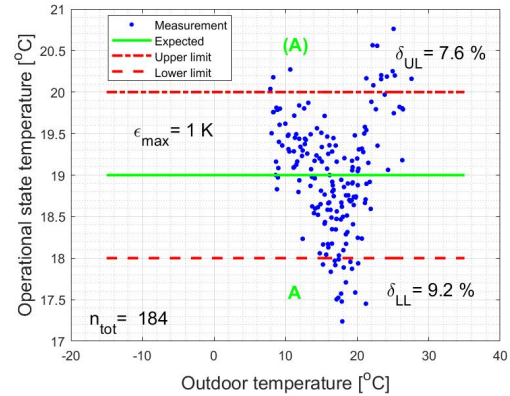


Figure 3B.7 Energy signature of Tcw_return

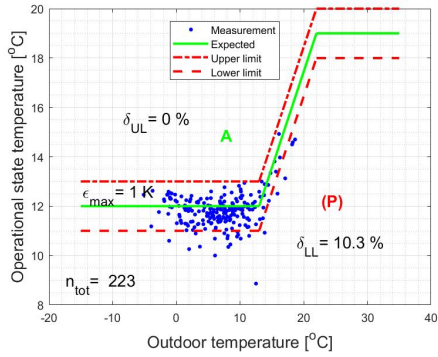


Figure 3B.8 Energy signature of Tenv_in

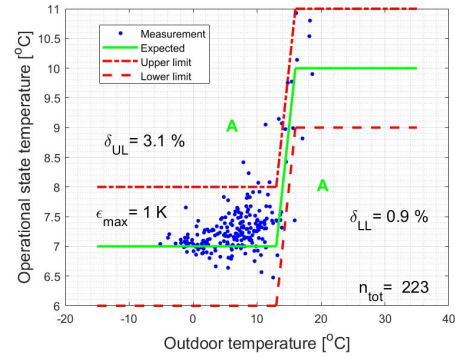


Figure 3B.9 Energy signature of Tenv_out

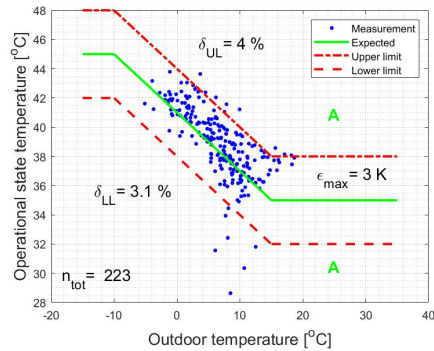


Figure 3B.10 Energy signature of Tcond_out

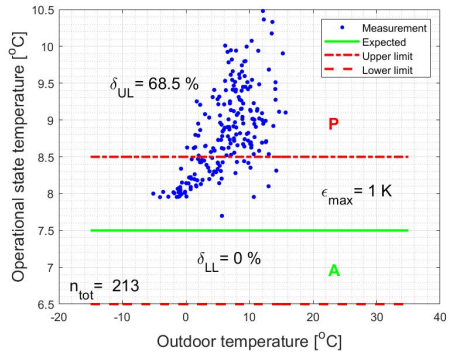


Figure 3B.11 Energy signature of Tcold_well_in

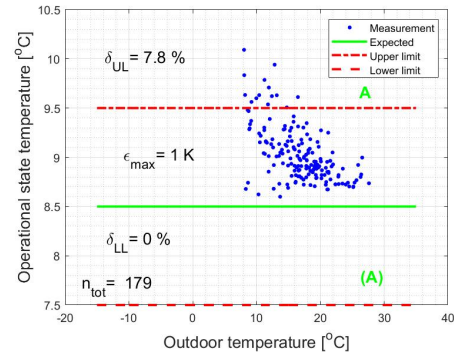


Figure 3B.12 Energy signature of Tcold_well_out

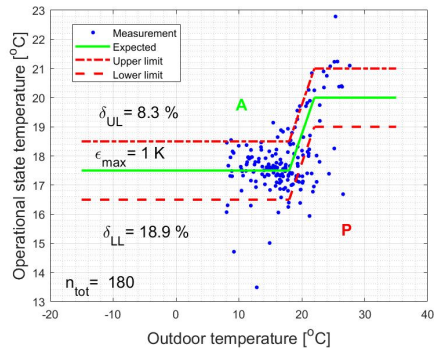


Figure 3B.13 Energy signature of Twarm_well_in

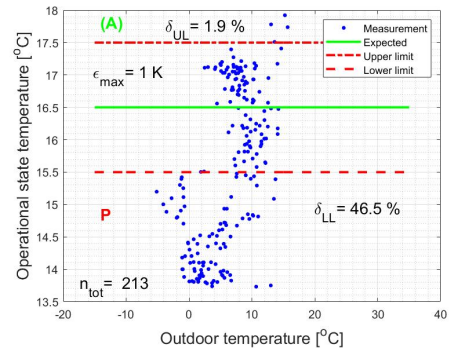


Figure 3B.14 Energy signature of Twarm_well_out

Appendix 3C. Results from monthly detection

This appendix presents some detection results from monthly detection periods. False detection results, deviating from the annual outcomes, are shown highlighted in grey background. Table 3C.1 shows the outcomes for the boiler system D.

Table 3C.1 Monthly energy balance symptoms of boiler system D

Grey background: Symptom is present (δ_{UL} =above upper limit, δ_{LL} =under lower limit, NA=not available, n_{day} =number of operational days)

| Symptom | Jan | Feb | Mar | Apr | May | Jun | Jul | Aug | Sep | Oct | Nov | Dec | Annual |
|------------------------|-----|-----|-----|-----|-----|-----|-----|-----|-----|-----|-----|-----|--------|
| ε [%] | -2 | -3 | -7 | -3 | -1 | 0 | -5 | 0 | -1 | -2 | -3 | -3 | -0.4 |
| Q_{boiler_mod} [GJ] | 60 | 35 | 66 | 12 | 3 | 0 | 3 | 0 | 0 | 0 | 1 | 13 | 198 |

Table 3C.2 shows the monthly deviation ε of the SCOP of the heat pump based on the days in the month for which the SCOP could be estimated. The heat produced monthly is divided by the work supplied by the heat pump monthly to estimate the measured monthly SCOP_{hp}. The reference SCOP_{exp} is calculated using Eq. (3.16).

As can be seen from this table, a monthly detection period leads to symptoms for June to September despite the fact that the annual SCOP for the heat pump apparently indicates a correct COP.

Table 3C.2 Monthly SCOP symptoms of the heat pump on a daily basis

Gray background: Symptom is present, ε =deviation between SCOP_{hp} and SCOP_{exp}

| Symptom | Jan | Feb | Mar | Apr | May | Jun | Jul | Aug | Sep | Oct | Nov | Dec | Annual |
|----------------------|-----|-----|------|------|------|-----|-----|------|------|-----|------|-----|--------|
| SCOP _{hp} | 4.5 | 4.5 | 4.4 | 4.5 | 4.7 | 4.2 | 3.9 | 0.0 | 4.9 | 4.9 | 4.7 | 4.7 | 4.5 |
| SCOP _{exp} | 4.5 | 4.5 | 4.5 | 4.7 | 4.8 | 5.0 | 5.0 | 5.0 | 4.9 | 4.9 | 4.7 | 4.7 | 4 |
| ε [%] | 1.1 | 0.0 | -1.2 | -3.3 | -2.5 | -16 | -23 | -101 | -1.3 | 1.6 | -0.9 | 0.0 | 12.5 |
| Q_{cond_mod} [GJ] | 316 | 282 | 166 | 102 | 33 | 21 | 7 | 0 | 8 | 33 | 115 | 192 | 1313 |

The maximum heat flux measured in each month is shown in Table 3C.3. As can be seen, capacity is low in the months May to November.

Table 3C.3 Symptoms for the capacity of the boiler

(grey background: symptom present)

| Symptom | Jan | Feb | Mar | Apr | May | Jun | Jul | Aug | Sep | Oct | Nov | Dec | Annual |
|-----------------------|-----|-----|-----|-----|-----|-----|-----|-----|-----|-----|-----|-----|--------|
| P _{boiler} | T | T | T | T | F | F | F | - | F | F | F | T | T |
| P _{max} [kW] | 394 | 380 | 400 | 311 | 227 | 67 | 22 | NaN | 56 | 63 | 62 | 377 | 400 |

Table 3C.4 presents the results for monthly symptoms for three OS variables considered in the case study: T_{cond_out}, T_{ew_supply} and T_{cold_well_in}. In this table δ_L and δ_H represent the monthly percentage by which the lower and upper limit thresholds are exceeded, calculated using Eq. (3.8). Those hours n_{tot} are shown in Table 3B.4 for each month. For those hours an exceeded threshold is added to n_{fault} as a counter. This table also shows the exchanged energy E_{month} during those hours.

Table 3C.4 Monthly OS symptoms

(grey background: incorrect detection)

(δ_{UP} =above upper limit, δ_{LL} =under lower limit, NA=not available, n_{tot} =number of operational hours or days, E_{month} =exchanged energy)

| Symptom | | Jan | Feb | Mar | Apr | May | Jun | Jul | Aug | Sep | Oct | Nov | Dec | Annual |
|---------------|-------------------|------|------|------|------|------|------|------|------|------|------|-----|------|----------|
| Tcond_out | δ_{UL} [%] | 0 | 0 | 0 | 11.1 | 9.1 | 20.0 | 75.0 | NA | 0 | 0 | 4 | 0 | 4 |
| | δ_{LL} [%] | 6.9 | 0 | 4.2 | 3.7 | 4.5 | 0 | 0 | NA | 16.7 | 5.9 | 0 | 0 | 3.1 |
| | n_{tot} [hr] | 347 | 316 | 208 | 120 | 33 | 23 | 3 | 0 | 7 | 33 | 155 | 247 | 223 days |
| | E_{month} [GJ] | 65 | 58 | 36 | 21 | 6 | 4 | 0 | 0 | 1 | 5 | 23 | 38 | |
| | | | | | | | | | | | | | | |
| Tew_supply | δ_{UL} [%] | 100 | NA | 0 | 17.6 | 4.5 | 4.2 | 8.0 | 20.0 | 53.3 | 17.4 | 0 | 0 | 22.8 |
| | δ_{LL} [%] | 0 | NA | 0 | 0 | 0 | 0 | 0 | 0 | 0 | 0 | 0 | 100 | 0.5 |
| | n_{tot} [hr] | 0 | 0 | 7 | 42 | 96 | 225 | 241 | 256 | 619 | 87 | 6 | 0 | 184 days |
| | E_{month} [GJ] | 0 | 0 | 3 | 18 | 53 | 157 | 213 | 140 | 297 | 37 | 2 | 0 | |
| | | | | | | | | | | | | | | |
| Tcold_well_in | δ_{UL} [%] | 17.9 | 10.7 | 16.0 | 70.4 | 94.7 | 88.9 | 100 | NA | 100 | 76.5 | 92 | 61.5 | 68.5 |
| | δ_{LL} [%] | 0 | 0 | 0 | 0 | 0 | 0 | 0 | NA | 0 | 0 | 0 | 0 | 0 |
| | n_{tot} [hr] | 398 | 370 | 291 | 140 | 32 | 16 | 2 | 0 | 6 | 32 | 174 | 265 | 213 days |
| | E_{month} [GJ] | 441 | 346 | 229 | 76 | 8 | 2 | 0 | 0 | 1 | 10 | 81 | 181 | |
| | | | | | | | | | | | | | | |

References

- [1] P. de Wilde, The gap between predicted and measured energy performance of buildings: A framework for investigation. Automation in Construction 41 (2014) 40-49. <https://doi.org/10.1016/j.autcon.2014.02.009>.
- [2] A. Taal, L. Itard, W. Zeiler, A referenced architecture for the integration of automated energy performance fault diagnosis in HVAC systems, Energy & Buildings 179 (2018) 144-155, <https://doi.org/10.1016/j.enbuild.2018.08.031>.
- [3] L. Haorong, Y. Daihong, J. Braun, A review of virtual sensing technology and application in building systems, HVAC&R Research, 17:5(2011) 619-645, <https://www.tandfonline.com/doi/abs/10.1080/10789669.2011.573051>.
- [4] BuildingEQ (2018). <http://www.buildup.eu/en/practices/cases/building-eq-tools-and-methods-linking-epbd-and-continuous-commissioning>
- [5] European Standard EN 15316-1:2017. Energy performance of buildings. Method for calculation of system energy requirements and system efficiencies. General and Energy performance expression, Module M3-1, M3-4, M3-9, M8-1, M8-2 (2017) CEN, Brussels.
- [6] W. Kim, S. Katipamula, A Review of Fault Detection and Diagnostics Methods for Building Systems. Science and Technology for the Built Environment, 24:1 (2017), 3-21, <https://doi.org/10.1080/23744731.2017.1318008>.
- [7] Z. Guo, X.Liu, W. Tao, R. Shah, Effectiveness–thermal resistance method for heat exchanger design and analysis. International Journal of Heat and Mass Transfer,

Volume 53, Issues 13–14 (2010), Pages 2877-2884.
<https://doi.org/10.1016/j.ijheatmasstransfer.2010.02.008>

[8] L.Gao, J. Zhao, Q. An, J. Wang, X. Liu, A review on system performance studies of aquifer thermal energy storage. *Energy Procedia* 142 (2017) 3537-3545.
<https://doi.org/10.1016/j.egypro.2017.12.242>

[9] W. Chung, Review of building energy-use performance benchmarking methodologies. *Applied Energy* 88 (2011) 1470-1479.
<https://doi.org/10.1016/j.apenergy.2010.11.022>.

[10] J. Liu, H. Chen, J. Liu, Z. Li, R. Huang, L. Xing, An Energy performance evaluation methodology for individual office building with dynamic energy benchmarks using limited information. *Applied Energy* 206 (2017) 193-205.
<https://doi.org/10.1016/j.apenergy.2017.08.153>

[11] Y. Wei, X. Zhang, Y. Shi, L. Xia, S. Pan, J. Wu, M. Han, A review of data-driven approaches for prediction and classification of building energy consumption. *Renewable and Sustainable Energy Reviews* 82 (2018) 1027-1047.
<https://doi.org/10.1016/j.rser.2017.09.108>.

[12] E.H. Borgstein, R. Lamberts, J.L.M. Hensen, Evaluating energy performance in non-domestic buildings: A review. *Energy and Buildings* 128 (2016) 734-755.
<https://doi.org/10.1016/j.enbuild.2016.07.018>.

[13] Z. Li, Y. Han, P. Xu, Methods for benchmarking building energy consumption against its past or intended performance: An review. *Applied Energy* 124 (2014) 325-334. <https://doi.org/10.1016/j.apenergy.2014.03.020>.

[14] H. Wang, P. Xu, X. Lu, D. Yuan, Methodology of comprehensive building energy performance diagnosis for large commercial buildings at multiple levels. *Applied Energy* 169 (2016) 14-27. <https://doi.org/10.1016/j.apenergy.2016.01.054>.

[15] R. Hitchin, I. Knight, Daily energy consumption signatures and control charts for air-conditioned buildings. *Energy and Buildings* 112 (2016) 101-109.
<https://doi.org/10.1016/j.enbuild.2015.11.059>.

[16] J. Bynum, D. Claridge, J. Curtin, Development and testing of an Automated Building Commissioning Analysis Tool (ABCAT). *Energy and Buildings* 55 (2012) 607-617. <https://doi.org/10.1016/j.enbuild.2012.08.038>.

[17] G. Anzaldi, A. Corchero, H. Wicaksono, K. McGlenn, A. Gerdelan, M. Dibley, Knoholem: Knowledge-Based Energy Management for Public Buildings Through Holistic Information Modeling and 3D Visualization (2013).
https://doi.org/10.1007/978-3-319-02332-8_5.

- [18] T. Maile, V. Bazjanac, M. Fisher, A method to compare simulated and measured data to assess building energy performance. *Building and Environment* 56 (2012) 241-251. <https://doi.org/10.1016/j.buildenv.2012.03.012>.
- [19] D. Choiniere, D. DABOTM: A BEMS assisted on-going commissioning tool (2008). Proceedings of the National Conference on Building Commissioning 2008. <https://www.bcxa.org/ncbc/2008/docs/Choiniere.pdf>
- [20] L. Belussi, L. Danza, Method for the prediction of malfunctions of buildings through real energy consumption analysis: Holistic and multidisciplinary approach of Energy Signature. *Energy and Buildings* 55 (2012) 715-720. <https://doi.org/10.1016/j.enbuild.2012.09.003>.
- [21] A. Costa, M. Keane, J. Torrens, E. Corry, Building operation and energy performance: Monitoring, analysis and optimization toolkit. *Applied Energy* 101 (2013), 310-306. (WBD). <https://doi.org/10.1016/j.apenergy.2011.10.037>.
- [22] L. Zhao, J. Zhang, R. Liang, Development of an energy monitoring system for large public buildings. *Energy and Buildings* 66 (2013) 41-48. <https://doi.org/10.1016/j.enbuild.2013.07.007>.
- [23] A. Ahmed, J. Ploennig, K. Menzel, B. Cahill, Multi-dimensional building performance data management for continuous commissioning, *Advanced Engineering Informatics* 24 (2010) 466-475. <http://dx.doi.org/10.1016/j.aei.2010.06.007>
- [24] C. Miller, Z. Nagy, A. Schlueter, Automated daily pattern filtering of measured building performance data. *Automation in Construction* 49 (2015) 1-17. <https://doi.org/10.1016/j.autcon.2014.09.004>
- [25] B. Bozkaya, R. Li, W. Zeiler, A dynamic building and aquifer co-simulation method for thermal imbalance investigation. *Applied Thermal Engineering* 144 (2018) 681-694. <https://doi.org/10.1016/j.applthermaleng.2018.08.095>.
- [26] Energiecentrale met warmte en koude opslag (WKO), ISSO-publicatie 39 (2017). ISSO. ISBN: 978-90-5044-307-4978-90-5044-307-4.
- [27] Y. Zhao, S. Wang, F. Xiao, A system-level incipient fault-detection method for HVAC systems (2013). *HVAC&R Research*, 19:5, 593-601. <http://hdl.handle.net/10397/23739>

4. P&ID-based automated fault identification for energy performance diagnosis in HVAC systems: 4S3F method, development of DBN models and application to an ATES system.

This chapter has been published as:

Arie Taal, Laure Itard, “P&ID-based automated fault identification for energy performance diagnosis in HVAC systems: 4S3F method, development of DBN models and application to an ATES system”, *Energy & Buildings* **224** (2020) 110289

In this chapter, the fault isolation in the 4S3F method is presented which is conducted on the thermal energy plant of the building of the Hague University of Applied Sciences in Delft. In addition, energy savings are estimated after the founded fault corrections.

4.1. Introduction

As noted in [1], for example, fault detection is the detection of the presence of faults in the functioning of a system by means of symptoms. To use healthcare as an analogy, faults can be seen as illnesses which lead to symptoms. These faults are isolated and evaluated in the diagnosis process.

Despite the many studies of building commissioning and energy management, building energy analysis systems with fully automated fault detection and diagnosis are rarely applied in practice, resulting in unnecessarily high energy consumptions. In [2] a first draft of the 4S3F method was presented. This method, based on data provided by the Building Management System (BMS), aims to achieve automated continuous energy diagnosis of complex heating, ventilation and air conditioning (HVAC) systems using a systematic approach based on the information contained in process & instrumentation diagrams (P&IDs) and the subsequent analysis of four categories of symptoms and three categories of faults (4S3F). This 4S3F method is present in the Building Energy Management System (BEMS), which can either be a separate application or be implemented in the BMS. The method was shown to overcome the problem of energy diagnosis systems seldom being used in practice because their design does not reflect how HVAC designers work. Furthermore, the process of using energy diagnosis to isolate faults is far from fully automated at present, there is little standardization of energy diagnosis, and few generic methods are applicable which can be applied regardless of the type of HVAC system. This

leads to solutions which are not only very specific to particular HVAC systems, but which are also time-consuming to implement.

In [2], a first draft of the 4S3F architecture was tested on a simple theoretical case. In the current article, the diagnosis phase in the 4S3F method is applied to a thermal energy plant with real sensor data for a whole year, in the assumption that symptoms have already been identified at this stage.

A great deal of research has been conducted on automated fault detection and diagnosis (FDD). Kim and Katipamula presented in [3] an overview of existing FDD methods for HVAC systems. Various diagnosis methods can be applied depending on the detection method. In the last decade, data-driven detection methods have been discussed, such as those based on regression formulas, artificial neural networks (ANN), principal component analysis (PCA) and support vectors, such as the support vector machine (SVM). Wang and Xiao [4] and Beghi et al. [5], for example, isolated sensor faults after PCA detection by means of the sensor contribution to the symptom. Li et al. [6] also estimated the contributions of possible faults to the symptom for the purpose of isolating faults. They used a support vector data description (SVDD) algorithm on chiller FDD to detect a symptom. In [7], Wang and Cui also applied PCA as a detection method and isolated the faults by means of rules using a fault diagnostic classifier.

Due to the data-driven nature of these machine learning techniques, their application to the identification of faults remains a complex process. Furthermore, these approaches to diagnosis depend on the specific method of data-driven detection applied. In addition, they rely on the availability of data on healthy operation and, for some methods, data on healthy operation combined with data on incorrect operation with known faults. Liang and Du [8], for example, applied an SVM classifier based on both normal and faulty conditions.

Besides data-driven methods, the application of model-based and rule-based methods is also commonly found in recent literature. Song et al. propose in [9] a model-based method in which faults are estimated by means of simulation, with a classification set up on the basis of the calculated symptoms. In rule-based detection methods, we see that the isolation of faults mainly takes place using a diagnosis rules table (see e.g., Zhao [10]). In DABO [11], an FDD application, rule tables are also used to isolate faults. Another method is a reference-based approach that compares the behaviour of similar components to isolate a faulty component. See [12] where this is applied to district heating substations. Despite the many solutions proposed, an approach to generic automated fault diagnosis that can be applied regardless of the type of HVAC system has yet to be developed, and the practical implementation of current methods calls for considerable effort. In particular, the IT-based nature of data-driven methods means that by their very nature they are far removed from the professional practice of HVAC engineers. Furthermore, HVAC systems are also becoming more complex due to the many possible combinations of components and complex controls that

incorporate a large number of sensors. Generic FDD methods are not available for these new systems. Moreover, HVAC systems consist of subsystems and a simultaneous diagnosis for these subsystems has yet to be proposed. In research, FDD takes place sequentially either top-down or bottom-up, but not in both directions, which could help enable quicker, more comprehensive and more accurate diagnoses. In addition all methods provide a true-false result for faults and this can lead to incorrect conclusions due to inaccuracies in measurements and method. In the 4S3F FDD architecture, the fault isolation part of the diagnosis is carried out using a diagnostic Bayesian network (DBN) method that largely solves these problems. The DBN method has been applied successfully to chillers [13], to VAV terminals [14] and to AHU [15 and 16]. However, these applications are still HVAC-specific. The automated fault isolation (AFI) in the 4S3F method overcomes this problem and has been demonstrated at the extensive thermal energy plant at The Hague University of Applied Sciences (THUAS) building in Delft, the Netherlands, using the data present in the building's BMS. The HVAC system that formed the focus of the study contains a gas boiler and a heat pump combined with an aquifer thermal energy storage (ATES) system for storage and supply of both heat and cold. All buffers and hydronic systems were also included. The analysis covers a whole year, based on data collected at 16-minute intervals, and demonstrates the practical usability of the 4S3F architecture for an existing HVAC system.

The basic 4S3F diagnosis architecture for energy performance is briefly presented in Section 4.2. In Section 4.3 the generic approach of AFI with the 4S3F approach is presented. Section 4.4 describes the HVAC system under consideration. In Section 4.5 the symptoms detected in the case study are presented, as they form the starting point for the fault diagnosis method. Section 4.6 describes the application of the AFI method applying DBN models. In this section the case study results are presented and evaluated and in section 4.7 the fault diagnosis without subsystems and fewer symptoms is discussed. Section 4.8 energy optimization and savings are discussed. Additionally, in Section 4.9, a sensitivity analysis is conducted on prior probabilities in the case study. Finally, in Section 4.10, conclusions are drawn, and recommendations made concerning the fault diagnosis element of the 4S3F diagnosis framework.

4.2. 4S3F architecture for energy performance detection and diagnosis

This section presents the salient points of the 4S3F architecture. For a detailed explanation of this architecture, see [2].

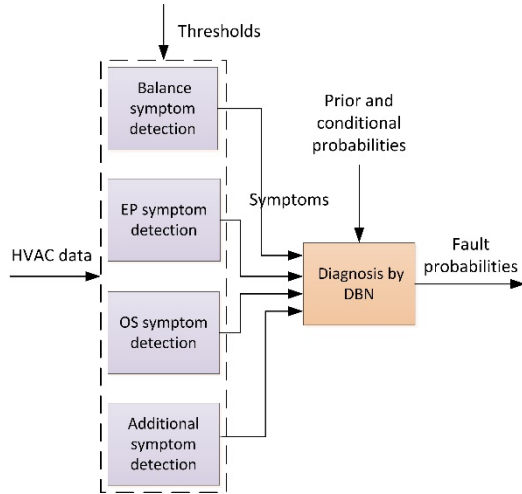


Figure 4.1 4S3F architecture for automated energy performance detection and diagnosis

The identification of symptoms starts with the detection of observable malfunctioning symptoms, based on the HVAC P&IDs (process and instrumentation diagrams) and the measurement points and set points present in the BMS, the main purposes of which are the control and monitoring of the HVAC system.

These symptoms are categorised in four main types (4S), see Figure 4.1: balance symptoms (energy, mass and pressure-based), energy performance (EP) symptoms, operational state (OS) symptoms and additional symptoms (based on additional information such as maintenance information). The results of the symptom detection phase are supplied to a diagnostic Bayesian network (DBN) model. In this model, symptoms are linked to possible faults. We distinguish three types of faults: faults in the models used to enrich BMS data (e.g., to estimate missing energy data or to set up balance models), component faults and faults affecting control components. In this paper, we demonstrate a DBN for energy performance purposes, in which we have taken into account that model faults are not present and that this has been checked. We define components as being not only trade components but also HVAC systems at different aggregation levels. Figure 4.2 shows the relationship between the four types of symptoms and the three types of faults as implemented in the 4S3F DBN models. The direction of the arrows in the DBN runs from the fault nodes to the symptom nodes. In other words, this figure shows which symptoms may be caused by a specific fault. The components and controls can be extracted from the HVAC P&ID diagram. The present paper focuses solely on the fault identification part (3F) of the 4S3F framework.

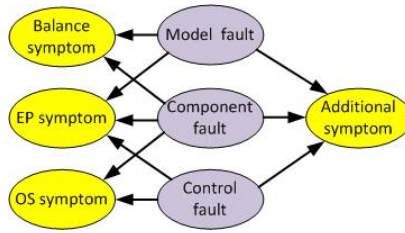


Figure 4.2 4S3F DBN structure

In the DBN diagnosis, the Present and Absent probabilities of the faults are estimated on the basis of the presence and absence of symptoms as established by the symptom detection.

The main advantages of applying DBN for fault isolation purposes, presented in [2], is that the structures of the DBN models can be extracted from P&IDs and that isolation of multiple faults takes place simultaneously. This also supports a system approach, because a DBN model can be built from DBN submodels and can be set up using aggregated DBN models from a DBN model library. A DBN model is easy to expand.

Due to its probability-based character, the DBN approach addresses uncertainties in measurements and in the FDD model and is to some extent insensitive to parameter values of the DBN nodes. It can handle conflicting symptoms and delivers results even when only a few symptom nodes are available because the outcomes are probabilities instead of Boolean. Furthermore, symptoms from all kinds of detection methods can be integrated.

4.3. The fault identification approach based on the 4S3F method

This section discusses the generic approach to identify faults from symptoms applying DBN models. As explained in Section 4.2, many different faults can lead to a single symptom. The reverse is also true: a fault can result in multiple symptoms. It is therefore necessary to conduct an analysis of the combination of all observed symptoms to determine the exact cause(s) of malfunctioning (the fault(s)). The 4S3F fault diagnosis method, as depicted in Figure 4.1, is based on Bayesian theory. Using the detected symptoms, the probability of occurrence of specific faults can be estimated.

Just as all possible symptoms can be identified once from the HVAC schematic, so all possible faults must also be identified once for each HVAC system, based on the HVAC P&ID (see for such a diagram Figure 4.11). This is a relatively simple once-only inventory, as was noted in [2], and will be demonstrated in Section 4.3.2. This inventory results in all possible faults being connected to all possible symptoms

through a DBN. The structure of the DBN closely follows the structure of the HVAC P&ID and its construction (also a once-only event) is therefore reasonably straightforward. A distinction can be made between component faults, control faults and model faults, see Figure 4.2. In the present paper, model faults are left out of the description in order to avoid excessively long descriptions and because a DBN with a model fault was already described in [2].

System levels on which DBN models are set up are discussed first, followed by how to establish the relationships between faults and symptoms from a P&ID. This section ends with the implementation of the DBN models.

4.3.1. System levels

As well for components as for controls levels are distinguished.

Components

According to [2], we should consider components on different levels, as a simultaneous diagnosis helps to isolate faults more accurately due to redundancy:

Level A: the total system

Level B: aggregated systems

Level C: (trade) components

Level D: subcomponents inside (trade) components

This also helps to define reusable diagnostic models that may be available in a library. For the sake of demonstration, complex DBN schematics are not shown in this paper, as we have made a conscious effort to limit the number of DBN nodes. This means that Level A (the complete system) and Level D (parts of components) are not shown, and only the faults at Levels B (aggregated systems) and C (components) are included. For instance, a malfunction in the heat pump is a possible fault but we will not specify the exact location within the heat pump at Level D, e.g., the compressor, evaporator, condenser or embedded control. In other words, the heat pump will be treated as a black box system, which is logical given that it is a commercially available component. In the authors' view, fault diagnosis at Level D could be implemented by component suppliers. Fault results from such as diagnosis could then be used as additional symptoms in the 4S3F method. For energy diagnosis purposes, we propose that the aggregated systems are based on generator, hydronic and emitter systems according to EN 15316-1:2017 [17].

Controls

As with components, for the purposes of this paper faults in the control system of each system are aggregated to one fault per system: for instance, the control of the

heat regeneration system may be faulty, but we do not specify whether the fault is in the temperature set point or in the timer setting. It may of course be possible and even desirable to consider both in practice, but that is not necessary to demonstrate the method within the context of this paper.

A control contains controllers which derive signals from sensors and send signals to components acting as actuators. These signals propagate information, as opposed to components which exchange energy. Control faults can be errors in controllers (e.g., control rules, set points), in connections with sensors and in actuators (e.g., broken wires and interruptions) and caused by incorrect design of the control circuit, including actuators. Generic controls at level B applied in thermal plants with an ATES system are the control of the ATES system, of the cold water, the hot water, and in addition, controls at Level C: the controls of the supplied condenser and evaporator water temperature of the heat pump.

The control parts of the P&ID can be based on guidelines (e.g., documents on hydronic systems, such as the ISSO standard for hydraulic systems [18 and 19]), which describe HVAC modules in the Netherlands.

4.3.2. Relationships between faults and symptoms

In this section, generic DBN (sub)models are discussed, along with their implementation.

As depicted in Section 4.3.1, components at Levels A to D can be defined. Generic fault isolation models can be developed once only for each type of component. The fact that this approach takes in balance, energy performance and operational state symptoms regardless of components and controls is what makes it generic. Components at lower levels can be combined to form generic subsystems and finally to generic aggregated systems as models for the thermal generator, hydronic and emitter systems. The first step is to construct the overall DBN model using DBN models for systems at level B and C, followed by setting the prior and conditional probabilities of the fault and symptom nodes. Again, this is done only once for each model, which can be saved in a model library.

It can be helpful to create a table that lists related errors and symptoms. See for instance Table 4.1, where such a generic model has been set up for a heat pump system (a generator system) at level B. The grey filled cells indicate the presence of a relation. As example, the cause of a low COP of the heat pump may be a malfunctioning heat pump, a too high set point in the control of the outlet water temperature of the condenser or a too low set point in the control of the outlet water temperature of the evaporator. However, it can also be approached on the other hand: if a fault is present, what symptoms can there be?

Table 4.1 Fault-symptom relation table for a heat pump system.

| Faults | <i>Heat pump</i> | <i>Control outlet water temperature of the evaporator</i> | <i>Control outlet water temperature of the condenser</i> |
|--|------------------|---|--|
| Symptoms | | | |
| <i>Heat pumps' capacity</i> | | | |
| <i>COP heat pump in heating mode</i> | | | |
| <i>EER heat pump in cooling mode</i> | | | |
| <i>Outlet water temperature evaporator</i> | | | |
| <i>Outlet water temperature condenser</i> | | | |

For the purposes of simplicity and accuracy, we propose that only strong relations should be set up and weak ones should be ignored. Such tables can easily be set up with reference to the HVAC P&ID (which depicts components at level B) as shown in Figure 4.3. In this figure, we see the controllers TC1 and TC2 which controls the evaporator outlet temperature (measured by sensor TT2) and the condenser outlet temperature (measured by TT3). The heat pumps' capacity is estimated by the temperature sensors TT3 and TT4, and the flow sensor FT2. The COP (coefficient of performance) is calculated from the supplied heat Q_{cond} and the compressor work E_{compr} , measured by ET1. And the EER (energy efficiency ratio) by the supply cold Q_{evap} and E_{compr} . Thus, we see that from the P&ID we can extract faults as well symptoms.

4.3.3. DBN models

As stated in Section 4.2, the DBN model calculates the posterior fault probabilities from the presence and absence of symptoms. An example of such a calculation is given in Appendix B of [20].

DBN schematics

From the relationships between the faults and symptoms, a DBN model is set up. As example, Table 4.1 results in the DBN model shown in Figure 4.4.

Since DBN models of aggregated systems at Level B as shown in Figure 4.4 are generic, this can be done once and then be reused.

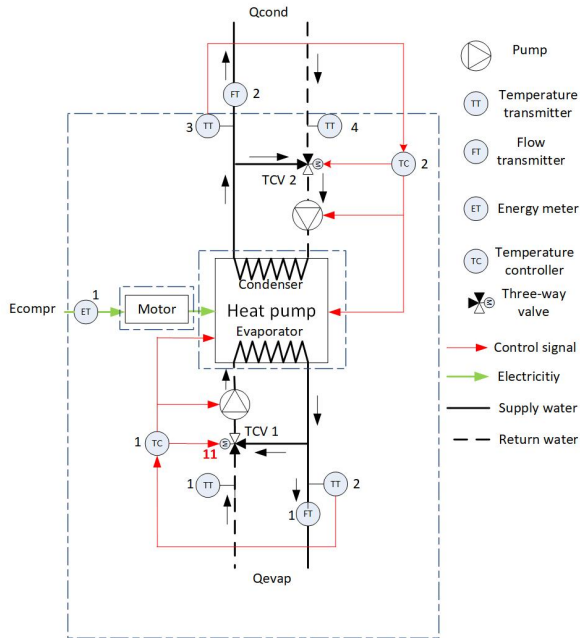


Figure 4.3 P&ID heat pump system.

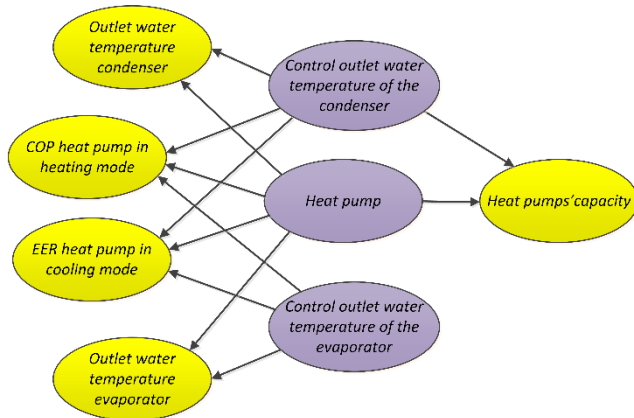


Figure 4.4 DBN schematic diagram of a heat pump system.

The software tool we used to construct our models is called GeNie [21]: a validated software application offering the possibility to create aggregated DBN models based on DBN submodels. This makes it possible to develop specific DBN models with the use of generic DBNs for components or systems, which shorten the implementation effort in the fault identification layer. Balance, energy performance and operational state symptom nodes are linked to fault models, such as heat pumps, boilers, cold

water systems, hydronic systems and ATEs systems. The links between fault and symptom nodes can be set up once only. Some links for faults and symptoms which concern several systems and components can be set up once only for well-known system configurations. These DBN models can be stored in a library.

Node states and probabilities

The parameters of DBN models are probabilities for the node states. The fault nodes are so-called parent nodes which contain prior probabilities for the state of the nodes. The corresponding child nodes, the symptom nodes, have conditional state probabilities that depend on the state of the connected parent nodes. First, the values of the prior probabilities must be set, followed by those of the conditional probabilities (see also [2], which proposes distinguishing between two states for the fault and symptom nodes: Present or Absent). The values only need to be set once when implementing the DBN model and can be based on HVAC expertise and later on historical data from the BMS.

- Prior probabilities of parent nodes

The absolute values of the prior Present and Absent probabilities for the events are chosen arbitrarily but their relative values are based on expert knowledge. For the sake of simplicity, we set separate fixed values for component faults and for control faults. The actual prior probabilities of component faults are set at 98%, which means that two out of 100 components are not functioning properly. However, the Absent prior probabilities of control rules are set lower to 95% because in practice energy performance often decreases due to faulty set control rules, changes in building use or incorrect changes to set points of the control system.

Figure 4.5 presents an example of the prior properties of a fault called *Control roof heating*. We distinguish between two states: Present or Absent with corresponding probabilities.

Node properties: Control roof heating

| State | Probability |
|---------|-------------|
| Present | 0.05 |
| Absent | 0.95 |

Figure 4.5 The implemented prior node properties of a fault called *Control roof heating* in GeNie

- Conditional properties of child nodes

The probabilities of the Present and Absent states of the symptom nodes depend on the state values of the fault nodes. In this case study, it is assumed that when one of

the parents is Present, the child value is Present with an arbitrary probability of 95%. This means there is an Absent probability of 5% for the child node when one or more of the parents are Present, because parent node faults can cancel each other out and lead to no symptom.

By way of example, Figure 4.6 presents the set properties in the dialogue box of a symptom node, in this case for a symptom called *SEERcw*. We have applied so-called Noisy-MAX nodes, in which we assume that the symptom is Absent when all parent states are Absent (LEAK=1).

Node properties: SEERcw

| Parent | Control cw | TSA ATES | Control ATES | Hydronic system cold water | Control evap | LEAK |
|---------|------------|----------|--------------|----------------------------|--------------|------|
| State | Present | Present | Present | Present | Present | |
| Present | 0.95 | 0.95 | 0.95 | 0.95 | 0.95 | 0 |
| Absent | 0.05 | 0.05 | 0.05 | 0.05 | 0.05 | 1 |

Figure 4.6 The implemented conditional node probabilities of a symptom called SEERcw in GeNie.

In future, the prior and conditional probabilities can be estimated more precisely as a result of experience and data mining. However, [20], in which the 4S3F method was conducted on a demand-controlled ventilation system, showed that the absolute values of the set probabilities are somewhat insensitive for the diagnosis results. In Section 4.9 we confirm that rough-set prior probabilities do not influence the outcomes fundamentally.

4.4. The thermal energy plant at The Hague University of Applied Sciences in Delft

The identification part of the 4S3F method is tested on the HVAC system of the THUAS building in Delft (see Figures 4.7 and 4.8). The ventilation of the building rooms is demand controlled by CO₂ concentration. In the classrooms and general living areas there is underfloor heating and cooling and in the staff rooms this has been extended with heat and cold ceiling panels.



Figure 4.7 The atrium of the THUAS building.



Figure 4.8 A staff room in the THUAS building.

Figure 4.9 shows the heat exchanger (8) with at the left a part the heat pumps' casing and in Figure 4.10 the headers (14) and (15) are presented.



Figure 4.9 The heat exchanger (8)



Figure 4.10 The headers (14) and (15)

The P&ID of the thermal energy plant in which these components are present, is presented in Figure 4.11. For the sake of simplicity, controllers are not depicted.

We have simplified this diagram based on generator, hydronic and emitter systems at level B. See Figure 4.12, in which relevant energy variables used for symptom detection are also depicted. In this figure, controllers for hot and cold-water supply temperatures (TC_{hw} and TC_{cw}), roof heating (TC_{roof}), regeneration (TC_{reg}) and ATES (TC_{ATES}) systems. Coupled control and sensor signals are also shown. These controls are explained in Section 4.6.1. Annual energy flows and efficiencies measured in 2013 are also depicted.

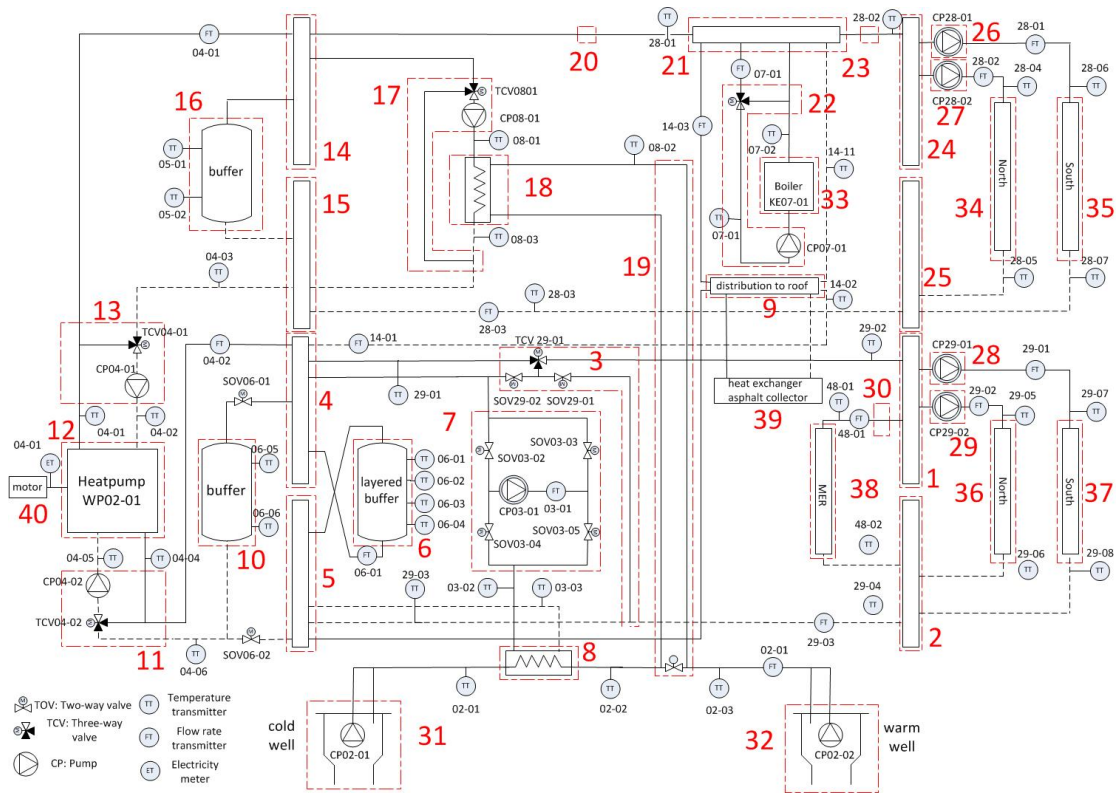


Figure 4.11 Principal diagram (P&ID) of the thermal energy plant at THUAS

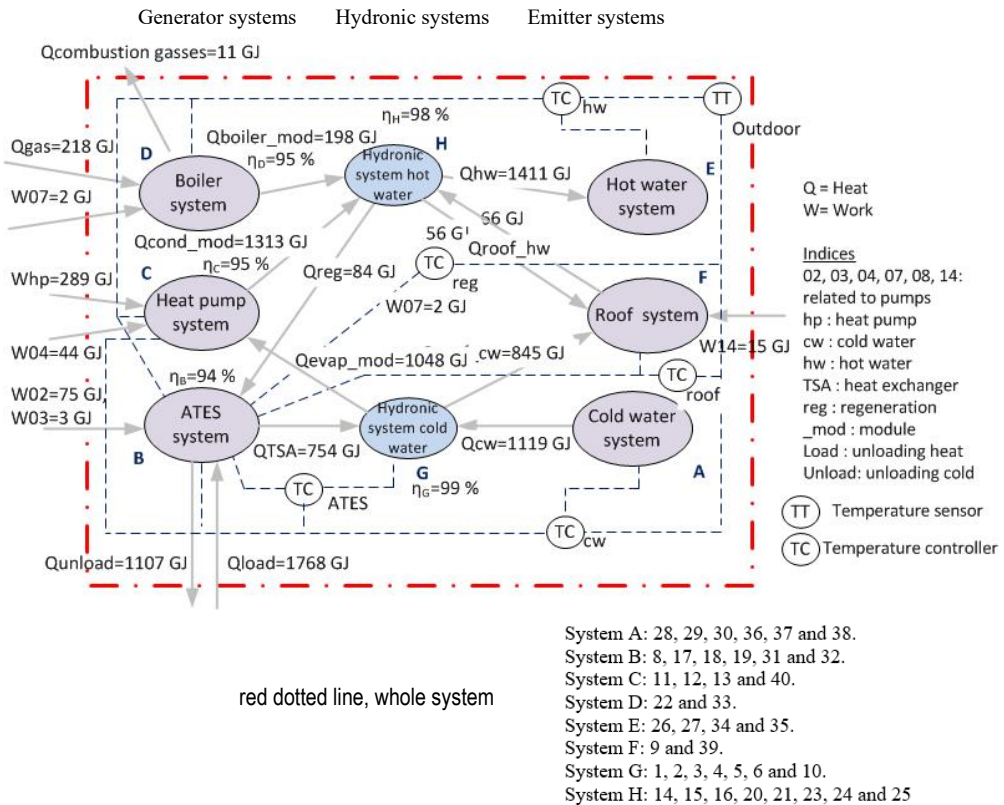


Figure 4.12 The relevant aggregated systems at Level A and at Level B
 (Consisting of systems A to and system controls).

In this figure, eight aggregated systems are present, based on systems 1 to 40 depicted in Figure 4.11. The determination of systems and subsystems is a one-off task, carried out based on the P&IDs as explained in [2].

In winter, heat is generated by a heat pump. When the heat loads are high, a gas boiler delivers additional heat. The heat source of the heat pump is warm water delivered by the warm well of an ATEs system, which presents the winter mode of the thermal energy generation system in a schematic. The ATEs system can also deliver heat to the parking lane on the roof to keep it free of ice.

In the summer months, cold water from the cold well of the ATEs system provides cooling. When cooling loads are high, the heat pump produces additional cold water on the evaporator side. This type of thermal energy plant with an ATEs system is common in the Netherlands: more than 2,000 of them have been installed in recent years and their operation is known to be often sub-optimal.

During the summer, heat from the heat pump condenser and the roof collector can be used to regenerate the warm well of the ATES system because the amount of thermal energy extracted from and supplied to the wells must be balanced annually in accordance with Dutch regulations. In Figure 4.12 the direction of the arrows shows positive heat transfer. Work supplied by pumps and the heat pump compressor is noted as W in these figures.

Measurement data are stored in the BMS at 16-minute intervals. The codes of the sensors and actuators (from 02 to 48) as implemented in the BMS were supplied by the designer of the HVAC system. As example, Figure 4.13 shows the flow sensor with code FT28-03 which is located in the hot water circuit depicted in Figure 4.11.



Figure 4.13 Flow sensor FT28-03

For the case study, the whole of the year 2013 is included due to the availability of an almost complete dataset.

4.5. Detected symptoms in the case study

In this section, the symptoms detected by the 4S3F method in the year of 2013 are listed and form the starting point for the automated fault identification. Table 4.2 summarises the annual results of the symptom detection process conducted in the case study. To estimate the presence or absence of a particular symptom, BMS sensor data are used. In a separate process, sensor data outliers are left out and missing data are filled in. Furthermore, biased data are corrected (also using the 4S3F method). This means that the data available is faultless.

Symptoms concerning efficiencies (η) constitute thermal energy losses in systems which are required to be lower than 2-4%, depending on the system. In addition, Table 4.2 shows the efficiency of the TSA heat exchanger of the ATES system η_{TSA} (87% according to design) and the efficiency of the thermal energy regeneration of the ATES system η_{reg} , which Dutch regulations stipulate must be 100% (i.e., each year, the same amount of thermal energy must be supplied to the aquifer as is used). These are defined as balance symptoms because they are calculated on the basis of energy balances. In addition to balance symptoms, we also identify energy

performance and operational state symptoms. The first are related to performance indicators such as the seasonal performance coefficient (SCOP) for the generation of thermal energy (a threshold of -5% is taken into account) and capacities (P) of components and systems realized as compared to those specified in the design (threshold of -10%). The second are symptoms regarding actual state values such as temperatures. Here we distinguish between controlled-based state values, which are set in a control system, and rule-based state values, which are those expected on the basis of the design. In the case study, a symptom is found when a controlled or design temperature is lower or higher than needed (+/- 1 to 3 K) for more than 10% of the days on which the associated system is operational. As Table 4.2 shows, 9 of the 31 possible symptoms of malfunctioning were shown to be present.

Table 4.2 Overview of the detection results from BMS data for the 31 possible symptoms found in the year 2013

(P= symptom present, A= symptom absent)

| Balance symptoms | | Energy performance (EP) symptoms | | | | Operational state (OS) symptoms | | | |
|----------------------|-----|----------------------------------|-----|---------------------|-----|---------------------------------|-----|----------------------------|-----|
| Efficiencies | A/P | Performance indicators | A/P | Capacity indicators | A/P | Controlled-based | A/P | Design-based | A/P |
| $\eta_{\text{sys}B}$ | A | SCOP _{hw} | A | Phw | A | Thw supply | P | Thw return | A |
| $\eta_{\text{sys}C}$ | A | SEER _{cw} | A | P _{cw} | P | T _{cw} supply | P | T _{cw} return | A |
| $\eta_{\text{sys}D}$ | A | SCOP _{Proof} | P | Php | A | T _{cond} out | A | T _{evap} in | A |
| $\eta_{\text{sys}G}$ | A | SCOP _{reg} | A | Proof | A | T _{evap} out | A | T _{cold} well out | A |
| $\eta_{\text{sys}H}$ | A | SCOP _{hp} | A | P _{reg} | A | T _{cold} well in | P | T _{warm} well out | P |
| PTSA | A | SEER _{hp} | A | PTSA | P | T _{warm} well in | P | | |
| η_{reg} | P | | | P _{boiler} | A | | | | |

B=ATES, C=heat pump, D=boiler, G=hydraulic cold water, H=hydraulic hot water, hp= heat pump, hw=hot water, cw= cold water)

Energy balance symptoms

Regeneration efficiency symptom η_{reg} was Present. This indicator represents the degree of thermal energy balance in the ATES system.

Energy performance symptoms

Symptom *SCOP_{Proof}* was Present, indicating that the roof heating system used more energy than expected. Furthermore, the thermal capacities of the cold-water system A (*P_{cw}*) and of the heat exchanger of the ATES system (*PTSA*) were lower than expected from the design values.

Operational state symptoms

In addition to the balance and EP symptoms, OS symptoms were detected: the hot water supply temperature to system H was too low and the cold-water supply temperature to system A too high. Unexpected temperatures were also found at the warm and cold wells of the ATES system.

4.6. Automated fault isolation in the case study

In this section, the AFI is conducted in the THUAS case study. The considered faults are discussed in Section 4.6.1. Section 4.6.2 presents the relationships between faults and symptom. Next, the implementation of the DBN models are presented in Section 4.6.3. And finally, in Section 4.6.4, the results of the fault isolation process.

4.6.1. Selected component and control faults

In aggregated hydronic systems A, E, G and H, we assume that only one fault can be present which covers faults in pipes, valves, heat exchangers, headers and pumps. In the other aggregated systems, multiple component faults are present. In the roof system F, faults in the roof collector (*TSA roof*) and hydronic system F can be present; in the heat pump system C, the heat pump (12) and the hydronic system can be present; in the boiler system D, we assume that the hydronic system D and the boiler can be faulty, and in the ATES system B, faults in the heat exchanger TSA (8) and hydronic system B are present. In total, therefore, there are 11 possible component faults to consider.

Control faults

From the control description of the thermal energy plant, which was present in the design document and the P&ID, the following five control faults at Level B, as depicted in Figure 4.13, can be distinguished:

- *Control ATES*
- *Control heat regeneration*
- *Control roof heating*
- *Control cw*
- *Control hw*

In addition, we take into account two controls at Level C in the heat pump system (system C):

- *Control cond*
- *Control evap*

We explain the implemented controls in the thermal energy plant of THUAS below in greater detail for the ATES and regeneration systems. The other five are described in Appendix A.

Control ATES

Control ATES depicts the faulty control of the ATES system. Figure 4.14 presents a simple schematic of the control of the ATES system B. When unloading cold water, the controller of the ATES system controls the flow rate of pump CP02-01 in the cold well to obtain the desired supply temperature in the warm well, measured by TT02-03. In the same way, the temperature of the supply water to the cold well is controlled when unloading heat from the ATES.

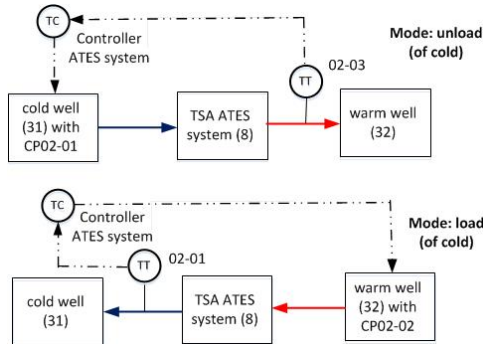


Figure 4.14 Control of the ATES system

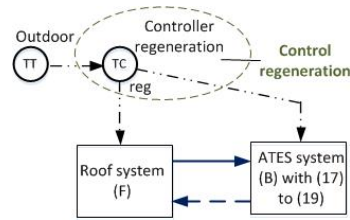


Figure 4.15 Control of the regeneration system

Control regeneration

Control regeneration depicts the control of the heat regeneration for the ATES system. The schematic of this control is shown in Figure 4.15. At high outdoor temperatures in summer, the roof and ATES systems are switched on. The roof system supplies heat to warm well 32 via systems 17 to 19.

4.6.2. Relationships between faults and symptoms.

We will examine 11 possible component faults. In addition, seven control faults are present. As seen in Table 4.2, 31 outcomes for symptoms are present. A DBN model is therefore built with 18 fault nodes and 31 symptom nodes.

Table 4.3 presents the completed Table 4.1 for the case study. As noted in Section 4.3.2 weak relations between faults and symptoms are ignored. For instance, the relation between the heat pump capacity *Php* symptom and the *Control ATES* fault: the table supposes no relation between the two because the warm water well temperature is thought always to be high enough to deliver heat to the evaporator of the heat pump. Only if the warm water well temperatures were to drop to an unrealistically low level (e.g., 4°C) would the heat pump be incapable of delivering enough heat.

Table 4.3 Main relations between the 31 symptoms and the 18 faults to build the DBN models
 hp= heat pump, hw=hot water, cw= cold water

| Component and control faults at level B (aggregated systems A to H) | Control supply temperature hw | Hydronic system hw E | Control supply temperature cw | Hydronic system cw A | Heat pump system C | Boiler system D | Control roof system F | Roof system F | Control ATEs system | ATES system B | Control regeneration | Hydronic system HW H | Hydronic system HW G |
|---|-------------------------------|----------------------|-------------------------------|----------------------|--------------------|-----------------|-----------------------|---------------|---------------------|---------------|----------------------|----------------------|----------------------|
| Component and control faults at Level C (components 1 to 40) | | | | | | | | | | | | | |
| Symptoms | | | | | | | | | | | | | |
| η_{sysB} | | | | | | | | | | | | | |
| η_{sysC} | | | | | | | | | | | | | |
| η_{sysD} | | | | | | | | | | | | | |
| η_{sysE} | | | | | | | | | | | | | |
| η_{sysH} | | | | | | | | | | | | | |
| η_{reg} | | | | | | | | | | | | | |
| η_{TSA} | | | | | | | | | | | | | |
| SCOPhw | | | | | | | | | | | | | |
| SEERcw | | | | | | | | | | | | | |
| SCOProof | | | | | | | | | | | | | |
| SCOPreg | | | | | | | | | | | | | |
| SCOPhp | | | | | | | | | | | | | |
| SEERhp | | | | | | | | | | | | | |
| P _{hw} | | | | | | | | | | | | | |
| P _{cw} | | | | | | | | | | | | | |
| P _{hp} | | | | | | | | | | | | | |
| Proof | | | | | | | | | | | | | |
| Preg | | | | | | | | | | | | | |
| PTSA | | | | | | | | | | | | | |
| Pboiler | | | | | | | | | | | | | |
| T _{hw_supply} | | | | | | | | | | | | | |
| T _{cw_supply} | | | | | | | | | | | | | |
| T _{cond_out} | | | | | | | | | | | | | |
| T _{evap_out} | | | | | | | | | | | | | |
| T _{in_cold_well} | | | | | | | | | | | | | |
| T _{in_warm_well} | | | | | | | | | | | | | |
| T _{hw_return} | | | | | | | | | | | | | |
| T _{cw_return} | | | | | | | | | | | | | |
| T _{evap_in} | | | | | | | | | | | | | |
| T _{out_cold_well} | | | | | | | | | | | | | |
| T _{out_warm_well} | | | | | | | | | | | | | |

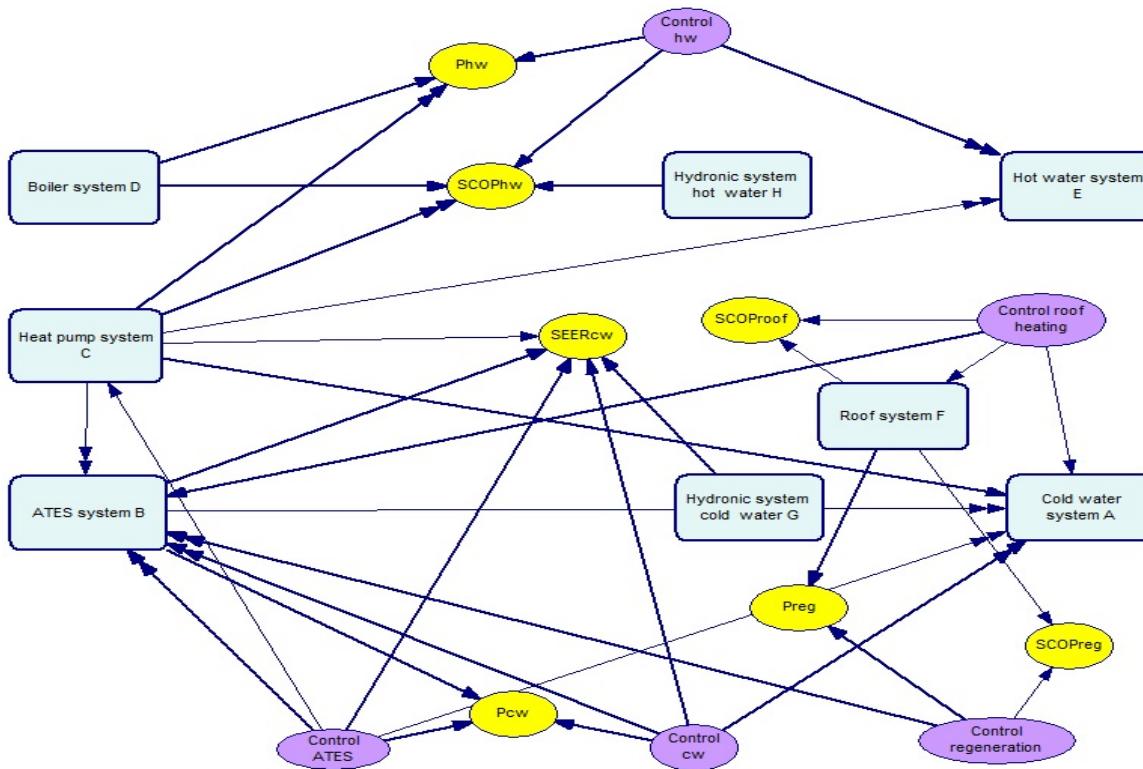


Figure 4.16 Overall DBN model at Level B with systems A to H.

4.6.3. The implementation of DBN models in GeNie

Based on Table 4.3, DBN models are built in GeNie. The overall DBN model is presented in Figure 4.16 and is constructed based on Figure 4.12. Both figures contain the eight main aggregated systems A to H at Level B, shown in blue. Fault nodes are shown in purple while symptoms which can be caused by more than one system at Level B, see Table 4.3, are shown in grey.

Figures 4.17 to 4.24 show the DBN models for systems A to H at Level C. As can be seen, these figures contain the 18 fault and 31 symptom nodes depicted in Table 4.2. These DBN models are extracted from the P&ID of Figure 4.11. Congruent to Figure 4.2, the arrow directions run from the fault nodes to the symptom nodes.

For example, Figure 4.18 shows that the fault node *TSA ATES* is linked to the symptom nodes η_{TSA} , *PTSA*, *Tcold_well_in*, *Twarm_well_in*, *Tcold_well_out* and *Twarm_well_out*, which are present in the DBN model of the ATES system. In addition, *TSA ATES* is linked to the symptoms *SEER_{cw}* and *P_{cw}* (see Figure 4.16), and *T_{cw_supply}* and *T_{cw_return}* (see Figure 4.17). The above is consistent with Table 4.3.

4.6.4. Fault isolation results

The symptom detection results presented in Table 4.2 are imported into the DBN model. This was done manually in our case study, but it is possible to automate this process. Note here that the symptoms were obtained using one year of 16-minute data and looking at yearly, monthly or weekly indicators. However, for the fault isolation itself, time steps are irrelevant and therefore not included in the DBN. Symptoms found over a period of less than a year (monthly, weekly, daily or even shorter timespans) can simply be fed into the DBN, resulting in shorter timespan outcomes.

We propose taking action when the Present probability outcome of a fault is higher than 30%. Isolation by the DBN resulted in four identified faults with 100% (see Figure 4.25): Present outcomes that led to 4 observed symptoms: *Control hw*, *Control ATES*, *Control regeneration* and *Control roof heating* are faulty.

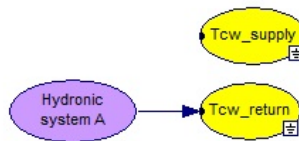


Figure 4.17 DBN model of the cold-water system A

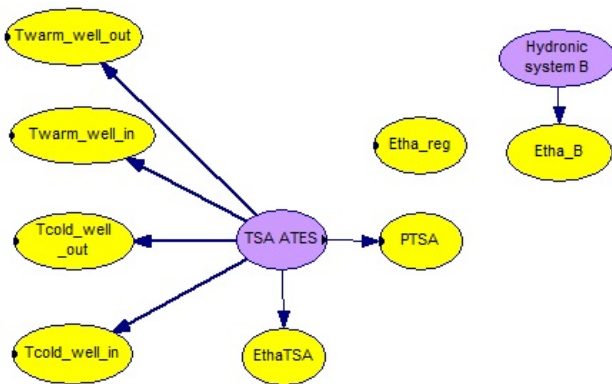


Figure 4.18 DBN model of the ATES system B.

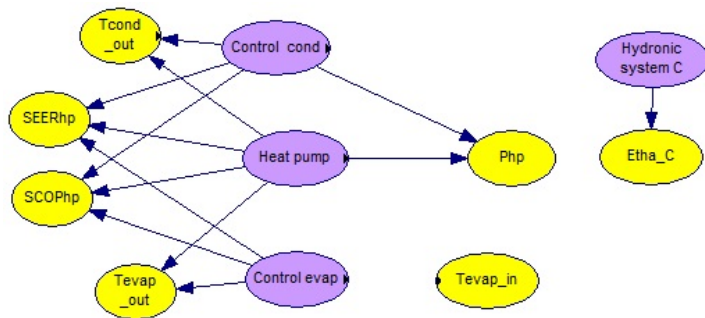


Figure 4.19 DBN model of the heat pump.

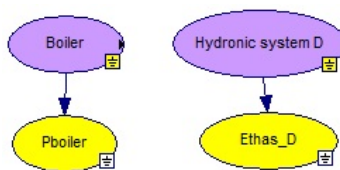


Figure 4.20 DBN model of the boiler system D. system C.

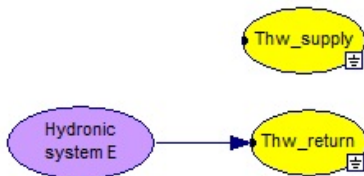


Figure 4.21 DBN model of the hot water system E.

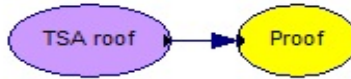


Figure 4.22 DBN model of the roof system F.

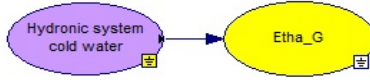


Figure 4.23 DBN model of the cold-water hydronic system G.

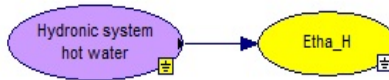


Figure 4.24 DBN model of the hot water hydronic system H.

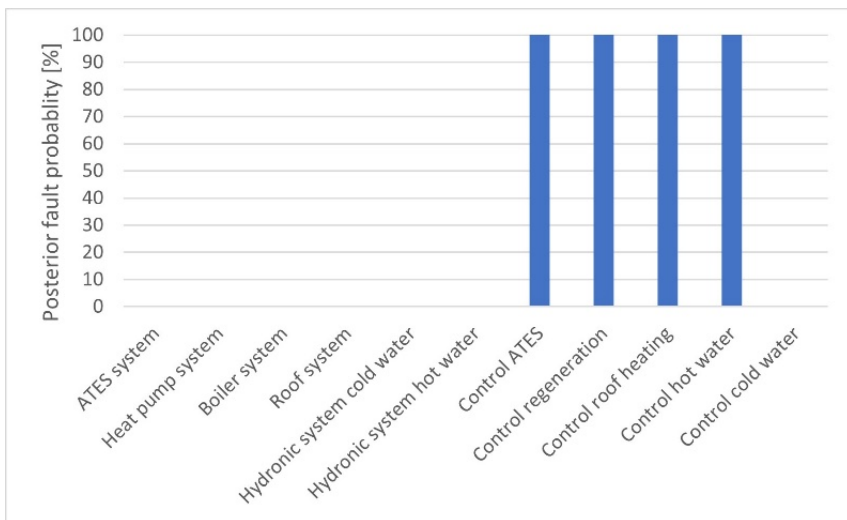


Figure 4.25 Posterior fault probabilities after diagnosis.

Discussion of the isolation results

We also contacted the maintenance company and the facility manager at THUAS to ask about other disruptions in the thermal power plant. They stated that there had been no thermal comfort complaints due to a malfunction in the thermal power plant. The four faults that were isolated would appear to be the only one's present. We will discuss them separately below.

Control hw

The control fault of the hot water system was identified as Present. This diagnosis result seems to be correct because detection revealed that the supply hot water temperature was often too low. Faults were not found in the installed capacities of the heat pump and the boiler. In addition, the control of the condenser seems to be correct, because no symptom was found in the condenser outlet temperature. Apparently, an excessively low supply water temperature is caused by *Control hw*.

Control ATES

The inlet water temperatures to the warm and cold well are too low and too high. As shown in Table 4.3, two main faults can cause this: *TSA ATES* or *ATES control*.

TSA ATES can be excluded because the efficiency of the heat exchanger efficiency η_{TSA} was correct. In addition, the capacity of the cold-water system A was low, while no thermal comfort complaints from users had been received. It would appear that the cold-water system A needs less capacity than stated in its design specifications. The resulting symptom was a lower-than-expected *PTSA* capacity. This leads to the justified conclusion that *ATES control* has been correctly identified as faulty, leading to excessively high and excessively low load temperatures for the ATES wells.

Control regeneration

No symptom was found for the capacity of the roof collector. *TSA roof* therefore seems to be correct. However, the thermal energy balance of the ATES system was incorrect, leading to an η_{reg} symptom, linked to the control of the regeneration system which is identified as Present.

Control roof heating

A survey of the 16-minute energy exchange to the roof showed that the roof was also heated by the boiler. This was not in conformity with the design. Adapting the control of the roof heating would therefore appear to be a reasonable course of action.

4.7. Effects of a DBN with only aggregated systems A to H (Level B)

The overall DBN model at aggregated Level B presented in Figure 4.16 contains DBN models of components at Level C. In this section, we discuss DBN models for aggregated systems A to H at Level B only, with and without capacity and operational state symptoms. This is to test the importance of the combined top-down/bottom-up approach in identifying faults. Figure 4.26 shows the DBN model at level B with both capacity and OS symptoms.

For the sake of simplicity, we have left out return water OS symptoms and efficiency symptoms. In Appendix 4B, the DBN models at Level B without capacity or OS symptoms are presented.

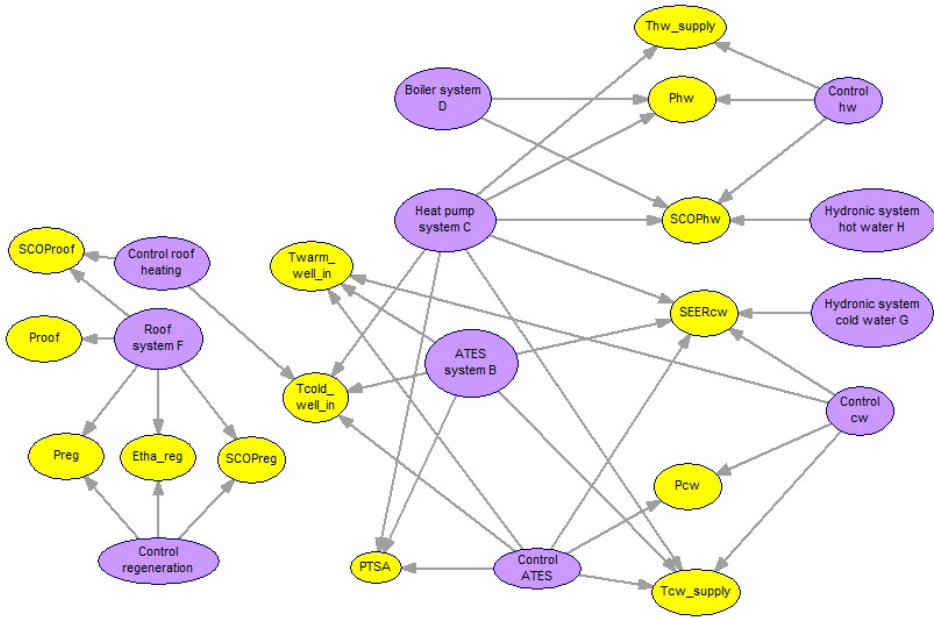


Figure 4.26 DBN model at Level B

Figure 4.27 presents the posterior fault present probabilities after diagnosis. In green the results from Section 4.6.4 (level B + C) are shown.

As this figure shows, diagnosis restricted to Level B with capacity and OS symptoms (orange) also isolates the four control faults. However, it is more difficult to find a fault inside the aggregated system at Level C (e.g., the control condenser or heat pump) if the heat pump system has been isolated as a fault.

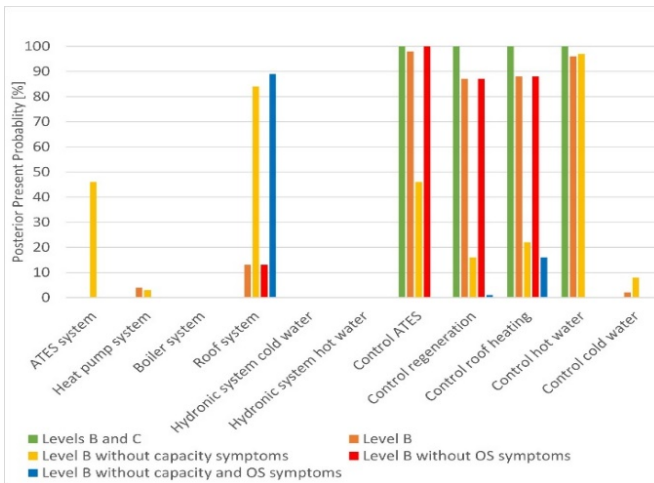


Figure 4.27 Posterior Present fault probabilities after diagnosis. (100 % is fully isolated as faulty)

As can be seen from this figure, faults are not isolated correctly when capacity or OS symptoms are missing.

In Figure 4.28 these incorrect outcomes (present fault probability above 30 %) are shown with the value 1.

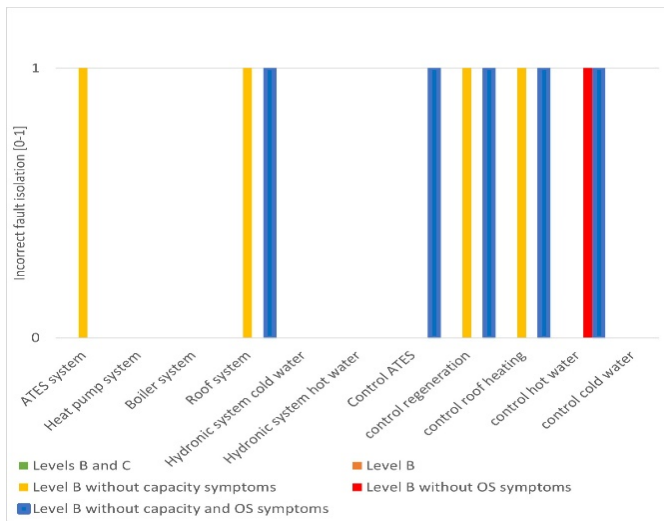


Figure 4.28 Incorrect fault isolation
(1=fault is Present)

Conclusion

Diagnosis using a DBN at Level B already delivers useful results. However, faults inside the DBN model cannot be isolated. Performance and capacity indicators, as well as operational state symptoms, are needed to isolate faults effectively. The correct and precise isolation of faults therefore requires the use of aggregated systems and their subsystems, at the same time as using multiple types of symptoms.

4.8. Fault analysis, correction and effect on energy usage

In this section, the evaluation process after fault isolation will be discussed with reference to the case study. The primary energy savings after fault correction will also be discussed. Unfortunately, it was impossible to carry out interventions, so we can only examine the energy savings due to corrections from a theoretical perspective. However, we checked manually whether the faults found were indeed errors by analyzing the BEMS data, consulting maintenance logs, interviewing the building manager and employees of the maintenance company, so that we can say with certainty that we have not overlooked any faults. We will discuss the four faults isolated by the energy performance diagnosis separately. In the Netherlands,

electricity is mainly generated by steam and gas power plants with an overall efficiency of 40%. We have taken this value into account when estimating primary energy.

Estimating energy waste and savings as a result of fault corrections is possible simply because of the availability of 16-minute data on energy levels in the BEMS.

4.8.1. Evaluation

4.8.1.1. Fault Control hw

As shown in Table 4.2, a symptom was detected for *Thw_supply*, the hot water supply temperature. An excessively low supply temperature could lead to thermal comfort complaints among users of the building, but the facility management at THUAS received no complaints to this effect. Excessively high supply temperatures were supposed to lead to lower energy performance, but again no such indications emerged. We nevertheless propose that the set values of the hot water supply controller should be checked to avoid user complaints in the future.

4.8.1.2. Fault Control roof heating

Calculations showed that part of the heat supplied to the roof was in fact supplied by the boiler (62 GJ) instead of the warm well of the ATES system. This was easy to correct by adjusting the roof control rules, and this was carried out in 2014 by the maintenance company.

4.8.1.3. Fault Control regeneration

The data suggests that the ATES system is not thermally balanced. As shown in Figure 4.12, the difference between stored cold ($Q_{load}=1768$ GJ) and heat ($Q_{unload}=1107$ GJ) was 661 GJ in 2013. An additional 661 GJ of heat therefore had to be supplied to the warm well (32). This can be achieved in several ways, which are explained below.

1. By means of the heat pump
This is the solution described in the design documentation. The roof would then serve as a heat source.
2. By supplying less heat to the roof
An analysis of the roof heating revealed that heat was being delivered even when outdoor temperatures were as high as 8°C, conditions in which there is no risk of ice. Adapting the outdoor set point and rules could reduce the heat required by 162 GJ.
3. Loading additional heat naturally from the roof
Analysis of the energy data shows that regeneration only took place in July and August, while the ATES system of the HVAC system was in discharge mode,

i.e., in cooling mode for the cold-water system A. Furthermore, the flow rates of the pumps for regeneration purposes were shown to be very low. By extending the time period and setting the flow rate of the pump to higher speeds, in theory an additional 885 GJ can be generated.

4.8.1.4. Fault Control ATES

The cold and warm well temperatures are higher and lower than the designed values. However, the lower warm well temperatures in load mode (when heat is delivered by the warm well) do not lead to a significant underperformance of the heat pump: the outgoing water temperatures of the evaporator show no symptoms and the SCOP and the capacity of the heat pump are as expected. In addition, the higher unload cold well temperatures have not led to problems in the cold supply. In light of this, a correction to the control of the ATES system would not lead to significant energy savings.

4.8.2. Primary energy savings

Here we will discuss the energy savings after correction in terms of primary energy. Figure 4.29 presents the primary energy consumption before and after corrections. We have assumed that electricity is generated with a mean SCOP of 0.4, which is commonly used in the Netherlands to calculate the primary energy ratio (PER). The SCOPs of components are known from design and actual performance. Before correction, the actual primary energy consumption of the thermal energy plant measured with BMS data from 2013 amounts to 1918 GJ/yr. After the adjustments described in Section 4.8.1, we see that the primary energy consumption is 1437 GJ / year due to the reduction of energy consumption for the roof and to a large extent for the ATES system. Thus, a primary energy saving of 481 GJ/yr (25.1%) is plausible, even though the thermal energy plant was assessed beforehand by experts and facility managers as performing well.

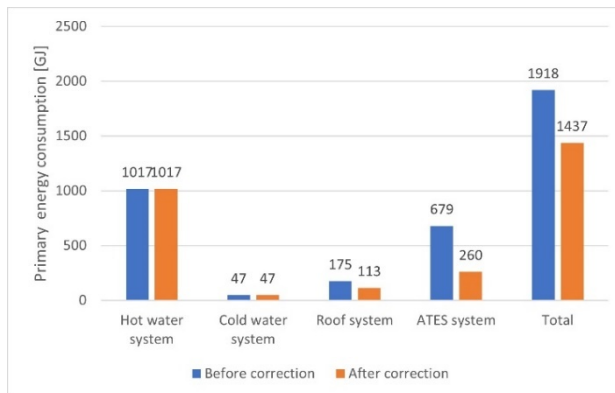


Figure 4.29 Primary energy consumption for the emitter systems and the ATES system.

4.9. Sensitivity analysis of the assumed probabilities in the fault layer

The prior fault probabilities of components and controls are difficult to estimate due to the lack of information about failures. Below, a sensitivity analysis is carried out to estimate the importance of accurate prior probabilities.

Table 4.4 presents the results of this experiment. In the case study, the prior Absent probabilities were set to 98% for components and 95% for the control rules. The prior fault probabilities for all control nodes vary for the sensitivity analysis.

The results of 5 faults for the reference probabilities are presented in the highlighted column 3 in Table 4.4. The second and fourth columns show the results for the posterior probabilities, with the prior fault Absent probabilities of the control systems being 90 and 99.9%. The latter is extremely high compared to the component probabilities because experience with HVAC maintenance has shown that control faults occur more often than component errors. Nevertheless, the 4 control faults are still isolated correctly among a wide range of prior probabilities.

Table 4.4 Influence of prior probabilities on the outcomes of the posterior fault Present probabilities

| | Prior Absent probabilities | | |
|-----------------------------|---------------------------------------|-----|------|
| Components | 98 | 98 | 98 |
| Control rules | 90 | 95 | 99.9 |
| | Posterior fault Present probabilities | | |
| <i>Control hot water</i> | 100 | 100 | 100 |
| <i>Control ATES system</i> | 100 | 100 | 100 |
| <i>TSA roof system</i> | 0 | 0 | 2 |
| <i>Control regeneration</i> | 100 | 100 | 100 |
| <i>Control roof heating</i> | 100 | 100 | 98 |

Given the simplicity and limited scope of our analysis, it is remarkable that in our experiments the Bayesian method correctly identifies possible faults even when the absolute values of prior and conditional probabilities are unknown. However, the sign of the differences (positive or negative) between prior probabilities helps in achieving a more accurate diagnosis. In practice, the HVAC maintenance technician is very knowledgeable about the frequency of faults present and this knowledge should be used by the HVAC engineers in designing the DBN. Alternatively, libraries of these values could be set up.

4.10. Conclusions and recommendations

In this article, the focus is on the fault diagnosis phase based on the 4S3F architecture. In the fault diagnosis phase symptoms identified on the basis of balance, EP and OS indicators (e.g., efficiency, performance factors, capacity indicators) are fed into a DBN model constructed from the P&ID. This DBN model is built from predefined

DBN models of aggregated systems (generator, hydronic and emitter systems) and corresponding subsystems (components and control systems).

4.10.1. Results from the case study

The potential of the fault diagnosis method has been demonstrated in the case study for a thermal energy plant with an ATEs system. A full year was covered to show how faults can be isolated automatically.

Although the 4S3F system normally considers three types of faults, for the sake of demonstration only two types of faults were included: component faults caused by faulty capacity, efficiency degradation or component failure, and control faults such as the incorrectly set point of a controller or the inaccurate control of a process mode. For the sake of simplicity, the prior fault Absent probabilities of all components were set to 98% and those of all control rules to 95%. In addition, all conditional fault Present probabilities were set to 95% when a symptom is present.

The proposed 4S3F framework was successful in diagnosing faults in a thermal energy generation plant. It shows that the results are adequate even when prior and conditional probabilities in the DBN nodes are assumed. A sensitivity analysis showed that other prior values lead to the same fault diagnosis results. Energy savings of up to 25% are possible after fault corrections.

In addition to the results of the energy performance diagnosis of the HVAC system examined, the article proposes a general approach for setting up a library of diagnosis models. These models for systems can be applied to other installations.

4.10.2. Recommendations

- Although the results are very promising, further research is desirable to extend the framework, improve its accuracy and make it even easier for practitioners to use. The diagnosis aspect of the framework should be applied to other systems, such as air handling systems and heat and cooling facilities in rooms.
- A guideline for the necessary dataset of the BMS needs to be drawn up to estimate energy amounts to and from systems.
- A generic library of diagnosis models is needed from which DBN models can be selected in specific cases. For the sake of this paper, we initiated such a generic library. A relevant research objective would be to detect the strong and weak relationships between symptom and fault nodes.
- Software is needed to implement the state values of the symptom nodes in the DBN model, feed in the set probabilities of the nodes, interface with the DBN model and automate the output of the DBN diagnosis.
- In this case study, GeNie has been used as the DBN software tool. Research is needed to identify the most suitable software tool, capable of handling the

libraries of DBN models and redundant symptom information in the right way. The software must be able to deal with the adapted probabilities of events based on information from data mining and should be suited to implementation in BEMS.

- In this case study, only main heat exchange components (heat pump, boiler, heat exchangers) were faults. The DBN model can be extended with fault nodes for all components at Level C (e.g., piping, pumps and valves).
- Further research is needed on implementation in DBN. In this paper, Boolean events (Present and Absent) were implemented, meaning that the prior and conditional probabilities give the probability of the event being Present or Absent. When more events for fault and symptom nodes are introduced, it may be possible to estimate the kind of fault, for instance in the case of a negative or positive deviation. It may then also be possible to weigh the degree of the estimated deviation. This can help influence the correction of faults.
- Lastly, research into ways of automating the evaluation aspect of the diagnosis should be conducted. The application of energy balance and EP symptoms in the detection phase ensures the availability of energy levels and performance indicators, which helps to estimate energy savings by corrections.

In future, research should be carried out to see whether the HVAC can be started up automatically by the BMS in a range of modes to speed up the estimation of a fault. For instance, the BMS could estimate bias errors in temperature sensors by starting the pumps and fans at night or at weekends when no heat or cold is needed. Faulty control rules could then also be observed.

Appendix 4A. Control systems for roof heating, and cold water, hot water, condenser and evaporator supply temperatures

Control roof heating system

The roof is heated when outdoor temperatures are low. Pumps in the roof system extract heated cold water from the hydronic cold water system G. The control for this purpose is presented in Figure 4A.1.

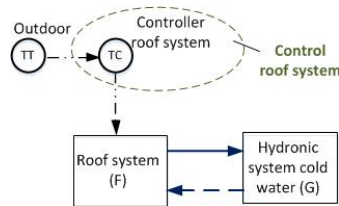


Figure 4A.1 Control roof heating system

Control cold water supply temperature (Control cw)

Figure 4A.2 is a schematic of the control of the cold-water supply temperature of the cold-water system G (*Control cw*). As the schematic shows, the controller of the cold-water supply activates the ATES systems (pump CP02-01 is turned on and off). The set point of the cold-water supply temperature is based on the outdoor temperature. This cold-water supply temperature is measured by TT29-02 and is controlled by the three-way valve TCV29-01 (depicted in Figure 4.11) in the hydronic system cold water G. When the supply temperature is not reached, the heat pump is set to deliver additional cooling.

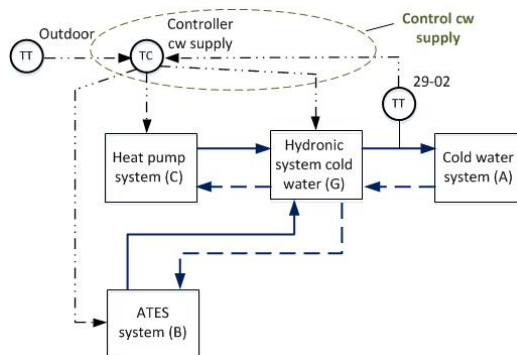


Figure 4A.2 Control of the supply temperature of the cold-water system

Control hot water supply temperature (Control hw)

The hot water supply temperature to system E is measured by sensor TT28_02 and controlled by the controller of the outlet condenser temperature at the heat pump.

However, when the set point value is not reached, the boiler system is turned on to derive the desired set point value. See Figure 4A.3. in which *Control hw* is shown.

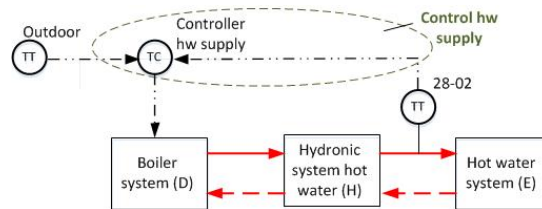


Figure 4A.3 Control of the supply temperature of the hot water system

Control condenser outlet temperature (*Control cond*)

The control of the condenser outlet temperature of the heat pump (*Control cond*) is presented in Figure 4A.4. The outlet condenser temperature is measured by TT04_01 and the heat pump system is controlled using set points and depends on the outdoor temperature.

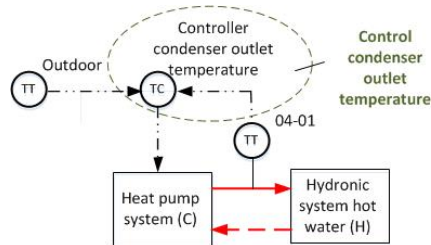


Figure 4A.4 Control of the condenser outlet water temperature

Control evaporator outlet temperature (*Control evap*)

The evaporator outlet temperature is controlled by TT04_04 and a controller. See Figure 4A.5 in which *Control evap* is shown.

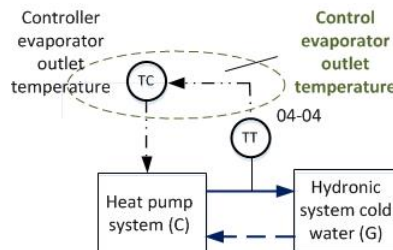


Figure 4A.5 Control of the evaporator outlet water temperature

Appendix 4B. DBN models with only aggregated systems A to H without capacity or OS symptoms

In this appendix, DBN models are presented at Level B with and without capacity or operational state symptoms. Figure 4B.1 presents the DBN model without capacity symptoms and Figure 4B.2 without OS symptoms. Figure 4B.3 then shows the DBN model without both capacity and OS symptoms. In this model, only performance indicators are present.

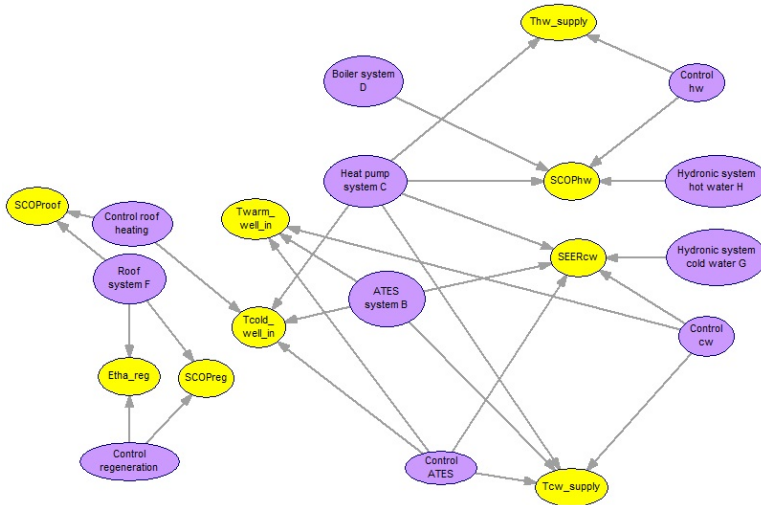


Figure 4B.1 DBN model at Level B without capacity symptoms

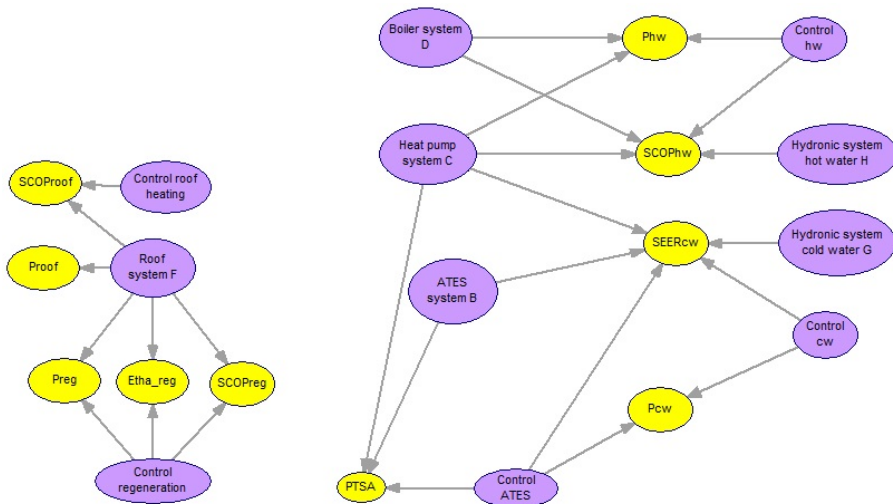


Figure 4B.2 DBN model at Level B without Operational State symptoms

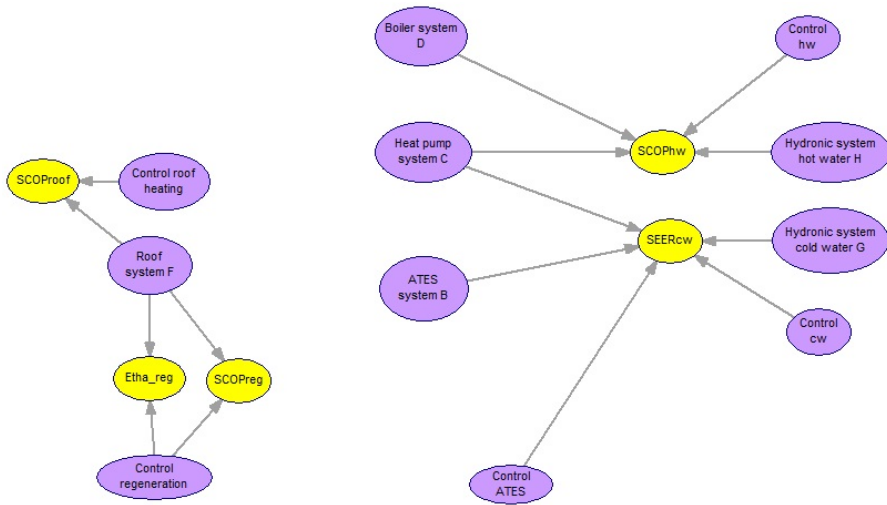


Figure 4B.3 DBN model at Level B without capacity and Operational State symptoms

References

- [1] N. Djuric, V. Novakovic, Review of possibilities and necessities for building lifetime commissioning, *Renewable and Sustainable Energy Reviews* 13 (2009): 486-492. <https://doi.org/10.1016/j.rser.2007.11.007>.
- [2] A. Taal, L. Itard, W. Zeiler, A referenced architecture for the integration of automated energy performance fault diagnosis into HVAC systems, *Energy & Buildings* 179 (2018): 144-155. <https://doi.org/10.1016/j.enbuild.2018.08.031>
- [3] W. Kim, S. Katipamula, A Review of Fault Detection and Diagnostics Methods for Building Systems. *Science and Technology for the Built Environment* 24(1) (2017): 3-21, <https://doi.org/10.1080/23744731.2017.1318008>.
- [4] S. Wang, F. Xiao, AHU sensor fault diagnosis using principal component analysis method. *Energy and Buildings* 36 (2004): 147-160. <https://doi.org/10.1016/j.enbuild.2003.10.002>
- [5] A. Beghi, R. Brignoli, L. Cecchinato, G. Menegazzo, M. Rampozzo, F. Simmini, Data-driven Fault Detection and Diagnosis for HVAC water chillers. *Control Engineering Practice* 53 (2016): 79-91. <https://doi.org/10.1016/j.conengprac.2016.04.018>
- [6] G. Li, Y. Hu, H. Chen, H. Li, M. Hu, Y. Guo, S. Shi, W. Hu, A sensor fault detection and diagnosis strategy for screw chiller system using support vector data description-based D-statistic and DV-contribution plots. *Energy and Buildings* 133 (2016): 230-245. <https://doi.org/10.1016/j.enbuild.2016.09.037>

- [7] S. Wang and J. Cui, A Robust Fault Detection and Diagnosis Strategy for Centrifugal Chillers, HVAC&R Research, 12(3) (2006): 407-428, https://www.researchgate.net/publication/268127435_A_Robust_Fault_Detection_and_Diagnosis_Strategy_for_Centrifugal_Chillers
- [8] J. Liang, R. Du, Model-based Fault Detection and Diagnosis of HVAC systems using Support Vector Machine method. International Journal of Refrigeration 30 (2007) 1104-1114. <https://doi.org/10.1016/j.ijrefrig.2006.12.012>
- [9] Y. Song, Y. Akashi, J. Yee, A development of easy-to-use tool for fault detection and diagnosis in building air-conditioning systems. Energy and Buildings 40 (2008): 71–82. <https://doi.org/10.1016/j.enbuild.2007.01.011>
- [10] X. Zhao, Lab test of three fault detection and diagnostic methods' capability of diagnosing multiple simultaneous faults in chillers, Energy and Buildings 94 (2015): 43–51. <https://doi.org/10.1016/j.enbuild.2015.02.039>
- [11] N. Ferretti, M. Galler, S. Bushby, D. Choinere, Evaluating the Performance of DABO and HVAC-Cx Commissioning Tools using the Virtual Cybernetic Building Testbed. Science and Technology for the Built Environment, 21(8) (2015): 1154-1164. <https://doi.org/10.1080/23744731.2015.1077670>
- [12] S. Farouq, S. Byttner, M. Boughalia, N. Nord, H. Gadd, Large-scale monitoring of operationally diverse district heating substations: A reference-group based approach. Engineering Applications of Artificial Intelligence 90 (2020) 103492. <https://doi.org/10.1016/j.engappai.2020.103492>
- [13] Y. Zhao, F. Xiaio, S. Wang, An intelligent chiller fault detection and diagnosis methodology using Bayesian belief network. Energy and Buildings 57 (2013) 278–288. <https://doi.org/10.1016/j.enbuild.2012.11.007>
- [14] F. Xiao, Y. Zhao, J. Wen, S. Wang, 'Bayesian network based FDD strategy for variable air volume terminals', *Automation in Construction* 41 (2014): 106-118. <https://doi.org/10.1016/j.autcon.2013.10.019>
- [15] Y. Zhao, J. Wen, F. Xiao, X. Yang, S. Wang, Diagnostic Bayesian networks for diagnosing air handling units faults – part I: Faults in dampers, fans, filters and sensors. *Applied Thermal Engineering* 111 (2017): 1272-1286. <https://doi.org/10.1016/j.applthermaleng.2015.09.121>
- [16] Y. Zhao, J. Wen, S. Wang, Diagnostic Bayesian networks for diagnosing air handling units faults – Part II: Faults in coils and sensors, *Applied Thermal Engineering* 90 (2015): 145-157. <https://doi.org/10.1016/j.applthermaleng.2015.09.121>
- [17] EN 15316-1:2017. Energy performance of buildings - Method for calculation of system energy requirements and system efficiencies - Part 1: General and Energy performance expression, Module M3-1, M3-4, M3-9, M8-1, M8-4.
- [18] Het ontwerp van hydraulische schakelingen voor verwarmen, ISSO-publicatie 44 (1998). ISSO.

- [19] Ontwerp van hydraulische schakelingen voor koelen, ISSO-publicatie 47 (2013). ISSO.
- [20] A. Taal, L. Itard, Fault detection and diagnosis for indoor air quality in DCV systems: Application of 4S3F method and effects of DBN probabilities. Building and Environment 174 (2020) 106632. <https://doi.org/10.1016/j.buildenv.2019.106632>
- [21] GeNie 2.1 (2016). BayesFusion. <http://download.bayesfusion.com>,

5. Fault detection and diagnosis for indoor air quality in DCV systems: Application of 4S3F method and effects of DBN probabilities.

This chapter has been published as:

Arie Taal, Laure Itard, “Fault detection and diagnosis for indoor air quality in DCV systems: Application of 4S3F method and effects of DBN probabilities”, *Building and Environment* 174 (2020), 106632

In this chapter, the 4S3F architecture is conducted on an end-user demand-controlled ventilation system in the building of the Hague University of Applied Sciences in Delft for indoor air quality purposes. Next to this, a sensitivity analysis of set prior and conditional DBN probabilities is conducted.

5.1. Introduction

Demand Controlled Ventilation (DCV) is claimed to be an effective method to achieve both high indoor air quality (IAQ) and energy savings. It determines the air flowrate to rooms according to the actual requirements in air-conditioned zones based on CO₂ concentration (see e.g., Fisk et al. [1] who presented an overview of DCV systems and ASHRAE standard 62.1 2013[2]). Most of the time the air flow rates are reduced significantly by DCV compared with conventional ventilation methods. In this article we focus on DCV systems controlling CO₂ concentration in workspaces. The benefits of DCV in comparison with constant air-volume systems are the reduction in heating and cooling load of the supply air and the decrease in power consumption of air handling unit (AHU) fans. Studies showed up to 40 % energy savings for fans. Tukur et al. [3] noted 25 % for an office building, Nielsen et al. [4] 35 % for family houses and Schibuola et al. [5] 40 % for a library. Zhang et al. [6] found energy savings for fans between 12 and 30 % for 15 locations in the United States. Thermal energy savings up to 25 % are depicted in [6].

Despite these positive results, generally in practice, the expected energy savings are not always realized. From a survey by Qin et al. [7] it followed that 20,9 % of the considered VAV terminals were ineffective, leading to poor IAQ and energy performance (see Lee and Yik [8], Wang [9], Guo et al. [10], who showed energy waste up to 30% for air systems, and Yu et al. [11] with energy waste between 25 and 50%). Many causes were identified in design, realization and operational stages, like faulty capacities of components, incorrect control of the DCV system or faulty sensors, see for instance Okochi and Yao [12], who stated that VAV systems can still be improved because faulty CO₂ and occupancy sensors are common due to aging

and incorrect sensor placement in rooms. Additionally, needed air ventilation capacities may have not been installed because of poor design or implementation. Moreover, CO₂ is used as proxy for indoor air quality and incorrect control of the indoor quality leads to health and comfort problems. Thus, neither energy savings or indoor quality are guaranteed.

Various types of DCV methods are available, such as occupancy presence control, relative humidity control and CO₂ control, see e.g., [13 and 14] and temperature control in VAV systems. CO₂-based DCV controlled method is most commonly used and we focus on it in this article.

Although CO₂ sensors could be placed in the rooms or in the room return air ducts, they are often installed in the main return air duct to limit costs. For instance, Shan et al. [9] proposed a multi-zone demand-controlled ventilation strategy using a limited number of CO₂ sensors in the main return air duct. However, nowadays the increased requirements for smart buildings, combined with the decrease of CO₂ sensor prices result in buildings being equipped with CO₂ and occupancy sensors in workspace. In these smart environments, DCV is controlled by both CO₂ concentration and occupancy. Many control strategies are available. Okochi et al. [12] presented an overview of controllers for VAV systems. Chenari et al. [14] presented also an overview of ventilation strategies. Conventional controllers are encountered (like P, PI PID) and predictive and adaptive controllers. For instance, Lu et al. [15] presented a dynamic DCV strategy using CO₂ balances equations, Goyal et al. [16] discussed the control of occupancy-based zone-climate, See also control strategies by Chao and Hu [17] and Wang [18].

More complex control systems lead to more chance of faults, meaning that the use of FDD (Fault detection and diagnosis) methods has become inevitable. Correction of the diagnosed faults will lead to better indoor air quality and lower energy consumption of fans and heating and cooling coils in the air handling units.

Kim and Katipamula [19] have recently presented an overview of FDD methods for HVAC systems including VAV systems. See for instance [7, 20 and 21] for VAV terminal units, Schein et al. [22] presented a method called VPACC (VAV box performance assessment control charts). FDD for the whole VAV systems is also available, see e.g., [23]. Most of the methods for VAV systems are based on expert rules [24] and can be combined with an approach with control charts using e.g., cumulative sum [24] and exponential weighted moving averages (EWMAs) [22] to eliminate transient influences and incidental outliers by measurements. In [7, 22 and 24] lists of faults and symptoms in VAV end-terminal systems are presented. Unfortunately, they are specific to the kind of considered system and generic FDD methods are still missing.

In the last decade data-driven methods were popular. Du and Jin [25] applied a principal component analysis (PCA) method to determine sensor faults and to correct them. Qi and Dong [26] proposed an FDD model for VAV systems based on neural

networks. An issue here is that data driven FDD methods use energy data based on sensors that may be faulty, and on heating, ventilation, air conditioning (HVAC) operation mode which is not always known. A novel approach is the use of Bayesian statistics. Xiao et al. [27] presented a diagnostic Bayesian network (DBN) for FDD of VAV terminals. Regnier et al. [28] proposes to apply it on AHU and VAV while Zhao et al. [29 to 31] applied DBN on AHU and chiller faults. Verbert et al. [32] also applied DBN on HVAC systems and Chen et al. [33] on whole building.

However, in all these FDD approaches the implementation does not occur simultaneously with the design of the HVAC system and its control. In [34], it was shown that the fact that FDD design does not take place concurrently with the design of HVAC and its control system, is a reason for the lack of use of FDD. The implementation of available FDD methods is complicated because it is time-consuming, and their structures deviate from HVAC design or control engineer practice.

In this article we apply the 4S3F framework which integrates these methods into an FDD architecture that can be set up by HVAC and control engineers during the design process and is based on Piping & Instrumentation Diagrams (P&IDs).

In [34] we have proposed a generic architecture for Energy Performance (EP) FDD, the so-called 4S3F method based on DBNs which can be setup simultaneously with HVAC design and implementation. This approach is based on HVAC P&IDs.

The advantages of the DBN approach as stated in [34] are:

- It is congruent to HVAC design and implementation practices.
- Fault identification takes place simultaneously at different system levels which prevent a complex top down or bottom up FDD approach.
- Outcomes are probabilities as an HVAC expert diagnoses.
- It delivers results even when information is missing or contradictory.
- It allows the application of all kinds of FDD methods to estimate or exclude symptoms and faults.

The examples in [34] are based on thermal energy plants in buildings. Here, we propose to apply it to DCV systems.

Section 5.2 introduces the 4S3F method and in section 5.3 the DCV system is explained. In sections 5.4 to 5.8 the DCV 4S3F method is applied in a case study for a lecturer room of a school building. Section 5.4 describes the 4S3F model in the case study. Then the results of the IAQ diagnosis are discussed. First, in section 5.5 basis analysis with the help of performance graphs is addressed from hourly available building management system (BMS) data. Then, in section 5.6 symptom results are shown from automated detection and finally the estimated faults are derived by applying diagnosis by a DBN model based on the 4S3F architecture in section 5.7. In section 5.8, the results are evaluated and in section 5.9 sensitivity of prior and

conditional probabilities regarding diagnosis results are discussed. Finally, conclusions are drawn from the case study and recommendations for further research are proposed in section 5.10.

5.2. The 4S3F FDD method for indoor air quality.

The reference EP FDD architecture described in [34] consists of four generic types of symptoms (4S): balance, energy performance (EP), operational state (OS) and additional symptoms. A balance symptom is present when a deviation in an energy, mass or pressure balance for a system is detected. When an energy performance metric, like a performance factor (e.g., coefficient of performance COP) or energy use shows a too low value an EP symptom is found while when a state value (e.g., temperature, flow rate, pressure, on-off state of a component) deviates unexpectedly in time, an OS (Operational State) symptom is detected. These state values could be measured by the BMS and are mostly depicted in an HVAC P&ID. Additional symptom based on for instance inspection or maintenance information, or from specific FDD methods of HVAC components can be added if needed. We recall that a symptom must be observable (is therefore the result of measurements) and symptoms can be identified by listing all measurement points (sensors) in the P&ID while a fault is the system ‘disease’ that leads to symptoms. Possible faults can be listed on the same way by observing the P&ID.

Three generic types of faults (3F), model, component and control faults, are present. The first ones are faults in assumptions in the models to estimate values for missing data. The second relates to HVAC components and systems which do not function properly. For instance, too low installed capacity, or too low efficiency by aging, or because it is defect. The last type concerns faults in the control of the HVAC components and system, for instance control of supply temperatures and on-off strategy of components like the control of the sequence of energy generators. Figure 5.1 shows relations between fault and symptom types in these 4 symptoms and 3 faults (4S3F) method.

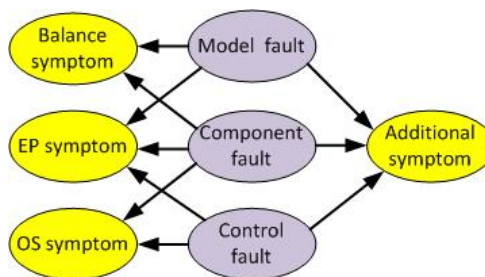


Figure 5.1. The 4S3F model: Relations between fault and symptom types.

For instance, a component fault could lead to balance, EP, OS and additional symptoms. In contrary, an EP symptom could be caused by a model, component or control fault. As can be seen there is no univocal relationship between faults and symptoms because more faults can lead to a same symptom. See [34] where this is explained in more detail.

With the help of a diagnostic Bayesian network (DBN) model, diagnosis takes place simultaneously in all components and systems. The DBN model of the 4S3F consists of the fault nodes which are linked to the symptoms nodes as shown in Figure 5.2. The fault nodes are so-called parent nodes with prior probabilities for their states and the symptom nodes are so-called child nodes with conditional probabilities for their states depending on the state of the fault nodes. The probabilities of the fault states, a value between 0 and 1, are calculated by the DBN when the states of the symptoms are known.

In this paper the 4S3F model developed for energy performance diagnosis is extended to DCV. This reference architecture supports all kind of DCV systems controlling CO₂ concentration at room level and is demonstrated on a quite common DCV system, see Figure 5.2.

5.3. Faults and symptoms of demand-controlled air ventilation systems

In this section generic faults and symptoms for DCV systems are identified and analysed. Figure 5.2 shows a P&ID, as used during design, of a frequently applied DCV system in which the supplied air flow rate is controlled by room dampers placed in end-terminals. The damper position depends on the presence of people and CO₂ concentration in the room. The air flow to the room is controlled by the CO₂ controller (CC) and the CO₂ concentration measured by the concentration transmitter (CT).

The fresh air to the rooms is supplied by the supply fan which is located in the Air Handling Unit. When room dampers are closed or partly opened, the supply and return fans in the AHU have to deliver less air flow. Usually, this can be controlled by a pressure controller (PC) which regulates the rotation speed of the fans. In the supply duct after the AHU the controlled supply pressure is measured by a pressure transmitter (PT). Controller VC opens and closes the inlet, recirculation and outlet dampers of the AHU and set the supply and return fans on and off by timers and ventilation demand.

There are also adapted versions of these control strategy (like Figure 5.2), at room level where also the presence of people (measured by a sensor indicated as PRT) and opened windows (measured by WT) are taken into account, as well as system level where the needed supply air flows are calculated by occupancy and CO₂ levels in the

rooms. In the specific case study (see section 5.4), the mechanical ventilation is shut down to avoid energy losses when the windows are open. It is very easy, using the P&ID in Figure 5.2, to list all possible symptoms and faults. This is done in Appendix A and forms the basis for the 4S3F architecture.

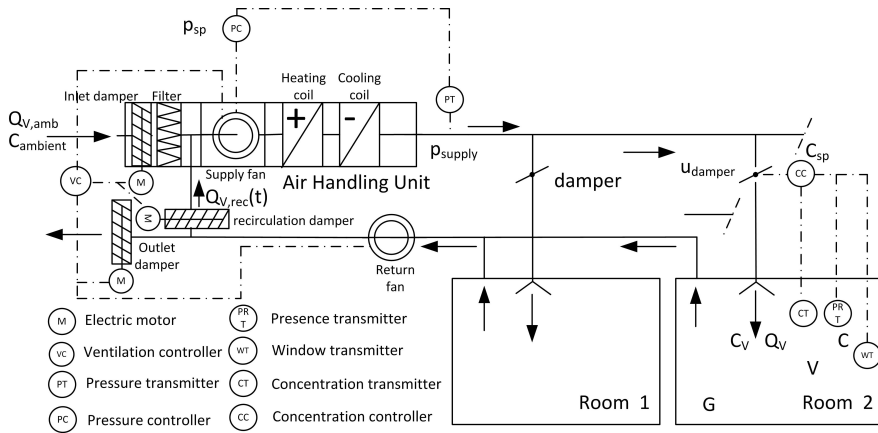


Figure 5.2. P&ID of a VAV system

G =CO₂ production in the room [kg/s].

C =CO₂ concentration in the room [ppm].

C_{sp} =setpoint of the maximum CO₂ concentration in the room [ppm].

p_{sp} =setpoint of static pressure of the supply air [Pa].

p_{supply} = Static pressure of the supply air [Pa].

C_v =CO₂ concentration of the supply air [ppm].

$C_{ambient}$ =CO₂ concentration of ambient air [ppm].

$Q_{v,ambient}$ =ambient air rate flow [m³/s].

Q_v =supply air rate flow to the room [m³/s].

$Q_{v,rec}$ =recirculated air flow rate [m³/s].

u_{damper} = damper position [0..100 %].

V =room air volume [m³].

5.4. 4S3F model for DCV systems in a case study

In this section the application of the 4S3F model to a real DCV system is shown. In the school building of The Hague University of Applied Science (THUAS) in the Netherlands a demand driven air ventilation system is present in which the air flow to the rooms is controlled by CO₂ concentration and occupancy.

The case study has been conducted on historical data of a room of the THUAS building. Hourly BMS data is available for the year 2015 and we will conduct

diagnosis on hourly basis which can also be done on actual BMS data. The location of this room 1.067, a lecturer room, is shown in Figure 5.3. In an occupied room, the air flow rate is increased when the CO₂ concentration exceeds 800 ppm and is decreased when it is below 600 ppm and the room is unoccupied. The designed supply air flow rate is 200 m³/h based on presence of 4 persons.

Most rooms of THUAS are located to an outer wall and contain windows. In each room of the building under consideration the CO₂ concentration is controlled by a damper which is present in the supply air duct to the room. A very specific control feature is that when one of the windows in the room is opened the mechanical air supply is stopped. This is to avoid energy losses. The presence is measured by a (passive infrared) PIR sensor and at the windows magnetic contacts are present which indicate an opened window. The supply air rate to a room is restricted by design and implementation of specific dampers with fixed maximum air flow rate setting. The air leaves the rooms by overflow to the corridors where return vents are present.

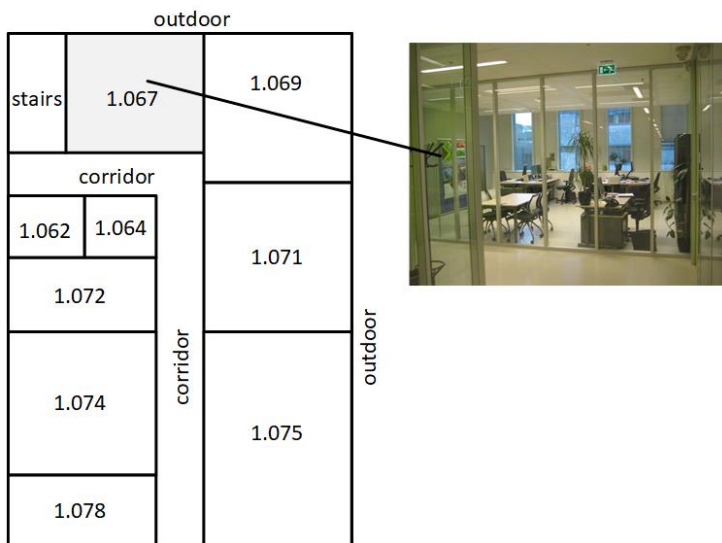


Figure 5.3. Considered building section

Too high measured CO₂ concentration in a room, one of the OS symptoms, could have, if present, many causes: by a faulty CO₂ sensor (e.g., broken), a faulty CO₂ measurement (e.g., biased value), missing connection to the BMS, a supply fan of the AHU which is not running, an occupancy sensor which is stuck, an occupancy measurement value is frozen, the damper of the VAV system which is broken or the control of it which is frozen. See Table 5.1. But also, by occupancy behaviour: the room occupancy can be higher than intended and in case of THUAS, one or more windows can be opened which leads to close the damper in order to save energy.

5.4.1. Considered faults in the case study

The faults in this case study are based on the generic faults presented in Appendix 5A in which faults are coded from F1 to F19. As simplification we do not look at the cause inside a component and cluster all faults concerning one component for the sake of demonstration. So, a broken or biased CO₂ sensor are clustered to one fault for the component CO₂ sensor, namely a faulty CO₂ sensor (F8). In addition, faults due to the AHU like damper (F4), filter (F5) and fan (F3) faults, and faults to control the AHU (F14, F15 and F17) are clustered to one component fault for the AHU because with the available BMS data in the case study it is not possible to distinguish the faults inside the AHU. However, when control values of the fan and dampers are present in the BMS, they could be separated. We have also clustered faults concerning the room damper (F7). A correct measured mechanical flow is important to detect symptoms. That is why we also take into account the air flow sensor qV as a fault (F11).

Table 5.1 presents the 9 faults which are considered in the case study. As can be seen 6 components and 3 control faults (CO₂, window and occupancy control) are distinguished. Three components are sensors: CO₂, PIR and qV sensors. Except fault F19, window control, which is specific for the THUAS building, all faults are generic for DCV systems with room control.

As can be seen model faults F1 to F2 are not taken into account in the case study because soft sensors were not applied. Furthermore, air leakage of ducts (F6) is ignored.

5.4.2. Considered symptoms in the case study

Table 5.1 also presents the 13 symptoms (depicted as **a** to **m** and based on the symptoms S1 to S13 presented in Appendix 5A,) that would be the observable result of the 9 faults identified in Section 5.4.1. Except for the balance symptoms, all symptoms are OS symptoms, meaning that the operational performance is compared to pre-set values. These pre-set values can be control setpoints and also expert rules. This approach is generic, but evidently, the setpoint values are DCV system specific.

Symptom *CO₂ unrealistic* (type S8 in Table A.1, type **a** in Table 5.1) is present when the measured CO₂ value is lower than the outdoor value or higher than an extreme value which indicates a non-realistic CO₂ measurement. When the BMS has not stored a CO₂ or a qV measurement, the value is not-a-number (NaN) which leads to symptom *CO₂ missing* or *qV missing* (both type S7, **b** and **f**). Symptom *qV unrealistic* indicates a negative value or a much higher value than should be possible on the basis of the design specifications (type S8, **e**). *High CO₂ and high qV* (type S4, **h**) represents that CO₂ is higher than the desired value with maximum air rate flow at

Table 5.1 Overview of faults and corresponding symptoms in the case study

(we have renumbered the faults and symptoms in Table 5A.1)

| FAULTS | | | | SYMPTOMS | | | |
|--------|-------------------------------|-----------|--|--|--|--------------------------|---|
| Nr | Description | Type | Explanation | Nr | Description | Type | Rules and thresholds |
| 1 | <i>Occupancy</i> | Control | The occupancy in the room is higher than according to the requirements. | h | <i>High CO₂ and high qV</i> | OS | CO ₂ >840 ppm and qV>200 m ³ /h PIR=1 |
| 2 | <i>CO₂ sensor</i> | Component | It can be broken or biased, or a cable is not connected or broken. | a b j | <i>CO₂ unrealistic</i> <i>CO₂ missing</i> <i>ΔCO₂ neighbours</i> | OS OS Balance | CO ₂ <360 or CO ₂ >3000 ppm CO ₂ =NaN ΔCO ₂ other rooms /CO ₂ on Saturdays from 0:00 to 6:00 am. |
| 3 | <i>AHU</i> | Component | It can be broken or the control of it is not right. | g m i | <i>qV_AHU=0</i> <i>qV=0</i> <i>High CO₂ and qV=0</i> | OS OS OS | qV_fan=0 and PIR=1 qV=0, PIR=1 and Δt=6 hrs. CO ₂ >840 ppm, qV=0 m ³ /h and PIR=0 |
| 4 | <i>PIR sensor</i> | Component | It can be broken or biased, or a cable is not connected or broken. | c d | <i>ΔCO₂ and PIR=0</i> <i>Presence outside working hours</i> | Balance OS | ΔCO ₂ >40 ppm, PIR=0 and Δt=1 hr. PIR=1 and 0:00<t<6:00 am |
| 5 | <i>Damper</i> | Component | The mechanical part of the damper or the electrical motor is stuck. | i k l m | <i>High CO₂ and qV=0</i> <i>High CO₂ and low qV</i> <i>Low CO₂ and qV>0</i> <i>qV=0</i> | OS OS OS OS | CO ₂ >840 ppm, qV=0 m ³ /h and PIR=0 CO ₂ >840 ppm, 0<qV<100 m ³ /h and PIR=0 CO ₂ <500 ppm, qV>0 m ³ /h and Δt=5 hrs. qV=0, PIR=1 and Δt=6 hrs. |
| 6 | <i>qV sensor</i> | Component | It can be broken, or a cable is not connected or broken. | e f | <i>qV unrealistic</i> <i>qV missing</i> | OS OS | qV>400 m ³ /h or qV<0 m ³ /h. qV=NaN |
| 7 | <i>BMS</i> | Component | A broken data-connection or software failure in the data logging leads to missing data. | f b | <i>qV missing</i> <i>CO₂ missing</i> | OS | qV=NaN |
| 8 | <i>Window control</i> | Control | The air supply to the room is stopped when a window is opened. | i | <i>High CO₂ and qV=0</i> | OS | CO ₂ >840 ppm, qV=0 m ³ /h and PIR=0 |
| 9 | <i>CO₂ control</i> | Control | The CO ₂ setpoints are not correct: too high at occupancy or too high at un-occupancy. Or delay times are too long. | k | <i>High CO₂ and low qV</i> | OS | CO ₂ >840 ppm, 0<qV<100 m ³ /h and PIR=0 |

room occupancy. In the same way *High CO₂ and qV=0* and *High CO₂ and low qV* (also both type S4, **i** and **k**) indicates too high CO₂ at absence or low value of the air flow rate to the room. During the weekends, when the building is unoccupied, the CO₂ values in rooms located close to each other should decrease to the same level. Symptom *ΔCO₂ neighbours* (type S1, **j**) is present when the CO₂ concentration in the room deviates 10 % from the mean value of the adjacent rooms at the end of Sunday night. When the CO₂ level is acceptable while an air flow rate is present, the symptom *Low CO₂ and qV>0* (type S5, **l**) is present because ventilation should not be needed. Symptom *qV_AHU=0* (type S6, **g**) is observable when the air handling unit does not supply air while the room is occupied. A room occupancy measured during night or weekend time also indicates the symptom *Presence outside working hours* (type S9, **d**). It could not be possible that the CO₂ concentration increases in the room while the PIR sensor indicates unoccupancy. Then symptom *ΔCO₂ and PIR=0* (type S1, **c**) is present. At last, when symptom *qV=0* (type S6, **m**) is observable when the room is occupied while ventilation is not present.

Notice that symptoms **c**, **h**, **i**, **k** and **m** are formed from combinations of measurements. To eliminate transient influences sufficient time periods should be taken into account.

As depicted in Table 5.1, some symptoms are only detected when they are present during more than one hour to avoid faulty detection by transient behaviour and incidental measurement outliers.

The chosen values in the rules are building specific and depend on the outdoor condition, the designed HVAC system and the HVAC control set points. The purpose of this article is not to optimize them, we have chosen values which obviously could be different in other systems. They are presented in the last column.

5.4.3. DBN model in the case study

In the 4S3F DBN method Bayesian statistics is applied which is based on relations between state probabilities of events. When the probability that event B is true (P(B)=1), the conditional probability P(A|B) that event A occurs while B is true, can be estimated using the DBN model. See Appendix 5B in which this is explained. In the DCV DBN events are faults which are linked to events for symptoms by arcs. When the true and false states of the symptoms are known, the posterior state (true or false) probabilities can be estimated.

Table 5.1 shows the links between the faults and symptoms in the DCV DBN model. This table is implemented straight forward in a DBN model. See Figure 5.4.

Set probabilities in the DCV DBN model

The values of the prior and conditional probabilities in the DCV DBN are based on assumptions. In the DCV DBN mode, the fault nodes (purple color) are parent nodes having prior probabilities which are set between 90 and 99 % true value. Thus, it is taken into account that some faults happen more often than others. For instance, a damper (1 % probability it is defect, see Appendix 5B) is seldom stuck while an opened window (5 % probability, see Appendix 5B) is more common. The symptom nodes (yellow color) have conditional probabilities which values indicates the probabilities that the symptom is present or absent

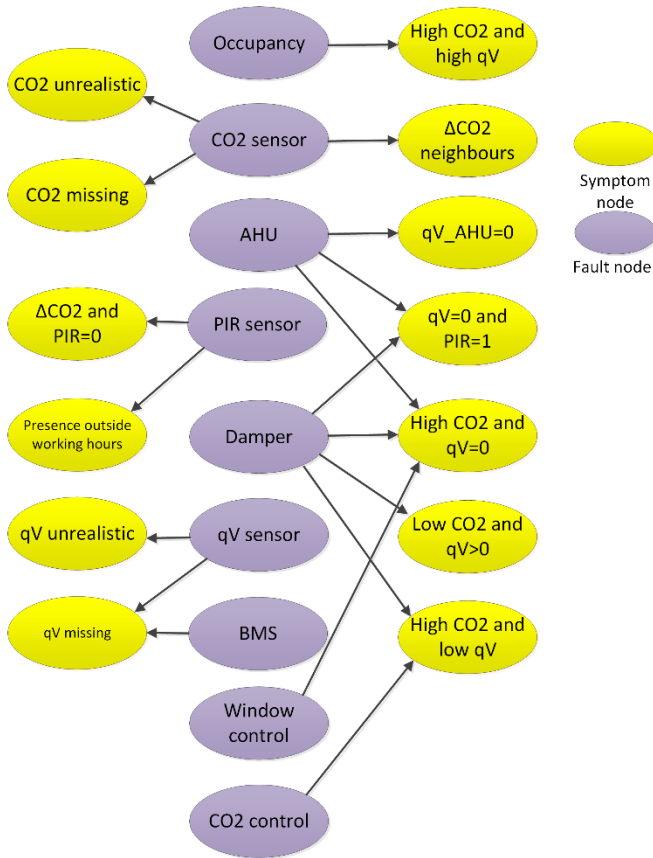


Figure 5.4. DBN model of DCV system in the case study (faults in purple, symptoms in yellow).

depending on the state of the parent nodes. As example we take symptom high CO₂ and no qV which can be caused by a disabled supply fan (AHU fault), by a frozen closed damper (Damper fault) or by opened windows (wrong Window control). The disabled supply fan leads with high probability (70 %, see Appendix 5B) to this symptom. This value is lower than 100 % because an opened window could deliver enough ventilation which does not lead to detection of the considered symptom. Another example is that an incorrect damper can be closed or opened. Only a frozen closed damper does not lead to mechanical ventilation. We assume that the probability of a frozen closed damper is as large as a frozen opened damper which lead to a conditional symptom probability of 50 % (see Appendix 5B) when the damper is faulty.

And at last, the example that windows are opened, thus mechanical ventilation is stopped. However, this will not always lead to high CO₂ concentration because the natural ventilation can be sufficient. So, we have assumed a conditional probability of 40 % that a opened window leads to too high CO₂ concentration.

Diagnosis can present fault probabilities in percentages. The absolute value is less important than the relative value. For instance, a diagnosed fault probability between 30 and 100 %

should lead to analyse the fault. We propose to look at the highest fault probabilities, e.g., higher than 30 % and start with the highest one for analysis purposes as an expert would do.

5.5. Monitoring results and descriptive analysis of BMS data

As background information, we address in this section first the measurements as energy signatures without using our 4S3F method for year 2015. Figure 5.5 shows the measured CO₂ concentration in the rooms 1.067, 1.069, 1.071 and 1.075 (the location was shown in Figure 5.3) during the year. Notice that weeks and days can be distinguished by peaks and valleys of the CO₂ levels and that they are low during end July and begin August (around 400 ppm) corresponding to an empty building during summertime. Furthermore, at the begin of the year the CO₂ concentration is higher, more than 2000 ppm!) than in the rest of the year. In most cases the CO₂ concentration stays below 1500 pp.

We see that the maximum air flow rate stays under 250 m³/h most of the time, which is higher than the designed value of 200 m³/h. Next, we see that during summer ventilation was off. Furthermore, we see a week pattern. Figure 5.7 depicts the CO₂ concentration of room 1067. The CO₂ concentration is around 800 ppm during room occupancy which is the set point value. Outliers are detected at the begin of the year and at the end of the autumn. The ambient concentration (400 ppm) is an assumption based on outdoor values in the Netherlands.

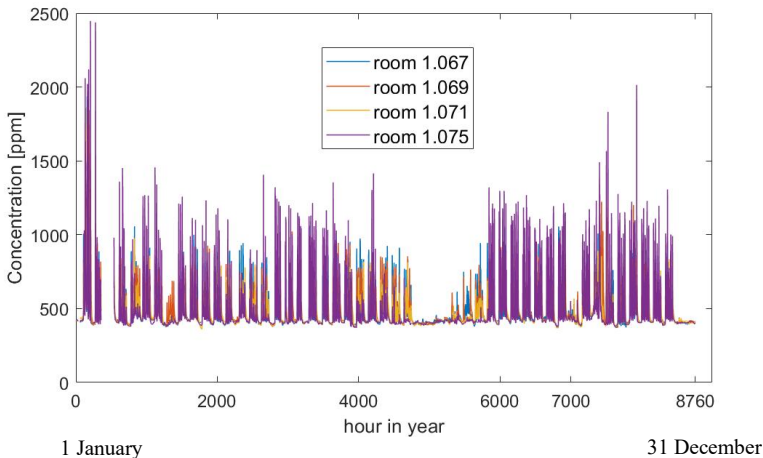


Figure 5.5. CO₂ concentrations in room 1.067, 1.069, 1.071 and 1.075.

Figure 5.6 shows the time series plot for the mechanical air flow rate to room 1.067. Figure 5.8 depicts that the room is nearly unoccupied during summertime and at Christmas time. In Figure 5.9 we see that the building is occupied from Monday to Friday (weekdays 2 to 6). Figure 5.10 shows that no air and a little bit of air was supplied on Sundays and Saturdays. The mean presence values are calculated by counting the hours that the room was occupied

during a day. The daily mean air flow rates were calculated by summarize the measured air flow rate for all days and divide it by the daily period of 24 hour.

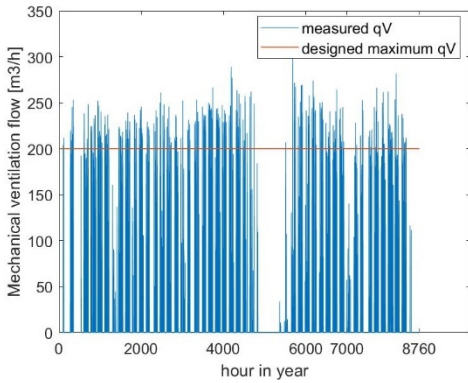


Figure 5.6. Air flow rate to room 1.067

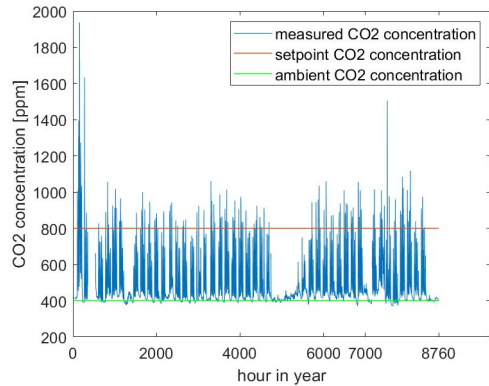


Figure 5.7. CO₂ concentration in room 1.067

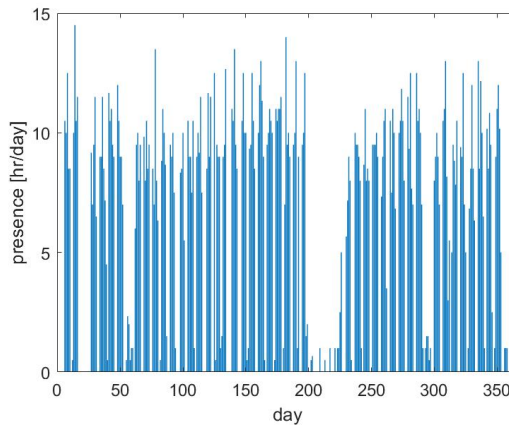


Figure 5.8. Occupancy of room 1.067

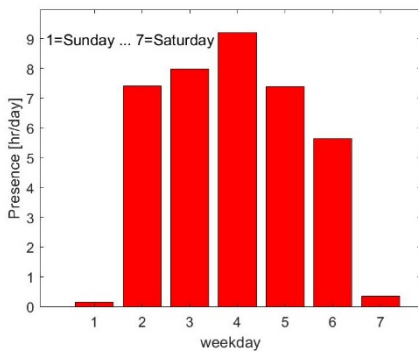


Figure 5.9. Presence during weekdays

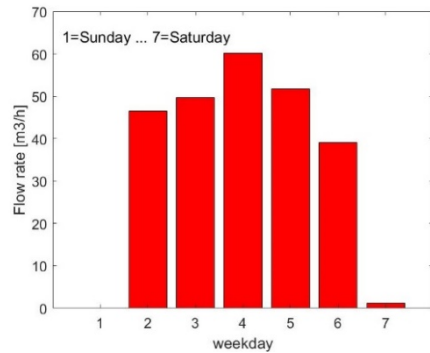


Figure 5.10. Mean air flow rate during weekdays

From these signatures, the presence of symptoms, e.g., the high CO₂ values at the begin of the year, is observed but does not lead to fault identification. It is almost impossible, also for the HVAC expert, to diagnose faults with these energy signatures or to optimize the system. Furthermore, symptoms can only be detected by outliers for which many (normal) data is needed, and automation is not possible.

5.6. Application of the 4S3F method: Detected symptoms

In this paper, we used historical BMS data on the year 2015. They were uploaded in Matlab, in which the rules and setpoints of Table 5.1 were used to detect symptoms. In an automated building energy management, they would be directly programmed into the BMS or could be an extension of the BMS. Figures 5.11 (a) to (m) present the detection results for the 13 distinguished symptoms. In these figures the value 0 indicates that the symptom is present and a value 1 it is not.

Figures 5.11 (a), 5.11 (b), 5.11 (e) and 5.11 (f) depict the detection results of symptoms **a**, **b**, **e** and **f** concerning the CO₂ and qV measurements. We see from these figures that the qV values and the CO₂ values are missing in some periods and that unrealistic values for these sensors are not present.

Figures 5.11 (c) and 5.11 (d) are about the occupancy sensor. These figures show that these symptoms for the PIR sensor are missing.

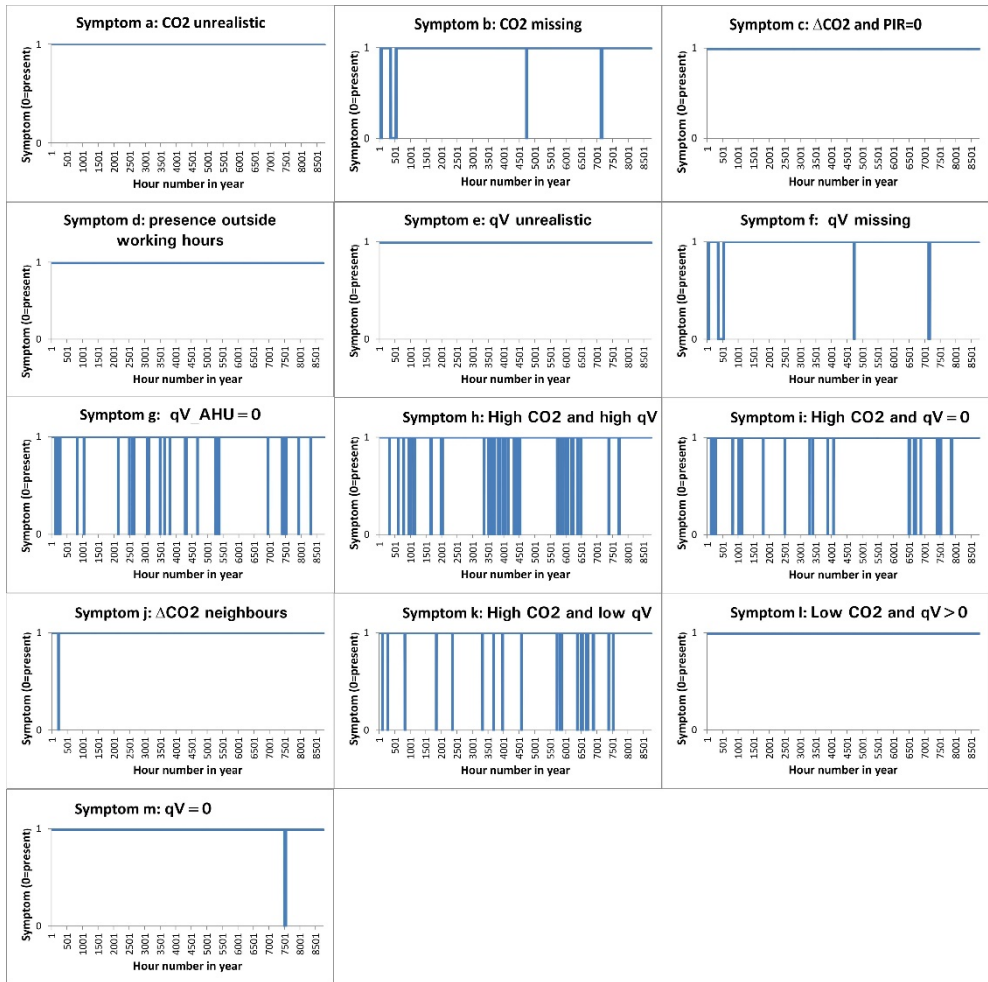
Figures 5.11 (h), 5.11 (i), 5.11 (k) and 5.11 (l) depict symptoms about CO₂ concentration and air ventilation flow. Figure 5.11 (h) shows that ‘*high CO₂ with high qV*’ is present. Notice that this symptom is often present during June and September.

Symptoms **i**, **k** and **l** are shown in Figures 5.11(i), 5.11(k) and 5.11(l). Symptom **l** is not present (ventilation while the CO₂ concentration is low) while the presence of symptoms **i** and **k** (thus high CO₂ while the ventilation is not present or low at occupancy) can be seen. Figure 5.11(j) depicts that symptom **j** (ΔCO_2 neighbours) happened once. In Figure 5.11(g) we see that the supply fan is sometimes off while the room is occupied. Figure 5.11(m) shows that symptom **m** ($qV=0$) is present only once.

This automated symptom detection is an improvement compared to the application of energy signatures as mentioned in section 5.5 in the sense that detection is automated and that a clear list of symptoms is generated. However, it is still complicated to find out the faults leading to symptoms. For example, one might estimate that sensor errors are absent from symptoms **a** to **f**, but it is more difficult to interpret symptoms **g** to **i** and **k**.

5.7. Application of the 4S3F method: Diagnosis results

In this section faults are isolated automatically from detected symptoms. The scheme depicted in Figure 5.4 is built in Genie. Then the absent and present symptoms detected in Figure 5.11 are fed to the DBN. Diagnosis has taken place for each hour in 2015. The diagnosis results are presented in Figure 5.12. The value 0 indicates that the fault is present and the value 1 it is absent.



(y-axis: 0=present, 1 = absent; hour 1=1 January, hour 8760=31 December)

Figure 5.11. Detected symptoms **a** to **m**

First, we address sensor faults. Figure 5.12(4) shows that the PIR sensor is always correct. Figures 5.12(2) and (7) show that the CO₂ and air flow sensor seems to be correct. As well CO₂ and air flow sensor faults are present once or twice. We ignore these outliers. The damper is diagnosed true because only one outlier was present, see Figure 5.12(5).

The diagnosis results for the other faults shown in Figures 5.12(1), (3), (6), (8) and (9) indicate that in 2015 the next faults were present:

- *Occupancy*
- *AHU*
- *Window control*
- *BMS*
- *CO₂ control*

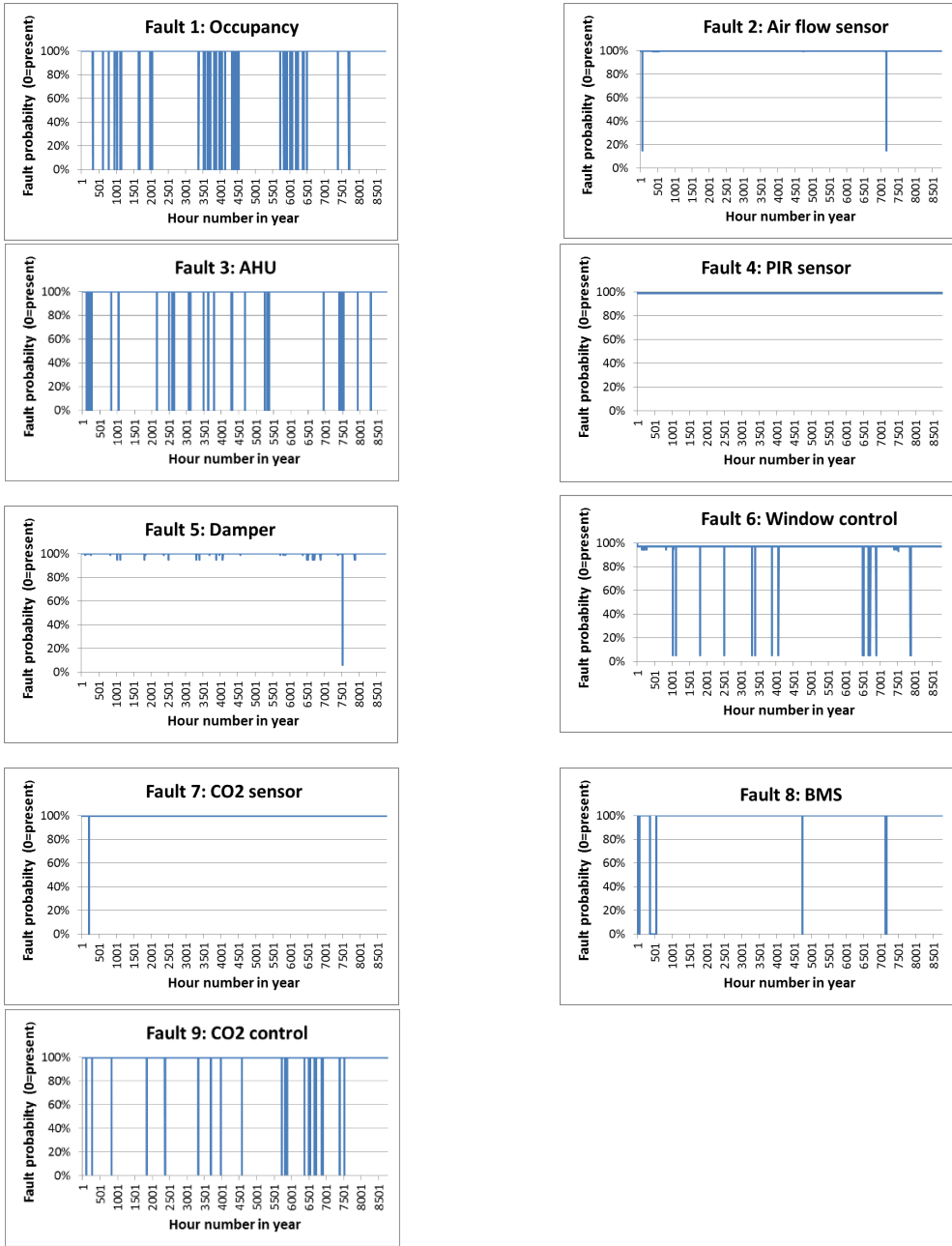


Figure 5.12. Faults 1 to 9
 (0=present, hour 1=1 January, hour 8760=31 December)

In Figure 5.12(1) we see that the occupancy of the room is too high. Figure 5.12(3) shows AHU faults and in Figure 5.12(6) depicts that one or more of the windows are opened in

some periods. Sometimes the data connection to the BMS is missing (see Figure 5.12(8)). From Figure 5.12(9) we see that the CO₂ control is not working correctly sometimes. In the next section the diagnosis results are discussed and validated with measured data and from facility manager information.

5.8. Evaluation of the diagnosis results

5.8.1. Findings from users and facility management

Occupancy information and information from the technical facility manager are used to analyze the diagnosis results. Below the findings are presented.

Fault 1: *Occupancy*

Room 1.067 is an office room for lecturers which was designed for an occupancy of 4 persons (800 ppm at a fresh air ventilation rate of 200 m³/h with an outdoor CO₂ concentration of 400 ppm). However, 6 workplaces are present in room 1.067 which, according to lecturers, are regularly fully occupied sometimes, so the room can be fully occupied especially in the busy education periods of June and September leading to higher occupancy than by design rules. Thus, signalized occupancy faults seem to be reasonably reliable.

Fault 3: *AHU*

AHU faults were estimated by diagnosis at the begin of January. It was known from the facility manager of THUAS that the supply fan in the AHU was off by malfunction of the AHU control from 6th to 12th January 2015 because this fan was set off automatically by a control rule to protect freezing of the AHU heater. However, it was not reset just in time but a few days later. Additionally, for some reasons, probably wrong signal connection with the BMS, the fan stayed off while ventilation was needed during 49 hours in year 2015. But we saw that after some hours the fan was set on and the fault was, probably automatically, restored. Thus, this fault was right diagnosed all the time.

Fault 6: *Window control*

The registered time that windows are opened, and the CO₂ concentration is higher than 800 ppm, is 58 hours. The BMS data contains also changes of the values of the contacts which registries opened windows. We have ignored consciously this data for diagnosis purposes which makes it possible to validate diagnosis outcomes concerning window control. Looking at this original BMS data, showed that one or both windows were opened during those hours. Thus, the diagnosis delivered correct results.

Faults 8: *BMS*

From the logbook at the facility manager, it was known that sometimes the data connection between the BMS and the data storage was broken.

Faults 9: *CO₂ control*

There were complaints, but nothing was done about it, because facility management thought it would come from the windows.

5.8.2. Conclusions from the case study

The case study shows the usefulness of the proposed 4S3F method for a DCV system. In almost all cases the diagnosis is correct. Only 4 outliers, one for the CO₂ sensor, one for the room damper and two for the q_v sensor were present. However, most of these false diagnoses can be prevented by using actual BMS data instead of hourly data based on a snapshot during an hour. Also, corresponding rules can be adapted. For instance, by taken into account the diagnosis results of the hours before or after the hour that the diagnosis takes place, or by changing the thresholds values in the rules. The faulty diagnosis could be corrected when another rule is introduced to estimate symptom k, for instance considering a whole day.

We have not adapted rules and thresholds in the case study because it was not our intention to optimize rules and thresholds in this article.

5.9. Sensitivity analysis of the set probabilities

Reference [34] states that the absolute values for as the prior and the conditional probabilities are not important but their relative values. A sensitivity analysis has been conducted on the DBN model presented in Figure 5.4 to investigate this statement.

5.9.1. Change of set probabilities of faults at an isolated symptom

First, we consider the effect of variable set probabilities when a symptom and its linked faults are isolated from the other DBN nodes. As example we have analysed symptom *High CO₂ and low q_v* which DBN model is presented in Figure 5B.1. In the case study the prior Absent probabilities of *Damper* and *CO₂ control* are set to 99 and 95 %. In addition, the conditional Present probabilities in the symptom node are set to 34 % and 90 % for a Present *damper* and Present *CO₂ control*. When the symptom *High CO₂ and low q_v* is set to be Present, The DBN calculated that the posterior Present probabilities of *Damper* and *CO₂ control* are 8 and 93%. Figures 5.13 to 5.16 present the results of a sensitivity analysis on prior and conditional probabilities. In Figure 5.13 the diagnosed posterior Present probabilities of the faults are presented as function from the prior Present probability of *Damper*. As can be seen, the posterior Present P(*Damper*) is still higher than those of *Window control* when its prior Present value is changed from the assumed 1 % in Table 5B.2 to 10 %.

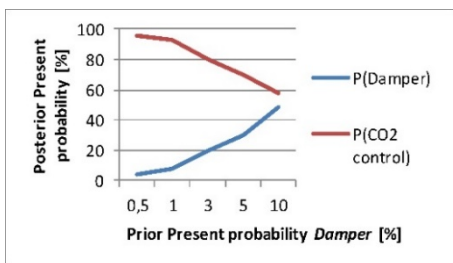


Figure 5.13. Effects prior probability *Damper*

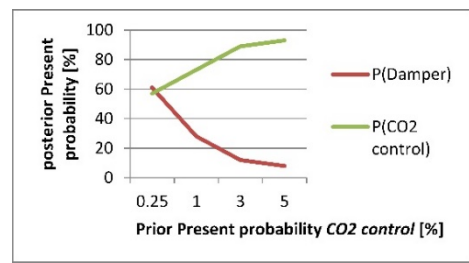


Figure 5.14. Effects prior probability *CO₂ control*

In the same way, we see that adapting of the prior Present probability of the CO_2 control from 0.5 to 5 % does not lead to other trends in fault identification. Figures 5.15 and 5.16 show the effects of changes of conditional Present probabilities. In a wide range of conditional Present probabilities, the outcome trends are the same.

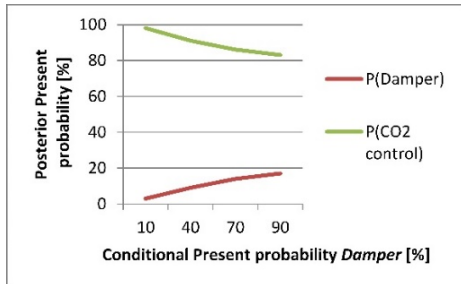


Figure 5.15. Effects conditional probability *Damper*

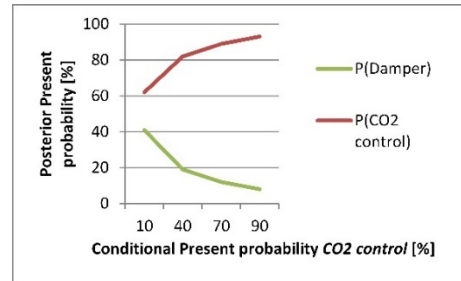


Figure 5.16. Effects conditional probability *CO2 control*

5.9.2. Change of set probabilities of faults on the diagnosis results

Here, we present the diagnosis results of the case study when some of the set probabilities concerning symptom *high CO₂ and no qV*, see the isolated DBN model in Figure 5.17, are changed arbitrary in such way that the differences with the probabilities of other nodes decrease.

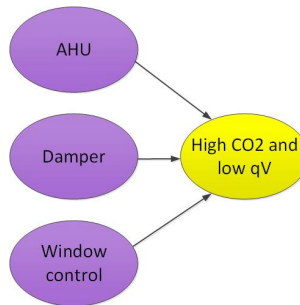


Figure 5.17. DBN model for symptom *high CO₂ and no qV*.

The next changes are made:

- Prior Present probability of *AHU* is set to 2 instead of 1 %.
- Prior Present probability of *Window control* is set to 2 instead of 5 %.
- Conditional Absent probability of *AHU* in *High CO₂ and qV=0* is set to 90 instead of 70 %.
- Conditional Absent probability of *Window control* in *High CO₂ and qV=0* is set to 20 instead of 40 %.

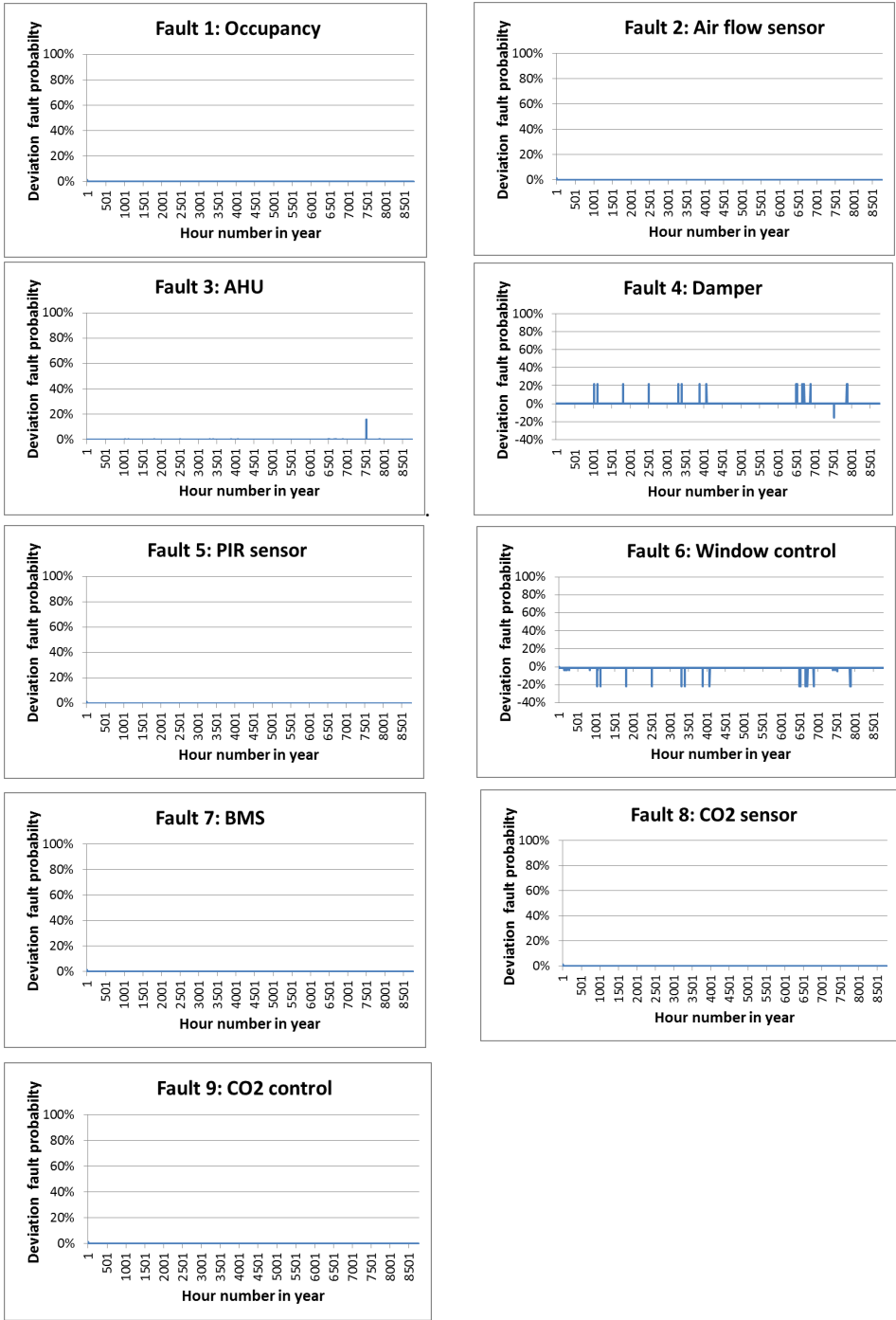
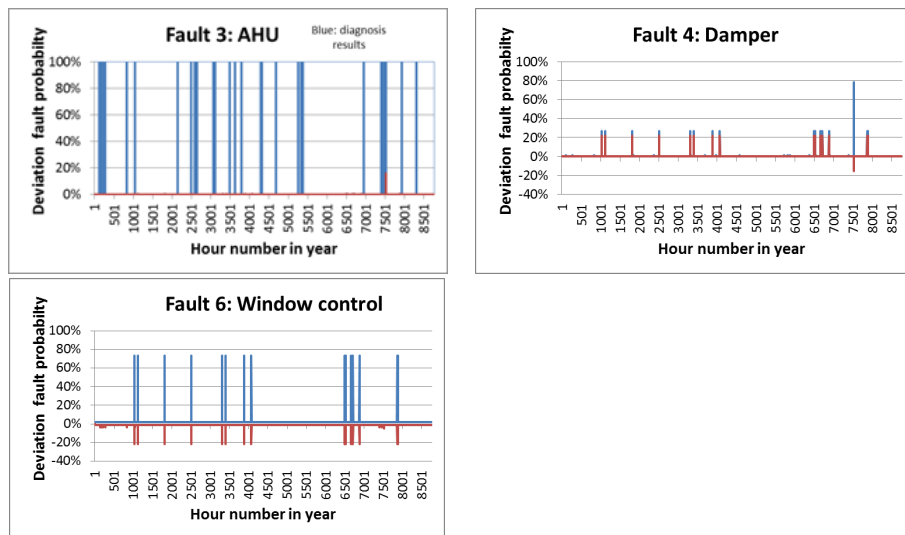


Figure 5.18. Diagnosis deviation by different set prior and conditional probabilities related to symptom *High CO2* and $qV=0$.

Figure 5.18 shows the differences between the estimated posterior fault probabilities and the results shown in Figure 5.12.

As can be seen, one outlier is present for *AHU*. Furthermore, *Damper* and *Window control* show deviations. However, even when the posterior fault probabilities presented in section 5.8 are corrected for these deviations, they stay higher than 30 % to take action for correction as noted in section 5.4. This can be seen from Figure 5.19 in which for faults 3, 4 and 6 the posterior fault probabilities are shown in blue and the deviations in red.

The sensitivity analyses show that variation in set prior and conditional probabilities did not lead to other diagnosis outcomes which confirms our statement that absolute values are of secondary importance. Detailed historical data on probabilities of the states is therefore not necessary, thus no detailed training data, but expertise about the relative frequency of errors occurring which is known by design and maintenance HVAC engineers. Also, component knowledge can be taken into account.



(red: deviation after changed set, blue: diagnosis results)

Figure 5.19. Effects on posterior probabilities at changed set probabilities to symptom *High CO2* and $qV=0$

5.10. Conclusions and recommendations

Conclusions

In this article the 4S3F FDD method for Energy Performance diagnosis has been applied on a DCV system. A generic set of symptoms and faults has been proposed and a case study has been conducted on the DCV system in a school building for the year 2015. This case study shows the usefulness of the proposed FDD method. In most cases the diagnosis seems correct despite arbitrary assumptions in symptom rules and for the probability values in the DBN model. Only 4 faulty diagnosis outliers were noted.

The DCV 4S3F method can be implemented simultaneously with the BMS system which are both based on HVAC P&IDs, like showed in Figure 5,2, as applied at HVAC design. Symptom rules and their thresholds depend on the specific DCV system. However, they can be estimated by the HVAC designer. Detection and diagnosis models could be obtained from libraries because of the generic approach in the 4S3F method. In addition, DCV faults are generic because of the generic character of the components and controls.

The sensitivity analyses in section 5.9 show that even when the set prior and conditional probabilities are varied in a wide range, this do not lead to other diagnosis outcomes as long as their relative values show the same trends as in reality.

Recommendations

Below recommendations are presented for improvement of the DCV FDD method.

Actual BMS data

In the case study hourly historical BMS data is used. The diagnosis can be proved applying real time actual BMS data. There is no limitation in the 4S3F method to use shorter periods. However, some rules have to be adapted to transient behaviour of the HVAC system and measurements outliers.

Extension with control signals from controllers

In practice, more actual BMS data is available like state and control values of actuators and controllers. The presented end-terminal system can be extended by these parameters to distinguish control and component faults of the damper and the supply fan.

Extension with AHU components

In the case study all faults in AHU are combined to one fault. One could distinguish damper, filter, fan and control faults to isolate the fault more precisely.

Recommendation to estimate and correct biased CO₂ sensors

Biased CO₂ sensors can be estimated faster and more accurately by implementing additional fully mechanical ventilation of each room during night-time. In this way a deviation in the CO₂ measurement can be estimated with the help of a mass balance symptom.

Counting persons

A simple method to count or calculate the number of persons in a room is helpful to estimate too high occupancy. This virtual sensor can be based on the increase of the CO₂ concentration and the supplied air flow. See e.g., Timilehin et al. [35] who presented an occupancy measurement survey.

Extension with specific FDD methods for components

As stated for the EP FDD, the FDD method for DCV systems can be extended with existing and new FDD methods for components as additional symptoms.

Extending the DCV FDD to VAV FDD

The proposed DCV FDD can be extended to VAV FDD by taking into account heat exchangers in the end terminals and thermal comfort control. In this way, thermal comfort indicators like air and wall temperatures and humidity can be integrated.

Optimizing the symptom rules

In the case study values in symptom rules are set up arbitrary and further studies are needed to determine optimal setpoints.

Setup of model libraries

We propose to set up model libraries for standard components and symptom rules.

Symptom rules with default thresholds.

DBN models including default prior and conditional probabilities for the fault and symptom nodes.

Automation of prior and conditional probabilities

As noted during the sensitivity analyses, the absolute values of the set probabilities are not very sensitive for the diagnosis results, but the relative values are. We propose to do research for automation of the set probabilities based on ranking of probabilities by HVAC expertise or by applying machine learning.

Integrating the DCV FDD with energy performance (EP) FDD

Misfunction of DCV systems leads to poor indoor climate but also to energy waste. Coupling the 4S3F method for energy performance diagnosis and Energy and the DCV 4S3F method gives the possibility for redundancy and therefore more accurate energy performance diagnosis.

Appendix 5A. Symptoms and faults of a DCV system

A symptom is an entity that can be observed directly and automatically from the sensors installed in the system. Finding all possible symptoms is just a matter of looking at all measurement points and analyzing what can be known from them. On the contrary, faults are anything that can go wrong. Symptoms and faults are derived from the observation of the P&ID in Figure 5.2 and summarized in Table 5A.1.

Faults F18 by over occupancy and F19 by window control are noted as control faults because people are not using the room or controlling the system as it was intended. In the first case, may be facility management allowed more persons in the room than allowed by design. The second because the occupants in the room let the windows too long opened which results in missing mechanical ventilation. A BMS fault could be a broken wiring or a software fault by failure of the communication application which lead to missing data. So, it is categorized as a component fault.

Table 5A.1 Faults and symptoms related to the DCV system of Figure 5.3.

| SYMPTOMS | |
|---------------------------------|--|
| Code | Balance symptoms |
| S1 | - Deviations in CO ₂ mass balances (e.g., the supplied CO ₂ mass must be equal to the discharged CO ₂ mass plus the increase of the CO ₂ mass) |
| S2 | - Deviations in air mass balances (e.g., by air flow rate sensor fault) |
| S3 | - Deviations in pressure balances (e.g., by air leakage which effects the supplied air rate.) |
| Operational state (OS) symptoms | |
| S4 | - The measured CO ₂ -concentration by CT is higher than the setpoint C _{sp} . |
| S5 | - Unexpected low or high CO ₂ concentration. |
| S6 | - Unexpected low or high air flows. |
| S7 | - Missing BMS data |
| S8 | - Unrealistic sensor data |
| S9 | - Presence outside working hours |
| Additional symptoms | |
| S10 | - Maintenance information |
| S11 | - Information from inspection. |
| S12 | - Sensor calibration information |
| S13 | - Complaints from occupants. |
| FAULTS | |
| Code | Model faults |
| F1 | - Model faults for virtual sensors, a physical missing state value is calculated by software from existing sensors, to estimate for instance presence and occupancy. E.g., by CO ₂ increase one could estimate the number of occupants in a room. |
| F2 | - Assumptions to set up CO ₂ - and air balances in the rooms. |
| Component faults | |
| F3 | - Supply fan or return fan, including electromotor, in the Air Handling Unit (AHU) is not working properly or broken. |
| F4 | - One of the dampers (also including electromotor) at the AHU is not working properly or broken. |
| F5 | - Inlet filter of the AHU is polluted which lead to low air flow to the building. |
| F6 | - Leakage of ducts or clogged ducts. |
| F7 | - Room damper (in which the motor is included) is broken. |
| F8 | - CO ₂ sensor is defective or biased. |
| F9 | - Presence sensor is defective or biased. |
| F10 | - Window contact sensor is defective or biased. |
| F11 | - Flow rate sensor is defective or biased. |
| F12 | - Data connection from the room sensors to the BMS is missing. |
| F13 | - Data connection to the BMS is missing. |
| F14 | - Data connection to the dampers of the AHU is broken. |
| Control faults | |
| F15 | - Control of the supply and return fan by controller PC is faulty |
| F16 | - Control of the CO ₂ concentration by controller CC is faulty. |
| F17 | - Control of the AHU dampers by controller VC is faulty. |
| F18 | - Room occupancy is higher than designed. |
| F19 | - Windows are opened while mechanical ventilation is needed. |

Appendix 5B. The construction of the 4S3F DBN

We consider a small part from the DCV DBN model of Figure 5.4 to show how the DBN calculates fault probabilities. Symptom *High CO₂ and low qV* is taken into account. From Figure 5.4 we see that this symptom can be caused by a faulty *CO₂ control* or faulty *Damper*. The faults linked to this symptom (notice that arcs go from the fault node to the symptom node) are isolated from other symptoms in this example which results in the DBN model shown in Figure 5B.1.

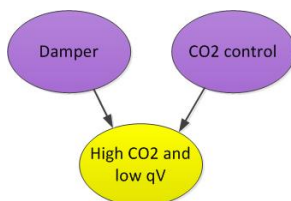


Figure 5B.1 DBN model for symptom *High CO₂ and low qV*.

Faults are parent nodes with prior probabilities. We define the probability as the number of presences per 100 observations divided by 100.

The prior probability that the damper is faulty (P(Damper)), has an arbitrary value of 1 % (see Table 5.B1) and the prior Present probability P(CO₂ control) is set higher to 5 % (see Table 5.B2) because from experience it is known that control faults occurs more often than component faults. These values can be adapted by historical values from the BMS and inspection of the logbook at the facility manager or by complaints from occupants.

In Genie [36], a DBN software tool, this can be implemented in tables for the node properties as shown in Tables 5.B1 and 5.B2. Symptoms are child nodes with conditional probabilities depending on the state of the fault node. Table 5.B3 presents possible node properties for symptom *High CO₂ and low qV* where a Present value for the symptom indicates the probability that the symptom is present. For the sake of simplification, it is assumed in this example that when one of the faults is present, the symptom is also present.

Table 5B.1 Conditional node properties *High CO₂ and low qV*
(Between parentheses: the prior probabilities).

| <i>Damper</i> | Present (0.01) | | Present (0.99) | |
|---------------------------------------|----------------|----------------|----------------|----------------|
| <i>CO₂ control</i> | Present (0.05) | Present (0.95) | Present (0.05) | Present (0.95) |
| <i>High CO₂ and low qV</i> | | | | |
| Present | 1 | 1 | 1 | 0 |
| Absent | 0 | 0 | 0 | 1 |

As can be seen symptom *High CO₂ and low qV* is present when *Damper* or *CO₂ control* is Present, otherwise Absent because both *Damper* and *CO₂ control* are Absent. In this example

we can easily calculate the probability that *High CO₂ and low qV* is Absent ($P(\text{High CO}_2 \text{ and low } qV^c)$), thus no symptom is present, when both faults are Absent because faults *Damper* and *CO₂ control* are statically independent of each other:

$P(\text{High CO}_2 \text{ and low } qV^c) = P(\text{Damper}^c \wedge \text{CO}_2 \text{ control}^c) = P(\text{Damper}^c) \cdot P(\text{CO}_2 \text{ control}^c) = 0.99 \cdot 0.95 = 0.9405 = 94.05\%$. In Table 5.B4 all calculated symptom probabilities are shown.

Table 5B.2 Calculated probabilities *High CO₂ and low qV* from the fault states.

| <i>Damper</i> | Present (0.01) | | Absent (0.99) | |
|-------------------------------|----------------|---------------|----------------|---------------|
| <i>CO₂ control</i> | Present (0.05) | Absent (0.95) | Present (0.05) | Absent (0.95) |
| Present | 0.05 % | 0.95 % | 4.95 % | 0 |
| Absent | 0 | 0 | 0 | 94.05 % |

Conversely, it is possible to calculate the Present probabilities $P(\text{Damper})$ and $P(\text{CO}_2 \text{ control})$ when the state of symptom *High CO₂ and low qV* is known. For instance the posterior Present probability of *Damper* can be calculated from $(0.05+0.95)/(0.05+0.95+4.95)=0.168=16.8\%$ when symptom *High CO₂ and low qV* is detected. Note that the posterior Present probabilities are estimated in the DBN from symptoms to faults while the DBN is set up from faults to symptoms. In Figures 5B.2 and 5B.3 two examples are presented for symptom *High CO₂ and low qV*. Figure 5B.2 shows the estimated symptom probabilities (94.1 % false) with the prior fault probabilities and Figure 5B.3 presents the estimated posterior fault probabilities when a symptom is detected (see that the *Damper* posterior Present probability is 16.8 % as mentioned earlier).

In Genie the type of the child nodes can be selected. In the general type, the child nodes have probabilities for each combination of parent states. Most of the time it is impossible or time consuming to define the fault probabilities of all these combinations.

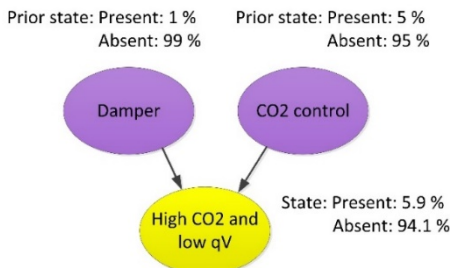


Figure 5B.2 Estimation of symptom probabilities
(Takes place during the setup of the DBN)

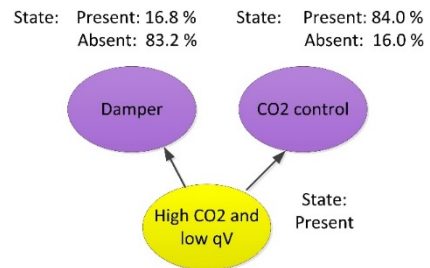


Figure 5B.3 Estimation of fault probabilities
(Takes place automatic by DBN during FDD process)

In the 4S3F method we apply so-called Noisy-Max nodes in which the Present parent state indicates the chances of the child states. Table B5 presents this for our DBN example. *High CO₂ and low qV* can be 66 % Absent when *Damper* is Present or 10 % Present when *CO₂ control* is Present. The conditional Absent probability by a present *Damper* is high because a frozen damper can be closed or largely opened which does not result in a small air flow rate. LEAK shows here the chance of the state properties when *Damper* and *CO₂ control* are

both Absent. Adjustment of the DBN example with the Noisy-Max node presented in Table 5.B3 leads both to 1 % Present values for *Damper* and *CO₂ control* when *High CO₂ and low qV* is Absent, while the Present values are 7.7 and 93.3 % when *High CO₂ and low qV* is Present.

Table 5B.3 Noisy-Max type for node High CO₂ and low qV in the DBN example

| State symptom ' <i>High CO₂ and low qV</i> ' | <i>Damper</i> Present | <i>CO₂ control</i> Present | LEAK |
|---|--------------------------|--|------|
| Present | 0.34 | 0.90 | 0 |
| Absent | 0.66 | 0.10 | 1 |

Noisy-Max nodes were applied for all DCV symptom nodes. The fault nodes, see Tables 5.B1 and 5.B2, have as first state the Present state because it is difficult to estimate the probabilities of the child node when one of the parent nodes is Absent independent of the state of the other parent nodes. In this way the Noisy-Max probabilities can be set up easily because the Absent state of LEAK can be set to 1 as we assume that the symptom is not detected when both faults are not present. Only an inaccurate model to detect symptoms could lead to a detected symptom while actually no faults are present. We have ignored this option.

As shown in Tables 5.B1, 5.B2 to 5.B5, only Present and Absent states are proposed for the fault and symptom nodes in the DCV DBN. However, it can be extended with more states when necessary.

References

- [1] W. Fisk, A. de Almeida, Sensor-based demand-controlled ventilation: a review. *Energy and Buildings* 29 (1998), 35–45. [https://doi.org/10.1016/S0378-7788\(98\)00029-2](https://doi.org/10.1016/S0378-7788(98)00029-2)
- [2] Ventilation for Acceptable Indoor Air Quality, ASHRAE Standard 62.1-2013 (2013). American Society of Heating, Refrigeration, and Air-Conditioning Engineers, Inc. Atlanta, GA, USA.
- [3] A. Tukur, K. Hallihan, K. Kissock, Energy Savings from Robust Control of Static Pressure Based upon Zonal Occupancy for Multiple-Zone VAV Systems (2016). Proceedings ACEEE Summer Study on Energy Efficiency in Buildings.
- [4] T. Nielsen, C. Drivsholm, Energy efficient demand controlled ventilation in single family houses *Energy and Buildings*, 42 (2010) 1995–1998. <https://doi.org/10.1016/j.enbuild.2010.06.006>
- [5] L. Schibuola, M. Scarpa, C. Tambani, Annual performance monitoring of a demand controlled ventilation system in a university library, *Energy Procedia* 101 (2016) 313-320. <https://doi.org/10.1016/j.egypro.2016.11.040>

- [6] J. Zhang, G Liu, R. Lutes, M. Brambley, Energy Savings for Occupancy-Based Control (OBC) of Variable- Air-Volume (VAV) Systems (2013). PNNL-22072. Pacific Northwest National Laboratory.
- [7] J. Qin, S. Wang, A fault detection and diagnosis strategy of VAV air-conditioning systems for improved energy and control performances. *Energy and Buildings* 37 (2005) 1035-1048. <https://doi.org/10.1016/j.enbuild.2004.12.011>
- [8] S. Lee, F. Yik, A study on the energy penalty of various air-side system faults in buildings, *Energy and Buildings* 42 (2010) 2–10. <https://doi.org/10.1016/j.enbuild.2009.07.004>
- [9] Y. Guo, J. Wall, J. Li, S. West, Intelligent Model Based Fault Detection and Diagnosis for HVAC System Using Statistical Machine Learning Methods (2013). *ASHRAE Transactions*. Vol. 119 Issue 1, Special section p1-8.
- [10] Y. Yu, D. Woradechjurnroen, D. Yu, A review of fault detection and diagnosis methodologies on air-handling units, *Energy and Buildings* 82 (2014) 550-262. <https://doi.org/10.1016/j.enbuild.2014.06.042>
- [11] S. Wang, Q. Zhou, F. Xiao, A system-level fault detection and diagnosis strategy for HVAC systems involving sensor faults, *Energy and Buildings* 42 (2010) 477–490. <https://doi.org/10.1016/j.enbuild.2009.10.017>
- [12] G. Okochi, Y. Yao, A review of recent developments and technological advancements of variable-air-volume (VAV) air-conditioning systems, *Renewable and Sustainable Energy Reviews* 59 (2016) 784-817. <https://doi.org/10.1016/j.rser.2015.12.328>
- [13] K. Shan, Y. Sun, S. Wang, C. Yan, Development and in-situ validation of a multi-zone demand-controlled ventilation strategy using a limited number of sensors. *Building and Environment* 57 (2012) 28-37. <https://doi.org/10.1016/j.buildenv.2012.03.015>
- [14] B. Chenari, J. Carrilho, M. da Silva, Towards sustainable, energy-efficient and healthy ventilation strategies in buildings: A review, *Renewable and Sustainable Energy Reviews* 59 (2016), 1426-1447. <https://doi.org/10.1016/j.rser.2016.01.074>
- [15] T. Lu, X. Lü, M. Viljanen, A novel and dynamic demand-controlled ventilation strategy for CO₂ control and energy savings in buildings. *Energy and Buildings* 43 (2011) 2499-2508. <https://doi.org/10.1016/j.enbuild.2011.06.005>
- [16] S. Goyal, H. Ingle, P. Barooah, Occupancy-based zone-climate control for energy-efficient buildings: complexity vs. performance, *Applied Energy* 106 (2013) 209-221. <https://doi.org/10.1016/j.apenergy.2013.01.039>
- [17] C. Chao, J. Hu, Development of a dual-mode demand control ventilation strategy for indoor air quality control and energy saving *Building Environ*, 39 (2004) 385–397. <https://doi.org/10.1016/j.buildenv.2003.11.001>

- [18] S. Wang, X. Xu, A Robust Control Strategy of Combined DCV and Economizer Control for Air-conditioning Systems. *Energy Conversion and management*, 43(18) (2002) 2569-2588. [https://doi.org/10.1016/S0196-8904\(01\)00193-5](https://doi.org/10.1016/S0196-8904(01)00193-5)
- [19] W. Kim, S. Katipamula, A Review of Fault Detection and Diagnostics Methods for Building Systems. *Science and Technology for the Built Environment* 24:1 (2017): 3-21. <https://doi.org/10.1080/23744731.2017.1318008>
- [20] H. Wang, Y. Chen, C. Chan, J. Qin, A Robust Fault Detection and Diagnosis Strategy for Pressure-independent VAV Terminals of Real Office Buildings, *Energy and Buildings* 43 (2011) 1774-1783. <https://doi.org/10.1016/j.enbuild.2011.03.018>
- [21] J. Seem, J. House, R. Monroe, On-line monitoring and fault detection (1999): 21-26. ASHRAE.
- [22] J. Schein, J. House, Application of control chart for detecting faults in variable-air-volume box. *ASHRAE Trans*; 109(2) (2003): 671-682.
- [23] A. Dexter and M. Benourats, A generic approach to identify faults in HVAC plants. *ASHRAE Trans*;102 (1) (1996): 550-556.
- [24] H. Wang, Y. Chen, C. Chan, J. Qin, An online fault diagnosis tool of VAV terminals for building management and control systems, *Automation in Construction* 22 (2012): 203-211. <https://doi.org/10.1016/j.autcon.2011.06.018>
- [25] Z. Du, X. Jin, PCA-FDA-based fault diagnosis in VAV systems. *HVACRes* 13(2) (2007):349–67. <https://doi.org/10.1080/10789669.2007.10390958>
- [26] H. Qi, W. Dong, A FDD model of VAV systems based on neural-networks and residual statistics. *Proceedings from 14th international conference on control, automation, robotics and vision, Phuket Thailand, 13-15th November 2016 (ICARCV 2016)*. 1555-1559.
- [27] F. Xiao, Y. Zhao, J. Wen, S. Wang, Bayesian network based FDD strategy for variable air volume terminals. *Automation in Construction* 41 (2014): 106-118. <https://doi.org/10.1016/j.autcon.2013.10.019>.
- [28] A. Regnier, J. Wen, Automated Fault Diagnostics for AHU-VAV Systems: A Bayesian Network Approach (2018). *International High Performance Buildings Conference*. July 2018. Paper 235. <https://docs.lib.purdue.edu/ihpbc/235>.
- [29] Y. Zhao, J.Wen, F. Xiao, X. Yang, S. Wang, Diagnostic Bayesian networks for diagnosing air handling units faults – part I: Faults in dampers, fans, filters and sensors. *Applied Thermal Engineering* 111 (2017): 1272-1286. <https://doi.org/10.1016/j.applthermaleng.2015.09.121>
- [30] Y. Zhao, J. Wen, S. Wang, Diagnostic Bayesian networks for diagnosing air handling units faults – Part II: Faults in coils and sensors. *Applied Thermal Engineering* 90 (2015): 145-157. <https://doi.org/10.1016/j.applthermaleng.2015.07.001>.

- [31] Y. Zhao, S. Wang, An intelligent chiller fault detection and diagnosis methodology using Bayesian belief network. *Energy and Buildings* 57 (2013): 278–288. <https://doi.org/10.1016/j.enbuild.2012.11.007>
- [32] K. Verbert, R. Babuska, B. De Schutter, Combining knowledge and historical data for system-level fault diagnosis of HVAC systems. *Engineering Applications of Artificial Intelligence* 59 (2017): 260-273. <https://doi.org/10.1016/j.engappai.2016.12.021>
- [33] J. Chen, J. Wen, T. Chen, O. Pradhan, Bayesian Networks for whole building level fault diagnosis and isolation (2018). *International High Performance Buildings Conference*. July 2018. Paper 266. <https://docs.lib.purdue.edu/ihpbc/266>.
- [34] A. Taal, L. Itard, W. Zeiler, A reference architecture for the integration of automated energy performance fault diagnosis into HVAC systems. *Energy & Buildings* 179 (2018): 144-155. <https://doi.org/10.1016/j.enbuild.2018.08.031>
- [35] T. Labeodan, W. Zeiler, G. Boxem, Y. Zhao, Occupancy measurement in commercial office buildings for demand-driven control applications: a survey and detection system evaluation. *Energy and Buildings*, 93 (2015), 303-314. <https://doi.org/10.1016/j.enbuild.2015.02.028>
- [36] GeNie 2.1 (2016), BayesFusion. <http://download.bayesfusion.com>,

6. Fault Detection, Diagnosis and Correction for hard and soft sensors in Building Energy Management Systems: A new extension of the 4S3F framework.

This chapter has been submitted as:

Arie Taal, Laure Itard, Wim Zeiler, “Fault Detection, Diagnosis and Correction for hard and soft sensors in Building Energy Management Systems”

In this chapter, the 4S3F architecture is conducted on hard and soft sensors which are of utmost importance to derive reliable values for detection purposes. By the nature of soft sensors, model faults are introduced. Sensor faults are estimated in a case study for the thermal energy plant of the building of the Hague University of Applied Sciences.

6.1. Introduction

Building energy management systems (BEMSs) are becoming increasingly important due to the need for a continuous realization of a high level of indoor comfort and a healthy indoor climate, alongside stringent legal requirements regarding energy use like the Energy Performance Building Directive (EPBD) in Europe [1]. The emergence of smart grids and complex controls for decentralized renewable energy systems also contribute to the increasing importance of BEMS. The energy consumption in the operational phase of a building is actually higher than expected from HVAC design. Continuous commissioning with energy management can help to reduce this unnecessarily high energy usage. Furthermore, a BEMS helps to detect and diagnose both poor thermal comfort and indoor air quality.

An energy diagnosis system is generally present in a BEMS using measured data from a building management system (BMS) that controls the HVAC system and stores the energy data, making the reliability of this data of the utmost importance. Despite the many studies regarding commissioning and energy management, see Kim and Katipamula [2] who presented recently an overview of heat, ventilation and air-conditioning (HVAC) fault detection and diagnosis (FDD) methods, building energy diagnosis systems are not often applied in practice because the implementation is complex, time consuming and there is a lack of standards. Literature presents many FDD methods to diagnose sensor faults. We come across several model-based, rule-based and data-driven methods, as presented in [2]. Much attention is paid to sensor faults due to their effects on the HVAC control. Most model-based methods, see e.g., [3 to 6], require accurate models for which setup is time-consuming while pure data-driven methods based on for instance artificial neural networks (ANN) (see e.g., [7 to 9]), Support vectors [10 to 13] and principal component analysis (PCA) [14 to 23] need

historical data for which it is important to know beforehand if it is faulty or faulty-free. This is generally not available for HVAC systems in existing buildings. In addition, many data-points cannot be handled in one data-driven method for a whole HVAC system, by which different models for each subsystem must be setup. Available rule-based methods [24 to 26] also have disadvantages that most rules are HVAC specific. Next to this, the fault isolation in most of these methods is not independent of the detection method used. Furthermore, which is the most important issue, these methods are far away from how engineers design and implement HVAC systems and knowledge of information technology is needed to set them up. Another point is that faults are estimated sequentially top-down or bottom-up while a mixed form in which estimation finds place simultaneously at different levels was shown to be more efficient in isolating faults and the effects of faults on energy consumption, see [27] and on indoor climate, see [28].

In [29] the 4S3F architecture was proposed for building energy diagnose purposes. It is based on systems engineering. This 4S3F method overcomes largely the disadvantages of pure model-based, rule-based and data-driven detection methods because it combines them in a generic way using DBN (diagnostic Bayesian network) for fault isolation. See [27 and 28]) where the method is demonstrated. In [29] the principle of the method was demonstrated with a simple example for a heat pump, in [27] for energy performance diagnosis of a thermal energy plant and in [28] for a demand-controlled ventilation system. In Taal and Itard [27 and 28] we assumed data were correct, neglecting the possibility of sensor faults. In the present article, a 4S3F method is proposed to diagnose sensor faults as well, showing that it is possible to diagnose simultaneously physical sensors (noted as hard sensor) faults as part of component faults and virtual sensors (also noted as soft sensor) faults as part of model faults while running for energy diagnosis purposes. The extended HVAC diagnosis system considered contains a heat pump combined with an Aquifer Thermal Energy Storage (ATES) system to generate heat and cold. The analysis covers part of the wintertime and therefore examines the energy measurement for heating, but also cooling required for a server room. In addition, demonstrating the framework, suggestions will be presented for the use of the framework in HVAC systems for sensor faults in general, especially for hot and cold-water systems. Several generic elaborations for standard components like headers and heat pumps and various detection and diagnosis models are proposed as well.

The case study in this paper demonstrates the practical usability of the framework and answers any concerns regarding the implementation of the framework, especially the facts that in practice there are fewer sensors placed than are ideally needed and that measurement contain uncertainties. In addition, the usage of standardized detection and diagnosis models and the simplifications which can be made in the DBN model while achieving an effective and efficient fault diagnosis are shown.

The applied 4S3F framework for BEMS is briefly presented in Section 6.2. Sections 6.3 to 6.6 discusses the generic approach for pre-processing, detection, diagnosis and correction for sensor faults. In Sections 6.7 to 6.11, the implementation of these processes in the 4S3F framework is elaborated further. Section 6.12 presents a sensitivity analysis applied to the prior probability values of sensor faults. Finally, conclusions and recommendations concerning further implementation of the 4S3F framework are drawn in section 6.13.

6.2. 4S3F framework for building energy performance

This section presents the headlines of the 4S3F framework for BEMSs applied on sensors. The presence of faults is determined by analyzing 4 different types of symptoms (4S), balance symptoms (energy, mass and pressure), energy performance (EP) symptoms, operational state (OS) symptoms and additional symptoms which are based on additional information as maintenance information.

The results of the detection phase are supplied to a DBN model. In this model symptoms are linked to possible faults. We distinguish three categories of faults (3F): faults of models used to estimate missing energy data or to set up balance models, component faults and faults to control components. Figure 6.1, from [29], shows the relationship between the 4 types of symptoms and the 3 types of faults implemented in DBN models.

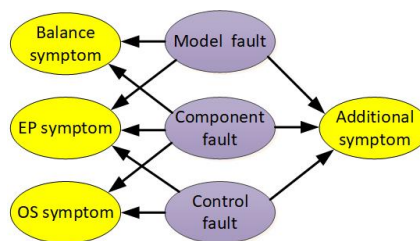


Figure 6.1. 4S3F structure.

The application of the 4S3F framework on sensor faults, is strongly based on system engineering for both detection and diagnosis of faults, applying energy, mass and pressure conservation laws for detection purposes applied to both aggregated systems and subsystems. Diagnosis finds place by DBNs by redundant analysis of fault symptoms. Furthermore, the 4S3F systematic is congruent to HVAC P&ID (process & instrumentation diagram) and it can be set up by the HVAC designer.

We consider hard sensors and their connections to the BMS as components. So, a fault in hard sensors will be classified as a component fault (e.g., a broken sensor). Soft sensors, obtained by enriching BMS data, for instance to estimate missing energy quantities by using measured temperatures and volume flow, will be considered as a model.

6.3. Generic pre-processing models for soft sensors

For symptom detection purposes, it could be necessary to apply soft sensors, a software approach to estimate missing state values or energy flow rates which are calculated from other sensors. It might also be necessary to replace BMS data missing by data connection or storage problems.

Existing BMSs are generally not equipped for automated energy performance FDD purposes. A standard like in the Netherlands ISSO 31 [30] which is a guideline for measurement points in HVAC systems, can help to estimate the desired systems and the necessary sensors which can be divided in hard and soft sensors.

Soft sensors for state values

The soft sensors embed models which contain (implicit) assumptions. Well-known models in pre-processing of missing state values are:

1. A model for mass flow rates estimation when only the status of an electro-mechanical apparatus is known. The unknown flow rate is estimated by applying documentation, like a pump characteristic and design values.
2. A model to estimate an unknown temperature with the help of other temperatures. When data points are missing, e.g., in older HVAC systems with few sensors, it could be possible to assume data from available measured data. In Figure 6.2 an example is shown for a header. When the temperature T2 is unknown, one can assume that this value is equal to the measured value of sensor TT03 or TT01.

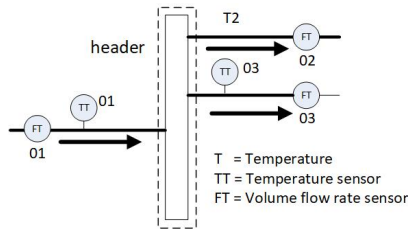


Figure 6.2. Header with unknown temperature.

3. A model to estimate a missing flow rate or missing temperature with the help of an energy balance. See Figure 6.3 which presents a model example for estimation of the missing temperature T_3 and volume flow rate q_{V3} at a three-way valve when T_1 , T_2 , q_{V1} and q_{V2} are known.
- 4.

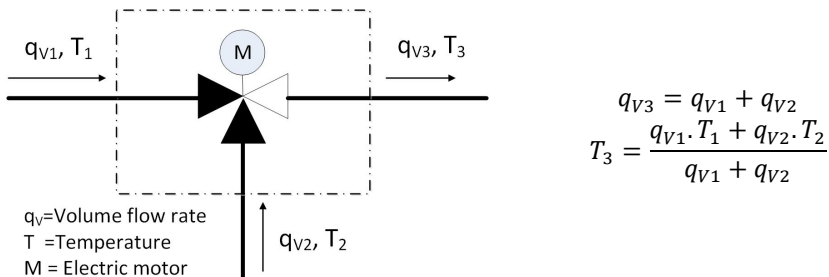


Figure 6.3. Model for a three-way valve.

5. A model for flow direction of measured mass flow rates.
6. A model to estimate the static pressure using the law of Bernoulli and taking account pressure losses by pipes, ducts and appendages.
7. A model to estimate the static pressure rise by a pump or fan turned on.

Soft sensors for thermal flow rates

Most BMSs have the possibility to store mass and thermal energy flow rates. However, this is not implemented for all HVAC components' input and output. It is common use to estimate thermal energy amounts from temperature and flow rate sensors:

1. Estimating exchanged enthalpy H by Eq. (6.1):

$$H = \sum \rho \cdot c \cdot q_v \cdot T \cdot \Delta t \quad (6.1)$$

With

ρ = density of the fluid [kg/m³]

c = specific heat capacity of the fluid [J/kgK]

q_v ,= volume flow rate [m³/s]

T = temperature [°C]

Δt = timespan at which q_v and T are considered constant [s]

2. Estimating exchanged heat Q by Eq. (6.2) with H_{in} the input enthalpy and H_{out} the output:

$$Q = \sum H_{in} - \sum H_{out} \quad (6.2)$$

3. Estimating exchanged mass m by Eq. (3.3):

$$m = \sum \rho \cdot q_v \cdot \Delta t \quad (6.3)$$

6.4. Generic approach for detection of symptoms related to sensors

In this section, general detection models and some examples for general rules are presented. In [27] and [28] examples of the 4S3F method were presented for a thermal energy-based HVAC plant and a DCV system. In these examples both EP and OS symptoms were applied and (energy) balance symptoms to detect unexpected energy losses. Examples of performance factors are coefficients of performance (COPs) and realized capacities of components. As operational states we understand physical state values such as temperatures, flowrates and pressures as well component states such as valve positions, rotation speed of pumps and on-off states of a heat pump. In this chapter we extend the use of energy balance symptoms with mass and pressure balance symptoms for sensor diagnosis purposes. Next to this we show that energy performance, operational states and additional symptoms help the sensor diagnosis.

In addition to [27], operational state symptoms related to the mode of the HVAC system are presented to exclude wrongly isolated faults in non-operational HVAC subsystems.

Independent of the type of sensor fault (broken, biased, wrongly installed or faulty modelled) the next symptoms could be detected when a sensor fault is present:

- Balance symptoms: Energy, mass and pressure balances are incorrect by faulty temperature or mass flow rates, or pressure sensor.

- Operational state symptoms
Examples of symptoms which could indicate malfunctioning sensors are:
 - Temperature deviations between measured values while the same are not expected. For instance, nearby located temperatures must be the same when the system is non-functional. Thus, the outlet water temperature of a system must have the same value as the inlet temperature when no energy is exchanged in the system. This can be realized by checking the water temperatures when the installation is not in heating or cooling operation, e.g., in weekends.
 - The flow rate sum to and from components, e.g., valves and headers, must be equal. This could be realized by checking the water flow rates every day before starting up the thermal energy plant.
 - Pressures must be equal to the atmospheric pressure when a flow machine is turned off.
 - Process mode states which indicate the presence of a sensor fault, we apply the HVAC mode (active or inactive state) of a subsystem as OS symptom to exclude a sensor fault within this system.
- Energy performance symptoms: for instance, COP and energy rate values which are unrealistic because they are calculated with faulty sensor values.
- Additional information from another FDD method for a trade component or from maintenance which indicate malfunctioning.

6.5. Generic approach for sensor fault isolation

Two types of sensor faults are distinguished: component (thus hard sensor faults) and model (soft sensor) faults as depicted in Figure 6.1.

The fault diagnosis in the 4S3F framework is based on Bayesian Theory by which posterior probabilities of faults with the help of the symptoms detected can be estimated without using an extensive trial and error method. The diagnosis method is built in a DBN model. In section 6.5.1, the generic structure of DBN models for sensor faults purposes is presented. Section 6.5.2 shows some generic DBN (sub)models for sensors as well as suggestions for the usage of HVAC process modes and values for fault probabilities. In addition, Section 6.5.3 presents generic DBN models for process modes as OS symptom and Section 6.5.4 the application of additional symptom nodes in DBN models. Next to this the use of subsystems is presented in Section 6.5.5. Finally, in Section 6.5.6, the DBN node states and probabilities are discussed.

6.5.1. Generic 4S3F structure of DBN models for sensor faults

The DBN model is built using GeNie [32], a software tool which uses the Bayesian software application Smile [33]. Examples of DBNs for diagnosis purposes are presented in [27, 28, 34 and 35]. However, we notice that a DBN model which includes many sensors could be

less readable because according to Figure 6.1 many connections can be present from sensor (component and model) nodes to symptom nodes. For instance, an energy balance symptom is linked to two flow sensors and four temperature sensors. We propose to reduce the number of links by introducing separate model fault sublayers by which hard sensor nodes are linked to symptom nodes. Therefore, the 4S3F structure in Figure 6.1 has been modified, see Figure 6.4. As can be seen, a link is added from the component type to the model type faults so that energy rate data and soft sensors can be calculated based on hard sensor values.

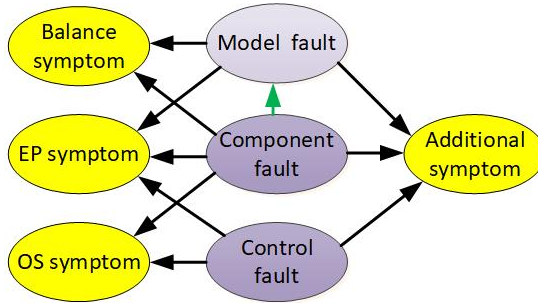


Figure 6.4. Adapted structure 4S3F model

Figure 6.5 presents the generic structure of the proposed sensor fault DBN model.

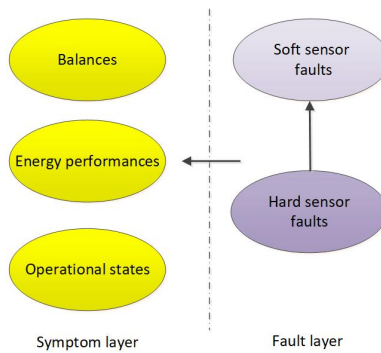


Figure 6.5. The generic DBN structure for 4S3F sensor fault diagnosis.

The proposed DBN model consists of the following kind of nodes which are connected with relationships by arcs:

- a. Hard sensor fault nodes (in purple) and soft sensor fault nodes (in light purple).
- b. Symptom nodes (yellow).

The symptom nodes are nodes which contain the conditional probabilities of symptoms: balance, EP, OS and additional symptoms.

For example, measured temperatures and flows (hard sensor data) are linked by enthalpy and heat nodes (soft sensors) to the balance nodes.

6.5.2. Generic sensor DBN models

DBN models should be implemented in the BEMS at the same time as the control in the BMS for efficiency considerations. However, they can be set up once and be available in a model library. In the case study, see Section 6.10, DBN models are applied for the headers, the heat pump, the boiler and the heat exchanger of the ATES system. As example, we present below a generic DBN model for a header.

Example: a generic enthalpy model for headers, including a soft sensor

The input and output enthalpies of a header can be calculated with Eq. (6.1). The schematic for a header can be extracted from a P&ID, see e.g., systems 1,2,4,5,14,15,21,24 and 25 depicted in Figure 6.13 which will be discussed later. As example, Figure 6.2 shows a schematic for such a header where the flow measured by FT01 is divided into flows measured by FT02 and FT03.

We suppose that T2 is a soft sensor which is modelled as being always equal to TT03. The corresponding DBN enthalpy model is presented in Figure 6.6 (the enthalpy nodes H are calculated from one temperature sensor TT and one flow sensor FT) in which T2 is a model node and the whole light purple row is a model sublayer containing soft sensor nodes.

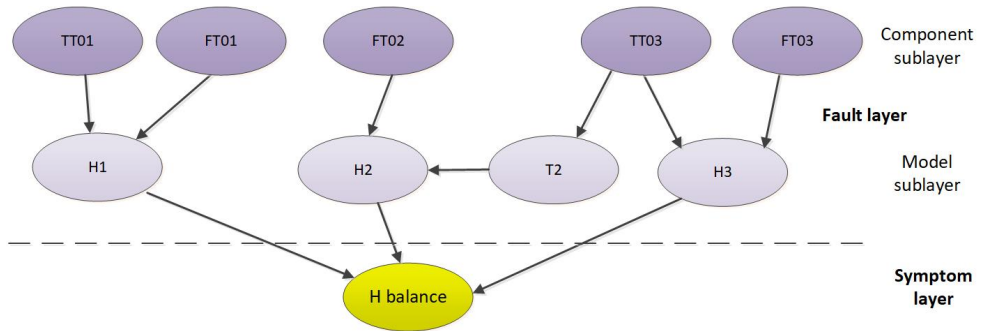


Figure 6.6. Generic DBN model for the energy balance of headers.

The corresponding DBN mass model (the incoming and outgoing mass are calculated from flow sensors) is shown in Figure 6.7.

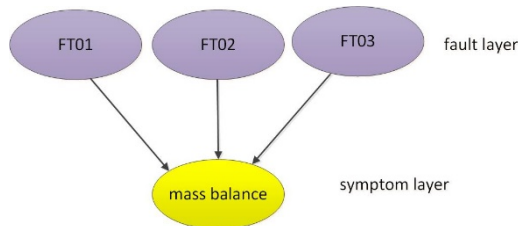


Figure 6.7. Generic DBN model for the mass balance of headers

These DBN models can be extended easily when more pipes are connected to the header. Another example, a DBN model for a heat pump system, is presented in [27].

6.5.3. Generic DBN model for process modes as OS symptom

Sensor faults can be incorrectly detected when the energy amounts of systems in which these sensors are installed are low. This can lead to a large deviation in a balance when in fact no or only a small amount of energy is transported. However, such additional information is relatively specific to systems or buildings, and it is likely to be more cumbersome to implement.

The faults in systems which deliver a small heat exchange can be excluded in the diagnosis which helps the isolation of the present faults. Depending on the heat and cold supply and demand of the building, process modes which indicate the on or (almost) off status of systems can be distinguished.

The process modes can be implemented in the DBN model by application of OS symptom nodes, so-called as negligible energy (NE) nodes are proposed, which indicate the presence of small energy amounts in the systems and set the faults in the sensor and model nodes in the fault layer of these systems to Absent. An example for this solution is shown in Figure 6.8 in which *NE01* is a negligible energy node.

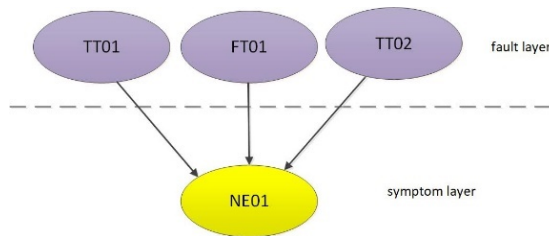


Figure 6.8. Example of a DBN Negligible energy node.

The fault nodes are set to true when the linked negligible energy symptom is Present. Figure 6.9 presents an example of a DBN NE node. When the symptom node *NE01* is set to Present, thus the exchanged energy amount is small, all sensor faults are set to Absent.

Node properties: NE01

| Parent | TT02 | TT01 | FT01 | LEAK |
|----------|---------|---------|---------|-------|
| State | Present | Present | Present | |
| ► Absent | 1 | 1 | 1 | 0.999 |
| Present | 0 | 0 | 0 | 0.001 |

Figure 6.9. Example of a DBN NE node

The fault nodes *TT01*, *TT02* and *FT01* are set to Absent when symptom *NE01* is Present. This is realized in GeNie by LEAK that here has the arbitrary value 0.001 (higher than 0) for the Present state of *NE01*.

6.5.4. Generic DBN model with an additional symptom

Symptoms which indicate the presence or absence of a sensor fault, for instance by another FDD method or from maintenance or inspection information can be added as an additional symptom. Figure 6.10 presents an example of such a DBN model for *TT01*, *FT01* and *TT02* as possible hard sensor fault nodes and an enthalpy balance (*Hbalance*) as symptom node. As additional information from sensor *TT01*, the symptom node *FDD TT01* is present.

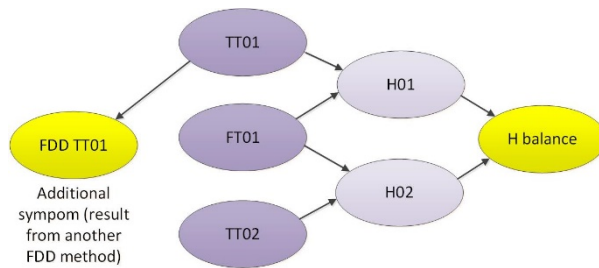


Figure 6.10. Example of DBN model with an additional symptom.

Possible prior probabilities of *FDD TT01* are shown in Figure 6.11.

Node properties: FDD TT01

| | | TT01 | Present | Absent |
|---------|--|------|---------|--------|
| Present | | 1 | 0 | |
| Absent | | 0 | 1 | |

Figure 6.11. Prior probabilities of the additional node *FDD TT01*.

The posterior outcomes for *TT01*, *FT01*, and *TT02* depend on the state of *FDD TT01* when the symptom *H Balance* is set to Present. Table 6.1 shows that all sensors have almost the same Present probability (34-35%) when the evidence of *FDD TT01* is Unknown. When *FDD TT01* is Present then *TT01* is set correctly to Present and set to Absent when *FDD TT01* is absent.

6.5.5. The use of aggregated systems in GeNie

GeNie offers the possibility to create aggregated DBN models from DBN submodels. In this way, it is possible to develop specific DBN models with the use of generic DBN models for

components or subsystems, which shorten the implementation effort of the specific DBN models.

Table 6.1 Posterior Present probabilities depending on the state of FDD TT01

| Posterior Present probabilities [%] | | | |
|-------------------------------------|-------------|-------------|-------------|
| | Sensor | | |
| State <i>FDD TT01</i> | <i>TT01</i> | <i>FT01</i> | <i>TT02</i> |
| Unknown | 34 | 35 | 34 |
| Present | 100 | 2 | 2 |
| Absent | 0 | 52 | 50 |

6.5.6. Node states and probabilities

In the nodes of the DBN models, the state probabilities of the Present and Absent events have to be set. The fault nodes are parent nodes which contain prior probabilities for the events of the nodes. The child nodes, like the enthalpy nodes, heat nodes and heat balance nodes, have conditional probabilities for the Present and Absent events that depend on the absence of the connected parent node faults, as presented in [27 and 28]. First, the set values of the prior probabilities should be determined, followed by those of the conditional probabilities.

Prior probabilities

The values for the prior state probabilities are chosen arbitrarily but based on expert knowledge. During the assessment period and considering past performance and the age of the equipment, it is assumed that less than 5% of the temperature and flow sensors are stuck or biased. So, there is a prior probability of 95% that the sensor readings are correct. This value is also assumed for the energy meter of the heat pump.

However, the prior Present probabilities of all assumptions of the pre-processing models are set higher, because, based on the authors' understanding of and experience with simulation models, the uncertainty is much higher. For straightforwardness, the prior Present probabilities for these model assumptions are all set to 10%. The influences of the above-mentioned choices will be discussed in section 6.12.

Conditional probabilities

The conditional probabilities of the child nodes depend on the state of the parent nodes. Parent node faults can compensate each other. Therefore, an Absent probability of 2% for the child node is set when one or more of the parents are Present.

In the future the prior and conditional probabilities can be fine-tuned by experience and data mining.

6.6. Generic approach of sensor corrections

The main types of corrections that can be distinguished are the repair of sensors or the adaptations and adding of models which are presented in sections 6.6.1 and 6.6.2 respectively.

6.6.1. Repair of hard sensors

Four causes for hard sensor faults are possible. The first one is that the measurement value is (temporarily) not available in the BMS, and the second is that the sensor is broken. Indicators for stuck sensors and missing measurements are unrealistic measured values and very high balance deviations, for instance higher than 40%. In the case of missing measurements, the necessary state values can be replaced, for example, by historical BMS data for the same conditions of HVAC processes using for instance a regression method or by replacing the missing data by calculated data from other available BMS data. If a sensor is broken it must be replaced. The third cause of fault sensor measurements could be that a sensor has been wrongly installed, and the fourth cause could be that of a drifting sensor. In the case of a high deviation, the measurement can physically be adjusted by:

- the displacement of the sensor when it is not installed correctly, which generally demands a high investment and will not often be applied in practice.
- the replacement of the sensor.
-

Or, in case of low deviations or when a physical solution is not possible, software-based corrections by:

- a bias correction
- the replacement of the measured value by a value calculated by a soft sensor which can also be applied in case the bias correction does not lead to adequate results.

6.6.2. Adaption of soft sensor faults

In case of a pre-processing model fault, another model has to be set up. Perhaps the model fault is easy to detect, and the model can be corrected by taking into account corrected heat losses for instance. However, a model expert has to be consulted when the necessary model adaption cannot be estimated. Fortunately, at the end of the implementation phase or at the beginning of the operational phase of the HVAC installation, the pre-processing model faults can be estimated for all possible process modes for the HVAC installation in an initial commissioning procedure.

6.7. The thermal energy plant in the building of The Hague University in Delft

6.7.1. System description

The proposed FDD framework was tested on the building of The Hague University of Applied Science (THUAS) in Delft. The THUAS building (see the atrium in Figure 6.12) was selected because it has a complex HVAC system with an advanced control system, and extensive measurement data is available for analyzing energy consumption and the indoor climate. The building mainly contains classrooms, offices for the lecturers and a restaurant.

In [27], which presents the application of the 4S3F method for energy performance purposes on the thermal energy plant of the THUAS building, the working of this systems is described.

Figure 6.13 shows the P&ID of this plant in which 37 sub-systems which exchange energy, are depicted as numbers. Hard sensors are indicated by code TT for temperature sensors and FT for flow rate sensors. The needed soft sensors needed for energy purposes are highlighted in yellow.



Figure 6.12. Inside the THUAS building

Heat is generated by a heat pump system and a boiler system and distributed to the hot water system in the building by a hot water hydronic system. Cold is generated by the cold well of the aquifer thermal energy storage (ATES) system and by the heat pump. By the cold-water hydronic system, the cold is transported to the cold-water systems of the building. In the winter, the parking roof is heated by the hot well of the ATES system. Because the ATES system has to be balanced over a year and more heat is extracted than cold from the ATES system, heat is regenerated to the hot well by the parking roof during summertime.

6.7.2. Detection and diagnosis systems

As noted in [29], balances are set up from small components, depicted in Figure 6.13, towards subsystems and the overall system. So not only the systems (1) to (30) are considered but also aggregated systems which combine components, for instance headers and buffers. Theoretically, many aggregated systems are possible. For instance, system (1) and (2) as well (2) and (3) can be combined and (1) to (3) etc. The order could be $30!$ thus more than 10^{32} combinations. It is not realistic and necessary to define all possible systems. Below, the selected systems are presented. First the aggregated systems (A), (B), (C), (D), (E), (F), (G) and (H), see Figure 6.14, which shows aggregated systems in the form of a block scheme in accordance with Figure 6.13. The arrow direction shows heat transferred Q and supplied work W to pumps and also the heat pump compressors electric work depicted as W .

In addition, the aggregated systems (I) and (II) are defined which contain the cold-water groups and the hot water groups. Finally, the overall system (III) is defined. Next, systems (a) to (d), are distinguished for couples of headers in the plants which are helpful for heat balances purposes: system (a) contains header 1 and 2, system (b) header 4 and 5, system (c) header 14 and 15 and system (d) header 24 and 25.

For each system, an energy balance can be set up with supplementary a mass balance.

Summarized, 45 energy and 8 mass balance symptom rules are available.

yellow marked:
soft sensors

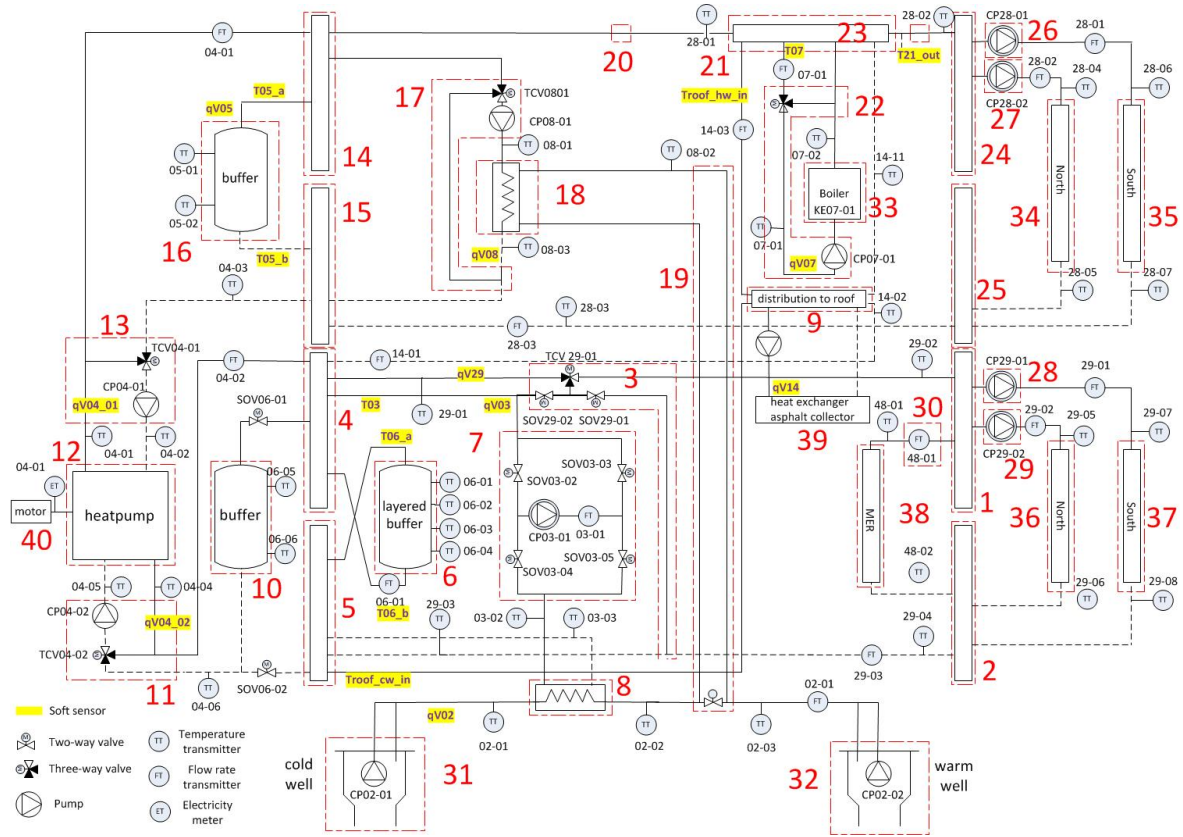


Figure 6.13. HVAC P&ID of the heat and cold generation system of THUAS including soft sensors.

6.8. Hard and soft sensors in the case study

6.8.1. Hard sensors

From Figure 6.13, 42 hard temperature, 15 hard flow rate sensors and one hard energy meter can be extracted. The installed temperature sensors are of the type of LG-Ni 1000 with an accuracy between 0.5 and 0.8 K depending on the operational temperature. The flow sensors have an accuracy of $\pm 0.5\%$ of reading which results in faults between 0.5% (at velocity > 1 m/s) and 2.5% (at low velocity). The BMS data is recorded every four minutes. The stored sensor data contains one decimal number leading to an increase of the inaccuracy of the stored temperature values of 0.1 K and of the flow rate sensors of 0.1 m³/h.

For the case study in this paper only the wintertime is reflected. The period of November 14th to December 11th, 2013 (28 days) was considered because of the availability of an almost complete set of 4 minutes energy data and the period is long enough to demonstrate the 4S3F principle.

6.8.2. Soft sensors for missing BMS data

Unfortunately, the sensors present have not been implemented for FDD purposes based on balance symptoms, so soft sensors had to be applied. When looking at Figure 6.13, it is obvious that some state values of the systems (1) to (30) are not measured. There are 16 missing data points, yellow highlighted depicted in Figure 6.14: qV04_01, qV04_02, qV05, qV07, qV08, qV14, qV29_01, Troof_cw_in, Troof_hw_in, T03, T07, T06_a, T06_b, T05_a, T05_b, and T21_out. In addition, the flow direction of FT02_01 and FT03_01 of the ATES system, depicted as qV02 and qV03, are not measured.

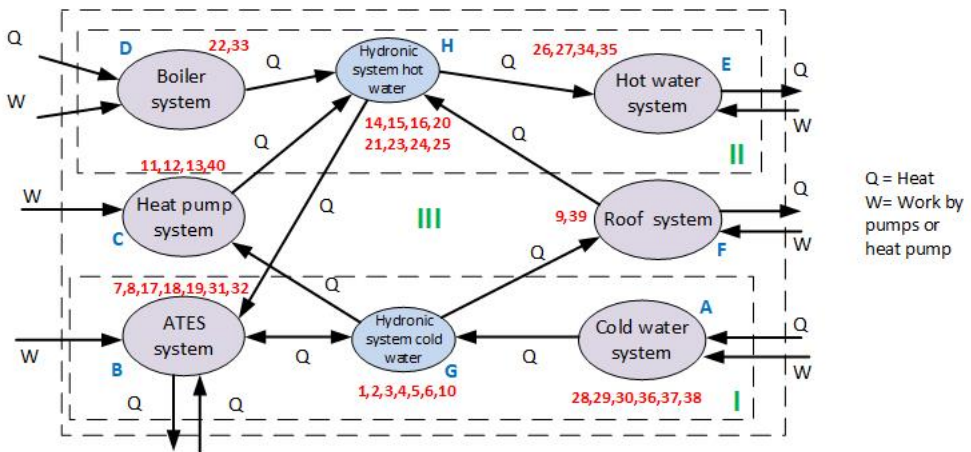


Figure 6.14. Aggregated systems in block scheme form.

The missing data are estimated by 18 soft sensors using pre-process models. With these models, which are models any HVAC expert could make, the energy and state values of the considered systems are now known and the balance equations which are needed in the

detection phase can be set up consulting the HVAC P&ID. Notice that needed sensors should be placed in new HVAC installations which is probably less expensive than set up, check and correction of pre-process models and will also result in more accurate FDD.

6.9. Fault symptom detection in the case study

In this section results of symptom detection in the case study is presented. A detection period of one day is taken into account. The reason for this choice is that daily analysis delivers in most cases of thermal energy diagnosis an adequate result. In the worst case, the delay is a few days for correcting the diagnosed fault. Furthermore, the detection models can be simple, and the proposed corrections are more robust than when a shorter detection timespan is applied by elimination of outliers and transient behaviour. Steady state models can be used for most HVAC systems meaning that energy and mass storage in the considered systems is neglected, which is good enough at daily level.

In the case study pressure balances are not analyzed because too few pressure sensors were installed to set up pressure balances. Furthermore, additional symptoms, like maintenance and inspection information, are not considered in this case study.

First, the results of balance detection are presented in Section 6.9.1. In addition, Section 6.9.2 describes the detection of energy performance symptoms, followed in Section 6.9.3 the results of operational state symptoms. Section 6.9.4 concludes with an overview of the symptoms detected.

In the case study, energy and mass balances are set up once for the 40 considered systems. This needs to be programmed only once in the BEMS. Then for all considered 28 days the percent deviations of the balances are calculated and compared with the set thresholds ε_{\max} .

6.9.1. Symptom detection by using balances

As noted earlier, analysis finds place on values aggregated on one day for a period of 28 days. The percentage deviation δ of the balances is calculated for every day with Eq. (6.4).

$$\delta = \frac{E_{out} - E_{in}}{E_{in}} \quad (6.4)$$

With

E = energy [J]

Thresholds for detection by balance symptoms

Due to inaccuracy of measurements and transient behaviour of the HVAC component band widths are needed for symptom detection. The design values are unknown, so we assumed an acceptable threshold of 5 % for daily heat balances and 3 % for daily enthalpy and mass balances. Energy-related thresholds include system heat gains and losses, which are assumed to be one or two percent due to the good insulation of components.

Results

Most systems indicated true balances. However, 20 systems (1), (2), (4) to (7), (11), (12), (22), (24), (25), (C), (D), (G), (a),(b),(e), (I) and (III) show faulty heat balance outcomes for

one or more days. Some examples of the results are shown in Appendix 6A.1. As can be seen no symptoms were detected in system (B) and (H). Contrary to these systems, the other examples show that the deviations are larger on most days than the threshold of 5%. It is shown that the absolute deviation of the heat balance for the overall system (III) is less than the threshold of 5% for most days.

6.9.2. Detection by using energy performance symptoms

Thresholds for detection by EP symptoms

Here, we assumed a threshold of 10 % for daily energy performance. Appendix 6A.2 presents results of the daily COP and EER for the heat pump. A too high EER is detected for most days.

6.9.3. OS Symptom detection

Operational states

Thresholds

The threshold for temperature deviations, belonging to OS symptoms, is set to 0.4 K, meaning $|\Delta T| < 0.4$ K.

Results

Results of the OS symptom detection are presented in Section 6A.3. It is shown that the temperature sensors TT04-04 deviates from TT04-04.

Process modes

The thermal energy thresholds are arbitrarily set at 2 GJ/day (maximum energy exchange is 11.3 GJ/day during the observed 28 days) and the heat pump work at 0.5 GJ/day which is maximum 2.1 GJ /day.

Results

As can be seen from Section 6A.4, some aggregated systems are inactive some days, especially on Sundays when the building is unoccupied.

6.9.4. Conclusions

Finally, in the balances of 19 systems faulty mass and heat balance outcomes were found for one or more days. In addition, it yields the symptom EERhp as Present, and further information shows that a temperature difference between TT04_04 and TT04_05, and TT04_06 is present. The detected symptoms are summarized in Table 6.2.

6.10. Sensor fault identification in the case study

This section presents the implementation of the diagnosis phase and shows fault isolation results for the case study.

In our experiment, 58 hard sensors (see Figure 6.14) are present, containing temperature transmitters (code TT), flow transmitters (code FT) and the work delivered to the heat pump

Table 6.2 Detected symptoms related to faults.

| Detected symptoms | Description of system |
|-------------------------------------|---|
| Balance system (1) Present | Cold water header |
| Balance system (2) Present | Cold water header |
| Balance system (4) Present | Cold water header |
| Balance system (5) Present | Cold water header |
| Balance system (6) Present | Buffer |
| Balance system (7) Present | Secondary water distribution ATES system |
| Balance system (11) Present | Evaporator group heat pump |
| Balance system (12) Present | Heat pump |
| Balance system (22) Present | Boiler module |
| Balance system (24) Present | Hot water header |
| Balance system (25) Present | Hot water header |
| Balance system (a) Present | Headers (1) and (2) cold water |
| Balance system (b) Present | Headers (4) and (5) cold water with buffers |
| Balance system (e) Present | Headers (24) and (25) hot water |
| Balance system (C) Present | Boiler system |
| Balance system (D) Present | Hydronic system cold water |
| Balance system (G) Present | Hydronic system hot water |
| Balance system (I) Present | Cold water circuit |
| Balance system (III) Present | Overall system |
| EER _{hp} too high Present | Heat to evaporator of the heat pump divided by compressor work. |
| Deviation TT04_04 – TT04_05 Present | Deviation water temperatures in evaporator group |
| Deviation TT04_04 – TT04_06 Present | Deviation water temperatures in evaporator group |

(code ET), and 18 models for soft sensors are made for missing state values. Thus 76 possible sensor faults are defined. Unfortunately, only 44 symptom rules are available, so the problem is undetermined.

First, the overall DBN model is set up by the use of DBN sub models which contain some of the considered systems (1) to (30) (as proposed in Sections 6.5.2 to 6.5.5), then the prior and conditional probabilities of the nodes are set (Section 6.5.6). It is assumed that a fault must be analyzed when the posterior probability is higher than 40 %.

6.10.1. The implementation of DBN models in GeNie

The overall DBN model in the case study is presented in Figure 6.15. As can be seen it is built up by generator systems (left), hydronic system (middle) and emitter systems (right) as shown in Figure 6.14 as blue nodes.

The overall DBN model consists of aggregated DBN models which are built up from the systems (1) to (30).

An example of a DBN submodel is presented in Figure 6.16 which shows the heat pump system (C). In this model the symptom nodes are yellow, the hard sensor fault nodes purple and the soft sensor fault nodes light purple. We see balance symptoms (depicted as *Q_{balance}*), OS symptoms (e.g., *TT04_04-TT04_05*) and EP symptoms (e.g., *COP_{hp}*). Hard sensor fault nodes (indicated as TT and FT) as well soft sensor fault nodes (e.g., *qV04_01*, *qV04_02* and the *H*'s and *Q*'s) are presented.

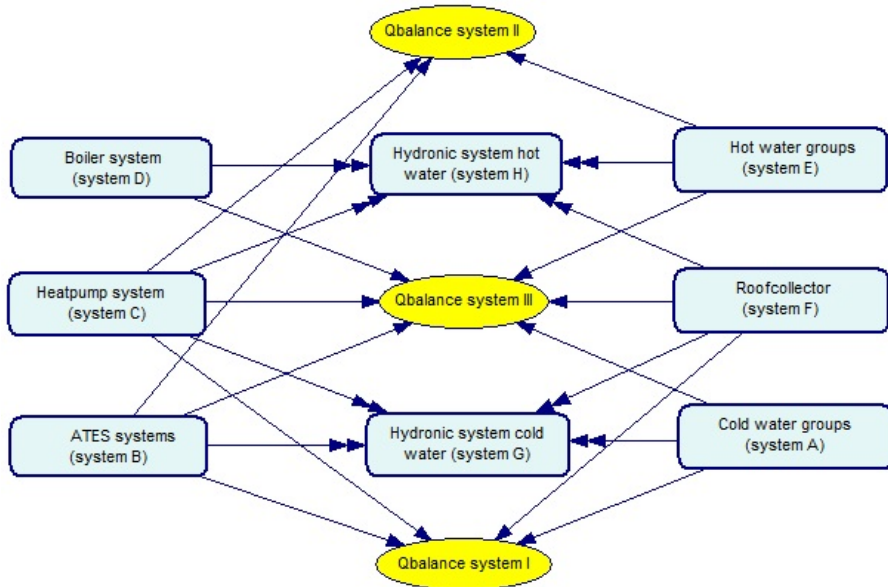


Figure 6.15. Overall DBN model of the thermal energy plant as built in GeNie

6.10.2. The implementation of negligible energy nodes as important OS symptom.

The considered HVAC system has different modes of operation. At the heat and cold demand side, the presence of heat demand of the roof collector (39), the hot water groups (34) and (35), and the cold demand of the systems (36) and (37) and of the server room (38) can be distinguished. In addition, energy may or may not be supplied by the heat pump (40), the boiler (33) and the wells of the ATES system (31) and (32).

Different load modes can be distinguished based on combinations of:

- System A: The cold demand of the server room (system (38)).
- System A: The cold demand by the North and South groups of the building (systems (36) and (37)).
- System B: The thermal energy delivered by the ATES system.
- System C: The electrical energy delivered to the heat pump system. See Figure 6.15 in which NE_{cond} and NE_{evap} are OS symptom nodes indicating the presence of the HVAC mode wherein the heat pumps condenser and evaporator have negligible capacity.
- System D: The heat delivered by the boiler system.
- System E: The heat demand by the North and South groups of the building (systems (34) and (35)).
- System F: The heat demand by the roof system.

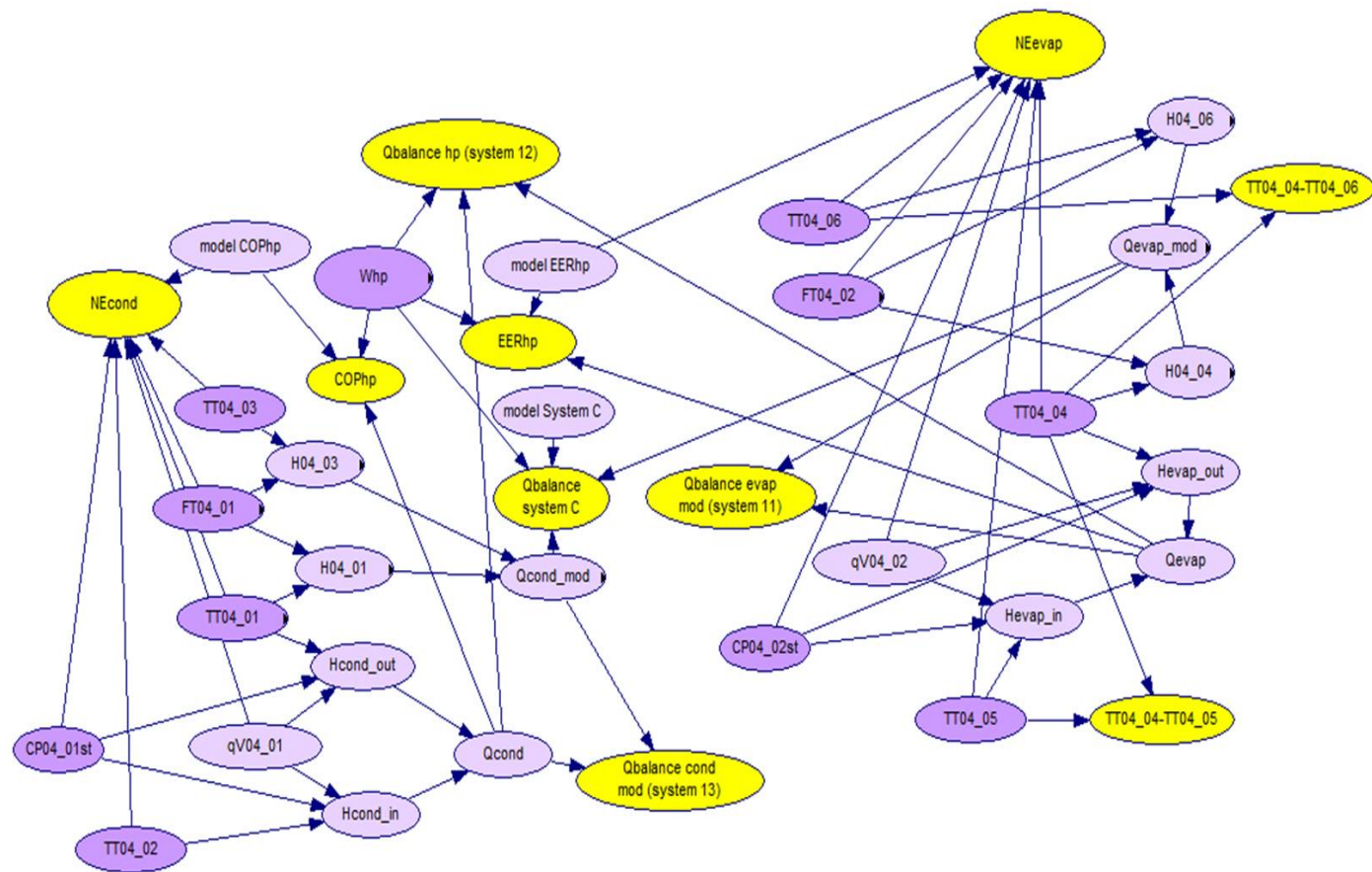


Figure 6.16. The implemented DBN model for the heat pump system (C)

6.10.3. Identification results

The detection results are imported in a DBN model. The main results of the diagnosis for the days on which the symptoms described in Table 6.2 are observed are presented in Figures 6.17 to 6.20 which show the results for some of the sensors. See the scheme in Figure 6.13 for the placing of these sensors. Figure 6.17 shows that the flow sensors FT28_01 and FT28_02 (the blue line is mostly invisible because the red line hides this line) have a high probability to be false (most days > 40 %).

In Figure 6.18 the sensor FT29_03 has a high probability to be faulty as well, while Figure 6.19 shows a high probability of TT04_04 being faulty. Furthermore, hard sensors CP07_01st, FT07_01, FT29_01, FT48_01, TT05_01, TT05_02, TT07_01, TT07_02 and TT29_07 (shown in Figure 6.20) were faulty by missing data-connection at the end of the 28 days period. In addition, models T06_a and T06_b (not shown) were sometimes reported as defective.

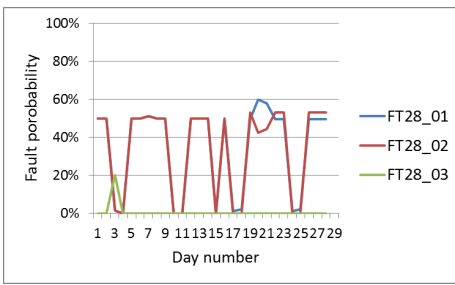


Figure 6.17. Fault probabilities of sensors FT28

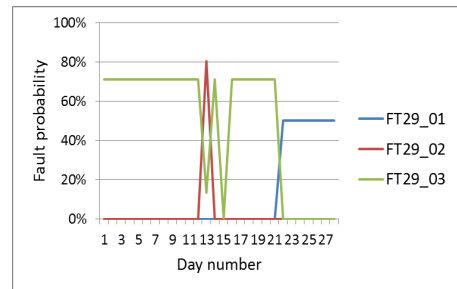


Figure 6.18. Fault probabilities of sensors FT29

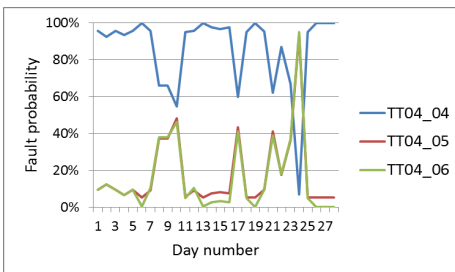


Figure 6.19. Fault probabilities of sensors TT04

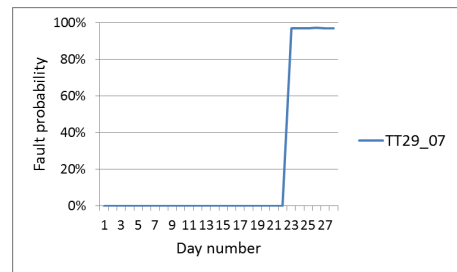


Figure 6.20. Fault probabilities of sensor TT29_07

Conclusion

Despite unambiguous detection results, the symptoms observed in Figures 6.19 to 6.20 lead to the detection of six possible sensor faults which are present:

- FT29_03 is faulty with a highest fault probability of more than 70%.
- TT04_04 is faulty with a highest fault probability of 100%.
- FT28_01 or FT28_02 is faulty with a highest fault probability of 50%.
- The soft sensors T06_a and T06_b were faulty with highest probability 92 and 96%.

6.11. Correction of sensor faults in the case study

In this section the results of the correction process are discussed. We address the proposed corrections in the case study.

6.11.1. Proposed corrections

In this section the proposed adaptations are summarized which are discussed in Appendix 6B.1.

FT29-03: The best fit was correction of FT29_03 by Eq. (6.5):

$$FT29-03_{corr}=FT48-01+FT29-01+FT29-02 \text{ [m}^3\text{/s]} \quad (6.5)$$

TT04-04 : Fitted by Eq. (6.6):

$$TT04-04_{corr}=TT04-04+1.25 \text{ [}^\circ\text{C]} \quad (6.6)$$

FT28-02 is adapted by Eq. (6.7).

$$FT28-02_{corr}=FT28-03-FT28-01 \text{ [}^\circ\text{C]} \quad (6.7)$$

The sensor diagnosis also resulted in soft sensor faults for T06_a and T06_b. Unfortunately, hard sensor data was missing to correct the applied models to easily adapt the models to these temperatures. We propose to omit corrections to these models.

6.11.2. Results after correction

The effects of the proposed adaptations are shown in Appendix 6B.2. As can be seen, the detection results show convincing outcomes for most days. However, because of the missing recorded data for systems (34) to (37), the outcomes for days 22 to 28 (system (a)) as well for days 19 to 28 (systems (b) and (III)) are still incorrect. Correction can be made for these systems by the replacement of the measured values by a model-based value by applying soft sensors in the enthalpy balances for the headers (1), (2), (24) and (25), which is left out of this case study. However, corrections could be made in the pre-processing part of the framework by using well-known solutions for missing data, like a regression method, to avoid wrong detection and diagnosis. Of course, the BMS has to be repaired as soon as possible. The pre-process can send a message to the responsible BMS technician. Discounting any missing data, most of the deviations in the daily energy balances remain under the threshold of 5%. Only 6 times a symptom was detected for 44 symptom nodes for 28 days which gives only 0.5% (fault) Present outcomes.

6.11.3. Meaning for energy analysis

The corrected calculated energy quantities can then be used for energy analysis. As can be seen in Appendix 6B.3, the differences between the energy output and input of the systems are almost invisible despite no correction has been taken place on the soft sensors T06_a and

T06_b. In this case no further action is proposed on finding adaptations of the models for the soft sensors T06_a and T06_b.

6.12. Sensitivity analysis of the assumed probabilities in the fault layer

The prior fault probabilities of sensors are difficult to estimate due to the lack of information about sensor failure. Below, a sensitivity analysis is applied on system C, the heat pump system. The process mode is considered in which the mass balance as well as the enthalpy balance of systems (4) and (5) are wrong. In addition, the heat balances of the systems (6) and (B) are wrong, and the deviation between TT04_04 and TT04_05 is large. In the case study, the prior Present probabilities of the sensors were set to 5%. The outcomes of the diagnosis with this prior probability delivered a posterior Present probability of 84 % for TT04-04. In the DBN model, these prior fault probabilities are varied for the sensitivity analysis. Table 6.3 presents the results of this experiment. The second column (in grey) shows the results of the case study for all prior Present probabilities being 5%. In the third column sensors TT04_04 and FT04_02 have a lower prior Present probability of 2%. Note that the posterior Present probability of the fault being in the temperature sensor TT04_04 decreases while it increases slightly for the sensors TT04_05 and TT04_06 which prior Present probabilities are still 5%.

Table 6.3 Influence of prior probabilities on the posterior probabilities.

| Sensor | Prior Present probabilities | | | |
|----------------|---------------------------------|----|----|----|
| <i>TT04_04</i> | 5 | 2 | 5 | 5 |
| <i>FT04_02</i> | 5 | 2 | 10 | 20 |
| <i>TT04_05</i> | 5 | 5 | 5 | 5 |
| <i>TT04_06</i> | 5 | 5 | 5 | 5 |
| | Posterior Present probabilities | | | |
| <i>TT04_04</i> | 84 | 70 | 80 | 74 |
| <i>FT04_02</i> | 11 | 7 | 21 | 38 |
| <i>TT04_05</i> | 21 | 33 | 24 | 30 |
| <i>TT04_06</i> | 8 | 12 | 8 | 7 |

In the case that *FT04_02* has a higher prior Present probability than *TT04_04* (see column 4) the posterior Present probability of the flow sensor increases while it decreases for the temperature sensor TT04_04. Larger differences between prior probabilities result in posterior probabilities of the same order for all sensors (see column 5). Still TT04_04 is detected as symptom in all cases. This sensitivity analysis, although not complete, shows that even when prior fault probabilities are not precisely known, the diagnosis delivers adequate results. Despite the simplicity and limited scope of our analysis, we notice that in our experiments the Bayesian method correctly identifies the temperature sensor TT04_04 as faulty when tested with a high belief of sensors (less than 5% of these sensors are stuck or biased).

When assumptions for prior and conditional probabilities are unsure, identification is more complicated. However, in that case, the 4S3F method still reduces the possible faults to a

limited number, which will help the HVAC expert to solve sensors faults with much less effort than nowadays.

6.13. Conclusions and recommendations

6.13.1. Conclusions

This article presents an extension of the 4S3F method to diagnose hard and soft sensor faults (component and model faults). The presented approach corresponds with how engineers design and diagnose HVAC systems with P&IDs and is applicable without knowledge of which sensors work well and/or are malfunctioning. The original 4S3F architecture has therefore been expanded with connections between component and model faults to implement soft sensor faults therein. Next to this, a novel operational state symptom node is presented which consider negligible energy amounts of systems and the application of additional symptoms from a separate FDD method for components is also discussed. A generic approach is presented for setting up the detection and diagnosis models for sensor FDD purposes.

Next to this generic part, the sensor FDD method is implemented in a case study of an existing HVAC system with real data. This case study shows that the 4S3F framework is successful in detecting and diagnosing sensor faults in the BEMS and is able to adapt measurements even when symptom thresholds are set arbitrarily. The sensitivity analysis for the prior probabilities shows that the diagnosis still delivers accurate results when the assumed prior probabilities are changed. Furthermore, the balance, EP and OS models for systems and DBN models in the cases study can be applied to other installations.

In addition, the assumptions that the heat losses are low in THUAS' HVAC system and that the storage term in the energy balances can be ignored during daily detection appeared to be correct.

6.13.2. Recommendations

Although the results are promising, further research is desirable.

First, a case study is needed to diagnose energy performance and sensor faults simultaneously. This research should provide answers to the questions such as which range of threshold values to use for the symptom detection, and to questions about sensor and energy performance diagnostic periods (from hourly to annual).

Diagnosis will be more accurate if all sensors necessary for energy analysis are installed. In the presented case study, some flow sensors and temperature sensors were both missing. A minimal set of sensors and meters should be estimated to realize good identification of measurement faults and inaccurate energy models. Standards for sensors to be installed should be used, e.g., [30] in The Netherlands.

In case a BEMS is set up sensors will be installed, and they can be checked for fault purposes when the installation is delivered by first commissioning.

It should also be researched if the HVAC can be started up automatically by the BMS in different modes to hasten the estimation of a fault. For instance, to estimate bias errors of

temperature and flow sensors, the BMS could start up the pumps and fans during nights or weekend days when no heat or cold is needed.

Further automation of the framework is necessary. To realize that:

- A generic library of detection models (including other systems like air handling systems and heat and cooling facilities in rooms) is needed from which balance models can be selected in a specific case. This library contains also models for OS and EP information.
- A generic library of diagnosis models is needed from which DBN models can be selected in a specific case.

For the sake of this paper, we started with such generic libraries.

- Software is needed to calculate the soft sensor values, the energy and the mass amounts in the processing. Next to this, automatic estimation of the presence of symptoms and translation of that to event values (Present or Absent) for the symptom nodes in the DBN model are needed. Finally, automation of the output of the DBN analysis is needed.
- Software should feed the probabilities of the fault and symptom nodes in the DBN models, which should be done once at setting up these models but can also be derived from generic DBN models.
- In this case study, GeNie is used as the DBN software tool. Research is needed into the most suitable software tool which can handle the libraries of DBN models and can handle redundant symptom information in the right way. The software has to deal with adapted probabilities of events based on information from data mining.

In addition, the implementation of prior and conditional probabilities in DBN models should be investigated further. In this paper, Boolean events (true and false) were implemented, meaning that the prior probabilities give the probability of the event to be true or false (e.g., 95% chance that TT04_04 works well and 5% chance it doesn't work). When more events for fault and symptom nodes are implemented (e.g., 85% chance that TT04_04 works well, 10% chance it is not well calibrated and has a bias, 5% chance it is broken), it may be possible to estimate the kind of fault, a defective or biased fault for example. It is also possible to weigh the degree of the estimated deviation. This can help the diagnosis and the correction of sensor faults.

Appendix 6A. Detection symptoms results

Symptom detection results from the THUAS sensor FDD case study are presented in this appendix. First, in Section 6A.1 results from balance symptom detection are shown, followed in Section 6A.2 by energy performance symptoms. In addition, operational symptom detection results are presented in Section 6A.3.

6.A.1. Balance symptom detection results

The next main assumptions in detection models are made.

- It is assumed that dynamic effects are small when a period of one day is considered. So, storage of (thermal) energy within the systems is ignored. The only exceptions are the buffers (6), (10) and (16).
- Heat losses of the systems are neglected because it is known that the components and pipes are insulated well.
- The hydronic system performs well. So, the direction of flows corresponds to the design.
- Leakage through closed valves is ignored.

Arbitrary, the threshold deviations for the balances ε_{\max} are based on expected inaccuracies by measurements and models. The assumptive threshold for the enthalpy and mass balances is set to 3 % while the heat balances are set higher to 5% because they are mainly calculated based on the former which results in higher balance deviations. Absolute deviations below these values, suppose that symptoms are not present.

Figures 6A.1 and 6A.2 show the deviation for the balances of the components (8), the heat exchanger of the ATES system, and the heat pump (12).

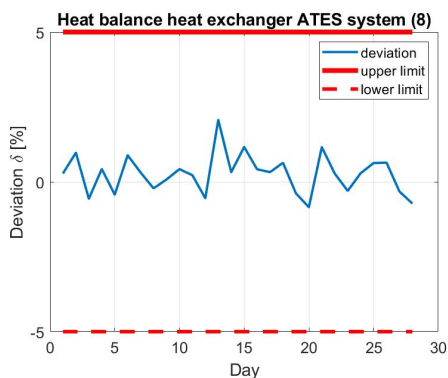


Figure 6A.1 Deviations of the heat exchanger ATES (8) before corrections

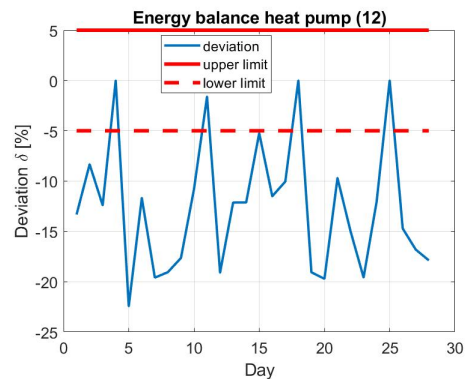


Figure 6A.2 Deviations of the heat pump (12) before corrections

The deviation of the heat balance of the heat exchanger lies far under the threshold of 5%. However, the absolute deviation of the heat balance of the heat pump, is most days far from the threshold of 5%.

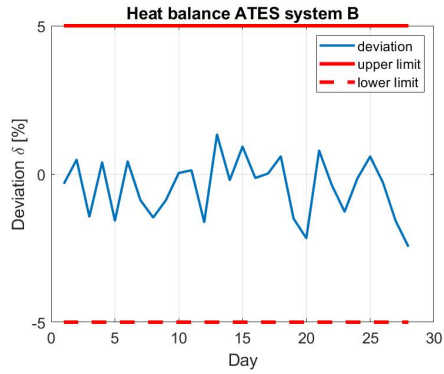


Figure 6A.3 Deviations of the ATES system before corrections.

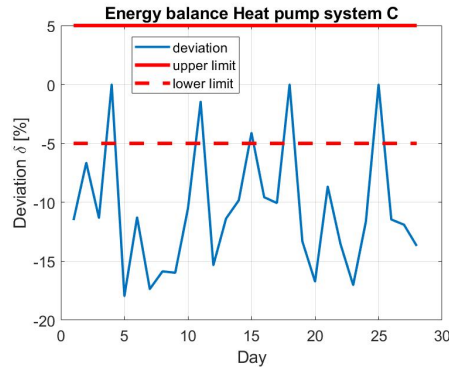


Figure 6A.4 Deviations of the heat pump system before corrections.

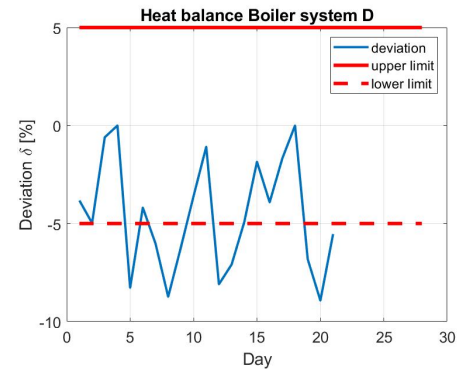


Figure 6A.5 Deviations of the boiler system before corrections.

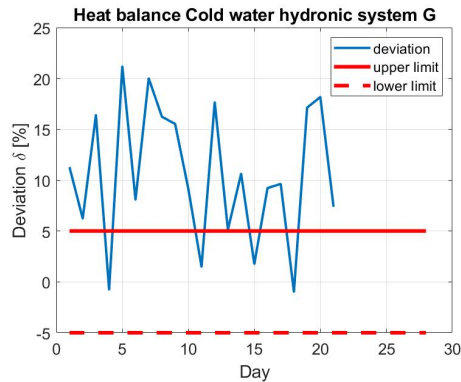


Figure 6A.6 Deviations of the hydronic system cold water before corrections

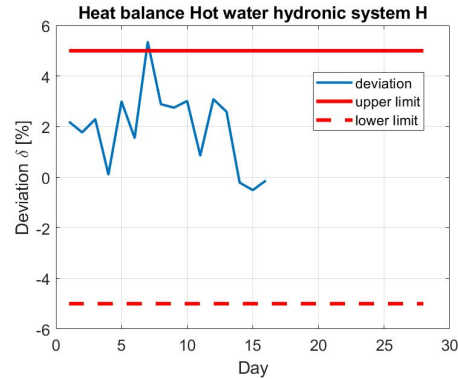


Figure 6A.7 Deviations of the hydronic system hot water before corrections

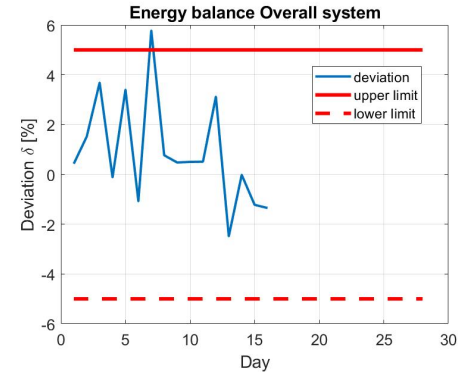


Figure 6A.8 Deviations of the thermal energy plant before corrections.

Figures 6A.3 to 6A.8 show the energy balance deviations of the aggregated system (B) to (D), (G), (H) and the overall system. As can be seen symptoms are structurally present for the systems (C), (D) and (G).

6.A.2. Energy performance symptom detection results

The COP and EER are defined as performance indicators which are independent of heat or cooling mode of the heat pump. Eqs. (6A.1 and 6A.2) show the formulas for these EPs.

$$COP_{hp} = \frac{Q_{cond}}{W_{hp}} [-] \quad (6A.1) \quad \text{and} \quad EER_{hp} = \frac{Q_{evap}}{W_{hp}} [-] \quad (6A.2)$$

With

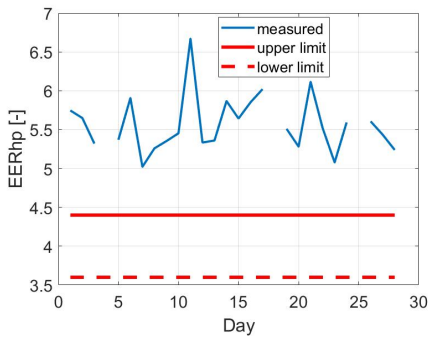
Q_{cond} =heat at the heat pumps condenser [kJ]

Q_{evap} =heat the heat pumps evaporator [kJ]

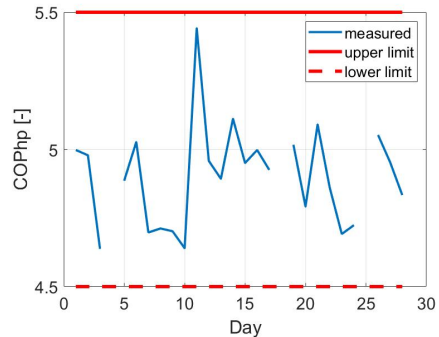
W_{hp} =supplied electric work to the compressor of the heat pump [kJ]

The EER and COP values of the heat pump must be realistic according to the manufactory data sheets. Figures 6A.9 and 6A.10 show the measured daily values.

Looking at the specifications of the heat pump and the mean water temperatures at the evaporator and condenser side of the heat pump (about 9 and 34°C), the daily COP_{hp} value should be about 5 and 4 for the EER_{hp}. Taking into account a threshold of 10% results in the next expected energy performance indicators: $4.5 < COP_{hp} < 5.5$ and $3.6 < EER_{hp} < 4.4$. All days, the EER_{hp} is higher than the upper limit of 4.4 (see Figure 6A.9). It is even higher than COP_{hp}. So, the calculated EER_{hp} based on the measured water temperatures is false. However, the COP_{hp} looks realistic because it is between the lower and upper limit values.



(blank gap:heat pump is off)
Figure 6A.9 Daily EER_{hp} before corrections



(blank gap:heat pump is off)
Figure 6A.10 Daily COP_{hp} before corrections

6.A.3. OS Symptom detection results

The water temperatures at the evaporator and condenser side of the heat pump: TT04_04, TT04_05, TT04_06, TT04_01 and TT04_02 are positioned next together in the technical room (see Figure 6.14 in which these sensors are depicted). The value of TT04_04 should reach the value of TT04_05 and TT04_06 when the heat pump is set off during a long period. As example, Figure 6A.11 shows the deviation between TT04_04 and TT04_05.

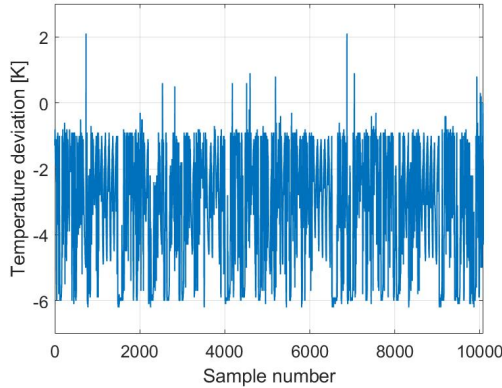


Figure 6A.11 Deviation between TT04_04 and TT04_05 before corrections

As can be seen TT04_04 and TT04_05 deviates from each other. The smallest deviation is about -1 K when the outliers are ignored. In Figure 6A.12, we see the temperature curves for TT04_04 and TT04_05 when the heat pump is turned off and there is no flow in cold water circuit 04. The number on the x-axis is the data storage number. An amount of 1 corresponds with a timestamp of 4 minutes. Number 1080 corresponds with Sunday November 17, 2013 at 00:00 hour and 1440 corresponds with Monday, November 18, 2013 at 00:00 hour. Figure 6A.12 shows that a higher deviation is detected between the sensors TT04_04 and TT04_05 than the set threshold of 0.4 K. Note: this figure shows also that every 360 minutes (6 hours) the temperature quickly decreases. This is caused by Pump CP03-01 in the secondary ATEs system which restarts every 6 hours for a short period of time, which is likely to be necessary for the pump to work properly. This affects the water temperatures at the heat pump because cold water is supplied from the buffer (6).

Deviations at the hot water circuit are not perceived. For instance, Figure 6A.13 shows a small temperature deviation between TT04_01 and TT04_02. We expect that TT04_02 to be equal to TT04_01 when the heat pump stays off. However, BMS data shows that the heat pump generates heat during Sunday night (after point 1440), resulting equilibrium could not be reached.

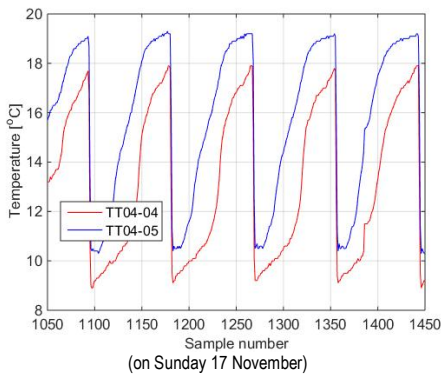


Figure 6A.12 Temperatures TT04_04 and TT04_05 before corrections

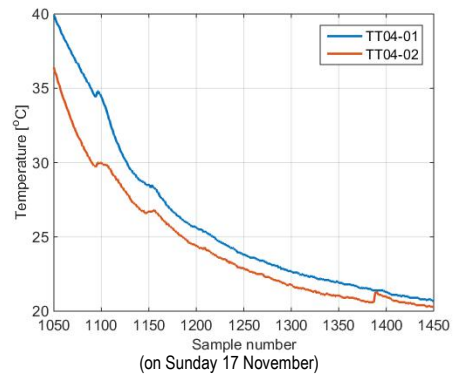
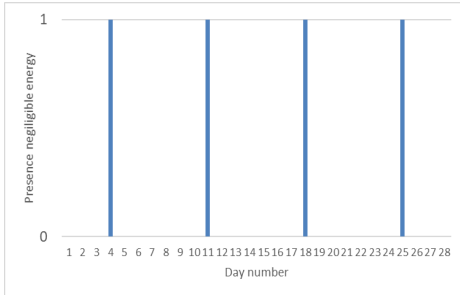


Figure 6A.13 Temperatures TT04_01 and TT04_02 before corrections

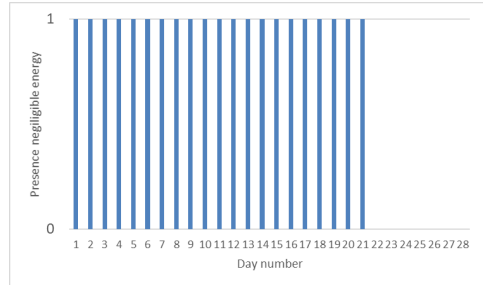
HVAC negligible energy results

Despite that the case study is conducted for wintertime, the heat pump was inactive for four days (on All Sundays, see Figure 6.14) and it can be seen from Figure 6A.15 that the boiler system was almost inactive all days. The roof system was active on the days 8, 9 and 20 (see Figure 6A.16).



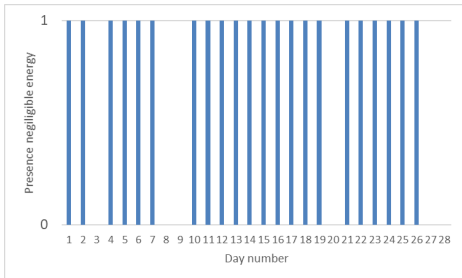
(0=Absent 1=Present)

Figure 6A.14 Negligible energy heat pump system



(0=Absent 1=Present)

Figure 6A.15 Negligible energy boiler system



(0=Absent 1=Present)

Figure 6A.16 Negligible energy roof system

Appendix 6B. Corrections in the case study

The corrections made in the case study are discussed in this appendix. The proposed corrections are presented in Section 6B.1. In Section 6B.2 the detection results after corrections are discussed and in Section 6B.3 the meaning for energy performance diagnosis.

6.B.1. Proposed corrections

The possible sensor fault FT29_03 is addressed first. Because we had not the opportunity to realize replacement and displacement of the sensors, we applied the soft sensor approach. The best fit was a bias correction of FT29_03 by Eq. (6.5):

$$FT29_03_{corr}=FT48_01+FT29_01+FT29_02 \text{ [m}^3\text{/s]} \quad (6.5)$$

This adaption leads to satisfying results (no symptoms are detected in system **(a)** anymore). TT04_04 can be simultaneously corrected. The OS information shows a bias around 1 K, see Figures 6A.11 and 6A.12. We have estimated a bias correction which results in the smallest deviation: +1.25 K. The measured TT04_04 will be corrected with this bias:

$$TT04_04_{corr}=TT04_04+1.25 \text{ [}^\circ\text{C]} \quad (6.6)$$

Where T04-04corr is the corrected temperature value.

And at last, a correction can be made simultaneously for FT28_01 or FT28_02. The diagnosis did lead to an ambiguous result. Both sensors can be faulty. Here, the soft sensor solution is also applied. Although the differences are not large, the proposed correction for FT28_02 fits better than that of FT28_01, so FT28_02 is adapted by Eq. (6.7).

$$FT28_02_{corr}=FT28_03-FT28_01 \quad (6.7)$$

6.B.2. Results after correction.

Figures 6B.1 to 6B.6 show the percent deviation of the systems **(B)**, **(C)**, **(D)**, **(G)**, **(H)** and **(III)** after the corrections. After the three proposed corrections, the detection results show convincing outcomes for most days, compared with Figures 6A.1 to 6A.6. However, because of the missing recorded data for systems **(34)** to **(37)**, the outcomes for days 17 to 28 (systems **(H)** and **(III)**) as well for days 21 to 28 (systems **(D)** and **(G)**) are still incorrect. Correction can be made for these systems by the replacement of the measured values by a model-based value by applying soft sensors in the enthalpy balances for the headers **(1)**, **(2)**, **(24)** and **(25)**, which is left out of this paper. However, the authors propose that the correction can be made in the pre-process part of the framework by using well-known solutions for missing data, like a moving average, to avoid wrong detection and diagnosis. Of course, the BMS has to be repaired as soon as possible. The pre-process can send a message to the responsible BMS technician. Discounting any missing data, most of the deviations in the daily energy balances remain under the threshold of 5%.

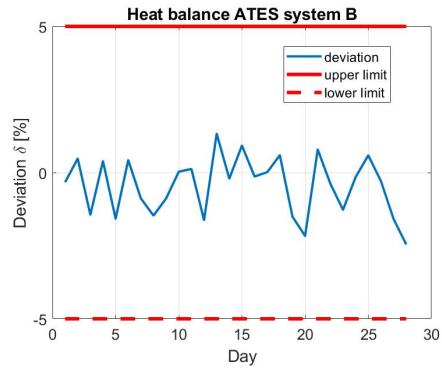


Figure 6B.1 Deviations of the ATES system after corrections.

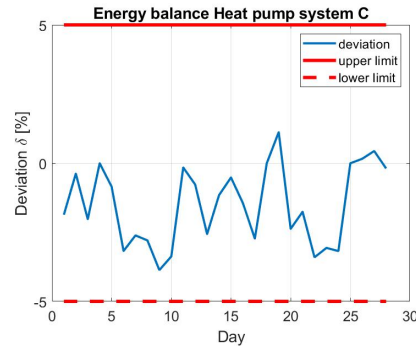


Figure 6B.2 Deviations of the heat pump system after corrections.

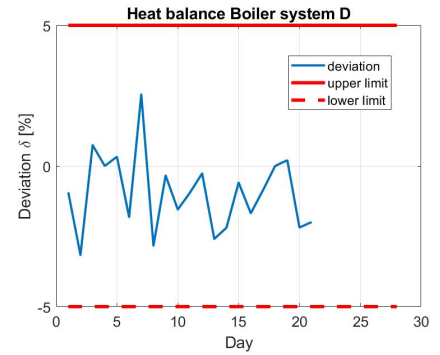


Figure 6B.3 Deviations of the boiler system after corrections.

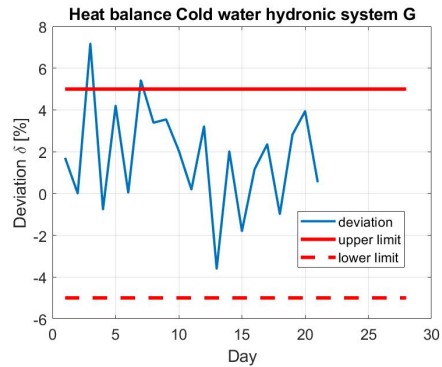


Figure 6B.4 Deviations of the hydronic system cold water after corrections.

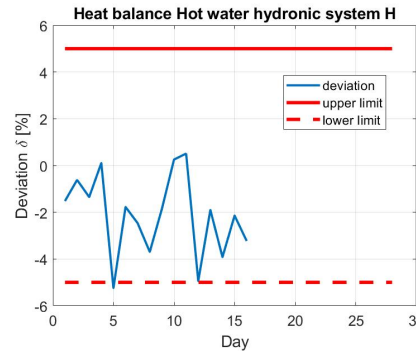


Figure 6B.5 Deviations of the hydronic system hot water after corrections.

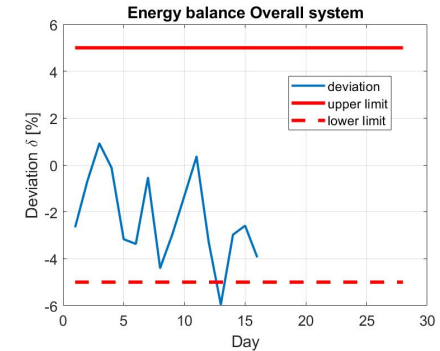


Figure 6B.6 Deviations of the whole system after corrections.

Figure 6B.7 shows the corrected EER_{hp} which is incorrect only twice despite the rough estimate of EER_{hp} .

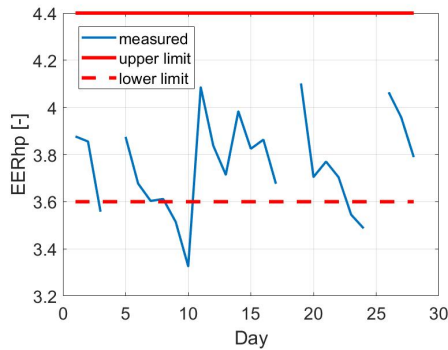


Figure 6B.7 Measured EER_{hp} after corrections

Figure 6B.8 shows the deviation between TT04_04 and TT04_5 after this correction. As can be seen the deviation is decreased to about zero.

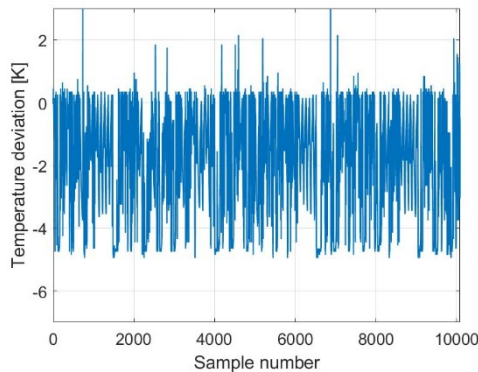


Figure 6B.8 Deviations between TT04_04 and TT04_05 after bias correction of TT04_04.

Figures 6B.9 to 12 present the exchanged energy for the boiler, the roof, the headers (4) and (5), and system (3) after corrections. The differences between the energy output and input of these systems are almost invisible. Only systems (4) and (5) show a visible deviation, which is easily explained because the case study was applied for a winter period in which the daily cold demands for the cold-water systems were low. Compared with the cold demand in the summer period, the absolute deviation of the presented cooling energy can be neglected.

The correction is satisfying because energy data is available for energy diagnosis purpose despite no correction has been taken place on the soft sensors T06_a and T06_b. In this case we propose no further action on finding adaptations of these sensors.

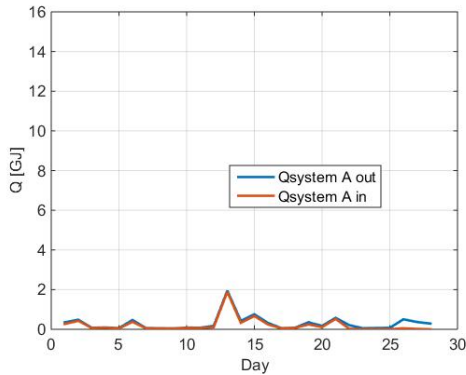


Figure 6B.9 Energy exchange boiler system after corrections

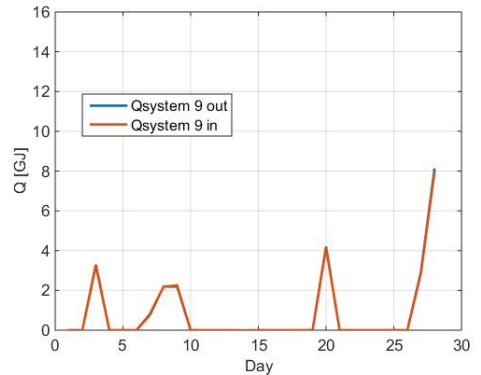


Figure 6B.10 Energy exchange roof after corrections

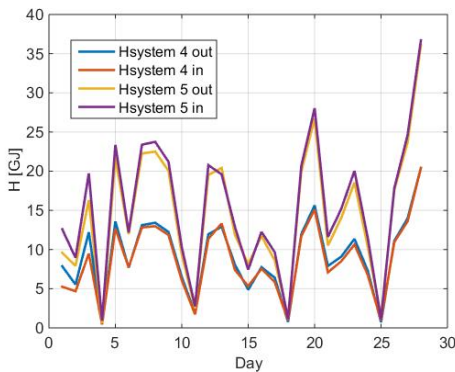


Figure 6B.11 Energy exchange systems headers (4) and (5) after corrections

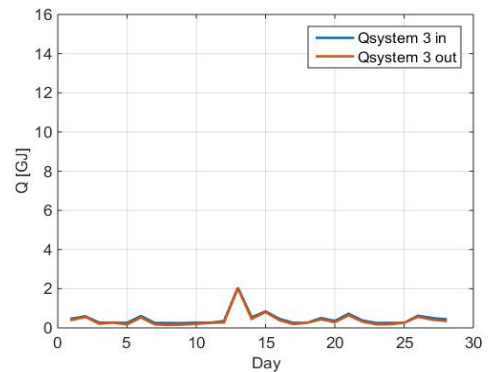


Figure 6B.12 Energy exchange system (3) after corrections

References

- [1] Energy Performance of building directive (EPBD) (2018). <https://ec.europa.eu/energy/en/topics/energy-efficiency/buildings>.
- [2] W. Kim, S. Katipamula, A Review of Fault Detection and Diagnostics Methods for Building Systems. *Science and Technology for the Built Environment*, 24:1 (2017), 3-21, <https://doi.org/10.1080/23744731.2017.1318008>.
- [3] S. Wang, J. Wang, Law-Based Sensor Fault Diagnosis and Validation for Building Air-Conditioning Systems. *HVAC&R Research*, 5:4 9 (1999): 353-380. <https://doi.org/10.1080/10789669.1999.10391243>.
- [4] S. Wang, J. Wang, Automatic sensor evaluation in BMS commissioning of building refrigeration systems, *Automation in Construction* 11 (2002): 59-73. [https://doi.org/10.1016/S0926-5805\(01\)00050-4](https://doi.org/10.1016/S0926-5805(01)00050-4)

- [5] J. Wang, S. Wang, J. Burnett, An integrated robust strategy for diagnosing sensor faults in building chilling systems, HVAC&R Research 8 (2002): 159-178.
<https://doi.org/10.1080/10789669.2002.10391434>
- [6] X. Yang, Z. Jin, Z. Du, Y. Zhu, Y. Guo, A hybrid model-based fault detection strategy for air handling unit sensors, Energy and Buildings 57 (2013): 132-143.
<https://doi.org/10.1016/j.enbuild.2012.10.048>
- [7] N. Kocyigit, Fault and sensor error diagnostic strategies for a vapor compression refrigeration system by using fuzzy inference systems and artificial neural network, international journal of refrigeration 50 (2015): 69-79.
<https://doi.org/10.1016/j.ijrefrig.2014.10.017>
- [8] Z. Du, B. Fan, J. Chi, X. Jin, Sensor fault detection and its efficiency analysis in air handling unit using the combined neural networks, Energy and Buildings 72 (2014): 157-166. <https://doi.org/10.1016/j.enbuild.2013.12.038>
- [9] M. Elmour, N. Meskin, M. Al-Naemi, Sensor data validation and fault diagnosis using Auto-Associative Neural Network for HVAC systems, Journal of Building Engineering 27 (2020): 100935. <https://doi.org/10.1016/j.jobe.2019.100935>
- [10] X. Yang, X. Jin, Z. Du, B. Fan, Y. Zhu, Optimum operating performance based online fault-tolerant control strategy for sensor faults in air conditioning systems, Automation in Construction 37 (2014): 145-154. <https://doi.org/10.1016/j.autcon.2013.10.011>
- [11] H.Han, B. Gu, J. Kang, Z. Li, Study on a hybrid SVM model for chiller FDD applications. Applied Thermal Engineering 31 (2011): 582-592.
<https://doi.org/10.1016/j.applthermaleng.2010.10.021>
- [12] S. Zidi, T. Moulahi and B. Alaya, "Fault Detection in Wireless Sensor Networks Through SVM Classifier," in IEEE Sensors Journal, vol. 18, no. 1, pp. 340-347, 1 Jan.1, (2018). <http://doi.org/10.1109/JSEN.2017.2771226>.
- [13] Y. Cheng, Q. Liu, J. Wang, S. Wan, T. Umer, Distributed Fault Detection for Wireless Sensor Networks Based on Support Vector Regression, Wireless Communications and Mobile Computing Volume (2018), 8 pages <https://doi.org/10.1155/2018/4349795>
- [14] S.W. Wang, F. Xiao, AHU sensor fault diagnosis using principal component analysis method. Energy and Buildings 36 (2004): 147-160
<https://doi.org/10.1016/j.enbuild.2003.10.002>
- [15] S. Wang, F. Xiao, Sensor Fault Detection and Diagnosis of Air-Handling Units Using a Condition-Based Adaptive Statistical Method, HVAC&R Research 12 (2006)
<https://doi.org/10.1080/10789669.2006.10391171>
- [16] F. Xiao, S.W. Wang, J.P. Zhang, A diagnostic tool for online sensor health monitoring in air-conditioning systems. Automatic and Construction 15 (2006): 489-503
<https://doi.org/10.1016/j.autcon.2005.06.001>
- [17] S.W. Wang, Y.Y. Qin, Sensor fault detection and validation of VAV terminals in air conditioning systems, Energy Conversion Management 46 (2005): 2482-2500.
<https://doi.org/10.1016/j.enconman.2004.11.011>
- [18] Z. Du., X. Jin, X. Yang, A robot fault diagnostic tool for flow rate sensors in air dampers and VAV terminals, Energy and Buildings 41 (2009): 279-286.
<https://doi.org/10.1016/j.enbuild.2008.09.007>

- [19] Z. Du, X. Jin, Detection and diagnosis for sensor fault in HVAC systems. *Energy Conversion and Management* 48(3) (2007): 693-702.
<https://doi.org/10.1016/j.enconman.2006.09.023>
- [20] Z. Du, X. Jin, Multiple faults diagnosis for sensors in air handling unit using Fisher discriminant analysis, *Energy Conversion and Management* 49 (2008): 3654-3665.
<https://doi.org/10.1016/j.enconman.2008.06.032>
- [21] S. Wang, Q. Zhou, F. Xiao, A system-level fault detection and diagnosis strategy for HVAC systems involving sensor faults, *Energy and Buildings* 42 (2010): 477-490.
<https://doi.org/10.1016/j.enbuild.2009.10.017>
- [22] F. Xiao, S. Wang, X. Xu, G. Ge, An isolation enhanced PCA method with expert-based multivariate decoupling for sensor FDD in air-conditioning systems, *Applied Thermal Engineering* 29 (2009): 712-722.
<https://doi.org/10.1016/j.applthermaleng.2008.03.046>
- [23] G. Hi, Y. Hu, An enhanced PCA-based chiller sensor fault detection method using ensemble empirical mode decomposition based denoising, *Energy and Buildings* 183 (2019): 311-324. <https://doi.org/10.1016/j.enbuild.2018.10.013>
- [24] J. Schein, S.T. Bushby, A Hierarchical Rule-based Fault Detection Diagnostic Method for HVAC Systems, *HVAC&R Research* 12 (2006): 111-125.
<https://doi.org/10.1080/10789669.2006.10391170>
- [25] J. Schein, S.T. Bushby, N.S. Castro, J.M. House, A rule-based fault detection method for air handling units. *Energy and Buildings* 38 (2006): 1485-1492.
<https://doi.org/10.1016/j.enbuild.2006.04.014>
- [26] H. Yang, S. Cho, C. Tae, M. Zaheeruddin, Sequential rule based algorithms for temperature sensor fault detection in air handling units, *Energy Conversion and Management* 49 (2008): 2291-2306.
<https://doi.org/10.1016/j.enconman.2008.01.029>
- [27] A. Taal, L. Itard, P&ID-based automated fault identification for energy performance diagnosis in HVAC systems: 4S3F method, development of DBN models and application to an ATES system. *Energy and Buildings* 224 (2020): 110289.
<https://doi.org/10.1016/j.enbuild.2020.110289>
- [28] A. Taal, L. Itard, Fault detection and diagnosis for indoor air quality in DCV systems: Application of 4S3F method and effects of DBN probabilities. *Building and Environment* 174 (2020) 106632. <https://doi.org/10.1016/j.buildenv.2019.106632>
- [29] A. Taal, L. Itard, W. Zeiler, A reference architecture for the integration of automated energy performance fault diagnosis into HVAC systems, *Energy & Buildings* 179 (2018): 144-155. <https://doi.org/10.1016/j.enbuild.2018.08.031>
- [30] Meetpunten en meetmethoden voor klimaatinstallatie (2014). ISSO-publicatie 31. Rotterdam, Stichting ISSO.
- [31] A. Taal, L. Itard P&ID-based symptom detection for automated energy performance diagnosis in HVAC systems. *Automation in Construction* 119 (2020), 103344.
<https://doi.org/10.1016/j.autcon.2020.103344>
- [32] GeNie 2.1 (2016), BayesFusion. <http://download.bayesfusion.com>.
- [33] Smile (2016), <http://download.bayesfusion.com>.

- [34] Y. Zhao, J. Wen, S. Wang, Diagnostic Bayesian networks for diagnosing air handling units faults – Part II: Faults in coils and sensors. *Applied Thermal Engineering* 90 (2015): 145-157. <https://doi.org/10.1016/j.applthermaleng.2015.07.001>
- [35] F. Xiao, Y. Zhao, J. Wen, S. Wang, Bayesian network based FDD strategy for variable air volume terminals, *Automation in Construction* 41 (2014): 106-118. <https://doi.org/10.1016/j.autcon.2013.10.019>

7. Discussion

This chapter discusses the overall findings of the thesis answering the research questions mentioned in chapter 1.4. First, the study outcomes are discussed followed by the limitations of the study.

7.1. Study outcomes

The main result of the current study is a new energy performance and fault detection and diagnosis (FDD) architecture that mimics diagnostic activities of HVAC (heating, ventilation, and air conditioning) engineers. The structure of the so-called 4S3F method consists of 4 types of symptoms (balance, energy performance, operational state and additional symptoms) and 3 types of faults (component, control and model faults) that can be obtained for the most part from P&IDs (process and instrumentation diagrams), applied in the design phase and for building management (BMS) purposes. The detection of symptoms takes place separately from the diagnosis based on Bayesian statistics by a diagnostic Bayesian network (DBN). The variety and number of researched HVAC systems in the case studies gives confidence that the 4S3F approach is workable on all kind of HVAC systems.

Chapter 2 showed the concept of how the 4S3F method can be built from a P&ID and presented the value of systems theory through redundant analysis of systems at multi-level. In the Chapters 3 to 6, the 4S3F approach has been successfully tested in case studies with real measurement data from the HVAC system of the building of The Hague University of Applied Sciences in Delft. It was applied to a thermal energy plant (containing a heat pump, boiler and an ATEs (aquifer thermal energy system) and a demand-driven ventilation system (DCV) as an end-user system. Energy consumption as well as a healthy indoor climate, and hard and soft sensor failures were discussed. The outcomes of chapter 3 were rules for annual balance, energy performance and operational state symptoms for a thermal energy plant. In Chapter 4 the DBN model for energy performance diagnosis purposes has been further researched at annual analysis to diagnose component and control faults. A main result was that the set absolute values for prior and conditional probabilities in the DBN are subordinate to the relative ones. It was shown that two states for symptom and fault nodes (true and false) were sufficient to isolate the present HVAC control faults. Application on a demand-controlled ventilation (DCV) system showed that the 4S3F method is also practicable on indoor air systems at daily time spans, see Chapter 5. In this case, undesirable control behaviour of the building users was counted as a control fault. And finally, in Chapter 6, the 4S3F method was applied on sensor faults. Supplementary to the other case studies, this case study showed that model faults can be isolated and additional symptoms help the diagnosis. Also, a shorter diagnosis time span (one day) was considered than at the energy performance diagnosis. Furthermore, redundant balance detection was successfully applied.

Below, the above is elaborated in more detail by answering the research questions presented in the Introduction. First, the main research question is discussed:

Which FDD architecture is suitable for HVAC systems in general to support the set up and implementation of FDD methods, including energy performance diagnosis?

After a literature study about energy performance metrics and FDD methods, and considering HVACs design approach with P&IDs, a novel FDD architecture, called 4S3F, was developed in this thesis. In this 4S3F architecture energy performance diagnosis is handled as an FDD method in the same way as FDD for components. With this architecture, the FDD system can be setup by HVAC & Control engineers in the same way as P&IDs using a library of detection and diagnosis models, regardless of the type of HVAC system.

The first insight was that in an FDD architecture for all kinds of systems, the detection of symptoms should be distinguished from the identification of the fault(s). This has been concurrently reported in other studies, for example, Zhao et al [1] presented an extremely useful extension of the FDD classification in 2019 [2] in Figure 1.2. In their very complete framework, symptom detection and fault identification are separated and there is an exhaustive categorization of FDD methods, the results of which can be embedded in the DBN models.

Second, the analysis of existing FDD methods and HVAC design processes has shown that the use of information embedded into P&ID's (Process and Instrument Diagrams) should be an essential component of an FDD method. Combining this information with measurement data from the building management system (BMS) leads to the possibility of determining symptoms of 4 categories (balance, energy performance, operational state, and additional information) and faults (model, component, and control) of 3 categories. In this way the FDD system can be setup concurrently in a similar way as the HVAC design by the HVAC and/or control engineers.

These insights lead to the 4S3F architecture in which the symptom detection and fault diagnosis phases are separated from each other (see Figure 7.1).

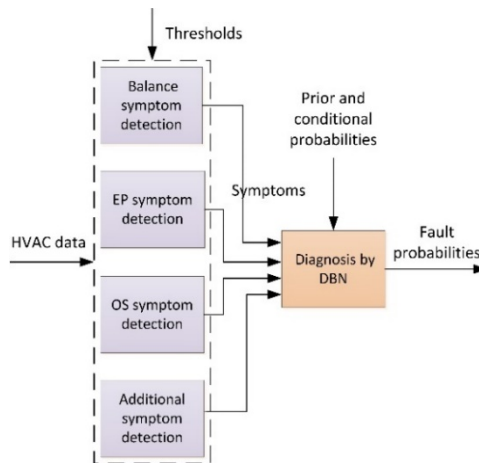


Figure 7.1 Separated detection and diagnosis phases in the 4S3F method.

For the symptom detection a set of symptom rules divided into four categories (balance, energy performance, operational state, and additional symptoms) was discussed and related

performance measures were developed, using efficiencies, seasonal performance factors, capacities, and control and design-based operational indicators.

As a diagnosis method, the DBN (Diagnostic Bayesian Networks) method was applied because of its system science nature which is present in P&IDs. This method includes HVAC expertise, and the results are probabilistic, diagnosing faults based on symptoms as HVAC engineers would.

Figure 7.2 shows the structure of the proposed 4S3F DBNs for all kind of HVAC systems. As can be seen three types of fault nodes are linked to four kinds of symptom nodes. The necessary information to set up a DBN for a specific HVAC system comes from the P&IDs. The links between symptoms and faults, and the set probability parameters in the DBN, are known from HVAC expertise. Knowledge of ICT and data analytics is limited at the stage of the set-up.

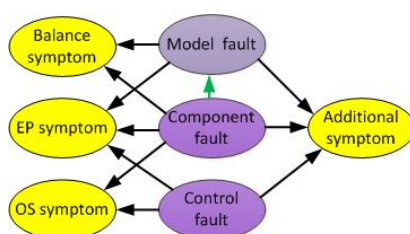


Figure 7.2 The 4S3F structure in a DBN model

In the 4S3F DBN the posterior probabilities of faults are identified by two states of symptoms: the presence or absence of symptoms.

Principle proofs of the 4S3F method have been performed on different types of HVAC components and systems, on the energy performance diagnosis of a thermal power plant (Chapter 3 and 4), a DCV system (Chapter 5) and hard and soft sensors (Chapter 6). The faults were correctly identified in all case studies. In this report, a start has been made with setting up symptom rule and DBN libraries. See Figure 7.3 which presents an overview of developed symptom rules and DBN models in the study.

The outcomes are discussed in more detail by specifically answering the four sub-questions defined in Chapter 1.4:

1. *How can HVAC P&IDs be used as a starting point for setting up an HVAC- specific FDD system, including energy performance diagnosis?*

The study revealed the usability of P&IDs for diagnosis of energy performance faults (Chapter 3 and 4), sensor faults (Chapter 6) and DCV (Chapter 5). In all experiments symptoms and faults were derived from them. In P&IDs, systems can be distinguished, relations between faults and symptoms can be depicted, and equations for exchanged energy amounts can be derived. See Figure 7.4 which shows an example how information from P&ID can be extracted for symptom detection and fault identification. It is common use that P&IDs contain information about set control values and capacities of components.

All presented 4S3F methods on sensor, energy performance and DCV show that one can set up an FDD system from P&IDs.

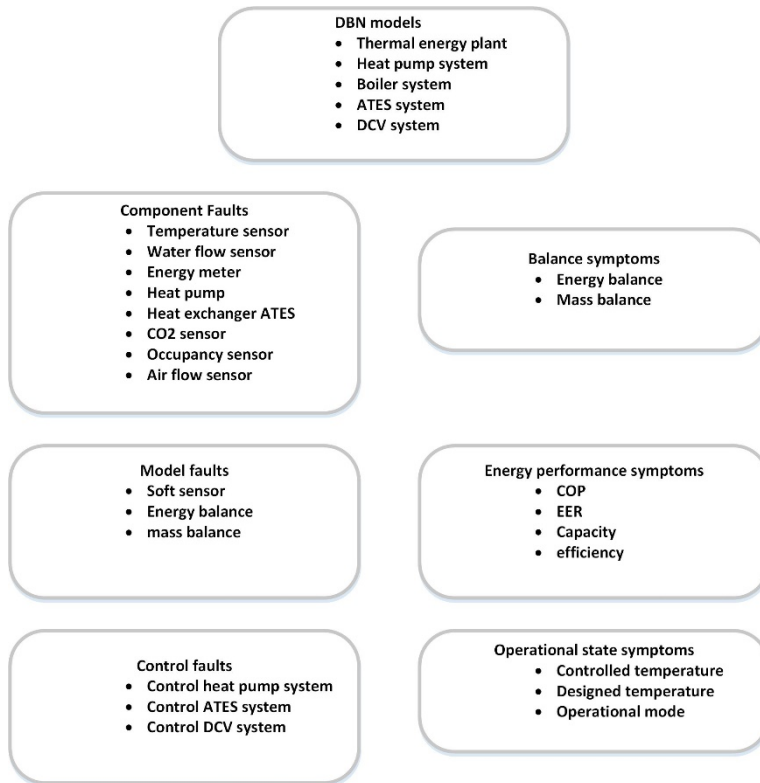


Figure 7.3 Faults and symptoms present in the case studie.

2. *How can the multiple system and subsystem levels in HVAC systems be reflected in and made useful for the FDD system?*

This question was addressed by looking at HVAC engineering practices where P&IDs are applied during design, implementation, and maintenance of HVAC systems. Different levels of systems can be distinguished. As example, Figure 7.4 presents a heat pump system which contains components and is part of a more aggregated thermal energy generation system. The case studies discussed in Chapters 4 and 6 for energy performance and sensor faults showed that FDD can take place simultaneously at different hierarchical levels, rather than by bottom-up or top-down approaches often described in literature. This is possible since DBNs support systems approach using specific nodes for aggregated systems and subsystems.

The hierarchical levels proposed are:

- Level A: whole HVAC system
- Level B: aggregated systems
- Level C: (trade) components
- Level D: subcomponents inside components

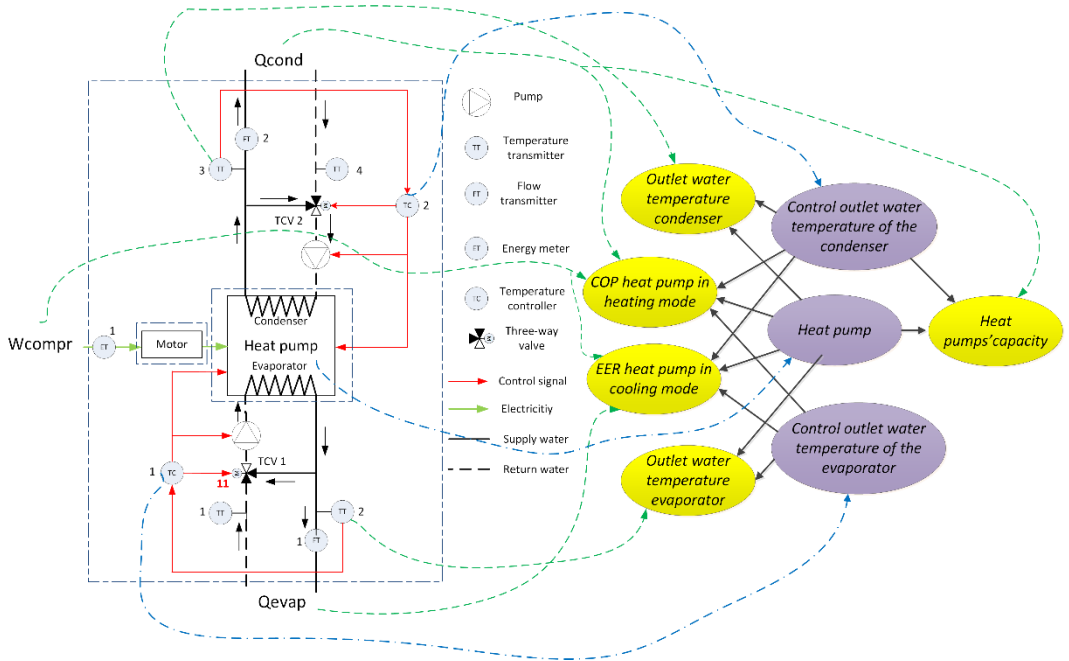


Figure 7.4 Extraction of a DBN model from a P&ID (purple: faults, yellow: symptoms)

In Chapter 2, simultaneous multi-level diagnosis was discussed. See Figure 7.5 which shows the aggregated system C made up of subsystems A and B. Redundant balances for these three systems allow much better isolation of sensor faults. In Chapter 6, this approach was successfully applied for sensor FDD.

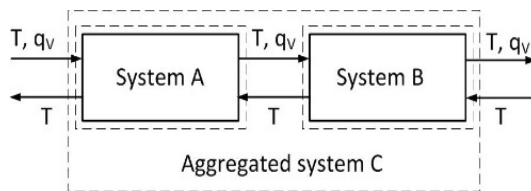


Figure 7.5 An aggregated system consisting of two sub-systems.

Figure 7.6 shows an example of DBN models at levels B and C. The DBN model of the heat pump system (containing components at level C), is an aggregated node in the DBN model at level B.

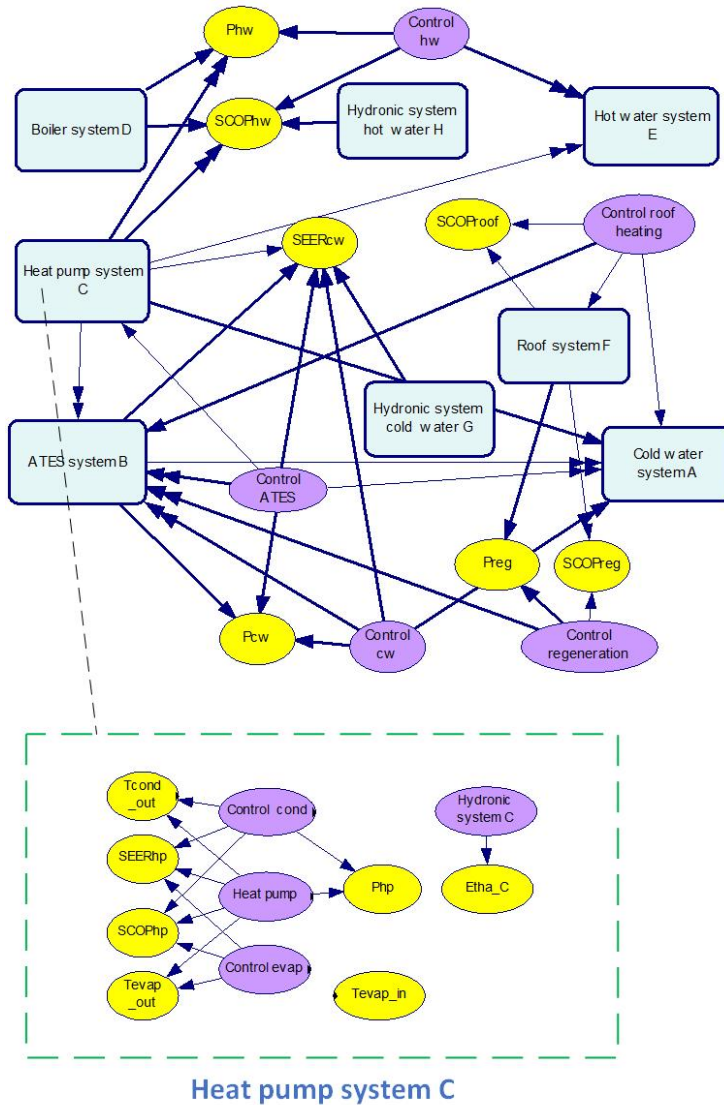


Figure 7.6 DBN model at level B containing components at level C.

3. Which methods need to be applied for symptom detection of the main categories of faults?

The input of the DBNs of the 4S3F method is the presence and absence of symptoms. Chapter 2 stated that all kind of model-, rule- and data-driven detection methods can be implemented in the 4S3F architecture. Based on our observations on how HVAC experts conduct energy diagnostics in practice, we have suggested classifying symptoms into four categories, as shown in Figure 7.2, which are successfully implemented in the case studies of Chapters 3, 5 and 6:

- a) **Balance symptoms:** based on balance deviations. This is a quantitative model-based approach, based on system theory. However, it does not use complex white box models, but just energy and mass balance equations on systems and subsystems.
In this thesis energy and mass balances are applied for energy performance analysis and sensor fault detection.
- b) **Energy Performance (EP) symptoms:** based on deviations in energy performance metrics. Both quantitative and qualitative model-based approaches can be applied here.
The usefulness of efficiencies, seasonal performance factors and realized capacities was demonstrated in this thesis.
- c) **Operational state (OS) symptoms:** based on deviations in the operational state from the expected state. This is either a quantitative model-based approach (comparing with simulation results), a qualitative model-based approach (rule-based) or a data-driven approach, in which historical data can be used to estimate outliers.
In the present study control and design-based operational indicators were applied. In addition, rules for indoor air quality detection purposes.
- d) **Additional symptoms:** based on additional information. This may be based on historical data or on maintenance or inspection data, but also on the results from a specific FDD method included in a component by the producer. Zhao [1] recently presented an overview of FDD methods from which this information can be extracted. They were classified into data-driven (classification, unsupervised learning and regression methods) and knowledge-driven (model-based and rule-based) methods.
In the present study, symptoms concerning negligible energy amount of HVAC subsystems were applied. In addition, it was shown how results from an external FDD method could be implemented.

The first category of symptoms is generic, while the last is generally system specific. While the second and third are generic, their set values are not. The detection in the case studies in the Chapters 3 and 6 showed that balances, which is directly linked to laws of energy and mass conservation, forms the foundation for the detection of symptoms. To estimate the balances, quantitative (thermodynamic) models are used. According to thermodynamics, the following energy balance applies for open systems when a time span is considered:

$$Q - W_t + H_{in} - H_{out} = \Delta H_{syst} \quad (7.1)$$

with

H=enthalpy

Q=net supplied heat

W_t=technical work

The indices *in* and *out* refers to the input and output of the system, and the index *syst* to the system content. The technical work includes both mechanical and electrical energy.

Contrary to most models found in literature, the models applied in the 4S3F method are very simple. If the timespan used for energy calculation is large enough to eliminate transient effects, these models are reduced to the fact that the sum of the inputs to a system should be equal to the sum of the outputs whereby $\Delta H_{\text{sys}}=0$.

As all systems are described in the HVAC schematic diagrams, it is easy to describe the balances simultaneously at HVAC systems' design.

Likewise, energy performance (EP) deviations, such as COPs, provide a generic way to detect symptoms, by comparing the performance of specific components relative to product specifications and the performance of systems to simulation results, benchmark values or guidelines. Examples include comparing efficiencies and performance factors of components to product specifications (see Chapters 3 and 6) or the yearly energy consumption to a benchmark. Energy performance measures based on seasonal values can be used, but also shorter times can be applied (day, hour etc.). The level of detail of the EP measures is not fixed in the reference architecture. Depending on aims and costs benchmark measures can be used or results from simulation models.

In addition, OS deviations emerge from the comparison between measured state values and their control set points (see Chapters 3, 5 and 6). These symptoms can be detected using rule-based and history-based models.

All types of symptoms other than the balance, EP and OS symptoms can be accommodated within the container term additional symptoms. Within this, subtypes can again be distinguished. For instance, additional information can contain results of specific component diagnosis methods already integrated in components by suppliers. In Chapter 6 an example of the integration of the outcomes from a diagnosis method for a component is discussed. Additional information may also include maintenance and inspection information on components regarding sensor and energy performance malfunctioning (to rule out the presence of faults in these components) or historical data trends (e.g., decrease of COPs of systems over the years due to ageing). Furthermore, the fault identification can be improved by the usage of so-called negligible energy (NE) symptom nodes which can exclude faults in non-operational HVAC subsystems. See Chapter 6 where such nodes are implemented. However, most additional information is relatively specific to systems or buildings, and it is likely to be more cumbersome to implement.

4. *Can the proposed FDD architecture easily be automated and applied on existing HVAC systems?*

All experiments conducted on an existing building have shown the usability of the 4S3F method despite missing data, faulty sensors, missing data points and missing design information concerning HVAC control accuracy. However, in practice the quantity of BMS data available can be low. This could lead to uncertainty of fault presence. Fortunately, one of the strengths of the DBN method is that still faults will be excluded and in the worst-case scenario more models, components and controls will be indicated as possibly defective. In Chapter 4 the sensitivity of faults at level B only is discussed. This experiment showed that fault probability outcomes will still indicate which part of the system should be tackled first.

7.2. Limitations of the study

In this section, the limitations of the present study are discussed.

A major limitation in the practical application is that the real time effort of HVAC engineers to design the FDD method is yet unknown. In particular, a protocol to set up a 4S3F method is lacking with the subject of how to divide the entire HVAC system into its subsystems. Furthermore, the detection and diagnosis steps in the case studies have been executed in a semi-automated manner with the software applications Matlab and Genie. Software based on Matlab was developed to convert BMS data to symptom data. Then, to exchange symptom results to the DBN model in Genie a C++ software tool, called GenieAnalyzer, was developed.

In addition, limitations of the study are further discussed below, based on the FDD phases as shown in Figure 1.1.

Pre-processing

Measurements comprise of outliers and missing data points. In the pre-processing phase, data must be cleared or replaced. This was out of the scope of this research but is of utmost importance. Blank data could be replaced by data from regression formulas based on pattern recognition by historical data (in Chapter 3, this was realized for missing daily energy). In addition, measurements must be transformed automatically into data in the correct form, for instance volume flow rate and temperature data must be converted to energy amounts and some soft sensor data to operational state values.

Furthermore, the sampling time of the measurement data from the heat and cold power plant in the case studies was 16 minutes. This may be insufficient for shorter diagnosis time spans.

Detection

The thermal energy plant of THUAS was divided into subsystems for which detection rules have been drawn up. Especially for sensor FDD, many subsystems were present, which meant that many balances had to be set up. Some of these balances required soft sensors. No research has been done on optimizing the number of subsystems.

The BMS (building management system) in the case studies contains many data points which were used for detection purposes. Hence, it is desirable to conduct the 4S3F method on other buildings with less or different sensors.

In this study, daily energy and mass balances were prepared with the assumption that the thermal storage term in the energy balances of most systems (an exception was made for the buffer tanks) could be neglected because the HVAC system has almost the same state after every night-time. This greatly simplifies the detection with balance symptoms because it can then be assumed that the energy output for each system must be equal to the energy input. The case studies on the thermal energy plant demonstrated that the storage term could rightly be neglected. In thermodynamically slow systems with a time constant on the order of a day (e.g., buffer vessels) or when the balances are set up for short times (e.g., hourly), it is necessary that the storage term is included.

Thresholds and number of exceedances in detection rules were set arbitrary in the case studies with HVAC knowledge. For instance, in the presented energy balance and energy performance detection rules, thresholds of 5% were assumed. In addition, an acceptable temperature deviation of 1 K (cold water system) to 3 K (warm water system) was used. The annual threshold exceedance of these operational state symptoms was set to 10%. However, these values depend strongly on the components and the set values of the controllers applied in the control systems. Moreover, the diagnosis time spam affects the rules. Furthermore, expected COPs were based on design specification and derived from guidelines. However, actual building use by occupants affects these energy performance measures.

The minimum number of symptoms required to arrive at a proper diagnosis has not been investigated. More, requires more effort, but will likely yield higher accuracy. However, this can also lead to misdiagnosis due to the possibility of contradictions and can complicate building a correct 4S3F DBN.

Diagnosis

A tool which generates automatically DBN models from the P&ID and runs the fault isolation based on automatic input generation from the detection phase is not available. Without such a software, the implementation can be time consuming.

Next to this, a limited amount of HVAC components and systems were considered: in the case studies a heat pump, an ATES system, heat exchangers and a DCV system. In addition, the 4S3F method has been isolated from other sub systems like the air handling units and thermal end-user systems. Furthermore, the building physical properties of the building and the influence of building occupancy on energy consumption are not taken into account. Also, novel thermal and electrical systems, as fuel cells and solar panels are not considered.

The prior and conditional probabilities in the DBN model were arbitrarily determined based on designers' experience. Despite this, the case studies showed that only relative values were important. However, in case of more DBN symptom and fault nodes which are linked to each other, it can be complex to estimate the conditional probabilities of the symptom nodes. The relative values of set probabilities in the DBN can be determined once and included in a guideline. More research could also be done on samples of buildings (rather than an individual buildings) to arrive at better values. Another possibility, for example, is to Pareto analysis performed on simulation models for most common HVAC systems to determine the probabilities or by performing data analysis on failure data from the BMS.

Unfortunately, it was not possible to create faults in an existing HVAC system to check the diagnosis for all kinds of faults.

Correction

Next to this, putting the 4S3F architecture into practice online and automatically correcting the faults was beyond the scope of the thesis. It is therefore tested on historical BMS data and not real time.

References

[1] Y. Zhao, T. Li, X. Zhang, C. Zhang, Artificial intelligence-based fault detection and diagnosis methods for building energy systems: Advantages, challenges and the future.

Renewable and Sustainable Energy Reviews 109 (2019): 85-101.
<https://doi.org/10.1016/j.rser.2019.04.021>.

[2] W. Kim, S. Katipamula, A Review of Fault Detection and Diagnostics Methods for Building Systems. Science and Technology for the Built Environment, 24(1) (2017): 3-21.
<https://doi.org/10.1080/23744731.2017.1318008>.

8. Conclusions

8.1 Overall conclusions

The main objective of this study was to develop a FDD architecture which combines knowledge present in P&IDs and HVAC expertise. The case studies presented proof of principles which have shown that the developed 4S3F method is promising.

The scientific contribution is a step forward towards a systematic and automated multi-system and multi-level fault and energy performance diagnosis by the novel 4S3F FDD architecture.

The proposed 4S3F framework meets the hypothesis mentioned in Chapter 1.4 that it must be possible to develop an automated generic FDD method for HVAC's energy performance diagnostic purposes based on systems theory approach, information from HVAC P&IDs and integrating diverse FDD methods already demonstrated. The congruence between the 4S3F and HVAC structure in P&IDs is believed to help promote the large-scale implementation of FDD, including energy performance diagnosis in HVAC systems. The primary symptom detection methods were balance (energy, mass and pressure) based and rule-based (energy performance indicators and operational states) but can be expanded to other types like statistical methods. The simultaneous redundant detection using balance symptoms on aggregated systems and associated subsystems improves the isolation of the faults which also finds place at multi-system level.

The DBN method as a diagnostic method overcomes the problems mentioned in Chapter 1, mainly because it is similar to how engineers design HVAC systems. In addition, it was successfully applied to both energy performance and component FDD. It is very promising that the 4S3F FDD method can be set up and implemented in parallel or even simultaneously with HVACs design and BMS implementation. When automated, this will considerably reduce the FDD implementation effort.

The case studies for sensor fault identification in a thermal energy plant, energy performance diagnosis of the same thermal energy plant and of a demand-controlled ventilation system showed the capability to diagnose with the 4S3F architecture. Component, control, and model faults can be isolated by four types of symptoms: balance, energy performance, operational state, and additional symptoms. Symptoms and faults can be extracted from the P&IDs of the HVAC system considered. The case studies provide confidence that the 4S3F method is generic and could therefore be applied to all types of HVAC systems. It can handle different FDD methods as model-based, rule-based, and data-driven which deliver symptoms for diagnosis purposes.

The diagnosis finds place by DBN models which are set up with expertise from HVAC engineers. Results from the diagnosis are posterior probabilities of faults. Even when less symptom or contradictory information is present, the diagnosis delivers usable outcomes. Multiple faults can be isolated simultaneously. The sensor fault diagnosis in a case study

demonstrated that many faults and symptoms can be diagnosed within seconds. It seems that extension of the DBN model with more nodes will not develop software runtime problems.

Furthermore, uncertainties in the FDD method can be processed in the set probabilities of the DBN model and by introducing model faults. It concerns incorrect or inaccurate measurements, incorrect balance models, inaccurate energy performance metrics and missing fault-symptom relations. The case studies demonstrated that absolute values of the prior and conditional probabilities in the DBN are less important than the relative ones which reduce the need to set these probabilities in a very accurate way.

Energy amounts needed for estimation of energy waste and energy consumption reduction by corrections could be simply determined by the standardized and systematic use of energy balances and energy performance indicators as symptoms, as done in the 4S3F method. These indicators and balances are not available in most rule-based and data-driven symptom detection methods.

And at last, in this thesis a start was made for a library of symptoms because most of the presented symptoms in the case studies are generic and consequently easily adaptable to specific HVAC systems. Detection symptoms and diagnosis models were developed for several components of a thermal energy system (generation and distribution systems) and a ventilation system (an emitter system). Figure 7.1 showed an overview of the applied kind of symptoms. Chapter 3 (operational state symptoms), 5 and 6 (balance, energy performance and operational state symptoms) presented examples of such models for a DCV end user system and an HVAC thermal energy plant. In addition, Diagnosis models, thus DBN models, were presented in Chapter 4 (component and control faults), 5 (component and control faults) and 6 (component and model faults).

Summarized, the next new insights and approaches can be concluded from the studies.

- a) P&IDs are the starting point for setting up an energy performance diagnostic system.
- b) Energy performance diagnosis can be conducted with DBNs.
- c) The 4S3F DBN mimics the way HVAC experts diagnose.
- d) It is possible to apply results from model-, rule- and data driven based FDD methods in the 4S3F DBN.
- e) The simultaneous diagnosis at multi-level is supported by the 4S3F DBNs.
- f) Many faults can be isolated at the same time.
- g) The simultaneous redundant detection using balance symptoms on aggregated systems and associated subsystems improves the isolation of the faults.
- h) The 4S3F architecture supports energy performance diagnosis of a thermal energy system as well a DCV system.
- i) Integration of energy performance diagnosis with component FDD is new.

- j) Uncertainties in the FDD method and inaccuracies in the measurement data can be processed in the 4S3F method.
- k) Application of model faults, especially soft sensors, in an FDD method is new.
- l) Absolute set probabilities of the fault and symptom nodes of the 4S3F DBN are less important than the relative ones.
- m) A start to classify rules for energy performance, balance and operational state symptoms was made.

8.2. Recommendations

This section presents recommendations for the design and implementation of the 4S3F method.

Elaboration of the 4S3F method

The symptoms presented in the case studies of this thesis could be extended with new versions. A library for detection symptoms should be set up. In addition, for diagnostic purposes, a DBN library must be established for HVAC systems.

Research should also be carried out into shortening diagnosis times. Furthermore, the optimal DBN structure must be developed.

Moreover, continuous 4S3F FDD using live data is necessary, mainly for the health and comfort of the user, whereas in this thesis only historical data has been used.

After automation, it is strongly recommended to conduct a case study to simultaneously setup the FDD method with HVAC design by the HVAC engineer.

The above recommendations are elaborated further in section 8.3.

Next to this, the 4S3F could be extended for multi-commodity energy grids at a block of buildings, district, and city level.

Automation

A procedure to set up the 4S3F model is recommended. Next to this, to help the implementation, automation of the FDD process is required to increase the acceptability of the 4S3F method. Furthermore, automation of the pre-processing is desirable. In the pre-processing step, missing and corrupted data and measured data outliers must be corrected automatically which was out of the scope of this thesis. However, much research has been conducted on this.

Specific recommendations for the automation of the 4S3F FDD method are addressed in this section. In the short term, within one to two years, the next software should be developed:

- Software to automate the pre-processing of BMS data: next to correction of corrupt data, soft sensor values and energy amounts could be estimated.
- A user interface for symptom detection, in which rules and default values can be adapted.
- Software for automated detection purposes is needed.
- A user interface to build DBNs.

- Software for diagnosis purposes which fill in automatically detection results and estimate posterior probabilities of the faults.
- Finally, a high-quality user interface to present diagnosis results and relevant information to correct faults would be relevant to advance the used of FDD in HVAC systems.

And after that:

- Software to select HVAC subsystems from a P&ID: It would be preferably automated from a (BIM) database containing P&ID information.
- Software to help the HVAC designer to select symptom models from an HVAC component and control library with default thresholds is needed.
- Probably, software is useful for automated adaption of set probabilities of DBN models by historical data.
- Next to this, software and methods which test sensors by starting up the HVAC system daily or in the weekend in different HVAC modes would be of great help to strengthen the diagnostic process.

Short term implementation in a real HVAC system

Extensive DBNs should be avoided because it complicates estimating the conditional probabilities of the symptoms. Therefore, the following is recommended when using the 4S3F method. Weak links between faults and symptoms should be neglected. However, at a minimum, balance symptoms must be present to isolate sensor failures. In addition, energy performance and operational state symptoms, as present in the case studies, are needed for energy performance analysis. Furthermore, DBN nodes must be present for the most used generator, distribution and emitter systems. Within these subsystems there are fault nodes for the main components, such as energy generators and heat exchangers. Afterwards, the DBN can be extended with additional symptoms and model faults.

In addition, it is recommended to start with daily FDD because heat gains and losses of systems and the storage period in energy balances can be ignored with daily FDD for well-insulated components, which greatly simplifies the energy balances.

The posterior fault probabilities should be presented in an automated way which could lead to advice stakeholders for correction purposes.

8.3. Further research

First, recent research work from the last year is discussed. In November 2020, M. Horrigan [1] published his PhD thesis. He focused on the operational phase of the building and considered only detection of faults which takes place by comparing operation data with forecast data from a calibrated simulation model. As stated in the present thesis, the disadvantage of this approach is that the prediction model could be trained with measurement data from a not optimally functioning installation. In addition, a changed building use should lead to an adjustment of the predictive model. Nevertheless, his research is valuable because

his symptoms could be applied in the 4S3F FDD. His study confirms that a multi-context approach has advantages over the commonly used bottom-up and top-down approaches.

Two recent studies present a DBN method as a tool for HVAC system diagnosis. First a thesis of Gao [2] from December 2020 is discussed. The DBN's, she presented, are also set up with expert knowledge and she also take in account the building typology such that a variety of HVAC systems can be considered. The structure of the DBNs supports multi-level diagnosis (component and sub-system levels are distinct). As with the 4S3F method, it does not go beyond the component level (i.e., trade products) and mainly distinguishes two fault conditions (normal and abnormal). Also, both component and control faults are recognized. Her design of the DBNs therefore largely corresponds to that of 4S3F. Since this has been done independently with 4S3F, that gives even more confidence in the 4S3F architecture. She confirms that absolute values for the prior probabilities are subordinate to relative values, so that she also uses raw values for these probabilities: two states and 0.9 for most normal conditions. Sometimes three states are distinguished. As with the 4S3F cases, the conditional probabilities vary.

In another study [3] only component faults for an air handling unit were considered. The DBNs are first setup on expert knowledge and adjusted afterwards based on data analysis. This resulted in more relations between faults and symptoms and, according to the expert, some relations were absent. A fault-symptom relation matrix is presented from which the DBN can be setup (in 4S3F a table was presented). Many rule-based symptoms were presented.

Both DBN studies confirm the choice of Bayesian networks over other FDD alternatives and present a structure of the DBNs largely similar to that of 4S3F. However, in contrast to the 4S3F approach, energy performance was not discussed, and no attention was paid to P&IDs drawn up by HVAC designers for setting up an FDD application. In addition, hard and soft sensor faults were not taken into account, and balance and EP symptoms were not taken into account in both DBN studies.

In view of the recommendations and recent studies, the following follow-up study is recommended below.

In the short term, faults in existing HVAC systems should be created to check the 4S3F method for all kinds of faults. This will be done for several buildings in one of the work packages of the recently started Dutch B4B project [4], in which research institutions and about twenty companies participate.

In the longer term, it is desirable that the FDD information is included in a building information model (BIM) and that a standard is available for this. The information required for the 4S3F FDD is strongly linked to design information. A central place where this information is available in the correct format is desirable. This includes P&ID based information, specifications of components and controls, and control settings. A BIM is suitable for this. In addition, changes during the realization or use of the building can be included in the BIM. It is also desirable to include pre-processed measurement data from the BMS in the BIM such as energy quantities and (for example average) operational state quantities that are directly usable for energy performance diagnosis. It is recommended that further research be conducted on this. In the KnoHoEM [5] project, for example, attention was paid to storage of measurement data in a BIM. Maintenance and inspection information and frequencies of types of faults can also be included.

8.3.1 Pre-processing

Most existing buildings do not contain many hard sensors, so soft sensors are needed to estimate energy amounts and status values. In the present study, some models are presented for soft sensors such as soft temperature and flow sensors. However, the overview is not exhaustive and should be supplemented, for example with a soft flow sensor, which can be derived from the specification of the fan and its speed.

8.3.1 Detection

New kind of symptoms should be investigated, to what extent they help to isolate errors. To include in the library, the following extensions may be considered:

Balances

- Pressure balances
- Energy and mass balances at room level which consider the internal heat production, heat flows through the building skin and storage of thermal energy in the construction.
- Mass and energy balance equations which consider non-stationary behaviour instead of steady state models.

Energy performance

- Time-based energy consumption symptoms. For instance, energy related patterns during day and night-time, and during weekends.

Operational states

- Flow rates
- Adding control signals for detection purposes which for instance support to identify a broken cable.

Additional information

- User information from occupants. For instance, complaints about thermal comfort.
- Incorrect HVAC modes (e.g., cooling with chiller instead of natural cooling).
- Predictive energy performance and IAQ models.

Next to this, results of existing or new component FDD methods, as statistical methods, can be implemented in the DBN.

Furthermore, it is recommended to investigate the minimum number and types of symptoms required to arrive at a proper diagnosis for all kinds of HVAC systems.

8.3.2 Diagnosis

It is desirable to conduct the 4S3F method on other buildings with a limited amount of data points such as houses. Furthermore, a study should be conducted on simultaneous diagnosis of energy performance, sensors, and indoor climate. In this study they were studied separately. Moreover, it is desirable to conduct research to optimize the division of an HVAC system into subsystems where the necessary sensors can be determined and research for the minimum data set for reliable energy performance symptom detection is required, for

application to existing buildings and dwellings where few sensors are present. On the other hand, redundant hard and soft sensors improve diagnosis of faulty sensors. Research is needed about the level of redundancy needed.

For diagnosis purposes, a DBN library with HVAC models for components and control systems is required to reduce the effort to set up a specific HVAC DBN. It is recommended to start with generator, distribution and emitter systems. For instance, models for an AHU, VAV systems and thermal energy generator systems as solar collector systems. Next to these systems, this library should also contain standardized HVAC components. For instance, models for valves, pumps, pipes and ducts but also models for control systems (supply temperatures, on-off strategies, timers) and sustainable energy generators. Furthermore, soft sensor models can be added, e.g., for the estimation of number of persons for occupancy purposes. A start is made in this thesis and can be realized in short term. It is recommended to expand the HVAC systems, such as air handling units and thermal terminals in building rooms. Next to this, solar panels and batteries can be considered. Furthermore, the building physical properties of the building and the influence of building users on energy consumption. For instance, by taken into account the thermal energy and air balances of rooms to exclude or include the effect of building physics on energy (including comfort and health) performance.

Moreover, as for diagnosis purposes, the optimal time interval for diagnosis is of utmost importance. Symptom detection and fault diagnosis could occur at short time frame (e.g., a sensor diagnosis at every minute) to annual diagnosis (e.g., annual SCOP of an ATES system). Is it possible to integrate different timespans in one integrated DBN model?

The relative values of prior and conditional probabilities in the DBN nodes can be estimated by experts. This can be done once and included in a guideline. More research could also be done on samples of buildings (rather than individual buildings) to arrive at better values. Another possibility, for example, is that Pareto analyses are performed on simulation models for most common HVAC systems to determine the probabilities or by performing data analysis on failure data from the BMS. In addition, a test procedure for set probabilities could be developed.

It can be hypothesized that more states in fault nodes helps to precisely identify the fault type. Moreover, the effect of more states (now Boolean) in symptom nodes can be considered which could help to accurately identify the fault type of a component or control system.

In the 4S3F method, DBN was chosen because it mimics the expert. Then DBN is an obvious choice. The present study concerned a proof of concept: to what extent does a DBN approach solve the identified problems? For this purpose, the software tool Genie based on Smile was used. In further research, it is certainly a recommendation to see whether other software which mimics engineer's' practice would not be (even) more suitable.

Energy balances have been used for sensor failures (chapter 6). They have also been used to determine unnecessary heat losses or gains in systems from system efficiencies (chapter 3). It is recommended to integrate these applications because anomalies in energy balances can be caused by sensor faults, but also by miscalculation of heat gains or losses (model errors) if not all exchanged energy can be measured. In addition, it is proposed to consider system

efficiency not as a balance symptom, but as a symptom of energy performance. The above needs to be worked out in more detail.

8.3.3 Correction

In addition, automation for decision making is desirable. For instance, by quantifying unnecessary energy losses, achievable energy gains by corrections and investment costs (for instance to redesign the HVAC system, to replace a sensor or to adapt control strategy).

Finally, looking at the developments in the field of energy flexibility, it could be interesting to develop the 4S3F method towards the determination of optimum control strategies, not only looking at set values in the system, but potentially better values.

References

- [1] M. Horrigan, An integrated statistical approach to bridge the operational performance gap in buildings (2020). PhD thesis. College of Engineering and architecture, UCD Energy Institute. Dublin.
- [2] T. Gao, Integrated building fault detection and diagnosis using data modelling and Bayesian networks (2020). PhD thesis. IMT Lille Douai and University of Lille. Lille.
- [3] T. Li, Y. Zhao, C.Zhang, J.Luo, X.Zhang. A knowledge-guided and data-driven method for building HVAC systems fault diagnosis. *Building and Environment* 198 (2021) 107850. <https://doi.org/10.1016/j.buildenv.2021.107850>.
- [4] Brains for buildings' energy systems (B4B). <https://brains4buildings.org>.
- [5] Anzaldi G., Corchero A., Wicaksono H., McGlenn K., Gerdelan A., Dibley M.J. (2014) Knoholem: Knowledge-Based Energy Management for Public Buildings Through Holistic Information Modeling and 3D Visualization. In: González Alonso I. (eds) *International Technology Robotics Applications. Intelligent Systems, Control and Automation: Science and Engineering*, vol 70. Springer, Cham. https://doi.org/10.1007/978-3-319-02332-8_5.

About the author

Arie Taal was born in 1956 in The Hague, The Netherlands. He obtained his B.Sc. degree at the Hague University of applied sciences, faculty Mechanical Engineering and his M.Sc. degree at the Faculty of Mechanical Engineering of the Technical University of Delft. Arie graduated in Mechanical Engineering, Climate control, in 1982 with a graduation project on energy savings by an active building shell. In the period from 1982 to 1989, he worked as HVAC researcher at two HVAC design firms. As designer he developed several HVAC systems, including the control systems, for large office buildings. From 1989 till now, he has been lecturer at the department of mechanical Engineering of The Hague University of Applied sciences. His specialism is thermal energy technology in the building environment. From 1999-2001 he was project leader of the research project “Climasim” which purpose was the development of an HVAC simulation approach with component models from a generic library. In the last years he teaches the energy transition from natural gas towards wind and solar energy.

In 2011, he started his PhD project part time: automated fault diagnosis, at HHS. During his PhD he was involved in educational activities as lecturer of “Smart building services”, “Sustainable energy generation”, “modelling and simulation of HVAC systems” and “Sustainable energy networks”. In addition, he is head of the curriculum commission of Mechanical engineering and was member at the research group of “Energy and Building” and nowadays member at the research group “Energy in Transition”.

List of publications

Journal papers

a. Published

[1] A. Taal, L. Itard, W. Zeiler, A reference architecture for the integration of automated energy performance fault diagnosis into HVAC systems, *Energy & Buildings* 179 (2018) 144-155. <https://doi.org/10.1016/j.enbuild.2018.08.031>

[2] A. Taal, L. Itard, Fault detection and diagnosis for indoor air quality in DCV systems: Application of 4S3F method and effects of DBN probabilities. *Building and Environment* 174 (2020) 106632. <https://doi.org/10.1016/j.buildenv.2019.106632>

[3] A. Taal, L. Itard, P&ID-based symptom detection for automated energy performance diagnosis in HVAC systems. *Automation in Construction* 119 (2020), 103344. <https://doi.org/10.1016/j.autcon.2020.103344>

[4] A. Taal, L. Itard, P&ID-based automated fault identification for energy performance diagnosis in HVAC systems: 4S3F method, development of DBN models and application to an ATEs system. *Energy and Buildings* 224 (2020): 110289. <https://doi.org/10.1016/j.enbuild.2020.110289>

b. Submitted

[1] A. Taal, L. Itard, W. Zeiler, Fault Detection, Diagnosis and Correction for hard and soft sensors in Building Energy Management Systems: A new extension of the 4S3F framework.

Conference proceedings

[1] Arie Taal, Yang Zhao, Wim Zeiler. Automatic commissioning of CO₂ sensors in air conditioning systems. Proceedings CIBSE Technical Symposium, London, UK 16-17 April 2015.

[2] Taal, A., Itard, L., Zeiler, W., & Zhao, Y. (2016). *Automatic detection and diagnosis of faults in sensors used in EMS*. 1-10. Paper presented at 12th REHVA World Congress (CLIMA 2016), May 22-25, 2016, Aalborg, Denmark, Aalborg, Denmark.

[3] Arie Taal, Laure Itard, Wim Zeiler. A Diagnostic Bayesian Network Method To Diagnose Building Energy Performance. Proceedings IBPSA 2019 Rome.

Bouwstenen is een publicatiereeks van de Faculteit Bouwkunde, Technische Universiteit Eindhoven. Zij presenteert resultaten van onderzoek en andere activiteiten op het vakgebied der Bouwkunde, uitgevoerd in het kader van deze Faculteit.

Bouwstenen en andere proefschriften van de TU/e zijn online beschikbaar via:
<https://research.tue.nl/>

Reeds verschenen in de serie

Bouwstenen

nr 1

Elan: A Computer Model for Building Energy Design: Theory and Validation

Martin H. de Wit

H.H. Driessen

R.M.M. van der Velden

nr 2

Kwaliteit, Keuzevrijheid en Kosten: Evaluatie van Experiment Klarendal, Arnhem

J. Smeets

C. le Nobel

M. Broos

J. Frenken

A. v.d. Sanden

nr 3

Crooswijk: Van 'Bijzonder' naar 'Gewoon'

Vincent Smit

Kees Noort

nr 4

Staal in de Woningbouw

Edwin J.F. Delsing

nr 5

Mathematical Theory of Stressed Skin Action in Profiled Sheeting with Various Edge Conditions

Andre W.A.M.J. van den Bogaard

nr 6

Hoe Berekenbaar en Betrouwbaar is de Coëfficiënt k in x -ksigma en x -ks?

K.B. Lub

A.J. Bosch

nr 7

Het Typologisch Gereedschap: Een Verkennende Studie Omtrent Typologie en Omtrent de Aanpak van Typologisch Onderzoek

J.H. Luiten

nr 8

Informatievoorziening en Beheerprocessen

A. Nauta

Jos Smeets (red.)

Helga Fassbinder (projectleider)

Adrie Proveniers

J. v.d. Moosdijk

nr 9

Strukturering en Verwerking van Tijdgegevens voor de Uitvoering van Bouwwerken

ir. W.F. Schaefer

P.A. Erkelens

nr 10

Stedebouw en de Vorming van een Speciale Wetenschap

K. Doevendans

nr 11

Informatica en Ondersteuning van Ruimtelijke Besluitvorming

G.G. van der Meulen

nr 12

Staal in de Woningbouw, Korrosie-Bescherming van de Begane Grondvloer

Edwin J.F. Delsing

nr 13

Een Thermisch Model voor de Berekening van Staalplaatbetonvloeren onder Brandomstandigheden

A.F. Hamerlinck

nr 14

De Wijkgedachte in Nederland: Gemeenschapsstreven in een Stedebouwkundige Context

K. Doevendans

R. Stolzenburg

nr 15

Diaphragm Effect of Trapezoidally Profiled Steel Sheets:

Experimental Research into the Influence of Force Application

Andre W.A.M.J. van den Bogaard

nr 16

Versterken met Spuit-Ferrocement: Het Mechanische Gedrag van met Spuit-Ferrocement Versterkte Gewapend Betonbalken

K.B. Lubir

M.C.G. van Wanroy

nr 17

**De Tractaten van
Jean Nicolas Louis Durand**
G. van Zeyl

nr 18

**Wonen onder een Plat Dak:
Drie Opstellen over Enkele
Vooronderstellingen van de
Stedebouw**
K. Doevendans

nr 19

**Supporting Decision Making Processes:
A Graphical and Interactive Analysis of
Multivariate Data**
W. Adams

nr 20

**Self-Help Building Productivity:
A Method for Improving House Building
by Low-Income Groups Applied to Kenya
1990-2000**
P. A. Erkelens

nr 21

**De Verdeling van Woningen:
Een Kwestie van Onderhandelen**
Vincent Smit

nr 22

**Flexibiliteit en Kosten in het Ontwerpproces:
Een Besluitvormingondersteunend Model**
M. Prins

nr 23

**Spontane Nederzettingen Begeleid:
Voorwaarden en Criteria in Sri Lanka**
Po Hin Thung

nr 24

**Fundamentals of the Design of
Bamboo Structures**
Oscar Arce-Villalobos

nr 25

Concepten van de Bouwkunde
M.F.Th. Bax (red.)
H.M.G.J. Trum (red.)

nr 26

Meaning of the Site
Xiaodong Li

nr 27

**Het Woonmilieu op Begrip Gebracht:
Een Speurtocht naar de Betekenis van het
Begrip 'Woonmilieu'**
Jaap Ketelaar

nr 28

Urban Environment in Developing Countries
editors: Peter A. Erkelens
George G. van der Meulen (red.)

nr 29

**Stategische Plannen voor de Stad:
Onderzoek en Planning in Drie Steden**
prof.dr. H. Fassbinder (red.)
H. Rikhof (red.)

nr 30

Stedebouwkunde en Stadsbestuur
Piet Beekman

nr 31

**De Architectuur van Djenné:
Een Onderzoek naar de Historische Stad**
P.C.M. Maas

nr 32

Conjoint Experiments and Retail Planning
Harmen Oppewal

nr 33

**Strukturformen Indonesischer Bautechnik:
Entwicklung Methodischer Grundlagen
für eine 'Konstruktive Pattern Language'
in Indonesien**

Heinz Frick arch. SIA

nr 34

**Styles of Architectural Designing:
Empirical Research on Working Styles
and Personality Dispositions**
Anton P.M. van Bakel

nr 35

**Conjoint Choice Models for Urban
Tourism Planning and Marketing**
Benedict Dellaert

nr 36

Stedelijke Planvorming als Co-Productie
Helga Fassbinder (red.)

nr 37

Design Research in the Netherlands

editors: R.M. Oxman
M.F.Th. Bax
H.H. Achten

nr 38

Communication in the Building Industry

Bauke de Vries

nr 39

**Optimaal Dimensioneren van
Gelaste Plaatliggers**

J.B.W. Stark
F. van Pelt
L.F.M. van Gorp
B.W.E.M. van Hove

nr 40

Huisvesting en Overwinning van Armoede

P.H. Thung
P. Beekman (red.)

nr 41

**Urban Habitat:
The Environment of Tomorrow**

George G. van der Meulen
Peter A. Erkelens

nr 42

A Typology of Joints

John C.M. Olie

nr 43

**Modeling Constraints-Based Choices
for Leisure Mobility Planning**

Marcus P. Stemerding

nr 44

Activity-Based Travel Demand Modeling

Dick Ettema

nr 45

**Wind-Induced Pressure Fluctuations
on Building Facades**

Chris Geurts

nr 46

Generic Representations

Henri Achten

nr 47

**Johann Santini Aichel:
Architectuur en Ambiguiteit**

Dirk De Meyer

nr 48

**Concrete Behaviour in Multiaxial
Compression**

Erik van Geel

nr 49

Modelling Site Selection

Frank Witlox

nr 50

Ecolemma Model

Ferdinand Beetstra

nr 51

**Conjoint Approaches to Developing
Activity-Based Models**

Donggen Wang

nr 52

On the Effectiveness of Ventilation

Ad Roos

nr 53

**Conjoint Modeling Approaches for
Residential Group preferences**

Eric Molin

nr 54

**Modelling Architectural Design
Information by Features**

Jos van Leeuwen

nr 55

**A Spatial Decision Support System for
the Planning of Retail and Service Facilities**

Theo Arentze

nr 56

Integrated Lighting System Assistant

Ellie de Groot

nr 57

Ontwerpend Leren, Leren Ontwerpen

J.T. Boekholt

nr 58

**Temporal Aspects of Theme Park Choice
Behavior**

Astrid Kemperman

nr 59

**Ontwerp van een Geïndustrialiseerde
Funderingswijze**

Faas Moonen

nr 60

**Merlin: A Decision Support System
for Outdoor Leisure Planning**

Manon van Middelkoop

nr 61

The Aura of Modernity

Jos Bosman

nr 62

Urban Form and Activity-Travel Patterns

Daniëlle Snellen

nr 63

Design Research in the Netherlands 2000

Henri Achten

nr 64

**Computer Aided Dimensional Control in
Building Construction**

Rui Wu

nr 65

Beyond Sustainable Building

editors: Peter A. Erkelens
Sander de Jonge
August A.M. van Vliet

co-editor: Ruth J.G. Verhagen

nr 66

Das Globalrecyclingfähige Haus

Hans Löfflad

nr 67

Cool Schools for Hot Suburbs

René J. Dierkx

nr 68

**A Bamboo Building Design Decision
Support Tool**

Fitri Mardjono

nr 69

Driving Rain on Building Envelopes

Fabien van Mook

nr 70

Heating Monumental Churches

Henk Schellen

nr 71

**Van Woningverhuurder naar
Aanbieder van Woongenot**

Patrick Dogge

nr 72

**Moisture Transfer Properties of
Coated Gypsum**

Emile Goossens

nr 73

Plybamboo Wall-Panels for Housing

Guillermo E. González-Beltrán

nr 74

The Future Site-Proceedings

Ger Maas

Frans van Gassel

nr 75

**Radon transport in
Autoclaved Aerated Concrete**

Michel van der Pal

nr 76

**The Reliability and Validity of Interactive
Virtual Reality Computer Experiments**

Amy Tan

nr 77

**Measuring Housing Preferences Using
Virtual Reality and Belief Networks**

Maciej A. Orzechowski

nr 78

**Computational Representations of Words
and Associations in Architectural Design**

Nicole Segers

nr 79

**Measuring and Predicting Adaptation in
Multidimensional Activity-Travel Patterns**

Chang-Hyeon Joh

nr 80

Strategic Briefing

Fayez Al Hassan

nr 81

Well Being in Hospitals

Simona Di Cicco

nr 82

**Solares Bauen:
Implementierungs- und Umsetzungs-
Aspekte in der Hochschulausbildung
in Österreich**

Gerhard Schuster

- nr 83
Supporting Strategic Design of Workplace Environments with Case-Based Reasoning
Shauna Mallory-Hill
- nr 84
ACCEL: A Tool for Supporting Concept Generation in the Early Design Phase
Maxim Ivashkov
- nr 85
Brick-Mortar Interaction in Masonry under Compression
Ad Vermeltfoort
- nr 86
Zelfredzaam Wonen
Guus van Vliet
- nr 87
Een Ensemble met Grootstedelijke Allure
Jos Bosman
Hans Schippers
- nr 88
On the Computation of Well-Structured Graphic Representations in Architectural Design
Henri Achten
- nr 89
De Evolutie van een West-Afrikaanse Vernaculaire Architectuur
Wolf Schijns
- nr 90
ROMBO Tactiek
Christoph Maria Ravesloot
- nr 91
External Coupling between Building Energy Simulation and Computational Fluid Dynamics
Ery Djunaedy
- nr 92
Design Research in the Netherlands 2005
editors: Henri Achten
Kees Dorst
Pieter Jan Stappers
Bauke de Vries
- nr 93
Ein Modell zur Baulichen Transformation
Jalil H. Saber Zaimian
- nr 94
Human Lighting Demands: Healthy Lighting in an Office Environment
Myriam Aries
- nr 95
A Spatial Decision Support System for the Provision and Monitoring of Urban Greenspace
Claudia Pelizaro
- nr 96
Leren Creëren
Adri Proveniers
- nr 97
Simlandscape
Rob de Waard
- nr 98
Design Team Communication
Ad den Otter
- nr 99
Humaan-Ecologisch Georiënteerde Woningbouw
Juri Czabanowski
- nr 100
Hambase
Martin de Wit
- nr 101
Sound Transmission through Pipe Systems and into Building Structures
Susanne Bron-van der Jagt
- nr 102
Het Bouwkundig Contrapunt
Jan Francis Boelen
- nr 103
A Framework for a Multi-Agent Planning Support System
Dick Saarloos
- nr 104
Bracing Steel Frames with Calcium Silicate Element Walls
Bright Mweene Ng'andu
- nr 105
Naar een Nieuwe Houtskeletbouw
F.N.G. De Medts

nr 106 and 107
Niet gepubliceerd

nr 108
Geborgenheid
T.E.L. van Pinxteren

nr 109
Modelling Strategic Behaviour in Anticipation of Congestion
Qi Han

nr 110
Reflecties op het Woondomein
Fred Sanders

nr 111
On Assessment of Wind Comfort by Sand Erosion
Gábor Dezsö

nr 112
Bench Heating in Monumental Churches
Dionne Limpens-Neilen

nr 113
RE. Architecture
Ana Pereira Roders

nr 114
Toward Applicable Green Architecture
Usama El Fiky

nr 115
Knowledge Representation under Inherent Uncertainty in a Multi-Agent System for Land Use Planning
Liyang Ma

nr 116
Integrated Heat Air and Moisture Modeling and Simulation
Jos van Schijndel

nr 117
Concrete Behaviour in Multiaxial Compression
J.P.W. Bongers

nr 118
The Image of the Urban Landscape
Ana Moya Pellitero

nr 119
The Self-Organizing City in Vietnam
Stephanie Geertman

nr 120
A Multi-Agent Planning Support System for Assessing Externalities of Urban Form Scenarios
Rachel Katoshevski-Cavari

nr 121
Den Schulbau Neu Denken, Fühlen und Wollen
Urs Christian Maurer-Dietrich

nr 122
Peter Eisenman Theories and Practices
Bernhard Kormoss

nr 123
User Simulation of Space Utilisation
Vincent Tabak

nr 125
In Search of a Complex System Model
Oswald Devisch

nr 126
Lighting at Work: Environmental Study of Direct Effects of Lighting Level and Spectrum on Psycho-Physiological Variables
Grazyna Górnicka

nr 127
Flanking Sound Transmission through Lightweight Framed Double Leaf Walls
Stefan Schoenwald

nr 128
Bounded Rationality and Spatio-Temporal Pedestrian Shopping Behavior
Wei Zhu

nr 129
Travel Information: Impact on Activity Travel Pattern
Zhongwei Sun

nr 130
Co-Simulation for Performance Prediction of Innovative Integrated Mechanical Energy Systems in Buildings
Marija Trčka

nr 131
Niet gepubliceerd

nr 132

Architectural Cue Model in Evacuation Simulation for Underground Space Design
Chengyu Sun

nr 133

Uncertainty and Sensitivity Analysis in Building Performance Simulation for Decision Support and Design Optimization
Christina Hopfe

nr 134

Facilitating Distributed Collaboration in the AEC/FM Sector Using Semantic Web Technologies
Jacob Beetz

nr 135

Circumferentially Adhesive Bonded Glass Panes for Bracing Steel Frame in Façades
Edwin Huveners

nr 136

Influence of Temperature on Concrete Beams Strengthened in Flexure with CFRP
Ernst-Lucas Klamer

nr 137

Sturen op Klantwaarde
Jos Smeets

nr 139

Lateral Behavior of Steel Frames with Discretely Connected Precast Concrete Infill Panels
Paul Teewen

nr 140

Integral Design Method in the Context of Sustainable Building Design
Perica Savanović

nr 141

Household Activity-Travel Behavior: Implementation of Within-Household Interactions
Renni Anggraini

nr 142

Design Research in the Netherlands 2010
Henri Achten

nr 143

Modelling Life Trajectories and Transport Mode Choice Using Bayesian Belief Networks
Marloes Verhoeven

nr 144

Assessing Construction Project Performance in Ghana
William Gyadu-Asiedu

nr 145

Empowering Seniors through Domotic Homes
Masi Mohammadi

nr 146

An Integral Design Concept for Ecological Self-Compacting Concrete
Martin Hunger

nr 147

Governing Multi-Actor Decision Processes in Dutch Industrial Area Redevelopment
Erik Blokhuis

nr 148

A Multifunctional Design Approach for Sustainable Concrete
Götz Hüsken

nr 149

Quality Monitoring in Infrastructural Design-Build Projects
Ruben Favié

nr 150

Assessment Matrix for Conservation of Valuable Timber Structures
Michael Abels

nr 151

Co-simulation of Building Energy Simulation and Computational Fluid Dynamics for Whole-Building Heat, Air and Moisture Engineering
Mohammad Mirsadeghi

nr 152

External Coupling of Building Energy Simulation and Building Element Heat, Air and Moisture Simulation
Daniel Cóstola

nr 153

**Adaptive Decision Making In
Multi-Stakeholder Retail Planning**

Ingrid Janssen

nr 154

Landscape Generator

Kymo Slager

nr 155

Constraint Specification in Architecture

Remco Niemeijer

nr 156

**A Need-Based Approach to
Dynamic Activity Generation**

Linda Nijland

nr 157

**Modeling Office Firm Dynamics in an
Agent-Based Micro Simulation Framework**

Gustavo Garcia Manzato

nr 158

**Lightweight Floor System for
Vibration Comfort**

Sander Zegers

nr 159

Aanpasbaarheid van de Draagstructuur

Roel Gijsbers

nr 160

'Village in the City' in Guangzhou, China

Yanliu Lin

nr 161

Climate Risk Assessment in Museums

Marco Martens

nr 162

Social Activity-Travel Patterns

Pauline van den Berg

nr 163

**Sound Concentration Caused by
Curved Surfaces**

Martijn Vercammen

nr 164

**Design of Environmentally Friendly
Calcium Sulfate-Based Building Materials:
Towards an Improved Indoor Air Quality**

Qingliang Yu

nr 165

**Beyond Uniform Thermal Comfort
on the Effects of Non-Uniformity and
Individual Physiology**

Lisje Schellen

nr 166

Sustainable Residential Districts

Gaby Abdalla

nr 167

**Towards a Performance Assessment
Methodology using Computational
Simulation for Air Distribution System
Designs in Operating Rooms**

Mônica do Amaral Melhado

nr 168

**Strategic Decision Modeling in
Brownfield Redevelopment**

Brano Glumac

nr 169

**Pamela: A Parking Analysis Model
for Predicting Effects in Local Areas**

Peter van der Waerden

nr 170

**A Vision Driven Wayfinding Simulation-System
Based on the Architectural Features Perceived
in the Office Environment**

Qunli Chen

nr 171

**Measuring Mental Representations
Underlying Activity-Travel Choices**

Oliver Horeni

nr 172

**Modelling the Effects of Social Networks
on Activity and Travel Behaviour**

Nicole Ronald

nr 173

**Uncertainty Propagation and Sensitivity
Analysis Techniques in Building Performance
Simulation to Support Conceptual Building
and System Design**

Christian Struck

nr 174

**Numerical Modeling of Micro-Scale
Wind-Induced Pollutant Dispersion
in the Built Environment**

Pierre Gousseau

nr 175

**Modeling Recreation Choices
over the Family Lifecycle**

Anna Beatriz Grigolon

nr 176

**Experimental and Numerical Analysis of
Mixing Ventilation at Laminar, Transitional
and Turbulent Slot Reynolds Numbers**

Twan van Hooff

nr 177

**Collaborative Design Support:
Workshops to Stimulate Interaction and
Knowledge Exchange Between Practitioners**

Emile M.C.J. Quanjel

nr 178

Future-Proof Platforms for Aging-in-Place

Michiel Brink

nr 179

**Motivate:
A Context-Aware Mobile Application for
Physical Activity Promotion**

Yuzhong Lin

nr 180

**Experience the City:
Analysis of Space-Time Behaviour and
Spatial Learning**

Anastasia Moiseeva

nr 181

**Unbonded Post-Tensioned Shear Walls of
Calcium Silicate Element Masonry**

Lex van der Meer

nr 182

**Construction and Demolition Waste
Recycling into Innovative Building Materials
for Sustainable Construction in Tanzania**

Mwita M. Sabai

nr 183

**Durability of Concrete
with Emphasis on Chloride Migration**

Przemysław Spiesz

nr 184

**Computational Modeling of Urban
Wind Flow and Natural Ventilation Potential
of Buildings**

Rubina Ramponi

nr 185

**A Distributed Dynamic Simulation
Mechanism for Buildings Automation
and Control Systems**

Azzedine Yahiaoui

nr 186

**Modeling Cognitive Learning of Urban
Networks in Daily Activity-Travel Behavior**

Şehnaz Cenani Durmazoğlu

nr 187

**Functionality and Adaptability of Design
Solutions for Public Apartment Buildings
in Ghana**

Stephen Agyefi-Mensah

nr 188

**A Construction Waste Generation Model
for Developing Countries**

Lilliana Abarca-Guerrero

nr 189

**Synchronizing Networks:
The Modeling of Supernetworks for
Activity-Travel Behavior**

Feixiong Liao

nr 190

**Time and Money Allocation Decisions
in Out-of-Home Leisure Activity Choices**

Gamze Zeynep Dane

nr 191

**How to Measure Added Value of CRE and
Building Design**

Rianne Appel-Meulenbroek

nr 192

**Secondary Materials in Cement-Based
Products:
Treatment, Modeling and Environmental
Interaction**

Miruna Florea

nr 193

**Concepts for the Robustness Improvement
of Self-Compacting Concrete:
Effects of Admixtures and Mixture
Components on the Rheology and Early
Hydration at Varying Temperatures**

Wolfram Schmidt

nr 194

Modelling and Simulation of Virtual Natural Lighting Solutions in Buildings

Rizki A. Mangkuto

nr 195

Nano-Silica Production at Low Temperatures from the Dissolution of Olivine - Synthesis, Tailoring and Modelling

Alberto Lazaro Garcia

nr 196

Building Energy Simulation Based Assessment of Industrial Halls for Design Support

Bruno Lee

nr 197

Computational Performance Prediction of the Potential of Hybrid Adaptable Thermal Storage Concepts for Lightweight Low-Energy Houses

Pieter-Jan Hoes

nr 198

Application of Nano-Silica in Concrete

George Quercia Bianchi

nr 199

Dynamics of Social Networks and Activity Travel Behaviour

Fariya Sharmeen

nr 200

Building Structural Design Generation and Optimisation including Spatial Modification

Juan Manuel Davila Delgado

nr 201

Hydration and Thermal Decomposition of Cement/Calcium-Sulphate Based Materials

Ariën de Korte

nr 202

Republiek van Beelden: De Politieke Werkingen van het Ontwerp in Regionale Planvorming

Bart de Zwart

nr 203

Effects of Energy Price Increases on Individual Activity-Travel Repertoires and Energy Consumption

Dujuan Yang

nr 204

Geometry and Ventilation: Evaluation of the Leeward Sawtooth Roof Potential in the Natural Ventilation of Buildings

Jorge Isaac Perén Montero

nr 205

Computational Modelling of Evaporative Cooling as a Climate Change Adaptation Measure at the Spatial Scale of Buildings and Streets

Hamid Montazeri

nr 206

Local Buckling of Aluminium Beams in Fire Conditions

Ronald van der Meulen

nr 207

Historic Urban Landscapes: Framing the Integration of Urban and Heritage Planning in Multilevel Governance

Loes Veldpaus

nr 208

Sustainable Transformation of the Cities: Urban Design Pragmatics to Achieve a Sustainable City

Ernesto Antonio Zumelzu Scheel

nr 209

Development of Sustainable Protective Ultra-High Performance Fibre Reinforced Concrete (UHPRC): Design, Assessment and Modeling

Rui Yu

nr 210

Uncertainty in Modeling Activity-Travel Demand in Complex Urban Systems

Soora Rasouli

nr 211

Simulation-based Performance Assessment of Climate Adaptive Greenhouse Shells

Chul-sung Lee

nr 212

Green Cities: Modelling the Spatial Transformation of the Urban Environment using Renewable Energy Technologies

Saleh Mohammadi

nr 213

A Bounded Rationality Model of Short and Long-Term Dynamics of Activity-Travel Behavior

Ifigeneia Psarra

nr 214

Effects of Pricing Strategies on Dynamic Repertoires of Activity-Travel Behaviour

Elaheh Khademi

nr 215

Handstorm Principles for Creative and Collaborative Working

Frans van Gassel

nr 216

Light Conditions in Nursing Homes: Visual Comfort and Visual Functioning of Residents

Marianne M. Sinoo

nr 217

**Woonsporen:
De Sociale en Ruimtelijke Biografie van een Stedelijk Bouwblok in de Amsterdamse Transvaalbuurt**

Hüseyin Hüsni Yegenoglu

nr 218

Studies on User Control in Ambient Intelligent Systems

Berent Willem Meerbeek

nr 219

Daily Livings in a Smart Home: Users' Living Preference Modeling of Smart Homes

Erfaneh Allameh

nr 220

Smart Home Design: Spatial Preference Modeling of Smart Homes

Mohammadali Heidari Jozam

nr 221

Wonen: Discoursen, Praktijken, Perspectieven

Jos Smeets

nr 222

Personal Control over Indoor Climate in Offices: Impact on Comfort, Health and Productivity

Atze Christiaan Boerstra

nr 223

Personalized Route Finding in Multimodal Transportation Networks

Jianwe Zhang

nr 224

The Design of an Adaptive Healing Room for Stroke Patients

Elke Daemen

nr 225

Experimental and Numerical Analysis of Climate Change Induced Risks to Historic Buildings and Collections

Zara Huijbregts

nr 226

Wind Flow Modeling in Urban Areas Through Experimental and Numerical Techniques

Alessio Ricci

nr 227

Clever Climate Control for Culture: Energy Efficient Indoor Climate Control Strategies for Museums Respecting Collection Preservation and Thermal Comfort of Visitors

Rick Kramer

nr 228

Fatigue Life Estimation of Metal Structures Based on Damage Modeling

Sarmediran Silitonga

nr 229

A multi-agents and occupancy based strategy for energy management and process control on the room-level

Timilehin Moses Labeodan

nr 230

Environmental assessment of Building Integrated Photovoltaics: Numerical and Experimental Carrying Capacity Based Approach

Michiel Ritzen

nr 231

Performance of Admixture and Secondary Minerals in Alkali Activated Concrete: Sustaining a Concrete Future

Arno Keulen

nr 232

World Heritage Cities and Sustainable Urban Development: Bridging Global and Local Levels in Monitoring the Sustainable Urban Development of World Heritage Cities

Paloma C. Guzman Molina

nr 233

Stage Acoustics and Sound Exposure in Performance and Rehearsal Spaces for Orchestras: Methods for Physical Measurements

Remy Wenmaekers

nr 234

Municipal Solid Waste Incineration (MSWI) Bottom Ash: From Waste to Value Characterization, Treatments and Application

Pei Tang

nr 235

Large Eddy Simulations Applied to Wind Loading and Pollutant Dispersion

Mattia Ricci

nr 236

Alkali Activated Slag-Fly Ash Binders: Design, Modeling and Application

Xu Gao

nr 237

Sodium Carbonate Activated Slag: Reaction Analysis, Microstructural Modification & Engineering Application

Bo Yuan

nr 238

Shopping Behavior in Malls

Widiyani

nr 239

Smart Grid-Building Energy Interactions: Demand Side Power Flexibility in Office Buildings

Kennedy Otieno Aduda

nr 240

Modeling Taxis Dynamic Behavior in Uncertain Urban Environments

Zheng Zhong

nr 241

Gap-Theoretical Analyses of Residential Satisfaction and Intention to Move

Wen Jiang

nr 242

Travel Satisfaction and Subjective Well-Being: A Behavioral Modeling Perspective

Yanan Gao

nr 243

Building Energy Modelling to Support the Commissioning of Holistic Data Centre Operation

Vojtech Zavrel

nr 244

Regret-Based Travel Behavior Modeling: An Extended Framework

Sunghoon Jang

nr 245

Towards Robust Low-Energy Houses: A Computational Approach for Performance Robustness Assessment using Scenario Analysis

Rajesh Reddy Kotireddy

nr 246

Development of sustainable and functionalized inorganic binder-biofiber composites

Guillaume Doudart de la Grée

nr 247

A Multiscale Analysis of the Urban Heat Island Effect: From City Averaged Temperatures to the Energy Demand of Individual Buildings

Yasin Toparlar

nr 248

Design Method for Adaptive Daylight Systems for buildings covered by large (span) roofs

Florian Heinzelmann

nr 249

Hardening, high-temperature resistance and acid resistance of one-part geopolymers

Patrick Sturm

nr 250

Effects of the built environment on dynamic repertoires of activity-travel behaviour

Aida Pontes de Aquino

nr 251

Modeling for auralization of urban environments: Incorporation of directivity in sound propagation and analysis of a framework for auralizing a car pass-by

Fotis Georgiou

nr 252

Wind Loads on Heliostats and Photovoltaic Trackers

Andreas Pfahl

nr 253

Approaches for computational performance optimization of innovative adaptive façade concepts

Roel Loonen

nr 254

Multi-scale FEM-DEM Model for Granular Materials: Micro-scale boundary conditions, Statics, and Dynamics

Jiadun Liu

nr 255

Bending Moment - Shear Force Interaction of Rolled I-Shaped Steel Sections

Rianne Willie Adriana Dekker

nr 256

Paralympic tandem cycling and hand-cycling: Computational and wind tunnel analysis of aerodynamic performance

Paul Fionn Mannion

nr 257

Experimental characterization and numerical modelling of 3D printed concrete: Controlling structural behaviour in the fresh and hardened state

Robert Johannes Maria Wolfs

nr 258

Requirement checking in the building industry: Enabling modularized and extensible requirement checking systems based on semantic web technologies

Chi Zhang

nr 259

A Sustainable Industrial Site Redevelopment Planning Support System

Tong Wang

nr 260

Efficient storage and retrieval of detailed building models: Multi-disciplinary and long-term use of geometric and semantic construction information

Thomas Ferdinand Krijnen

nr 261

The users' value of business center concepts for knowledge sharing and networking behavior within and between organizations

Minou Weijs-Perrée

nr 262

Characterization and improvement of aerodynamic performance of vertical axis wind turbines using computational fluid dynamics (CFD)

Abdolrahim Rezaeiha

nr 263

In-situ characterization of the acoustic impedance of vegetated roofs

Chang Liu

nr 264

Occupancy-based lighting control: Developing an energy saving strategy that ensures office workers' comfort

Christel de Bakker

nr 265

Stakeholders-Oriented Spatial Decision Support System

Cahyono Susetyo

nr 266

Climate-induced damage in oak museum objects

Rianne Aleida Luimes

nr 267

Towards individual thermal comfort: Model predictive personalized control of heating systems

Katarina Katic

nr 268

Modelling and Measuring Quality of Urban Life: Housing, Neighborhood, Transport and Job

Lida Aminian

nr 269

Optimization of an aquifer thermal energy storage system through integrated modeling of aquifer, HVAC systems and building

Basar Bozkaya

nr 270

Numerical modeling for urban sound propagation: developments in wave-based and energy-based methods

Raúl Pagán Muñoz

nr 271

Lighting in multi-user office environments: improving employee wellbeing through personal control

Sanae van der Vleuten-Chraibi

nr 272

A strategy for fit-for-purpose occupant behavior modelling in building energy and comfort performance simulation

Isabella I. Gaetani dell'Aquila d'Aragona

nr 273

Een architectuurhistorische waardestelling van naoorlogse woonwijken in Nederland: Het voorbeeld van de Westelijke Tuinsteden in Amsterdam

Eleonore Henriette Marie Mens

nr 274

Job-Housing Co-Dependent Mobility Decisions in Life Trajectories

Jia Guo

nr 275

A user-oriented focus to create healthcare facilities: decision making on strategic values

Emilia Rosalia Catharina Maria Huisman

nr 276

Dynamics of plane impinging jets at moderate Reynolds numbers – with applications to air curtains

Adelya Khayrullina

nr 277

Valorization of Municipal Solid Waste Incineration Bottom Ash - Chemical Nature, Leachability and Treatments of Hazardous Elements

Qadeer Alam

nr 278

Treatments and valorization of MSWI bottom ash - application in cement-based materials

Veronica Caprai

nr 279

Personal lighting conditions of office workers - input for intelligent systems to optimize subjective alertness

Juliëtte van Duijnhoven

nr 280

Social influence effects in tourism travel: air trip itinerary and destination choices

Xiaofeng Pan

nr 281

Advancing Post-War Housing: Integrating Heritage Impact, Environmental Impact, Hygrothermal Risk and Costs in Renovation Design Decisions

Lisanne Claartje Havinga

nr 282

Impact resistant ultra-high performance fibre reinforced concrete: materials, components and properties

Peipeng Li

nr 283

Demand-driven Science Parks: The Perceived Benefits and Trade-offs of Tenant Firms with regard to Science Park Attributes

Wei Keat Benny Ng

nr 284

Raise the lantern; how light can help to maintain a healthy and safe hospital environment focusing on nurses

Maria Petronella Johanna Aarts

nr 285

Modelling Learning and Dynamic Route and Parking Choice Behaviour under Uncertainty

Elaine Cristina Schneider de Carvalho

nr 286

Identifying indoor local microclimates for safekeeping of cultural heritage

Karin Kompatscher

nr 287

Probabilistic modeling of fatigue resistance for welded and riveted bridge details. Resistance models and estimation of uncertainty.

Davide Leonetti

nr 288

Performance of Layered UHPFRC under Static and Dynamic Loads: Effects of steel fibers, coarse aggregates and layered structures

Yangyueye Cao

nr 289

Photocatalytic abatement of the nitrogen oxide pollution: synthesis, application and long-term evaluation of titania-silica composites

Yuri Hendrix

nr 290

Assessing knowledge adoption in post-disaster reconstruction: Understanding the impact of hazard-resistant construction knowledge on reconstruction processes of self-recovering communities in Nepal and the Philippines

Eefje Hendriks

nr 291

Locating electric vehicle charging stations: A multi-agent based dynamic simulation

Seheon Kim

nr 292

De invloed van Lean Management op de beheersing van het bouwproces

Wim van den Bouwhuisen

nr 293

Neighborhood Environment and Physical Activity of Older Adults

Zhengying Liu

nr 294

Practical and continuous luminance distribution measurements for lighting quality

Thijs Willem Kruisselbrink

nr 295

Auditory Distraction in Open-Plan Study Environments in Higher Education

Pietermella Elizabeth Braat-Eggen

nr 296

Exploring the effect of the sound environment on nurses' task performance: an applied approach focusing on prospective memory

Jikke Reinten

nr 297

Design and performance of water resistant cementitious materials– Mechanisms, evaluation and applications

Zhengyao Qu

nr 298

Design Optimization of Seasonal Thermal Energy Storage Integrated District Heating and Cooling System: A Modeling and Simulation Approach

Luyi Xu

nr 299

Land use and transport: Integrated approaches for planning and management

Zhongqi Wang

nr 300

Multi-disciplinary optimization of building spatial designs: co-evolutionary design process simulations, evolutionary algorithms, hybrid approaches

Sjonnie Boonstra

nr 301

Modeling the spatial and temporal relation between urban land use, temperature, and energy demand

Hung-Chu Chen

nr 302

Seismic retrofitting of masonry walls with flexible deep mounted CFRP strips

Ömer Serhat Türkmen

nr 303

Coupled Aerostructural Shape and Topology Optimization of Horizontal-Axis Wind Turbine Rotor Blades

Zhijun Wang

nr 304

Valorization of Recycled Waste Glass and Converter Steel Slag as Ingredients for Building Materials: Hydration and Carbonation Studies

Gang Liu

nr 305

Low-Carbon City Development based on Land Use Planning

Gengzhe Wang

nr 306

Sustainable energy transition scenario analysis for buildings and neighborhoods - Data driven optimization

Shalika Saubhagya Wickramarachchi Walker

nr 307

In-between living and manufactured: an exploratory study on biobuilding components for building design

Berrak Kirbas Akyurek

nr 308

Development of alternative cementitious binders and functionalized materials: design, performance and durability

Anna Monika Kaja

nr 309

Development a morphological approach for interactive kinetic façade design: Improving multiple occupants' visual comfort

Seyed Morteza Hosseini

nr 310

PV in urban context: modeling and simulation strategies for analyzing the performance of shaded PV systems

Ádám Bognár

nr 311

Life Trajectory, Household Car Ownership Dynamics and Home Renewable Energy Equipment Adoption

Gaofeng Gu

nr 312

Impact of Street-Scale Built Environment on Walking/Cycling around Metro Stations

Yanan Liu

nr 313

Advances in Urban Traffic Network Equilibrium Models and Algorithms

Dong Wang

nr 314

Development of an uncertainty analysis framework for model-based consequential life cycle assessment: application to activity-based modelling and life cycle assessment of multimodal mobility

Paul Martin Baustert

nr 315

Variable stiffness and damping structural joints for semi-active vibration control

Qinyu Wang

nr 316

Understanding Carsharing-Facilitating Neighborhood Preferences

Juan Wang

nr 317

Dynamic alignment of Corporate Real Estate to business strategies: An empirical analysis using historical data and in-depth modelling of decision making

Howard Cooke

nr 318

Local People Matter: Towards participatory governance of cultural heritage in China

Ji Li

nr 319

Walkability and Walkable Healthy Neighborhoods

Bojing Liao

nr 320

Light directionality in design of healthy offices: exploration of two methods

Parisa Khademagha

nr 321

Room acoustic modeling with the time-domain discontinuous Galerkin method

Huiqing Wang

nr 322

Sustainable insulating lightweight materials for enhancing indoor building performance: miscanthus, aerogel and nano-silica

Yuxuan Chen

nr 323

**Computational analysis of the impact of
façade geometrical details on wind flow and
pollutant dispersion**

Xing Zheng

nr 324

**Analysis of urban wind energy potential
around high-rise buildings in close proxim-
ity using computational fluid dynamics**

Yu-Hsuan Jang

The Heating, Ventilation and Air Conditioning (HVAC) sector is responsible for a large part of the total global energy consumption, a significant part of which is caused by incorrect operation of controls and incorrect maintenance. HVAC systems are becoming increasingly complex, especially due to multi-commodity energy sources, and as a result, the potential for failures in systems and controls will increase. That is why energy performance diagnostic systems are paramount. However, despite much research on Fault Detection and Diagnosis (FDD) methods for HVAC systems, they are rarely applied. An important reason is that the proposed methods differ from the design approaches of HVAC designers who use process and instrumentation diagrams (P&IDs).

The presented study made a step forward towards a systematic and automated multi-system and multi-level fault and energy performance diagnosis by developing an energy performance FDD architecture based on information embedded in P&IDs. The new FDD method, called the 4S3F method, combines systems theory with data analysis. In this 4S3F method, the detection and diagnosis phases are separated. The symptoms and faults are classified into 4 types of symptoms (balances, operating conditions (OS) and energy performances (EP) anomalies and additional information) and 3 types of faults (component, control and model faults).

The 4S3F method has been applied to the thermal energy plant of the building of the Hague University of Applied Sciences in Delft, containing a ATEs system, a heat pump, a gas boiler and hot- and cold-water hydronic systems. The conducted case studies presented that the 4S3F method unambiguously diagnosed the causes of failures. In addition, they showed that the 4S3F architecture largely solves the problems present with existing FDD methods that can be realized through a strict distinction between causes (faults) and effects (symptoms), allowing multiple detection methods to be used. The diagnosis by Bayesian diagnostic networks (DBNs) supports simultaneous multi-HVAC-level diagnosis of multiple faults and overcomes by posterior probabilities of the possible faults, problems associated with incorrect diagnosis results due to measurement inaccuracies and uncertainties in the FDD method. Furthermore, it was shown that both energy performance analysis and component FDD are applicable with the 4S3F architecture. In addition, classifications for symptoms and faults were presented. Sensitivity analysis on the identified probabilities in the DBN of the case studies showed that the absolute values are subordinate to the relative ones which helps the setup of the 4S3F method.



DEPARTMENT OF THE BUILT ENVIRONMENT